

Dissertation zur Erlangung des Doktorgrades
der Fakultät für Chemie und Pharmazie
der Ludwig-Maximilians-Universität München

**Synthesis of natural modified nucleosides and their
mass spectrometric quantification in cells and tissue**

**Synthese von natürlichen modifizierten Nucleosiden und deren
massenspektrometrische Quantifizierung in Zellen und Gewebe**

Daniel Globisch

aus

Kaiserslautern

2011

Erklärung

Diese Dissertation wurde im Sinne von § 13 Abs. 3 bzw. 4 der Promotionsordnung der LMU München vom 29. Januar 1998 von Prof. Dr. T. Carell betreut.

Ehrenwörtliche Versicherung

Diese Dissertation wurde selbstständig, ohne unerlaubte Hilfe erarbeitet.

München, den 02.02.2011



Daniel Globisch

Dissertation eingereicht am: 03.02.2011

1. Gutachter: Prof. Dr. T. Carell

2. Gutachter: Prof. Dr. S. A. Sieber

Mündliche Prüfung am: 11.03.2011

Danksagung

An erster Stelle danke ich meinem Betreuer *Prof. Dr. Thomas Carell* für die interessante Themenstellung, die exzellenten Arbeitsbedingungen und die große wissenschaftliche Freiheit. Seine Motivationsstärke, aufbauenden Ratschläge und Begeisterung für die Bioorganik haben entscheidend zum Erfolg dieser Arbeit und meinem Interesse an der Forschung beigetragen. Vielen Dank für die hervorragende Unterstützung während meiner gesamten Promotionszeit.

Den Mitgliedern der Prüfungskommission danke ich für ihre Bemühungen und den zeitlichen Aufwand bei der Evaluierung der Arbeit. *Prof. Dr. Stephan A. Sieber* danke ich recht herzlich für die Übernahme des Koreferats. Darüberhinaus bin ich ihm für die Hilfe bei allen massenspektrometrischen Fragestellungen zu großem Dank verpflichtet, wobei sich neben anregenden Diskussionen auch eine hervorragende und unkomplizierte Kooperation ergab. *Prof. Dr. Martin Biel* danke ich für die erfolgreiche Kooperation.

Frau *Slava Gärtner* und Frau *Sabine Voß* danke ich für die hervorragende Hilfsbereitschaft bei allen bürokratischen und organisatorischen Fragen. Den Mitarbeitern der NMR-Spektroskopie und Massenspektrometrie an der LMU danke ich für die schnelle Aufnahme von NMR- und Massenspektren.

Meinen Kooperationspartnern *Dr. Stylianos Michalakos* und *Susanne Koch* bei *Prof. Dr. Martin Biel* und *Kerstin Kurz* bei *Prof. Dr. Stephan A. Sieber* danke ich für eine unkomplizierte und angenehme Zusammenarbeit. Meinen arbeitskreisinternen Kooperationspartnern *Tim Gehrke*, *Ines Thoma* und *Christian Trindler* danke ich für den Einblick in andere interessante Themengebiete des Arbeitskreises Carell.

Meinen Bachelorstudenten *Ines Thoma* und *Ellen Broda*, meinem Forschungspraktikanten *Florian Huber* und meiner amerikanischen Austauschstudentin *Emma Cating* danke ich für ihre hohe Einsatzbereitschaft und Motivation beim Bearbeiten der Projekte.

Dem gesamten Arbeitskreis Carell danke ich für vier wunderschöne Jahre in denen ich viele bayrische Traditionen kennenlernen und viele großartige außeruniversitäre Ereignisse erleben durfte, wobei ich viele Freunde gewonnen habe. *Christian Deiml*, *Martin Münzel*, *Tobias Brückl*, *Thomas Reißner*, *Christian Trindler* und *Andreas Glas* danke ich für die lustigen Stadionbesuche, Championsleague-Abende im Fürstenegger und Junta-Abende. Ich wünsche euch allen viel Erfolg bei euren Projekten und Doktorarbeiten. Bedanken möchte ich mich auch beim gesamten tRNA und DNA Quantifizierungsteam mit denen viele Projekte

erfolgreich bearbeitet und hunderte bis schätzungsweise tausende Proben analysiert werden konnten. Den größten Anteil hierbei hatten *Tobias Brückl*, *Martin Münzel*, *Mirko Wagner*, *Dr. Markus Müller* und *Veronika Reiter*. Ein besonderer Dank gilt *Mirko Wagner* für das Engagement in „seinem“ Zellkulturlabor. Hilfreiche Diskussionen und entscheidende Anregungen bekam ich neben den bereits genannten Personen von *Dr. Sabine Schneider*, *Tim Gehrke*, *Christian Deiml*, *Christian Trindler*, *Thomas Reißner*, *Ines Thoma* und *Dr. David Pearson*.

Martin Münzel, *Dr. Sabine Schneider*, *Dr. Markus Müller*, *Tim Gehrke* und *Mirko Wagner* danke ich ganz besonders für das sehr gute und gewissenhafte Korrekturlesen dieser Arbeit.

Mit *Andreas Glas*, *Tobias Brückl* und *Martin Münzel* danke ich meinen engsten Begleitern, die darüber hinaus zu echten Freunden geworden sind. Mit *Andreas Glas* verbrachte ich 3 Jahre in einer Box und konnte von ihm lernen wie man mit bayrischer Gelassenheit zum Erfolg kommen kann. Neben wissenschaftlichen Diskussionen konnte ich mich mit ihm zu jeder Zeit über die aktuellsten Sportereignisse unterhalten.

Die produktiven Diskussionen mit *Tobias Brückl* in den vergangenen vier Jahren werden für mich immer unvergessen bleiben. Zusammen starteten wir das Quantifizierungsprojekt und zerbrachen uns die Köpfe teilweise bis tief in die Nacht über das erfolgreiche Gelingen der Projekte. Die Zusammenarbeit mit ihm hätte nicht besser sein können und trug maßgeblich zum Erfolg unserer Doktorarbeiten bei. Neben wissenschaftlichen Themen fanden wir immer Zeit für private Gespräche und lustige Momente. Danke für diese Zeit!

Nachdem Tobias und Andreas fertig wurden, ersetzte *Martin Münzel* beide in einer Person. Er übernahm den Abzug in meiner Box und wurde Projektpartner meines zweiten Projekts. Seine Zielstrebigkeit gepaart mit seiner sympathischen Art machten ihn zu einem perfekten Mitstreiter. Neben fruchtbaren wissenschaftlichen Diskussionen konnten wir auch immer über die verschiedensten Sportarten diskutieren und in der Freizeit zusammen Fußball spielen.

Ständige Unterstützung erhielt ich von meinen Eltern *Gabriele* und *Axel*, meinem Bruder *Julian Globisch* und meinen Großeltern. Eure Hilfe während der Doktorarbeit und darüber hinaus war unheimlich wichtig für mich. Deshalb gehört Euch ein Dank von ganzem Herzen!

Mein letzter und größter Dank geht an *Patricia Burkert*, die mich zu jeder Sekunde der letzten vier Jahre unterstützt und aufgebaut hat. Ich danke dir für die Geduld, wenn es des Öfteren ein bis zwei Stunden länger als versprochen gedauert hat. Eine bessere Unterstützung und ein größeres Verständnis für meine Freude an der Forschung kann ich mir nicht vorstellen.

Parts of this thesis work were published or presented on conferences

Publications

- 1) D. Globisch*, M. Münzel*, M. Müller, S. Michalakis, M. Wagner, S. Koch, T. Brückl, M. Biel, T. Carell. “Tissue Distribution of 5-Hydroxymethylcytosine and Search for Active Demethylation Intermediates”
PloS One **2010**, *5*, e15367.
- 2) M. Münzel, D. Globisch, C. Trindler, T. Carell “Efficient Synthesis of 5-Hydroxymethylcytosine Containing DNA”
Org. Lett. **2010**, *12*, 5671–5673.
- 3) M. Münzel*, D. Globisch*, T. Brückl, M. Wagner, V. Welzmilller, S. Michalakis, M. Müller, M. Biel, and T. Carell. “Quantification of the Sixth DNA-Base Hydroxymethyl-dC in the Brain”
Angew. Chem. Int. Ed. **2010**, *49*, 5375–5377. (Selected as Hot Paper and Highlighted in *Chem. Eng. News* **2010**, *88* (No 27), 24–25.)
- 4) T. Brückl*, D. Globisch*, M. Wagner, M. Müller, and T. Carell. “Parallel isotope based quantification of modified tRNA nucleosides”
Angew. Chem. Int. Ed. **2009**, *48*, 7932–7934. (Selected as Hot Paper and Highlighted in *Chem. Eng. News* **2009**, *87* (No 38), 35.)

* These authors contributed equally to this work

Conference Presentations

NAR award winner for Poster Presentation: 8th Nucleic Acid Conference (NACON VIII), Sheffield, England, 09/2010. “*The Sixth DNA Base 5-Hydroxymethylcytosine in Mammalian Brain*”

Presented in: *Nucl. Acids Res.* **2010**, 38, 7871–7875.

Oral Presentation: 3rd EuChemMS Chemistry Congress, Nuremberg, Germany, 08/2010. “*Quantification of the sixth DNA nucleoside 5-Hydroxymethylcytosine and modified tRNA nucleosides by HPLC-MS*”

Poster Presentation: Bayer Ph.D. Student Course 2010, Cologne, Germany, 07/2010. “*Synthesis of Natural Modified Nucleosides for Quantitative HPLC-MS Analysis*”

Poster Presentation: Gordon Research Conference on Bioorganic Chemistry, Proctor Academy, Andover, NH, USA, 06/2009. “*Quantitative Analysis of Modified tRNA Nucleosides*”

Poster Presentation: Synthesefest 2009 – A Celebration of Organic Chemistry in Munich, Munich, Germany, 03/2009. “*Synthesis of Hypermodified Adenosine Derivatives Present in tRNA*”

Poster Presentation: EMBL Conference on Chemical Biology 2008, Heidelberg, Germany, 10/2008. “*Synthesis of Hypermodified tRNA-Nucleosides*”

Poster Presentation: 3rd Nucleic Acid Chemical Biology Ph.D. Summer School, Odense, Denmark, 06/2007. “*Synthetic approach to the natural tRNA modification Wybutosine (*yW*)*”

Other Publications

- 5) Y. M. Loksha, D. Globisch, R. Loddo, G. Collu, P. La Colla, E. B. Pedersen. "A Novel Synthetic Route for the Anti-HIV Drug MC-1220 and its Analogues"
ChemMedChem **2010**, *5*, 1847–1849.

- 6) D. Globisch, N. Bomholt, V. V. Filichev, E. B. Pedersen. "Stability of Hoogsteen Type triplexes – Electrostatic attraction between duplex backbone and TFO using an intercalating conjugate"
Helv. Chim. Acta **2008**, *91*, 805–818.

- 7) Y. M. Loksha, D. Globisch, E. B. Pedersen, P. La Colla, G. Collu, R. Loddo. "Synthesis and Anti-HIV-1 Evaluation of 1,5-Disubstituted Pyrimidine-2,4-diones"
J. Heterocyclic Chem. **2008**, *45*, 1161–1166.

Conference Article

- 1) E. B. Pedersen, A. M. A. Osman, D. Globisch, M. Paramasivam, S. Cogoi, N. Bomholt, P. T. Jørgensen, L. E. Xodo, V. V. Filichev. "Triplex glue by synthesizing conjugated flexible intercalators"
Nucleic Acids Symp. Ser. **2008**, *52*, 37–38.

Table of contents

Table of contents.....	ix
1. Summary	1
2. Zusammenfassung	7
3. Introduction	13
3.1 Gene expression	13
3.2 Natural modified nucleotides.....	14
3.3 tRNA.....	15
3.4 Modifications at position 37.....	18
3.4.1 Structure and distribution in organisms	18
3.4.2 Function	20
3.4.2.1 Structural role.....	20
3.4.2.2 Codon-anticodon interaction	22
3.4.2.3 Frameshift prevention and translocation.....	23
3.4.2.4 Aminoacylation	25
3.4.2.5 Diseases	26
3.5 Summary	27
4. Aims of the Project.....	29
5. Synthesis of modified tRNA nucleosides	33
5.1 The t⁶A carbamoyl family	33
5.2 Methylated adenosine modifications.....	35
5.3 N⁶-Acetyladenosine.....	37
5.4 Synthesis of modifications.....	38
5.4.1 Synthesis of t ⁶ A	38
5.4.2 Synthesis of isotope-labeled t ⁶ A	39
5.4.3 Synthesis of g ⁶ A.....	39
5.4.4 Synthesis of m ⁶ A and m ⁶ ₂ A	40
5.4.5 Synthesis of m ⁶ t ⁶ A.....	41
5.4.6 Synthesis of isotope-labeled m ⁶ t ⁶ A.....	44
5.4.7 Synthesis of Am and m ¹ A.....	46
5.4.8 Synthesis of ac ⁶ A.....	47
5.5 Overview.....	47
5.6 Building blocks for RNA synthesis	48
6. Quantification method	51
6.1 Extraction and purification of tRNA	52
6.1.1 Extraction of tRNA.....	52
6.1.2 Purification of tRNA.....	52
6.2 Enzymatic hydrolysis of tRNA	54

6.3	HPLC-ESI-MS.....	55
6.4	Stock solutions	57
6.5	Calibration curves	58
6.6	Accuracy of quantification.....	60
7.	Results tRNA modifications	63
7.1	Differences between <i>E. coli</i> , mammalian tissue, and cell lines	63
7.2	Strategy.....	65
7.3	Porcine tissue	67
7.4	Cancer cell lines	79
7.5	Phylogenetic analysis.....	81
7.6	Pathogenic bacteria	88
7.7	Stress response.....	89
8.	Modified nucleosides in DNA	95
8.1	5-Hydroxymethylcytosine	95
8.2	Quantification of hmC by HPLC-ESI-MS	96
8.3	Distribution of hmC in mammalian tissue	99
8.4	hmC as a putative intermediate in the demethylation process?.....	106
8.5	hmC in cancer cell lines	110
9.	Outlook.....	113
10.	Experimental Section	115
10.1	General chemical materials and methods	115
10.2	Tissue samples, bacterial strains, and cell culture.....	116
10.3	Biochemical materials	117
10.3.1	Equipment.....	117
10.3.2	Bacterial strains and cell lines.....	118
10.4	Biochemical methods.....	119
10.4.1	Bacterial strains and growth conditions	119
10.4.2	tRNA purification	120
10.4.2.1	tRNA extraction.....	120
10.4.2.2	tRNA purification	121
10.4.3	DNA isolation from tissue samples and cancer cell lines	122
10.4.4	Enzymatic digestion of tRNA	122
10.4.5	Enzymatic digestion of DNA.....	123
10.4.6	HPLC-ESI-MS.....	124
10.4.6.1	Mass filter	124
10.4.6.2	Calibration curves.....	125
10.4.7	Separation of mitochondria and cytosol.....	126
10.4.8	<i>In vitro</i> translation assay	127
10.4.9	Immunohistochemistry	127
10.5	Phylogenetic analysis.....	128
10.6	Syntheses	129

10.6.1	Synthesis of t ⁶ A	129
10.6.2	Synthesis of ¹³ C ₄ , ¹⁵ N-t ⁶ A	138
10.6.3	Synthesis of g ⁶ A.....	140
10.6.4	Synthesis of m ⁶ A, d ₃ -m ⁶ A, m ⁶ ₂ A, and d ₃ -m ⁶ ₂ A	142
10.6.5	Synthesis of m ⁶ t ⁶ A	148
10.6.6	Synthesis of d ₃ -m ⁶ t ⁶ A	155
10.6.7	Synthesis of Am, d ₃ -Am, and d ₃ -m ¹ A.....	161
10.6.8	Synthesis of ac ⁶ A.....	164
10.6.9	Synthesis towards incorporation of t ⁶ A into RNA.....	166
10.6.10	Synthesis towards incorporation of m ⁶ t ⁶ A into RNA.....	171
11.	Abbreviations.....	177
12.	References	181

1. Summary

Natural nucleic acids are the molecules of life. They contain the genetic information of every organism and are involved in many biological processes. Additionally, they were involved for the development of life on earth. All nucleic acids contain natural modified nucleotides, which are incorporated in complex processes and are of tremendous importance for regulation and accuracy of transcription and translation in every organism. Over 120 different modifications were detected in all natural nucleic acids and the number is still increasing. tRNA is the most heavily modified nucleic acid and it additionally contains the broadest structural variety of modifications. So far, the function and role of single tRNA modifications has been investigated. Natural modified nucleosides were only rarely investigated in a context based manner. To overcome this limitation, we developed a method which allows quantification of in principle all tRNA modifications in parallel. This is similar to *proteomics* and *metabolomics* research in which the complete proteome or metabolome of a cell is quantified in parallel, respectively.

The method is based on HPLC-ESI-MS analysis. It enables precise quantification of tRNA modifications by using isotope-labeled stable internal standard molecules for each modification (*Figure 1*). In addition, the method was extended to allow quantification of DNA modifications.

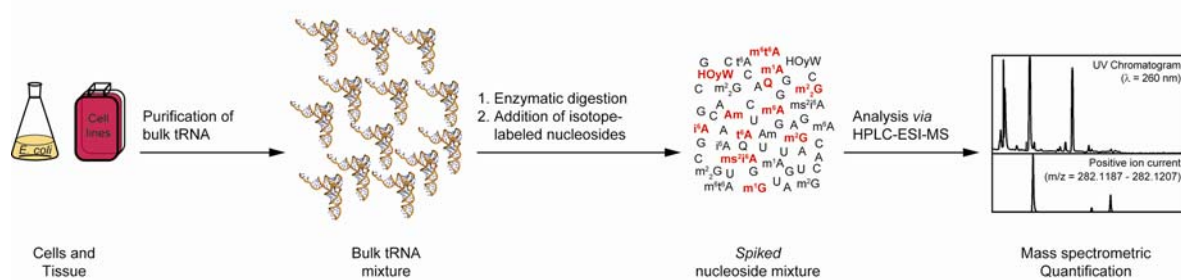


Figure 1: Representative workflow of the LC-MS based quantification method for tRNA nucleosides which is applicable for all kind of cells. Extension of this method allows quantification of DNA, rRNA, and mRNA modifications.

The method starts with isolation and purification of tRNA or DNA, followed by complete enzymatic digestion of tRNA or DNA to the nucleosides. Afterwards the isotope-labeled nucleosides are spiked to the natural nucleoside mixture, which is analyzed *via* HPLC-ESI-MS experiments (*Figure 1*). In these measurements, the specific mass area of the natural

modification is compared with the area of the added corresponding isotope-labeled nucleoside.

Modified tRNA nucleosides

Availability of isotope-labeled reference compounds is essential for accurate quantification of the corresponding natural occurring modified nucleoside. Therefore, in total 13 nucleosides including six isotope-labeled derivatives were synthesized and used in this thesis work (Figure 2).

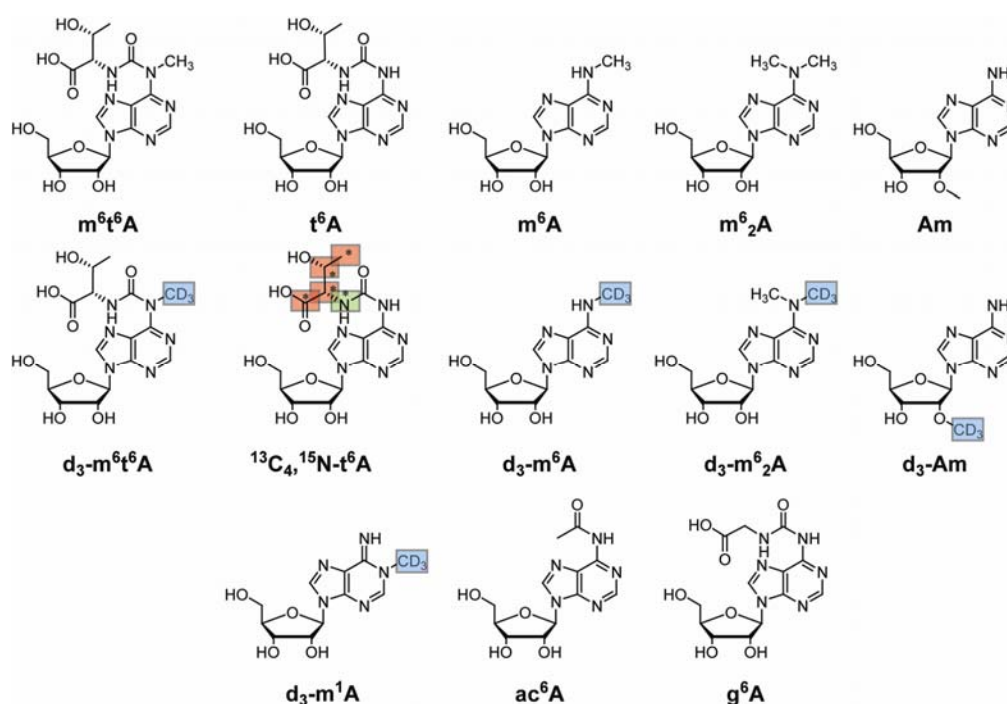


Figure 2: The 13 modified nucleosides synthesized in this Ph.D. thesis work.

These six isotope-labeled nucleosides as well as eleven other modifications synthesized in the group of Prof. T. Carell were used as internal standards for quantification of tRNA modifications in different bacterial species, mammalian tissues, and human cell lines.

In a first project we identified quantitative differences between healthy tissues and cancer cell lines especially for the modified tRNA nucleosides t^6A and ms^2i^6A (Figure 3A). The modification t^6A is upregulated in all cell lines compared to the liver tRNA values. In addition, the mitochondria specific modification ms^2i^6A could not be detected in any cancer cell line, but is present in significant amounts in liver tRNA. The absence in cancer cells is attributed to the Warburg effect, which describes an impaired mitochondrial activity in tumors. Furthermore, we analyzed the ms^2i^6A content in different tissues and found high

levels in tissues with high mitochondrial activities (*Figure 3B*). The data correlate well with the mitochondria specific Cytochrome C oxidase activity (*Figure 3C*). In summary, the $ms^{2,6}A$ content represents mitochondrial activity and can be used as marker to differentiate between healthy and tumor tissues.

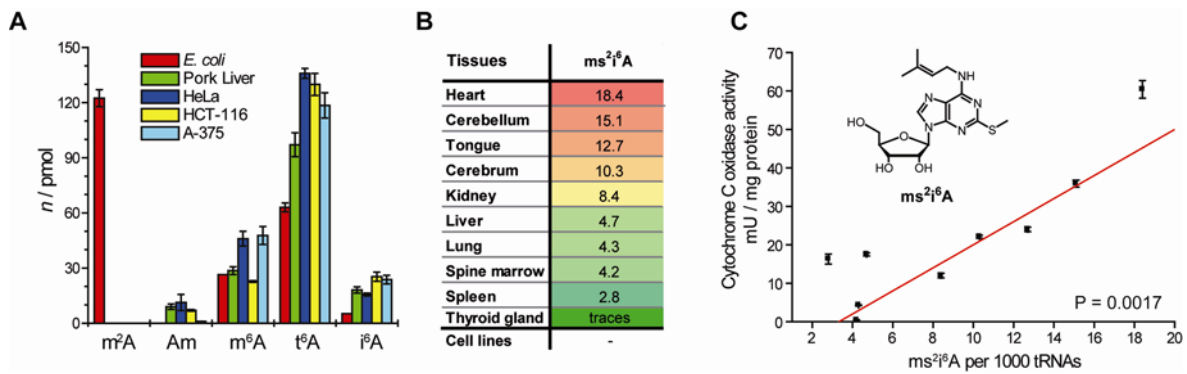


Figure 3: A) Differences of tRNA modification levels between *E. coli*, liver tissue and three cancer cell lines. B) Tissue dependency of $ms^{2,6}A$. C) Correlation of $ms^{2,6}A$ with Cytochrome C oxidase activity.

The tRNA modification levels of 11 further nucleosides were determined in 10 different cell lines and 10 different tissues (*Figure 4A*). These results revealed that tissues contain significantly different modification levels. tRNA from liver and cerebellum is most heavily modified, whereas heart and cerebrum exhibit lowest modification levels. These results are in line with *in vivo* protein synthesis rates from literature. Therefore, an *in vitro* translation system was established and used in this thesis to further support this hypothesis. High *in vitro* translation activity correlated with the modification level (*Figure 4B*). All cancer cell lines showed similar or higher levels than liver as the most heavily modified tissue. This can be explained by the high proliferation rates of cancer cells, which necessitates high protein synthesis rates (*Figure 4A*).

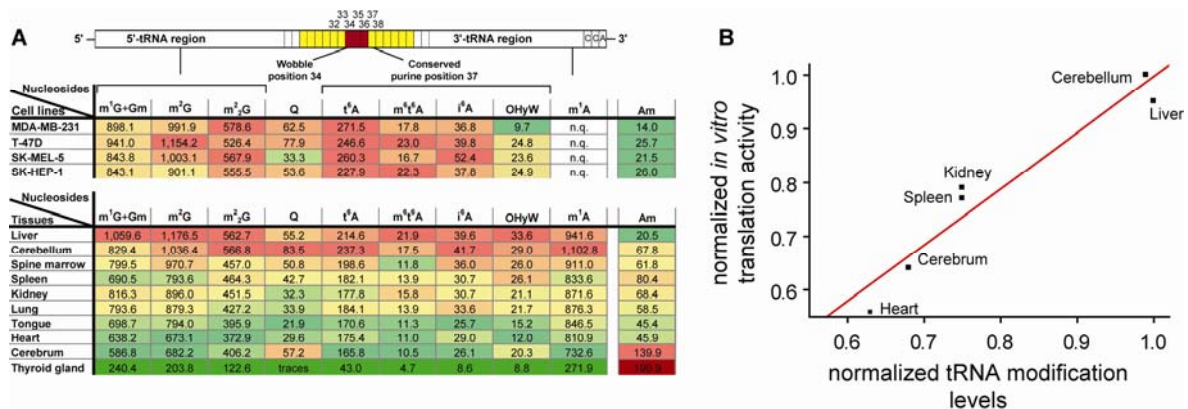


Figure 4: A) Quantitative data of cancer cell lines and tissues colored according to the amount. B) Correlation of total tRNA *in vitro* translation activity with normalized nucleoside levels.

In a further project the tRNA modification levels of 11 different prokaryotic species were investigated. Analysis of bacteria from different parts of the phylogenetic tree revealed large tRNA modification level differences. With these data, combined the mammalian tissue values and data from two yeast strains, we performed a Cluster correlation analysis. This analysis yielded clustering according to phylogenetic correlations (*Figure 5A*). Eukaryotic and prokaryotic organisms cluster separately from each other and the two yeast strains are differentiated from mammalian tissues. Furthermore, Gram-positive and Gram-negative bacteria are clearly separated from each other and even bacteria from the same genus can clearly be differentiated. These results show the high accuracy of our quantitative data and hint at an evolutionary controlled development of tRNA modifications.

In addition, the response of the tRNA modification pattern to external stimulation was analyzed in *E. coli*. Indeed, variations in the tRNA modification values were detected after applying different pH stress conditions or antibiotic treatment (*Figure 5B*).

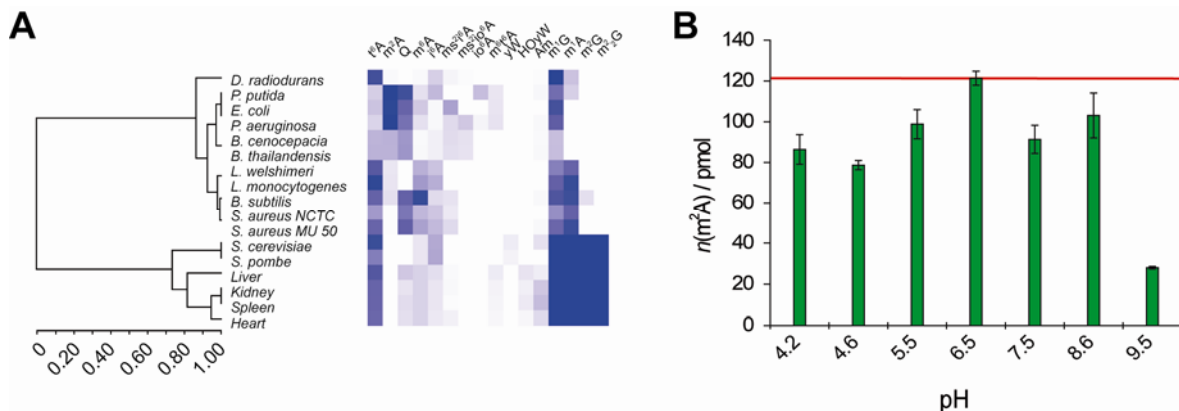


Figure 5: A) Cluster analysis of determined quantitative tRNA modification data for prokaryotes and eukaryotes. B) tRNA modifications variations depending on pH stress.

The sixth DNA base 5-hydroxymethylcytosine

Methylation of cytosine at the 5-position (mC) is an epigenetic marker, which is known for many decades. It is of high importance to block expression of specific genes. In 2009, the modification 5-hydroxymethylcytosine (hmC) was detected as a novel base in purkinje neurons of the mammalian cerebellum. Enzymes of the *Tet* family were identified to convert mC to hmC. These observations indicate that hmC has an epigenetic role, which is not clarified yet.

Using our quantification method, we analyzed the hmC and mC content in the mammalian body. Analysis of different tissues revealed that hmC is distributed over the whole

mammalian body with significantly varying amounts from 0.03% to 0.7% hmC/dG depending on the tissue type (*Figure 6A*). However, mC values are constant around 4.2%. Interestingly, tissues from the central nervous system (CNS) contain the highest amount of hmC. Medium values were found for tissues like kidney, heart, and lung. Lowest values could be detected in liver, spleen and pituitary gland, which is located in the brain. All these results indicate an important role of hmC in the nervous system. Therefore, we analyzed the mammalian brain in more detail and again found strongly varying values of hmC in different brain regions (*Figure 6B*). An interesting fact is that regions with a high cognitive role (cerebral cortex, hippocampus) contain high hmC values. Furthermore, an age dependency for the hmC values in hippocampus could be shown (*Figure 6C*).

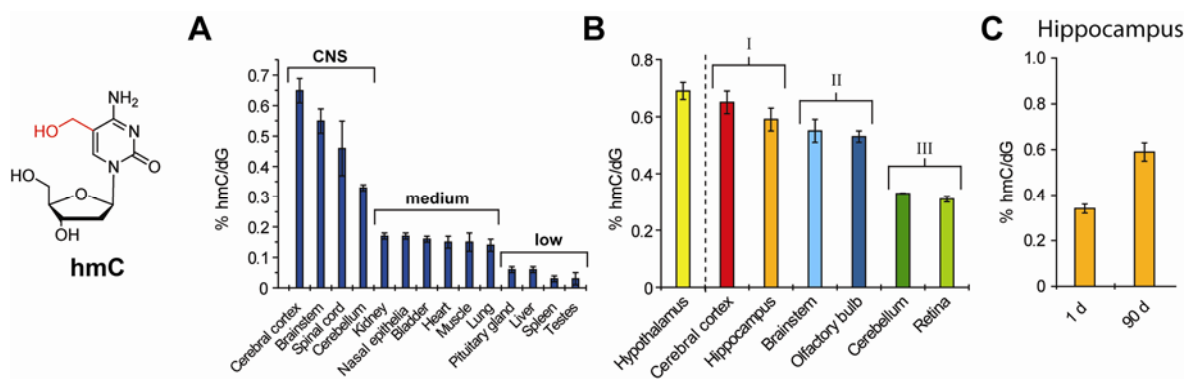


Figure 6: A) hmC distribution in the mammalian body. B) hmC distribution in different brain regions. C) Age dependency of hmC in hippocampus.

2. Zusammenfassung

Natürliche Nucleinsäuren sind die Moleküle des Lebens. Sie tragen die genetische Information in jedem Organismus und sind in viele biologische Prozesse involviert. Zusätzlich waren sie sehr wichtig für die Entwicklung des Lebens auf der Erde. Alle Nucleinsäurearten enthalten natürlich modifizierte Nucleotide, welche in komplexen Prozessen synthetisiert werden. Diese Modifikationen sind von großer Bedeutung für die Regulierung und Genauigkeit der Transkription und Translation in jedem Organismus. Über 120 unterschiedliche Modifikationen sind bisher bekannt und zusätzlich steigt die Zahl der neu entdeckten Modifikationen immer weiter. Transfer-RNA (tRNA) besitzt die größte Anzahl und Strukturvielfalt an Modifikationen. Bisher wurden die Funktionen von einzelnen tRNA Modifikationen untersucht und teilweise aufgeklärt. Allerdings wurden natürliche Modifikationen selten im Zusammenhang als Gesamtheit untersucht. Um diese Lücke zu schließen, wurde im Rahmen dieser Doktorarbeit eine Methode entwickelt, welche die parallele Quantifizierung von grundsätzlich allen tRNA-Modifikationen ermöglicht. Diese Methode ist sehr ähnlich zu den *Proteomics* und *Metabolomics* Forschungsbereichen bei denen jeweils das gesamte Proteom oder Metabolom einer Zelle parallel quantifiziert wird.

Die von uns entwickelte Methode basiert auf der HPLC-ESI-MS Analyse und ermöglicht präzise Quantifizierung von tRNA-Modifikationen unter Verwendung von stabilen isotope markierten internen Standardmolekülen (*Abbildung 1*). Zusätzlich wurde die Methode erweitert, um die Quantifizierung von DNA Modifikationen zu ermöglichen.

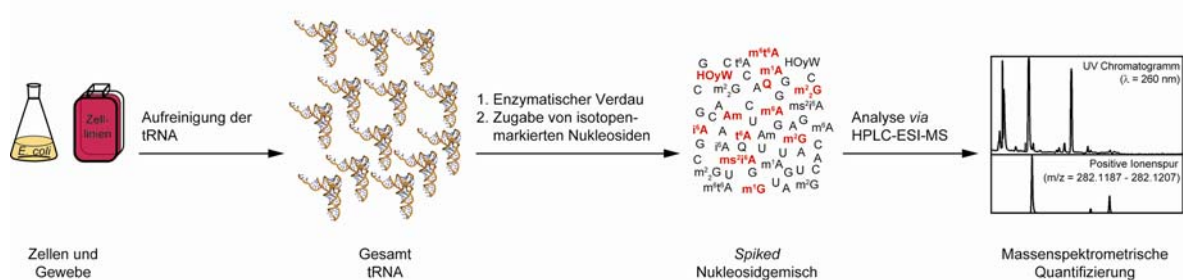


Abbildung 1: Repräsentative Darstellung der LC-MS basierenden Quantifizierungsmethode für tRNA Nucleoside, welche auf alle Zellarten anwendbar ist. Eine Erweiterung dieser Methode ermöglicht die zusätzliche Quantifizierung von DNA, rRNA und mRNA Modifikationen.

Die Methode beginnt mit der Isolierung und Aufreinigung von tRNA oder DNA. Nach dem quantitativen enzymatischen Verdau der Nucleinsäuren zu Ihren Nucleosiden werden die

isotopenmarkierten Nucleoside zugegeben und die Nucleosidlösung mittels HPLC-ESI-MS analysiert (*Abbildung 1*). In diesen Messungen werden die Flächen der spezifischen Massensignale des natürlichen Nucleosids und der entsprechenden isotopenmarkierten Verbindung verglichen.

Modifizierte tRNA Nucleoside

Die Verfügbarkeit von isotopenmarkierten Referenzverbindungen ist essentiell für die präzise Quantifizierung der entsprechenden natürlich vorkommenden Nucleoside. Dafür wurden im Rahmen dieser Arbeit insgesamt 13 Nucleoside synthetisiert und verwendet, von denen 6 isotopenmarkiert sind (*Abbildung 2*).

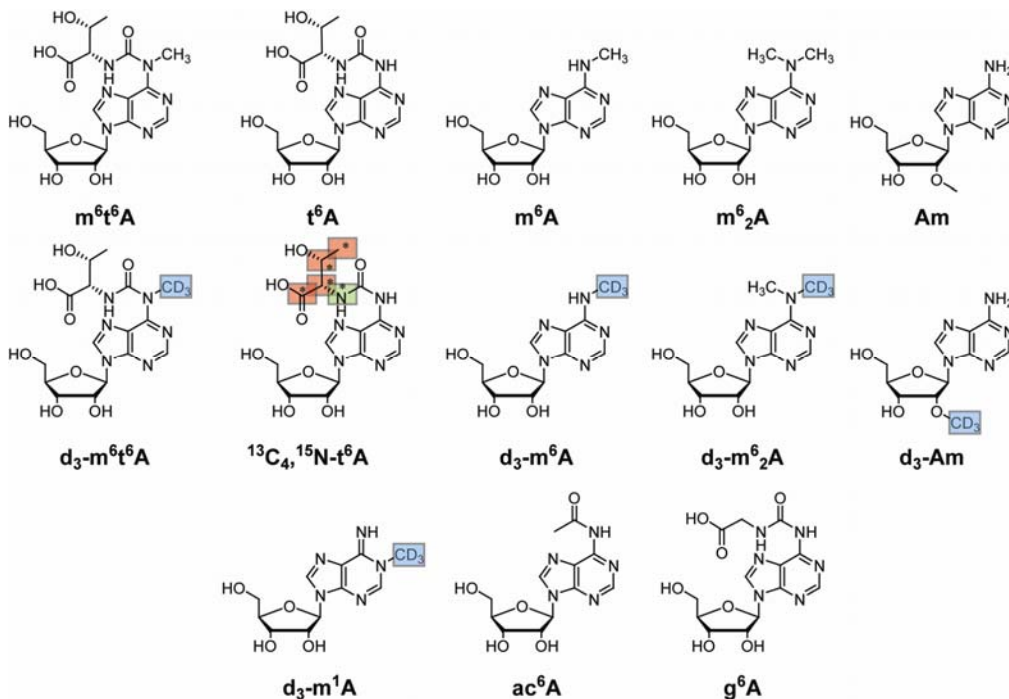


Abbildung 2: Die 13 modifizierten Nucleoside, die im Rahmen dieser Doktorarbeit synthetisiert wurden.

Diese 6 isotopenmarkierten Nucleoside und 11 weitere Modifikationen aus der Gruppe von Prof. T. Carell wurden als interne Standards zur Quantifizierung von tRNA-Modifikationen in verschiedenen Bakterienarten, Säugetiergeweben und menschlichen Zelllinien verwendet.

In einem ersten Projekt wurden quantitative Unterschiede der modifizierten tRNA Nucleoside zwischen gesundem Gewebe und Krebszelllinien insbesondere für die Modifikationen t⁶A und ms²i⁶A gefunden (*Abbildung 3A*). In allen Zelllinien ist die Modifikation t⁶A im Vergleich zur Leber-tRNA hochreguliert. Zusätzlich konnte die mitochondrienspezifische Modifikation ms²i⁶A nicht in Krebszelllinien gefunden werden, während sie in signifikanten

Mengen in Leber-tRNA vorkommt. Die Abwesenheit in Krebszellen ist in Übereinstimmung mit dem Warburg-Effekt. Dieser besagt, dass die mitochondriale Aktivität in Tumoren beeinträchtigt ist. Des Weiteren analysierten wir den ms^2i^6A -Gehalt in verschiedenen Geweben und entdeckten besonders hohe Mengen in Geweben mit hoher mitochondrialer Aktivität (Abbildung 3B). Der jeweilige ms^2i^6A -Gehalt korreliert sehr gut mit den entsprechenden mitochondrienspezifischen Cytochrom C Oxidase-Aktivitätswerten (Abbildung 3C). Zusammengefasst repräsentieren die ms^2i^6A -Werte die mitochondriale Aktivität und können als Marker zur Unterscheidung von gesundem und Tumorgewebe verwendet werden.

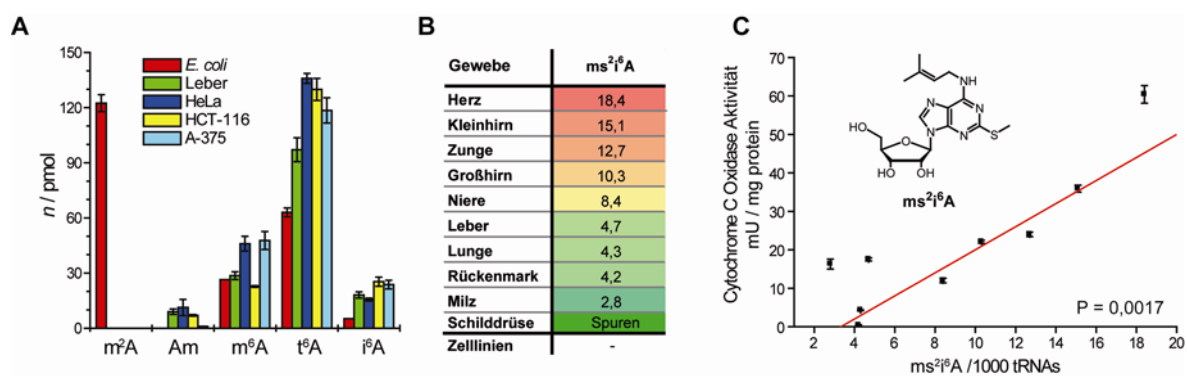


Abbildung 3: A) Unterschied der tRNA-Modifikationswerte zwischen *E. coli*, Lebergewebe und drei Krebszelllinien. B) Gewebeabhängigkeit der ms^2i^6A -Werte. C) Korrelation von ms^2i^6A mit der Cytochrome C Oxidase-Aktivität.

Zusätzlich wurden die tRNA-Modifikationslevel von 11 weiteren Nucleosiden in 10 Zelllinien und 10 Säugetiergeweben untersucht (Abbildung 4A). Diese Resultate zeigen, dass verschiedene Gewebetypen signifikant unterschiedliche Modifikationswerte besitzen. Während die tRNAs in Leber und Kleinhirn am Höchsten modifiziert sind, ist der tRNA-Modifikationsgrad in Herz und Großhirn am geringsten. Diese Resultate sind in Übereinstimmung mit *in vivo* Proteinsyntheseraten aus Literaturdaten. Um diese Beobachtung zu stärken wurde im Rahmen dieser Doktorarbeit ein *in vitro*-Translationssystem etabliert. Hohe *in vitro* Translationsaktivitäten der tRNA in unterschiedlichen Geweben korrelieren sehr gut mit hohen Modifikationswerten (Abbildung 4B). Alle Krebszelllinien besitzen entweder gleiche oder höhere tRNA-Modifikationswerte, als das höchstmodifizierte Lebergewebe. Dieses Resultat kann durch die schnell proliferierenden Krebszelllinien erklärt werden, die eine hohe Proteinsyntheserate benötigen (Abbildung 4A).

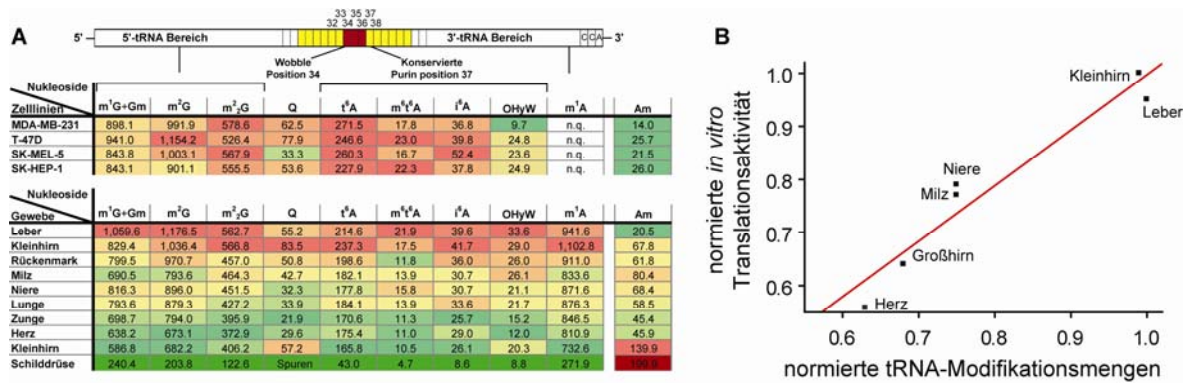


Abbildung 4: A) Übersicht der quantitativen Daten von Krebszelllinien und Säugetiergeweben. B) Korrelation der *in vitro* Translationsaktivität von Gesamt-tRNA mit den normierten Nukleosidwerten.

In einem weiteren Projekt wurden 11 unterschiedliche Bakterienarten untersucht. Die Analyse von Bakterien aus verschiedenen Bereichen des phylogenetischen Baums zeigt große Unterschiede in den tRNA-Modifikationswerten. Diese Werte zusammen mit den Daten von den Säugetiergeweben und zwei Hefestämmen wurden mit Hilfe eines *Cluster*-Algorithmus analysiert. Diese Analyse erzielte Zusammenhänge in Übereinstimmung zu phylogenetischen Korrelationen (*Abbildung 5A*). Eukaryotische und prokaryotische Organismen spalten unterschiedlich voneinander auf. Zusätzlich sind die beiden Hefestämme deutlich von den Säugetiergeweben zu unterscheiden. Auch Gram-positive und Gram-negative Bakterien sind deutlich voneinander getrennt und sogar Bakterien der gleichen Gattung sind eindeutig unterscheidbar. Diese Resultate zeigen die sehr hohe Genauigkeit unserer quantitativen Werte und deuten auf eine evolutionskontrollierte Entwicklung der tRNA-Modifikationen hin.

Zusätzlich wurde untersucht, ob das tRNA-Modifikationsmuster aufgrund von äußerem Stress in *E. coli* sich verändert. Tatsächlich wurden Variationen der tRNA-Modifikationslevels nach Anwendung von unterschiedlichen pH Bedingungen oder Antibiotika gefunden (*Abbildung 5B*).

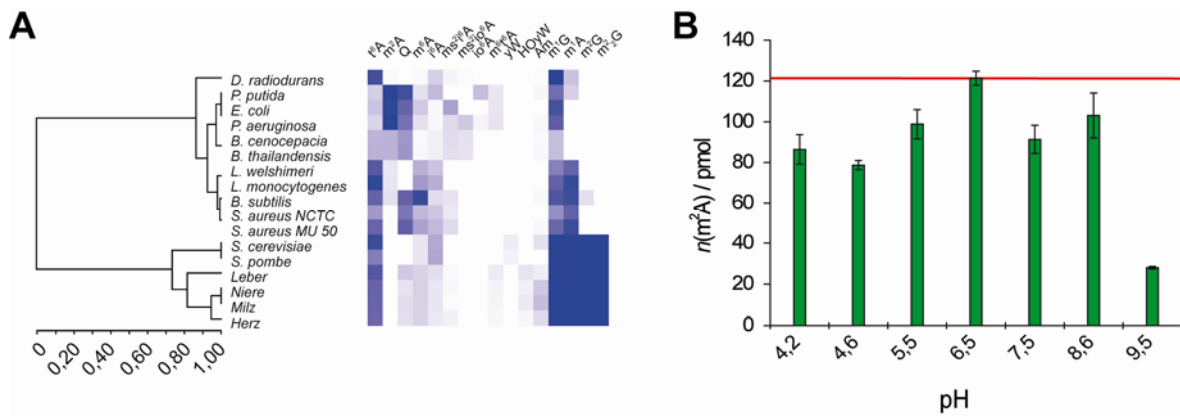


Abbildung 5: A) Clusteranalyse der quantitativen tRNA-Modifikationswerte von Prokaryoten und Eukaryoten. B) tRNA-Modifikationsänderung nach Anwendung von pH Stressbedingungen bei *E. coli*.

Die sechste DNA-Base 5-Hydroxymethylcytosin

Die Methylierung von Cytosin in Position 5 (mC) ist ein epigenetischer Marker, der seit vielen Jahrzehnten bekannt ist. Die wichtige Aufgabe dieser Modifikation ist es, die Expression bestimmter Gene zu unterdrücken. Im Jahr 2009 wurde die DNA-Modifikation 5-Hydroxymethylcytosin (hmC) als neue Base in Purkinje-Nervenzellen des Säugetierkleinhirns entdeckt. Enzyme der *Tet* Familie wurden identifiziert, die mC zu hmC modifizieren. Diese Entdeckungen deuten auf eine epigenetische Rolle von hmC hin, die bisher noch ungeklärt ist.

Mit Hilfe unserer Quantifizierungsmethode analysierten wir den hmC und mC Gehalt im Säugetierkörper. Analysen von verschiedenen Geweben zeigen, dass hmC im gesamten Säugetierkörper vorkommt. Das Verhältnis hmC/dG ist Gewebespezifisch und liegt zwischen 0,03% bis 0,7% (Abbildung 6A). Im Gegensatz dazu haben wir konstante mC Werte von jeweils ungefähr 4,2% gefunden. Interessanterweise besitzen Gewebe des Zentralnervensystems (ZNS) hohe hmC Werte. Mittlere Werte wurden für DNA aus Niere, Herz und Lunge detektiert. Die geringsten Werte wurden für Leber, Milz und Hypophyse gefunden, welche sich im Gehirn befindet. Diese Resultate deuten auf eine wichtige Funktion von hmC im Nervensystem hin. Deshalb untersuchten wir das Säugetiergehirn im Detail und haben erneut unterschiedliche Werte detektiert (Abbildung 6B). Eine interessante Entdeckung sind hohe hmC Werte in Regionen mit kognitiven Funktionen (Großhirnrinde und Hippokampus). Zusätzlich wurde eine Abhängigkeit der hmC Werte vom Alter der Tiere im Hippokampus gezeigt (Abbildung 6C).

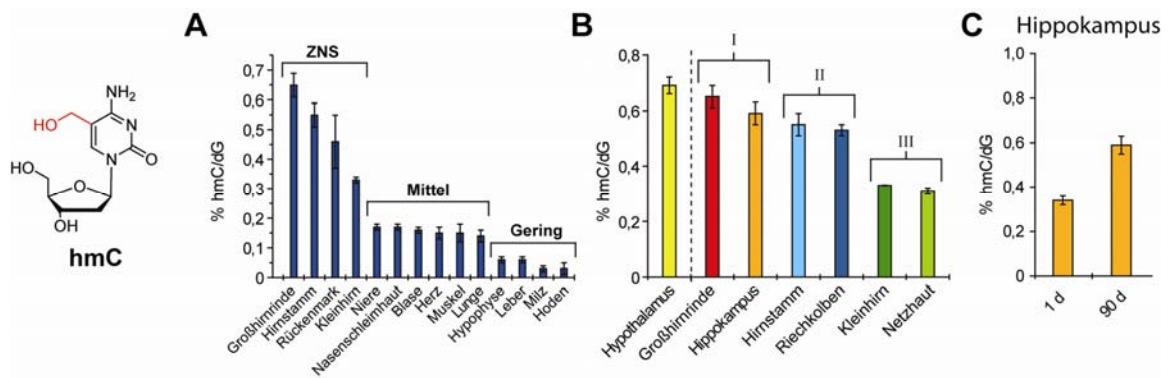


Abbildung 6: A) hmC-Verteilung im Säugetierkörper. B) hmC-Verteilung in verschiedenen Gehirnregionen der Maus. C) Altersabhängigkeit von hmC im Hippokampus von Mäusen.

3. Introduction

3.1 Gene expression

Gene expression is one of the most crucial processes in the life of an organism, where the genetic information is converted in a two step procedure into proteins. The genomic DNA containing this information is transcribed to messenger RNAs (mRNAs) in a process called transcription (*Figure 7*).^[1] This is followed by translation of the mRNAs into proteins by the ribosome, using its ribosomal RNA and the transfer RNA (tRNA). These three different RNA types, mRNA, rRNA, and tRNA are the main macromolecules involved in translation, which exhibit different functions. The mRNA carries the genetic information as a triplet code in form of trinucleotide codons. The tRNA serves as an adapter molecule linking an anticodon to the corresponding amino acid. In the ribosome a tRNA is matched to the appropriate codon on mRNA and the peptide chain is elongated by transferring the amino acid to the previous tRNA. After final peptide coupling the full length protein is released from the ribosome.^[1]

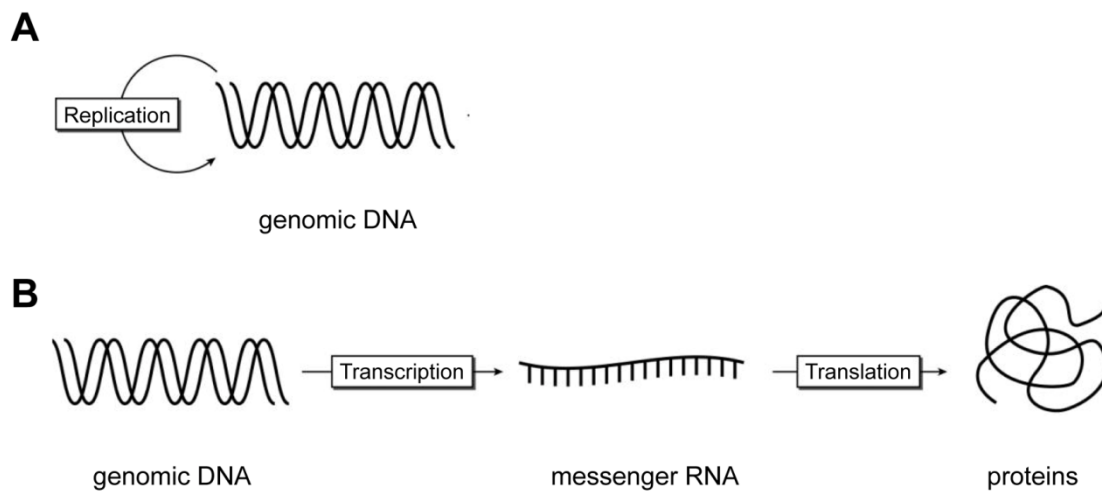


Figure 7: Schematic illustration of the replication of genomic DNA and gene expression.^[2] A) Replication of genomic DNA. B) Gene expression. Transcription to single stranded messenger RNA. Messenger RNAs are translated to proteins at the ribosome with tRNAs carrying the amino acids. The full length proteins are released to the cytosol.

The genetic code is assembled with 64 three letter codes, which are grouped into 16 different boxes according to the first two letters (*Figure 8*). These codon boxes are mainly degenerated to decode a single amino acid with up to six codons. Thus, 61 codons are used for incorporation of 20 natural amino acids and in addition three stop codons are present to terminate protein synthesis.

		SECOND				
		U	C	A	G	
U	FIRST	UUU Phe	UCU Ser	UAU Tyr	UGU Cys	U C A G THIRD, WOBBLE
		UUC Phe	UCC Ser	UAC Tyr	UGC Cys	
		UUA Leu	UCA Ser	UAA Stop	UGA Stop	
		UUG Leu	UCG Ser	UAG Stop	UGG Trp	
C	FIRST	CUU Leu	CCU Pro	CAU His	CGU Arg	U C A G THIRD, WOBBLE
		CUC Leu	CCC Pro	CAC His	CGC Arg	
		CUA Leu	CCA Pro	CAA Gln	CGA Arg	
		CUG Leu	CCG Pro	CAG Gln	CGG Arg	
A	FIRST	AUU Ile	ACU Thr	AAU Asn	AGU Ser	U C A G THIRD, WOBBLE
		AUC Ile	ACC Thr	AAC Asn	AGC Ser	
		AUA Ile	ACA Thr	AAA Lys	AGA Arg	
		AUG Met	ACG Thr	AAG Lys	AGG Arg	
G	FIRST	GUU Val	GCU Ala	GAU Asp	GGU Gly	U C A G THIRD, WOBBLE
		GUC Val	GCC Ala	GAC Asp	GGC Gly	
		GUA Val	GCA Ala	GAA Glu	GGA Gly	
		GUG Val	GCG Ala	GAG Glu	GGG Gly	

Figure 8: The genetic code with 64 different codons subdivided in 16 boxes containing four codons with the same first two nucleotides. Different degenerated codons are colored: 6-fold in orange, 4-fold in green, 3-fold in blue, 2-fold in yellow, and 1-fold in red. The three stop codons are colorless.

3.2 *Natural modified nucleotides*

The correct synthesis of proteins is of tremendous importance and optimized by every organism. All steps require tight regulation, fine tuning and proofreading. A mechanism evolved by nature is the modification of the four canonical bases A, C, G, and T(U) in DNA and RNA. Modified nucleosides are present in every cellular nucleic acid and range from simple methylations up to attachments of large side chains to the canonical bases, which are then called hypermodifications.^[3-6] However, every single modification changes the properties of any RNA type to improve different parts of gene expression.^[7-13]

Mammalian DNA is built up by the canonical bases and two natural cytosine modifications (*Figure 9*). 5-Methylcytosine (mC) was discovered in the 1950s, which is attracting protein

complexes to block expression of specific genes. Even though many reports describe the role of this epigenetic marker it is still subject of research regarding the development of life and memory formation.^[13-19] In addition, the Fe(II) and ketoxyglutarate dependent *Tet* enzymes can convert mC to 5-hydroxymethylcytosine (hmC), which was found in 2009 to be a novel modification present in DNA of the cerebellum in mammals.^[20-21] It was speculated that hmC could play a role in cell development or an active demethylation process. Nevertheless, the function of this modification still remains to be elucidated.

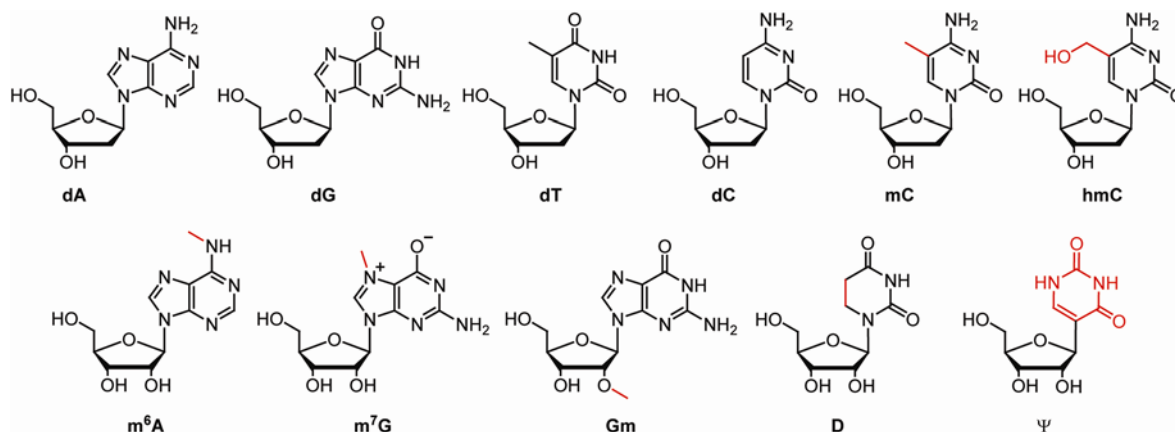


Figure 9: The first row shows the canonical DNA nucleosides dA, dG, dT, and dC with the two modified cytosine derivatives mC and hmC present in mammalian DNA. The representative modifications m⁶A, m⁷G, Gm, D, and Ψ from rRNA and mRNA are depicted in the second row.

Mainly simple modifications, such as various methylations, which are either present at the base or the 2' position, are found in mRNA and rRNA. While *N*⁶-methyladenosine (m⁶A), 7-methylguanosine (m⁷G), and 2'-*O*-methylguanosine (Gm) can be found in mRNA and rRNA, dihydrouridine (D) and pseudouridine (Ψ) are present in rRNA (Figure 9).^[4]

3.3 tRNA

Nevertheless, the majority of all nucleic acid modifications exists in tRNAs with up to 20% modified nucleotides. So far, 92 different tRNA modifications have been identified in all organisms, while the number of new detected modifications is still increasing.^[22-24] The tRNA is built up by three different loops, a variable loop and the specific CCA tail (Figure 10). The dihydrouridine stem and loop (DSL) and the thymidine stem and loop (TSL) are important for the 3D structure of a tRNA. The anticodon stem and loop (ASL) contains the anticodon and on the other end of the tRNA the specific CCA tail can be found at the amino acid acceptor stem. Modifications are present in most positions of the tRNA, but can mainly be found in the three different loops. These are incorporated during the different stages of the tRNA

maturation process. For the DSL and TSL it was partially shown that the modifications are already incorporated in tRNA precursors before splicing.^[25] These modifications are responsible for the correct folding of the tRNA and thus play an important structural role.^[8] The tertiary tRNA structure is additionally stabilized with Mg^{2+} ions that bind to different positions in the tRNA and also contribute to A and P site binding at the ribosome.^[26-27] Modifications, which are placed in the anticodon are finally incorporated to obtain the mature tRNA. It is proposed that they evolved during development of life to optimize each tRNA for correct translation.^[9-11, 25]

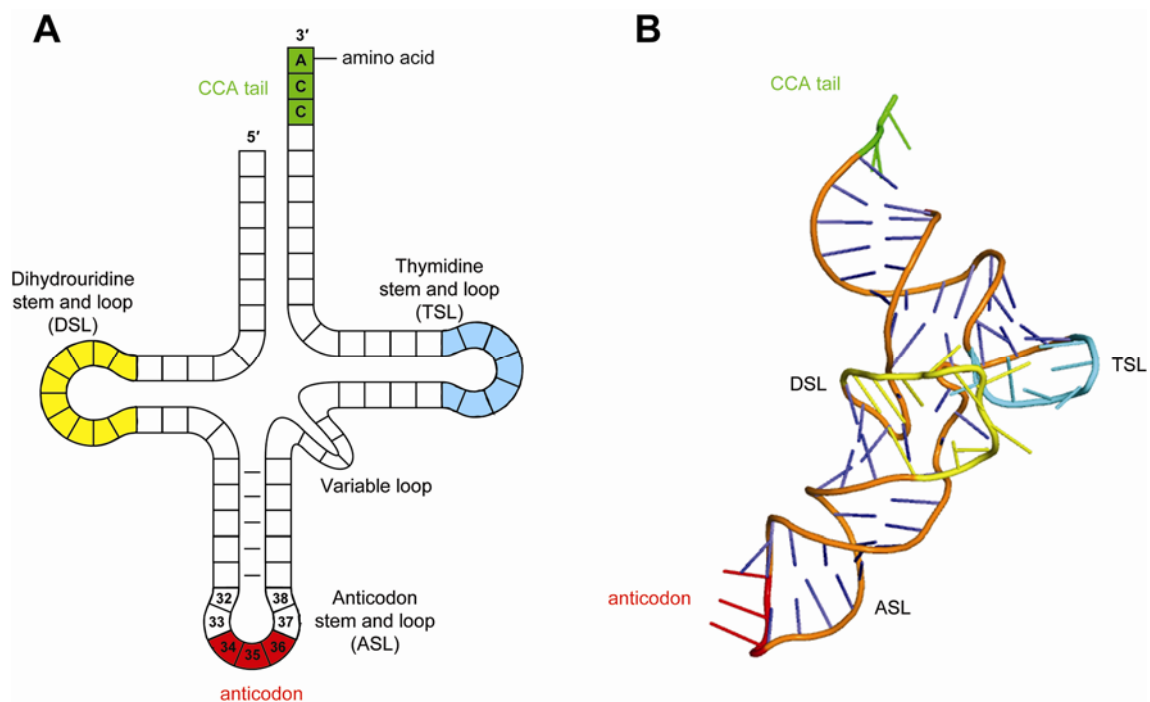


Figure 10: Structures of tRNA with the three loops of DSL (yellow), TSL (blue) and ASL. The anticodon is coloured in red and the CCA tail in green. A) 2D cloverleaf structure of tRNA B) 3D structure of representative *E. coli* tRNA^{Phe} ^[28]

The anticodon loop (position 32 to 38) is one of the modification richest parts of tRNAs with the highest modification diversity of all natural nucleic acids.^[4-5, 7] Outside the anticodon loop mainly simple modifications like methylations, thiolations or Ψ can be found. Anticodon loops have special sequences with conserved positions in all identified tRNAs of the three domains of life (Figure 11). The conserved pyrimidine position 32 is either unmodified, contain monomethylations, Ψ , or 2-thiocytidine (s^2C), while position 33 is unmodified and almost exclusively U.^[5, 29-30] The highest structural diversity of tRNA modifications is present at position 34, the so called wobble position and at position 37, which is directly 3'-adjacent to the anticodon. These modifications enable wobble base pairing and are a tool for efficient

reading of degenerated codons. The wobble position mainly contains a large diversity of uridine derivatives, inosine (I), 2'-*O*-methylated nucleosides, and nucleosides of the complex queuosine family.^[5, 29-30] The fold of the ASL is described as a U-turn motif, which was already indicated in the first crystal structures of yeast tRNA^{Phe}.^[31-32] The loop of this 17-mer has an almost 180° reverse of the backbone to align the anticodon bases which are stacking to each other. Intrastrand hydrogen bonds stabilize the U-turn structure. Positions 32 and 38 can form an additional intrastrand base pair to extend the anticodon stem.^[33]

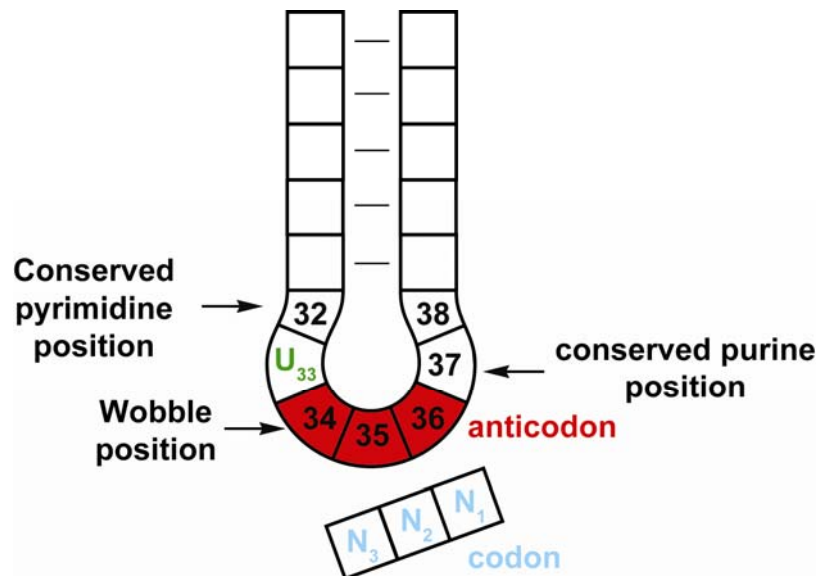


Figure 11: Anticodon stem and loop (ASL) with the anticodon loop from nucleotide 32 to 38. The anticodon is marked in red color. In position 32 is a conserved pyrimidine or its modification is present. Position 33 is mainly a uridine (green), while the three anticodon nucleotides are varying. While the wobble position can be modified the two modifications 35 and 36 are always unmodified. Position 37 is a conserved purine position, which is heavily modified, while position 38 is unmodified and mainly A.^[29-30, 34]

3.4 Modifications at position 37

3.4.1 Structure and distribution in organisms

Modifications at position 37 are of large structural diversity, ranging from simple methylation up to complex hypermodifications and are strongly dependent and specific for the anticodon sequence. This position contains exclusively purines and tRNA sequence analysis from different organisms revealed that A is occurring in 80% and G in 20% at this position.^[27, 35] Here adenosine derivatives are the most abundant modifications, which are either modified at position 2, 6 or both together.^[4-5, 7] So far, 16 modified nucleosides including 12 adenosine derivatives were identified at position 37 in tRNAs of organisms from all domains of life and can only be found at this position (*Figure 12*). In addition, the modification 1-methylinosine (m^1I) and the three guanosine derived modifications 1-methylguanosine (m^1G), wybutosine (yW), and hydroxywybutosine ($OHyW$) can also be found in the anticodon loop. While the tricyclic modifications yW and $OHyW$ are specific for this position, the m^1G and m^1I can also be found at other tRNA positions. These 16 nucleosides at position 37 can be classified in four different groups.

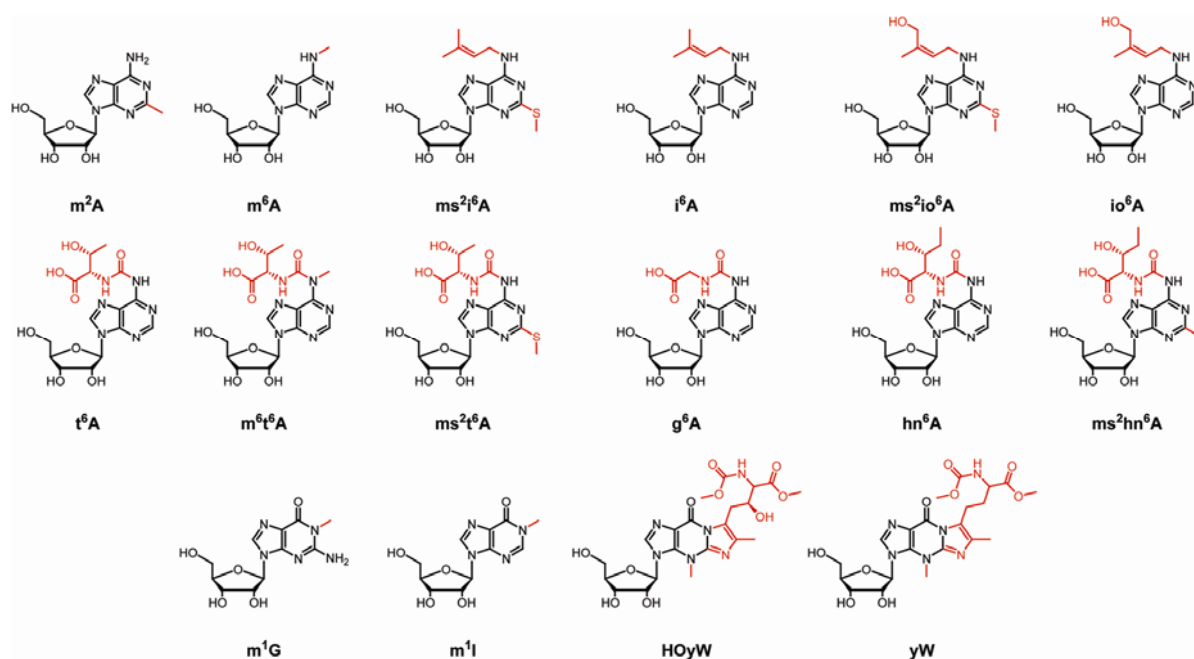


Figure 12: Modified nucleosides exclusively present 3'-adjacent to the anticodon at position 37.

The monomethylated nucleosides 2-methyladenosine (m^2A), N^6 -methyladenosine (m^6A), m^1G , and m^1I are synthesized by *S*-adenosylmethionine (SAM) dependent enzymes in a one step methylation process. Only m^1I is deaminated prior to methylation. The modification m^1G

is present in all three domains of life, while m^2A and m^6A are only present in bacterial tRNA.^[3, 5] The nucleoside m^6A is additionally present in mitochondrial tRNA of eukaryotes. The nucleoside m^1I is exclusively present at position 37 in tRNA^{Ala} of eukaryotes.^[4-5, 7]

The second class of modified nucleosides carries an isopentyl moiety at the N^6 -position, which are modified by the *Mia* enzyme family. The simplest representative is N^6 -isopentenyladenosine (i^6A), while an additional methylthio group is attached at position 2 in the further modified nucleoside 2-methylthio- N^6 -isopentenyladenosine (ms^2i^6A). These modifications are present in bacteria as well as in eukaryotes. The two *cis*-hydroxylated modifications 2-methylthio- N^6 -(*cis*-hydroxyisopentenyl)adenosine (ms^2io^6A) and N^6 -(*cis*-hydroxyisopentenyl)adenosine io^6A are completing the class of isopentyl derivatives and are occurring in bacterial tRNA (*Figure 12*).^[4-5, 7]

The third group carries different amino acids attached to adenosine *via* a carbonyl group in position 6 at the exocyclic amine. These hypermodified nucleosides are located in the anticodon loop 3'-adjacent to the anticodon of tRNAs reading ANN codons (N is standing for any of the canonical nucleosides A, C, G, or U). The main representative N^6 -threonylcarbamoyladenosine (t^6A) is present in all organisms and contains a L-threonine moiety linked to position 6 *via* a carbonyl moiety. It is together with m^1G the only modified nucleosides present at position 37 in all three domains of life. Additional methylation at this position occurs in some prokaryotic and eukaryotic tRNAs to obtain the modified nucleoside N^6 -methyl- N^6 -threonylcarbamoyladenosine (m^6t^6A). Two further modifications contain glycine and hydroxynorvaline instead of threonine in N^6 -glycinylylcarbamoyladenosine (g^6A) and N^6 -hydroxynorvalylcarbamoyladenosine (hn^6A), respectively (*Figure 12*). Furthermore, a methylthio moiety attached to the purine at position 2 was detected in the two modified nucleosides 2-methylthio- N^6 -threonylcarbamoyladenosine (ms^2t^6A) and 2-methylthio- N^6 -hydroxynorvalylcarbamoyladenosine (ms^2hn^6A).^[4-5, 7]

The fourth group is built up by the two wybutosine derivatives yW and OHyW, which are present in eukaryotic tRNA^{Phe}. These modifications are the only tricyclic modified bases detected in tRNA until today (*Figure 12*). Interestingly, the modified nucleoside m^1G is the first intermediate in the biosynthetic cascade to yW and OHyW. These two modifications are present only in eukaryotic organisms and are completely absent in prokaryotic or archaeal organisms. In eukaryotes yW is present in the unicellular organism yeast and in plants. The further hydroxylated and rarely described nucleoside OHyW is present in mammals as well as plants.^[4-5, 7]

3.4.2 Function

Biochemical, biological and chemical studies of modifications at position 37 were mainly performed for the most common nucleosides t^6A , ms^2t^6A , i^6A , ms^2i^6A , m^1G , and yW . The influence of these modifications in the appropriate ASL was investigated to elucidate the impact on anticodon loop stabilization, codon-anticodon interaction, frameshift prevention, translocation and aminoacylation.

3.4.2.1 Structural role

Modifications at position 37 are important for stabilization of ASL structure and to prearrange the anticodon. Structural and conformational effects were investigated by either solution studies of synthetic ASLs with NMR, Xray crystallography of whole tRNAs or tRNAs in complex with the ribosome. 17mer RNA strands were used as minimum tRNA mimic to simulate the 7-membered loop and 5-membered doublestranded stem region of an ASL (*Figure 11*).

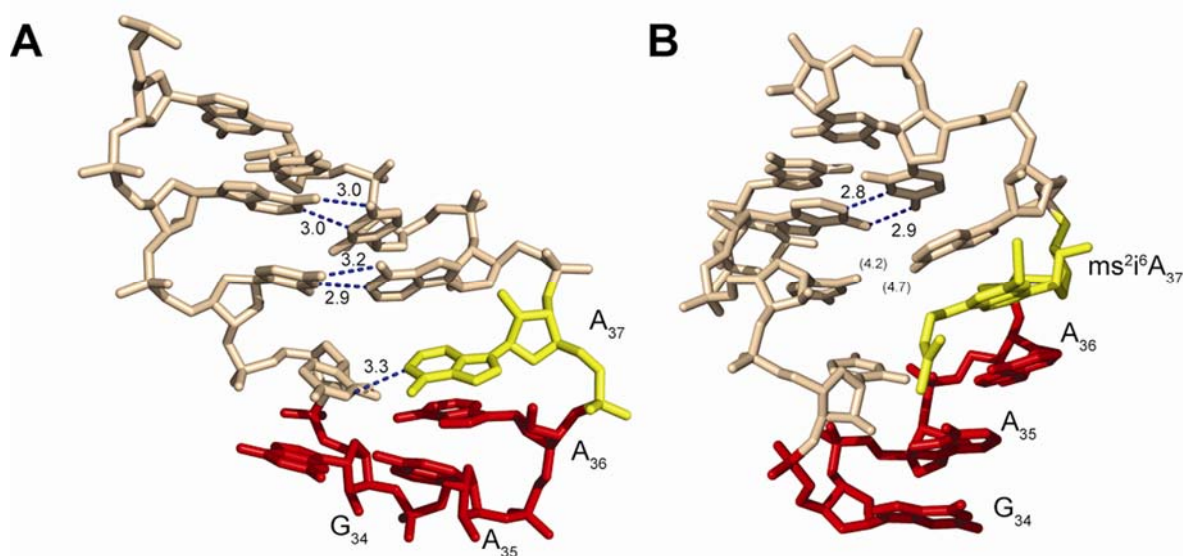


Figure 13: Different conformations of the anticodon loop of *E. coli* tRNA^{Phe}. A) Unmodified ASL with intramolecular hydrogen bonds.^[33] B) ASL with incorporated ms^2i^6A and prearranged anticodon bases for interaction with the codon.^[28]

NMR studies have shown that incorporation of modifications results in a reduced thermal stability and free energy (ΔG), but contribute significantly to increased entropic values (ΔS).^[36-38] The enhanced entropy and higher flexibility of the ASL is required to overcome the entropic penalty for A site binding.^[27] Comparison of modified and unmodified ASLs of *E. coli* tRNA^{Phe} with ms^2i^6A at position 37 shows the importance of modifications for the

structure.^[28, 33] Incorporation of the modification leads to a conformational change. The anticodon bases are prearranged in the modified structure, whereas they are orientated in different directions in the unmodified ASL (*Figure 13A*). Modification ms^2i^6A base stacks with the A_{36} to stabilize the anticodon prearrangement. In addition the hydrophobic isopentyl moiety is flexible and can contribute to anticodon codon interactions. The hydrogen bonds between A_{38} and U_{32} are disrupted in the modified ASL, which increases the mobility of the loop (*Figure 13B*).^[33, 39]

A main focus of ASL studies was put on the $tRNA^{Lys}_{UUU}$ sequences which contain t^6A in *E. coli* tRNA and ms^2t^6A in the mammalian tRNA at position 37 with the two different modified uridine nucleosides 5-methylaminomethyl-2-thiouridine (mnm^5s^2U) and 5-methoxycarbonylmethyl-2-thiouridine (mcm^5s^2U) at the wobble position, respectively. In general t^6A derivatives are found in codons starting with U and especially in pyrimidine rich codons, which require special stabilization. This nucleoside stacks over the first codon anticodon base pair to promote base stacking of positions 35 and 36. This stabilizes the weak $U_{36} \cdot A_1$ anticodon-codon binding. Furthermore, t^6A was described to enhance the stability of a G·U mismatch base pair at the wobble position in binding studies of whole tRNAs.^[40] NMR structures of modified ASLs with t^6A and ms^2t^6A reveal inhibition of the noncanonical intrastrand binding $C_{32} \cdot A^+_{38}$ by neutralization of A^+ with the ionized carboxylic acid of threonine.^[41-42] In contrast, the hydrophobic character of the methyl group in m^1G supports $Cm_{32} \cdot A^+_{38}$ base pairing in $tRNA^{Phe}$. When m^1G is further modified to yW the anticodon loop loses flexibility, resulting in three defined, slowly exchanging conformations.^[43] Thus, this anticodon loop significantly differs to the structure of ASLs with m^1G . Furthermore, ASLs with the incorporated modifications i^6A , ms^2i^6A , and yW influence Mg^{2+} binding to bases in the anticodon loop.^[26-28, 33, 39]

Interestingly, an extra hydrogen bond in t^6A between nitrogen N1 of the base with the amine of the coplanar orientated ureido group forms a third ring, which is similar to the tricyclic base yW (*Figure 14*).^[38, 44-45] This tricyclic structure leads to an additional stabilization by base stacking of the first codon base pair in complex with the mRNA. Furthermore, the 2-methylthio moiety in ms^2t^6A is slightly destabilizing this “third ring hydrogen bond”. This causes a significant conformational change compared to t^6A containing ASLs and results in a so-called stair-stepped conformation of the anticodon bases, which are unstacked in ASLs lacking ms^2t^6A .^[46]

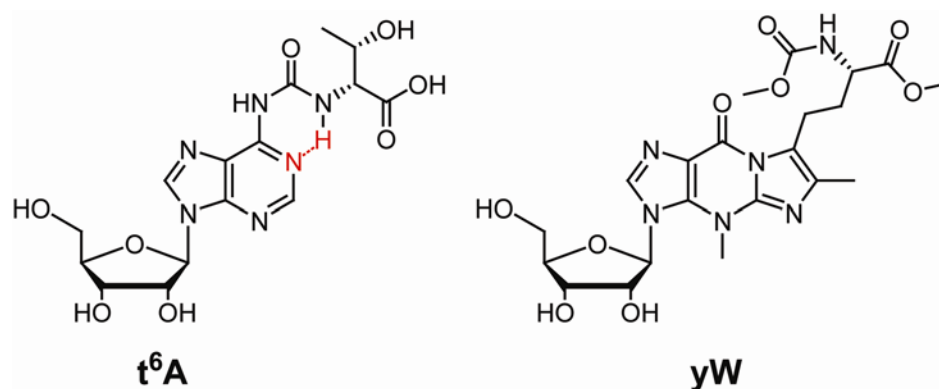


Figure 14: The modified nucleoside t^6A as the quasi-tricyclic nucleoside with the hydrogen bond between N1 and the ureido amino group (red) and the tricyclic nucleoside yW .

3.4.2.2 Codon-anticodon interaction

Codon-anticodon interaction properties of modifications were determined with specifically programmed 30S ribosomal subunit containing the appropriate mRNA. In these studies the binding abilities of unmodified, partially modified, and totally modified ASLs were compared. The importance of the 2'-hydroxyl groups in the anticodon was shown in contrast to DNA derivatives.^[47] Afterwards chemical incorporation^[47] of modified nucleosides as phosphoramidites enabled more detailed investigations.^[38, 42, 44, 46, 48-50] Binding abilities to programmed ribosomes were investigated for different unmodified ASL sequences, which naturally contain various modifications. Only 5 of in total 21 unmodified ASL sequences could bind strongly to the cognate anticodon in the peptidyl tRNA binding site (P site).^[51] Dissociation rates determined for eight modified and unmodified tRNAs from *E. coli* in the P site as well as the aminoacyl tRNA binding site (A site), also revealed the high impact that these modifications have. Unmodified tRNAs are dissociating faster compared to the fully modified tRNAs with either m^2A , ms^2i^6A or t^6A at position 37.^[52]

The ASL of *Escherichia coli* (*E. coli*) tRNA^{Lys} with the anticodon UUU contains t^6A at position 37 and is very similar to the human tRNAs^{Lys1,2,3}. Binding studies with poly-A programmed ribosomes revealed that this ASL, containing only t^6A has very similar binding affinities than the native *E. coli* tRNA^{Lys}, whereas the unmodified ASLs were only binding weakly to the ribosome.^[37, 51, 53] The fully modified ASL, which additionally contains the wobble modification mm^5s^2U , has the same binding affinity to the ribosome as the mature tRNA. In addition, it showed a significant enhanced binding ability to the wobble codon AAG. Thus, ASLs can be used as minimal mimics of a tRNA structure for the investigations of the modification properties. Interestingly, a further study with the ASLs from yeast

tRNA^{Phe} showed the importance of the modification m¹G, which is present at position 37 in this tRNA.^[36] In contrast to t⁶A, the completely unmodified ASL was still binding to the ribosome with an affinity of up to two-thirds relative to the mature tRNA. However, modified ASLs require incorporated m¹G, because modifications in the stem or at the wobble position without m¹G resulted in drastically reduced binding affinities. Thus m¹G has a stabilizing effect on the codon-anticodon interaction.

3.4.2.3 Frameshift prevention and translocation

About 20 to 40 peptide bonds are formed in one second and discrimination between cognate, near-matched and non-cognate tRNAs in the A site is the major factor for correct translation. Nevertheless, errors occur at a frequency of 10⁻³ to 10⁻⁴.^[9, 54] The charged tRNA in the P site can slip by one nucleotide before the next cognate tRNA binds to the A site or after the complex translocation process, when the tRNA loaded with the peptide chain is transferred from the A site to the P site. Frameshift events can either occur as +1 frameshift, with addition of one nucleotide or as -1 frameshift with deletion of 1 nucleotide. A defective cognate or non-cognate tRNA can more easily cause frameshift (*Figure 15*).^[55-56] These frameshifts lead to truncated and malfunctioning proteins, while missense errors would in contrast only cause minor activity loss of proteins.

Investigations clearly prove that modifications 3'-adjacent to the anticodon are improving frame maintenance and translocation. Furthermore, it was postulated that the main biological Darwinian force for the development of new modifications for position 37 and/or the wobble position is frame maintenance, contributing to uniform ribosomal binding to all tRNAs.^[57]

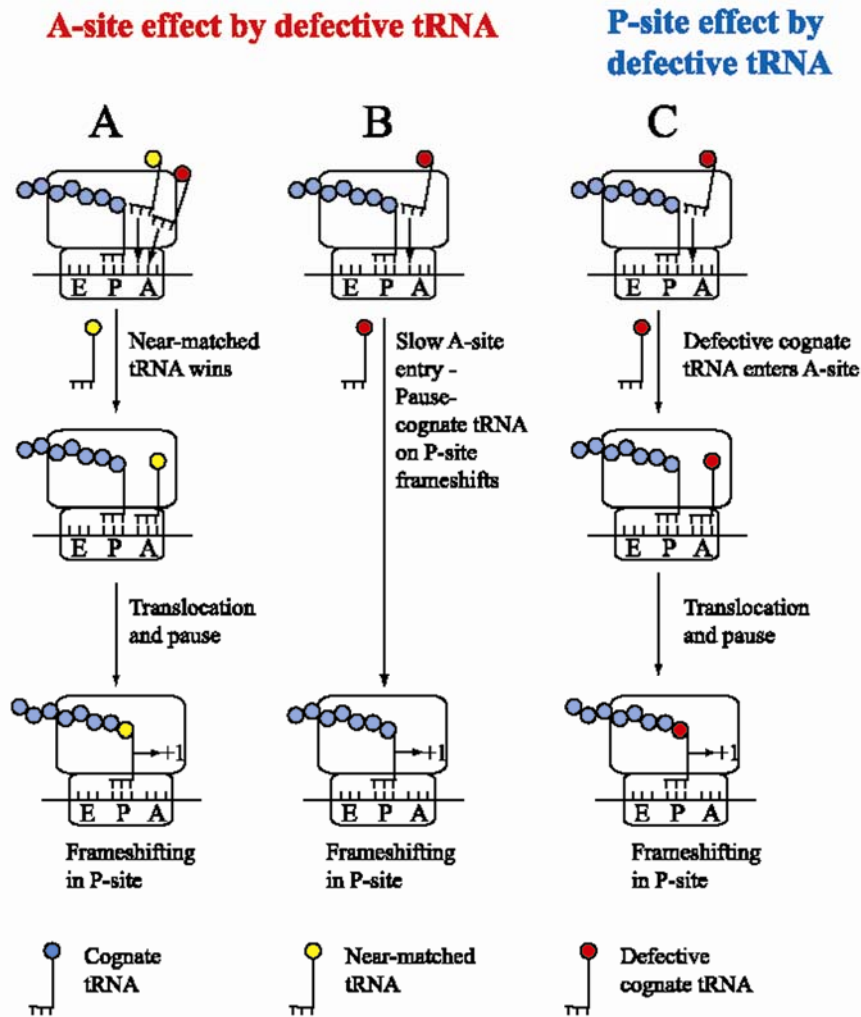


Figure 15: Three possible situations in which frameshift events are possible. A) Frameshift in the case of a near-matched tRNA. B) Frameshift in the case of a cognate tRNA. C) Frameshift in the case of a defective cognate tRNA.^[56]

Influence of modified nucleosides in frameshift prevention was shown for the first time in a mutant of *Salmonella typhimurium*, which lacks the methyltransferase modifying G to m¹G by the group of Björk in 1989.^[58] It was shown that the methyl group in position 1 of guanosine inhibits base pairing with C as well as prevents +1 frameshifts but not -1 frameshifts.^[57, 59-60] This modification is present in all three domains of life and was suggested to be an early modification in the development of life, because of sequence similarities of the modifying enzyme *trmD* throughout. It was also argued that this modification evolved in an early stage of translation improvement to obtain long chain peptides, since its absence leads to impaired growth rates in prokaryotes and eukaryotes.^[61] In addition, the isopentyl modifications (ms²)i(o)⁶A also prevent +1 frameshifts. Mutants lacking either the 2-methylthio moiety (i⁶A or io⁶A) or are unmodified (A) showed significant increased frameshift rates by up to 8 fold compared to the natural modified tRNA (ms²i(o)⁶A). Moreover, wobble modifications and

yW-derivatives in rabbit liver tRNA also prevent frameshift events.^[62] These observation can be explained by the fact that the +1 frameshift is sensitive to the rate of codon recognition in the empty A site because of slow selection or low concentration of cognate tRNA. In contrast, -1 frameshift can only occur by slippage of the strongly bound deacylated tRNAs in the E site as well as the peptidyl-tRNA.^[60]

Moreover it was shown that tRNA modifications of tRNA^{Val} and tRNA^{Lys} are important for the translocation. In tRNA^{Val} the modification m⁶A and the wobble modifications are only important for translocation of wobble codons, whereas it is not influencing cognate codons. In contrast, both modifications t⁶A₃₇ and mnmU₃₄ are necessary for correct translocation in tRNA^{Lys}, whereas tRNAs lacking modifications were unable to translocate at all. Interestingly, the modifications in tRNA^{Phe} are not important for this step. Thus modifications are important depending on the nature of the tRNA and if the codon is a wobble or a cognate codon.^[52, 63]

3.4.2.4 Aminoacylation

To date numerous examples are known where the tRNA modification strongly influences correct aminoacylation and mischarging. Aminoacylation of the cognate tRNA is of tremendous importance for correct protein synthesis.

For instance, the arginyl-tRNA synthetase additionally attaches Arg to the wrong yeast tRNA^{Asp} with a factor of 300-500 times when the modification m¹G at position 37 is unmodified.^[64-65] Correct aminoacylation in *E. coli* tRNA^{Ile} depends on the wobble modification lysidine (k²C). If this modification is lacking, the tRNA is charged with reduced activity by IleRS and is in addition mischarged with methionine by MetRS.^[66] These tRNAs have similar codons AUA (Ile) and AUG (Met) and can specifically be differentiated only by the presence or absence of the modification k²C.^[67] Thus, single modification exchange can completely convert the identity of a whole tRNA.^[68-69]

In addition, the specific lysinyl-tRNA synthetase (lysRS) of *E. coli* tRNA^{Lys} is unable to charge the unmodified tRNA lacking t⁶A.^[52] Also less efficient *in vivo* aminoacylation rates were found with tRNAs lacking ms²io⁶A in *S. typhimurium*. Higher influence on aminoacylation was detected for mutants without the isopentyl moiety compared to those lacking the 2-methylthio group.^[70] The activity of *E. coli* glutamyl-tRNA synthetase also requires m²A at position 37 as well as the wobble modification mnm⁵s²U.^[71] Furthermore,

modification present in the anticodon loop result in significantly decreased lysine-incorporation rates. Important to note is the fact, that the rates were diverse influenced depending on the modification position.^[72]

The reasons behind all these observations can be obtained from crystal structures providing insights into the interaction of aminoacyl-tRNA synthetases with the anticodon.^[73-75] In the crystal structure of methionyl-tRNA synthetase (MetRS) from *Aquifex aeolicus* in complex with the unmodified tRNA^{Met} shows the interaction with the inside of the tRNA L-shape and a distorted anticodon loop. Nevertheless, the enzyme binds to positions A38, A35, and C34, while bases U36 and A37 are pointing in the opposite direction resulting in a conformational change of the whole anticodon loop.^[72] Comparison with IleRS-tRNA^{Ile} and ValRS-tRNA^{Val} complexes by superposition revealed that they provide hydrophobic pockets for interaction with positions 37 as well as 34 and 38.^[74-75] Therefore, all anticodon loop nucleotides are important for recognition and correct aminoacylation.

3.4.2.5 Diseases

Some tRNA modifications present in the anticodon are associated with diseases. For example, the modifications ms²i⁶A and queuosine (Q) present in tRNA of *S. flexneri* are important for the expression of the virulence factor *VirF*, which is incorrectly expressed in mutants lacking the corresponding modifying enzymes. Mutants lacking *MiaA*, the enzyme for the first biosynthetic step of ms²i⁶A, have reduced expression rates with constant mRNA levels of the virulence factor.^[76-77]

The anticodon loop of human tRNA^{Lys3} is a primer of the human immunodeficiency virus type 1 (HIV-1). The complex with the specific viral reverse transcriptase and the viral genome is only possible with the presence of the modifications ms²t⁶A₃₇ and mcm⁵s²U₃₄ in the anticodon loop. Unmodified or partly modified tRNAs show reduced binding constants.^[78-79]

In addition, the two taurine-containing wobble modifications 5-taurinomethyluridine (τ m⁵U) and 5-taurinomethyl-2-thiouridine (τ m⁵s²U) are absent in cells with the mitochondrial diseases myopathy, encephalopathy, lactic acidosis, and stroke-like episodes (MELAS) and myoclonus epilepsy associated with ragged red fibers (MERRF).^[80-83] Lack of both modifications results in mitochondrial dysfunction due to a deficient translational systems.

3.5 *Summary*

The diversity and important regulatory functions of tRNA modifications in the anticodon loop at position 37 indicate the evolutionary specialization. Unique tRNA anticodon loop properties are obtained by this diversity to enable translation with high accuracy. These results show the importance of every modification present in the anticodon stemloop as essential recognition elements for correct binding to the codon. Especially, modifications at the position 37 are responsible for accuracy of the translational process by decreasing the dipeptide synthesis rate and increasing the rejection rate of noncognate codons.^[84] It was proposed that modified nucleosides at position 37 developed by evolutionary pressure to maintain accurate translation.^[51] Absence of modifications causes frameshift and aminoacylation errors, inefficient translation and is even associated with diseases.

So far structure-function relationship studies were mainly investigated on the single tRNA modification level or of modifications as part of a whole tRNA molecule. Tissues and species specific analysis of the whole tRNA modification pattern can provide penetrating insights into the regulation of organisms, which probably results in the observation of new biological functions as well as new disease correlations.

4. Aims of the Project

Modified RNA nucleosides are of high diversity in structure and to date more than 120 different modifications are known.^[3-5, 35] Databases are available by now, where modifications have been collected and classified according to type of modification as well as their occurrence in each domain of life and even in different organisms. Modified tRNA nucleosides are the most investigated RNA type and have the largest variety with up to 90 different modifications known today. Up to now quantification of these modifications was performed with radioactive labeled 2D TLC analysis and by UV peak integration of HPLC chromatograms.^[85-94] The results from these studies showed that the abundance as well as the modification levels for some hypermodified tRNA nucleosides vary depending on the tissue and that some alterations of modified levels are associated with diseases.^[78-83, 95]

In the era of *omics* research the central scientific approach is the study of broad biological systems as a whole, putting individual components in context to each other. The main *omics* areas described so far are *genomics*, *metabolomics*, *proteomics*, and *transcriptomics*.^[96-101] Since the development of mass spectrometers with improved sensitivity, most of these areas are using mass spectrometric (MS) based methods. For example, *proteomics* research which has rapidly developed in the last decades analyzes bulk protein mixtures *via* nano-liquid chromatography-tandem MS (nano-LC-MS/MS). *Metabolomics* is also using HPLC-MS based methods for the analysis of more than 100 compounds in parallel.^[102-103]

Stable isotope-labeling with amino acids in cell culture (SILAC) or isotope-coded affinity tagging (ICAT) are two proteomic methods in which heavy atom labels are inserted either *via* the cell culture medium or by selective reaction of a linker with a reactive group of the analyte, respectively.^[104-106] These methods use heavy atom labeled samples, which are measured in parallel as an internal reference in order to enable comparative analysis of protein expression levels. Furthermore previous reports have shown applicability of this method for quantification of two uridine modifications and DNA modifications.^[107-110]

HPLC-ESI-MS, which involves chromatographic separation and mass spectrometric analysis, is a perfect tool for the parallel quantification of tRNA modifications. First of all this combined method is advantageous to quantify compound amounts by UV-peak integration of HPLC chromatograms, because of higher sensitivity without background interference. In

addition, the natural nucleosides from isolated tRNAs and the corresponding added isotope-labeled reference molecules can be distinguished by their different molecular weights.

The aim of this thesis was to develop and optimize a method for the parallel quantification of in principle all modified tRNA nucleosides in different cell types as depicted in *Figure 16*. For successful establishment each of the subdivided steps had to be optimized:

- 1) Synthesis of isotope-labeled internal standard nucleosides
- 2) Isolation and purification of tRNA
- 3) Enzymatic digestion of bulk tRNA with spiking of isotope-labeled nucleosides
- 4) HPLC-ESI-MS-analysis
- 5) Analysis of data

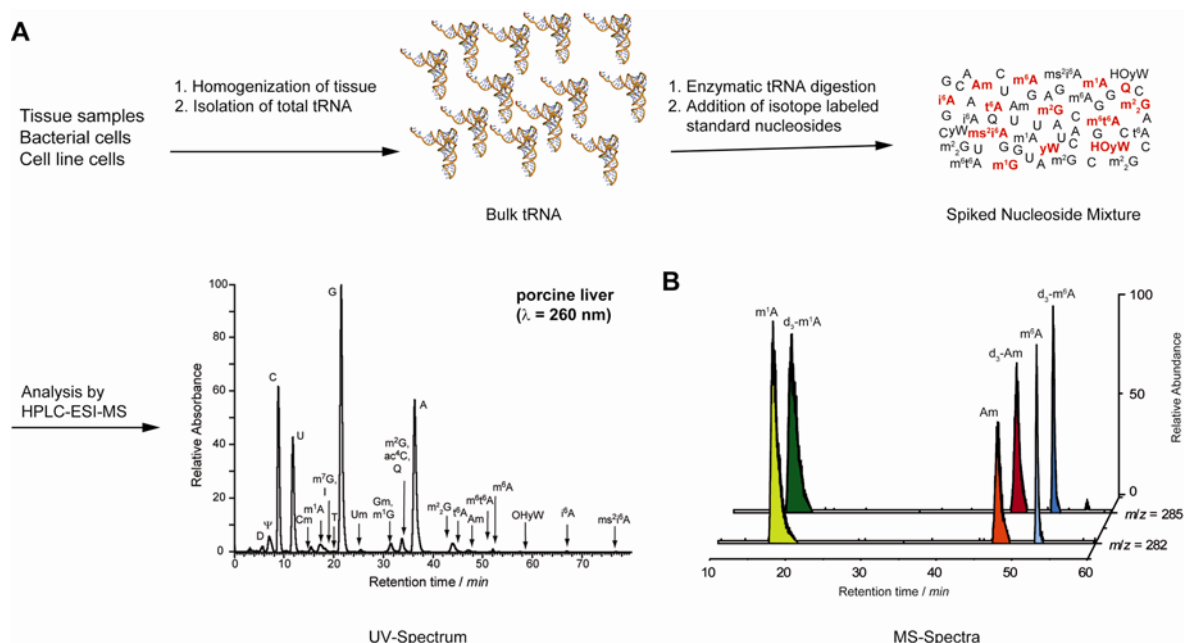


Figure 16: Workflow of the LC-MS quantification method for tRNA nucleosides. A) The process starts with isolation and purification of bulk tRNA out of any cell type followed by enzymatic digestion of tRNA. Then isotope-labeled nucleosides were added and the samples were subsequently analyzed with HPLC-ESI-MS. B) Representative depiction of the specific ion currents of monomethylated adenosine derivatives in parallel (front signals) and their corresponding isotope-labeled derivatives (back signals).

With the optimized HPLC-MS based quantification method analysis of tRNA modifications was envisioned in order to gain deeper insights regarding their tissue specificity, phylogenetic relationship as well as their association with diseases. Due to the presence in every organism and high importance for life of every organism this thesis work should contribute to extend the *omics* research with analysis of natural modified nucleosides.

During this thesis work the DNA modification 5-hydroxymethylcytosine (hmC) was detected in mammalian tissue for the first time in 2009.^[20-21] Thus, the second aim of this thesis was to extend our method to enable quantification of the DNA modifications hmC and 5-methylcytosine (mC). Analysis of these modifications in the whole mammalian body was envisioned to enable gaining deeper insight into presence and function of hmC in correlation to mC.

The quantification method for DNA nucleosides includes the following steps (*Figure 17*):

- 1) Preparation of tissue samples and extraction of genomic DNA
- 2) Enzymatic digestion of bulk DNA with spiking of isotope-labeled nucleosides
- 3) HPLC-ESI-MS-analysis
- 4) Analysis of data

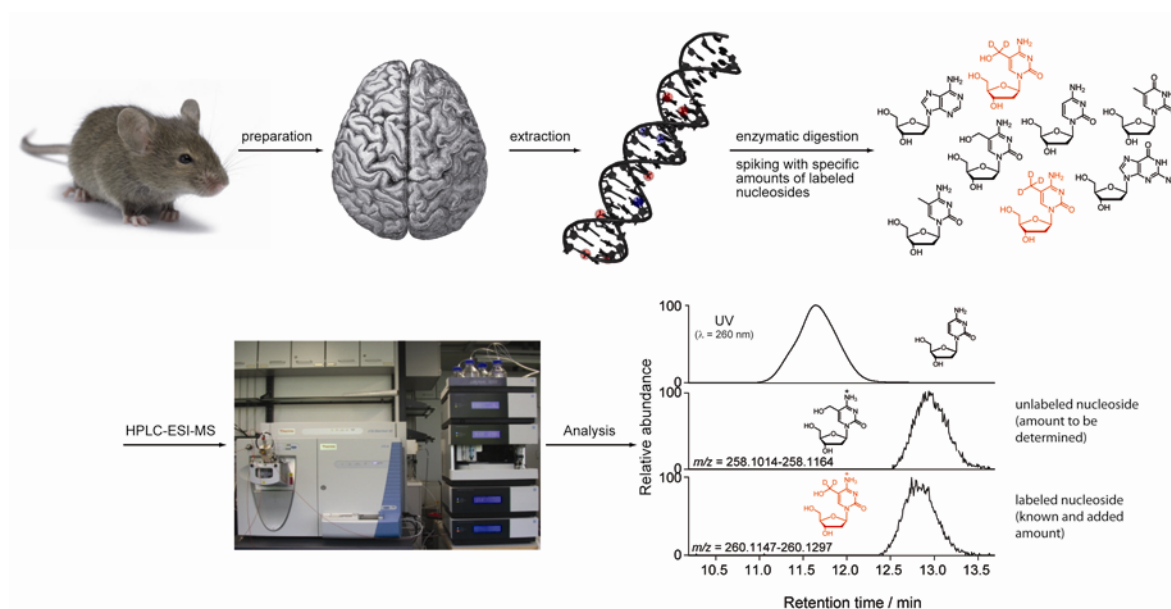


Figure 17: Workflow of the LC-MS quantification method for the two DNA nucleosides hmC and mC. After preparation of mouse tissue samples, the genomic DNA was extracted and subsequently digested to the nucleosides. After spiking with the isotope-labeled derivatives of hmC and mC the samples were analyzed via HPLC-ESI-MS.

5. Synthesis of modified tRNA nucleosides

Synthesis of modified nucleosides is fundamental for our method, because every present tRNA nucleoside can be quantified as long as isotope-labeled reference molecules are available. The different chromatographic and ionization properties of each modified nucleoside require a specific reference molecule for each investigated nucleoside. Isotope-labeled derivatives of the natural molecules are the best choice to enable precise quantification. A similar method allowed to quantify dihydrouridine (D) in relation to uridine in *E. coli* tRNA and 23S rRNA.^[110]

The most common nucleosides present in tRNA of bacteria and eukaryotes were synthesized as isotope-labeled derivatives. An efficient synthetic route is of high importance to insert isotope-labels due to limited commercial availability of labeled reagents. We took care that the synthesized isotope-labeled nucleosides have at least three *Da* difference to avoid contamination of natural ¹³C isotopes in the extracted tRNA nucleosides. The natural occurring nucleosides were synthesized as well, which we used for measuring calibration curves and assignments of modifications.

The nucleosides synthesized in this Ph.D. thesis are modified adenosines and mainly belong to two modification classes. The first class includes nucleosides of the carbamoyl family and the second class contains different methylated adenosine derivatives. Half of these modifications are present at position 37 of different decoding tRNAs and thus directly involved in codon-anticodon interaction.^[7] The other modifications are present all over the tRNA except the anticodon stem-loop and mainly stabilize the 3D structure.^[7-8] Therefore, a broad variety of adenosine modifications with diverse functions were synthesized. The syntheses of the modified nucleosides as well as their isotope-labeled derivatives are described after a short summary of their first detection in organisms and known biosynthetic pathways.

5.1 *The t⁶A carbamoyl family*

A very important group of modified nucleosides are *N*⁶-threonylcarbamoyladenine (*t*⁶A) and its derivatives, which are exclusively present in tRNA at position 37. Together with *N*¹-methylguanosine (*m*¹G) they are the only modified nucleoside present at position 37 in all three domains of life.^[3-7, 49] The main member *t*⁶A contains a L-threonine moiety attached to

adenosine *via* a carbonyl group at position 6. Additional methylation at this position occurs in some tRNAs to obtain the modified nucleoside m^6t^6A . Two further modifications contain glycine and hydroxynorvaline instead of threonine in g^6A and hn^6A , respectively (Figure 18). Furthermore, a methylthio moiety attached to the purine at position 2 was detected in the two modified nucleosides ms^2t^6A and ms^2hn^6A .

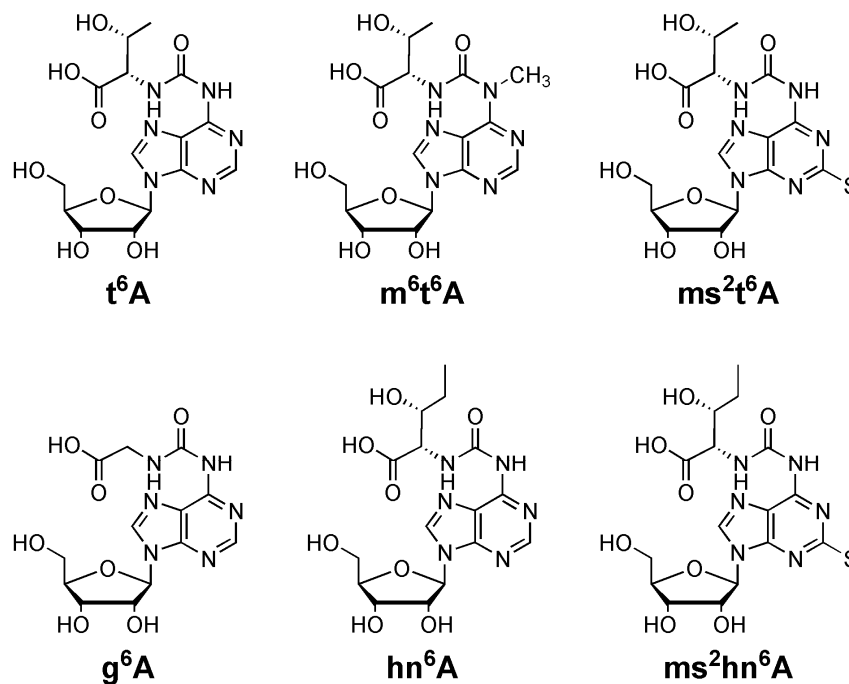


Figure 18: The modified tRNA nucleoside t^6A and its derivatives m^6t^6A , ms^2t^6A , g^6A , hn^6A , and ms^2hn^6A .

These hypermodified nucleosides are located in the anticodon loop 3'-adjacent to the anticodon of tRNAs reading ANN codons (N is standing for any of the canonical nucleosides A, C, G, or U). The nucleoside t^6A was first isolated and characterized from *E. coli*, yeast, and calf liver tRNA in 1969.^[111-112] It is the main representative of this modification class and is also present in archaeal organisms.^[90, 92] Recently, the protein family YrdC/Sua5 has been assigned as modifying enzymes for this modification.^[113] Studies towards the analysis of the biosynthetic pathway of t^6A formation elucidated an ATP-dependent process requiring L-threonine and bicarbonate. These biosynthetic studies were investigated with purified enzyme and t^6A -deficient tRNA.^[114-115]

The same enzyme also incorporates glycine in assays lacking threonine.^[114] This observation could probably explain the detection of the modification g^6A in traces from isolated tRNAs in yeast, which has only been reported once.^[116]

The methylated modification m^6t^6A was first detected in *E. coli* in 1972 and in wheat embryo tRNA^{Thr}_{GGU} two years later.^[117] Although the modifying enzyme has not been identified or isolated yet, biosynthetic studies proved that the methyl group is inserted after t^6A formation via the cofactor *S*-adenosylmethionine (SAM).^[118] In this study, the gene *tsaA* was assigned to encode the m^6t^6A specific methyltransferase, which is only methylating t^6A in absence of a cytidine in position 32. This hints for a proofreading of the methyltransferase in regard to C₃₂.^[119]

The modification ms^2t^6A is also present at position 37 and was first identified in mouse liver tRNA in 1979.^[120-121] It is furthermore part of bacterial and eukaryotic tRNA and the modifying enzyme responsible for insertion of the 2-methylthio moiety by further modification of t^6A has recently been described.^[122]

To complete the list of modified t^6A derivatives hn^6A and ms^2hn^6A were isolated from thermophilic bacteria and archaea in 1992. No biosynthetic studies have been published for the synthesis of hn^6A . It is speculated that the enzyme, which inserts the 2-methylthio group in ms^2t^6A catalyzes the last biosynthetic step for biosynthesis of ms^2hn^6A .^[122]

5.2 Methylated adenosine modifications

Methylation of nucleosides is one of the simplest modifications and occurs in a large variety of RNA species. Monomethylation of adenosine occurs at four different positions at the base and at the 2'-*O* position of the sugar. The monomethylated adenosine modifications 1-methyladenosine (m^1A), 2-methyladenosine (m^2A), N^6 -methyladenosine (m^6A), 8-methyladenosine (m^8A), 2'-*O*-methyladenosine (Am), and the important dimethylated nucleoside N^6,N^6 -dimethyladenosine (m^6_2A) are depicted in *Figure 19*. The first isolation of the methylated adenosine derivatives m^2A , m^6A , and m^6_2A from total RNA of *E. coli*, *Aerobacterium aerogenes* and yeast was reported in 1958.^[123-124] Until today progress in purification and analytical tools led to detection of more methylated nucleosides and their assignment to specific RNA species and domains.^[3-7] All modifying enzymes are methyltransferases requiring SAM as methyl donor.

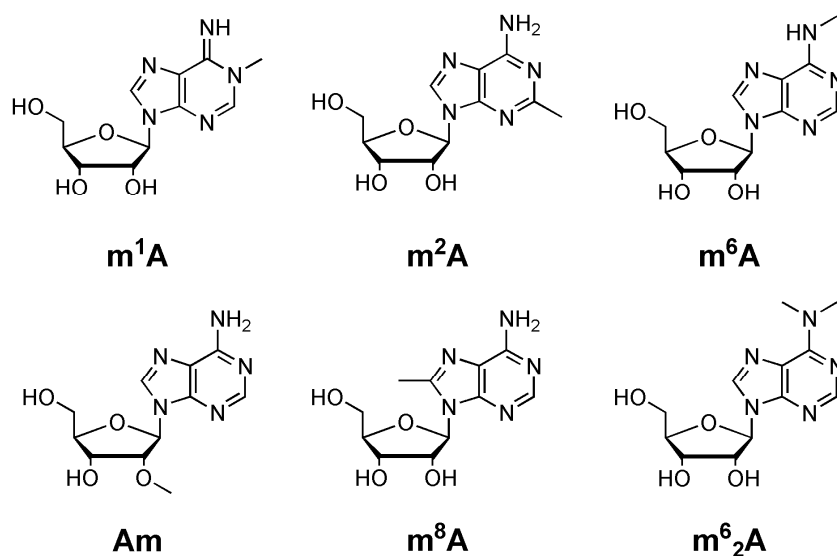


Figure 19: Overview of the monomethylated adenosine modifications 1-methyladenosine (m^1A), 2-methyladenosine (m^2A), N^6 -methyladenosine (m^6A), 8-methyladenosine (m^8A), 2'-*O*-methyladenosine (Am), and the dimethylated N^6,N^2 -dimethyladenosine (m^6_2A).

The base modification m^1A was first identified in 1961 as a RNA nucleoside. This modification is mainly present in tRNA of all three domains of life either at position 9 or in the T-loop at position 58.^[125-126] It was also found to be present in all three rRNA subunits of eukaryotes.^[127] Due to its charged betaine structure it possesses a special character and enables intramolecular binding to stabilize the 3D structure of the tRNA. The modification m^1A is e.g. present in 23 of the 34 tRNA sequences of *S. cerevisiae*.^[35] Recently, the bipartite structure of the tRNA m^1A_{58} methyltransferase from *S. cerevisiae* was found to be conserved in humans as well as the methyltransferase that catalyses the formation of m^1A at position 9 of archaeal tRNA.^[125, 128]

The nucleoside m^2A is only present in bacterial tRNA at position 37 and was isolated for the first time in 1958.^[124] The methyl group is attached to the purine base in a rarely occurring carbon-carbon bond for adenosine derivatives in tRNA.^[3]

Methylation at position 6 of adenosine is a widespread modification present in all three domains of life and was found to occur in tRNA, rRNA, mRNA, and small nuclear ribonucleic acid (snRNA). The assignment of this modification is problematic, because of the instability of the two modified nucleosides m^1A and m^6t^6A . Harsh basic and acidic conditions were applied in early protocols for isolation of nucleosides from different RNAs. Both nucleosides could decompose or rearrange to yield m^6A , which could lead to misinterpretation. Databases indicate m^6A as a modification present in tRNA and rRNA of archaea, prokaryotes, and eukaryotes, while it is exclusively present in mRNA and snRNA of

eukaryotic organisms. In tRNA it was found to be present at position 37 adjacent to the anticodon.^[5] The modification m⁶A represents the major modification present in mammalian mRNA but the function is still unknown, although it was found about 35 years ago. A recent study from 2010 claims that a role of m⁶A to promote splicing seems less likely, while a function in translational control or message recycling remains a possibility.^[129]

Methylation in the 2'-*O*-position of RNA nucleosides is largely abundant in all types of RNA (tRNA, mRNA, and rRNA) and mainly for all four canonical nucleosides. Methylation in the 2'-*O*-position of RNAs enhances the stability, but the biological role in tRNA is not clarified yet. Most commonly 2'-*O*-methylation is present in 7 different positions in eukaryotes and bacteria.^[35] Biosynthesis is either guided by a small nucleolar ribonucleoprotein (snoRNP) complex in rRNA and snRNA or by independently modifying methyltransferases in bacterial and eukaryotic tRNA.^[130] The adenosine methylation was detected in yeast tRNA^{His} placed at position 4, which is the only 2'-*O*-methylated position in a tRNA duplex region.^[130-131] Nevertheless, this modification is largely conserved in eukaryotes and also present in humans, which hints at a specific but unknown role. In other positions Am is deaminated to obtain the modification Im.

In 2009, the modification m⁸A was identified in rRNA of *E. coli* for the first time and already proven to be involved in resistance to antibiotics.^[132-133]

Two adjacent dimethylated nucleosides m⁶₂A occur in the highly conserved 3' end in nature of the small ribosomal subunit in all organisms with only few exceptions. Furthermore, it has been shown, that they are stabilizing the structure of ribosomal subunit complexes and that the methyl groups are stimulating the interaction between rRNA subunits and the initiation factor IF-3.^[134] Specific methyltransferases were identified in all three domains of life.^[135]

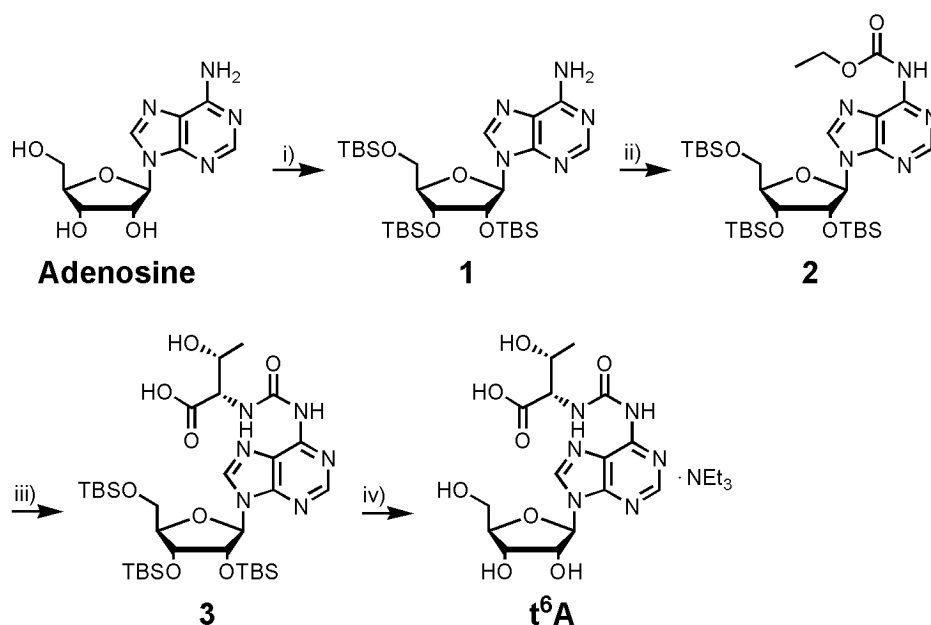
5.3 *N*⁶-Acetyladenosine

Recently, *N*⁶-acetyladenosine (ac⁶A) was detected as a novel tRNA nucleoside in the hyperthermophilic methanogen *Methanopyrus kandleri*.^[136] The only acetylated modifications detected before have been two cytidine compounds with the acetylation at position 4 (ac⁴C and ac⁴Cm). Therefore ac⁶A is the only acetylated purine known so far. It is assumed that this modification is a minimal analogue to t⁶A.^[136] However, the function, position or the biosynthesis of this new modification is still unknown.

5.4 Synthesis of modifications

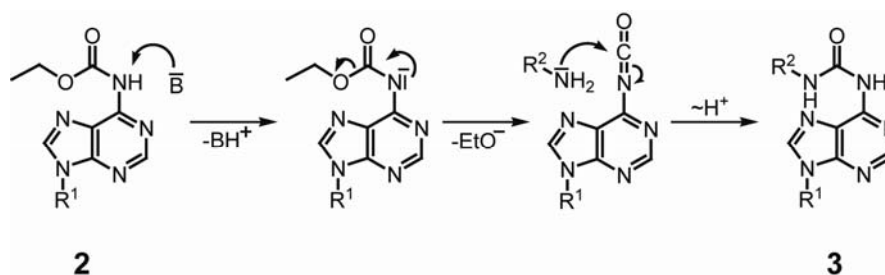
5.4.1 Synthesis of t⁶A

Several synthetic routes were reported for the synthesis of the nucleoside t⁶A.^[48, 50, 137] A straightforward synthetic route was selected for the synthesis according to literature procedures (*Scheme 1*). In contrast to previous syntheses the alcohols were protected as TBS-ethers instead of acetylation.^[138] Acetylation was avoided due to the use of compound **1** as intermediate in the synthesis of further nucleosides described in this chapter, which are instable under basic conditions. This intermediate was functionalized to a carbamate using ethylchloroformate as the electrophile, which introduced the carbonyl function together with ethanolate as leaving group for subsequent substitution.



Scheme 1: Synthesis of the nucleoside t⁶A. i) TBSCl, imidazole, DMF, rt, 19 h, 81%; ii) ethylchloroformate, pyridine, 0 °C to rt, 5 h, 72%; iii) L-threonine, pyridine, 125 °C, 8.5 h, 80%; iv) NEt₃·3HF, CH₂Cl₂, rt, 20 h, 65%.

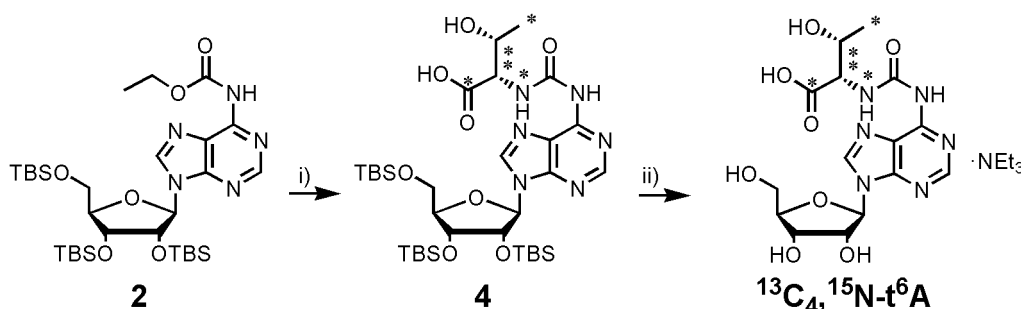
Precursor **2** was treated with L-threonine to yield the sugar protected t⁶A (**3**). The base catalyzed mechanism starts with deprotonation of the acidic proton at the exocyclic amine with subsequent loss of ethanolate. The isocyanate intermediate is attacked by the amine of L-threonine to form the product after final proton transfer (*Scheme 2*). Deprotection with NEt₃·3HF cleaved the TBS groups to obtain final product t⁶A after purification *via* HPLC (*Scheme 1*).



Scheme 2: Mechanism of the base catalyzed conversion of the carbamate **2** to the urea derivative **3**. R^1 = TBS protected ribose, R^2 = L-threonine residue.

5.4.2 Synthesis of isotope-labeled t^6A

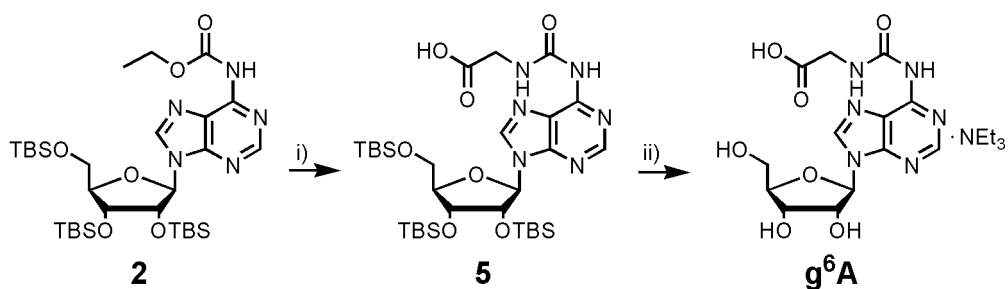
The same route for the synthesis of t^6A was chosen to insert the heavy atom label (*Scheme 3*). Commercially available $^{13}C_4,^{15}N$ -L-threonine was used to react with carbamate **2** to yield the sugar protected heavy atom labeled t^6A (**4**). Deprotection with $NEt_3 \cdot 3HF$ resulted in the isotope-labeled compound $^{13}C_4,^{15}N$ - t^6A .



Scheme 3: Synthesis of the heavy atom labeled derivative of t^6A . i) $^{13}C_4,^{15}N$ -L-threonine, pyridine, 125 °C, 6.5 h; ii) $NEt_3 \cdot 3HF$, CH_2Cl_2 , rt, 72 h, 45% (over two steps).

5.4.3 Synthesis of g^6A

Synthesis of the modified nucleoside g^6A was performed using the same strategy as for t^6A .^[137] Advanced intermediate **2** was treated with glycine to achieve compound **5**, followed by deprotection of the TBS groups to obtain the modified nucleoside g^6A (*Scheme 4*). The obtained product was utilized as reference compound after purification *via* HPLC.

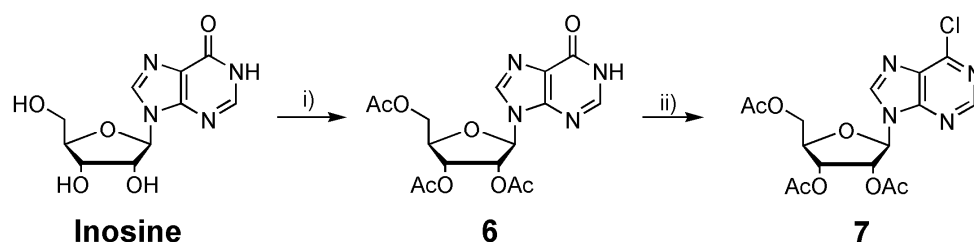


Scheme 4: Synthesis of nucleoside g^6A . i) glycine, pyridine, 125 °C, 6 h, 69%; ii) $NEt_3 \cdot 3HF$, CH_2Cl_2 , rt, 48 h, 6%.

A heavy atom labeled derivative of this modification was not synthesized, because we did not detect g^6A in any of the investigated tRNA samples. Glycine was only inserted into tRNA in assays with threonine depleted medium to form g^6A as described in literature.^[116] However, the synthetic procedure of the natural occurring modification enables rapid synthesis of a heavy atom labeled derivative by using for example $^{13}C_2$ -glycine, which could be used as internal standard in quantification experiments.

5.4.4 Synthesis of m^6A and m^6_2A

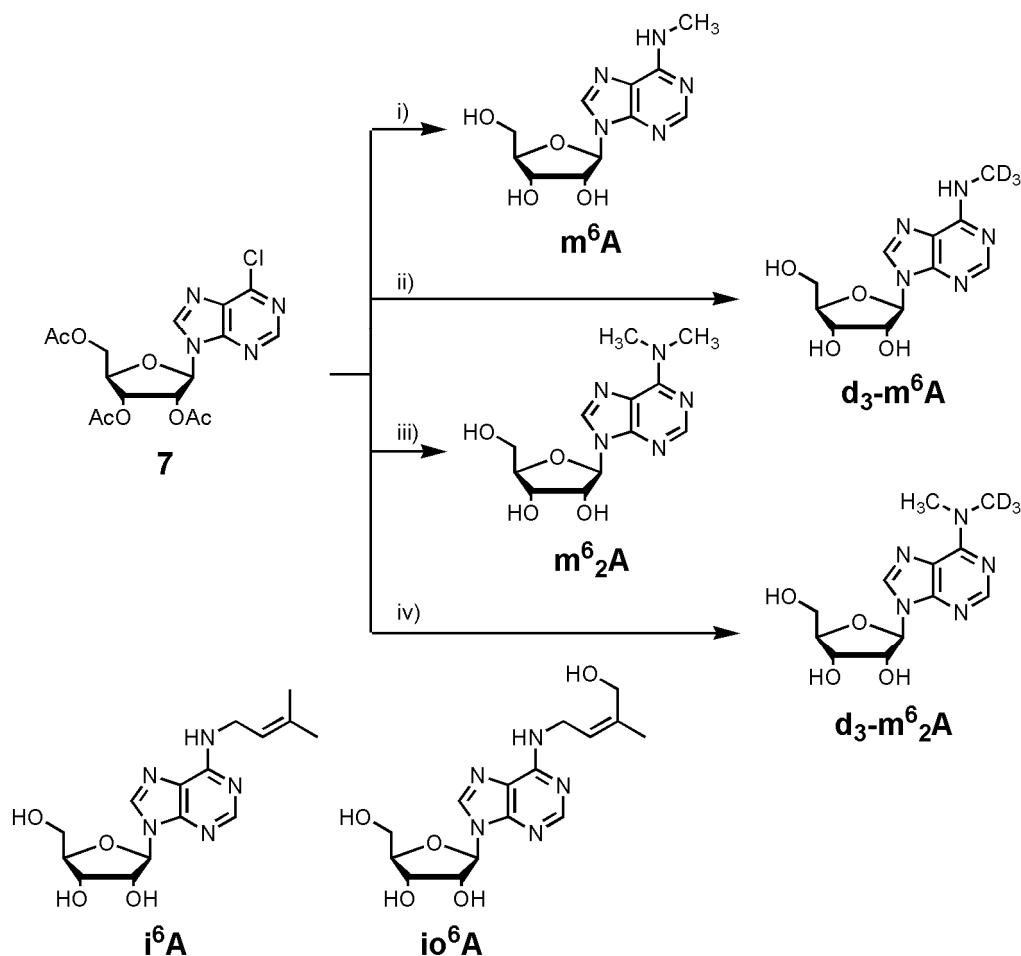
A divergent synthetic route was used for the synthesis of both derivatives m^6A and m^6_2A from only one precursor. After acetylation of the inosine alcohol groups (**6**) the carbonyl function at position 6 was converted into a chloro function to yield intermediate **7** using the *Vilsmeier* reagent *N*-chloromethylene-*N,N*-dimethylammoniumchloride^[139] (*Scheme 5*). This reagent allows better handling with precise amounts compared to other chlorinating reagents like $POCl_3$. It gave the product in excellent yields.^[139]



Scheme 5: Synthesis of the intermediate **7**. i) Ac_2O , pyridine, DMF, 75 °C, 0.5 h, 87%; ii) *Vilsmeier* reagent, CH_2Cl_2 , 40 °C, 24 h, 93%.

Precursor **7** was treated with different amines to synthesize the natural nucleosides m^6A , m^6_2A and their heavy atom labeled derivatives d_3-m^6A and $d_3-m^6_2A$, respectively. Additionally, it was used by Dr. T. Brückl to synthesize the isopentyl nucleosides i^6A , io^6A , and their isotope-labeled derivatives. Details for the synthetic procedures and analytical data are

described in his Ph.D. thesis.^[140] In total, precursor **7**, which is available in large quantities in two steps, allowed rapid and efficient synthesis of four nucleosides m^6A , m^6_2A , i^6A , and io^6A and of the four corresponding heavy atom labeled derivatives in a divergent route (*Scheme 6*).

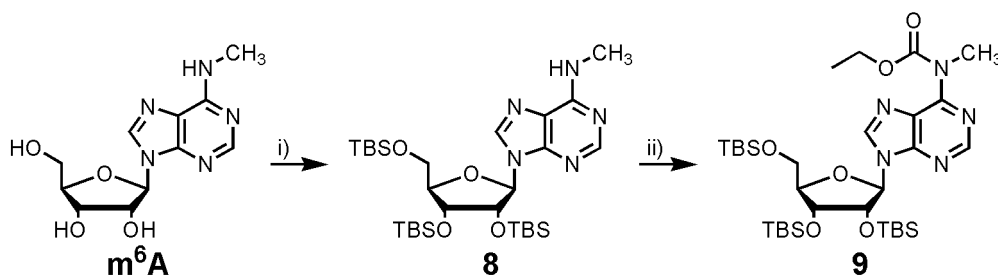


Scheme 6: Synthesis of the modified nucleosides m^6A , $d_3\text{-}m^6A$, m^6_2A , and $d_3\text{-}m^6_2A$. The two nucleosides i^6A and io^6A were also synthesized from intermediate **7**. i) MeNH_2 (33% in EtOH), EtOH, rt, 18 h, 93%; ii) $d_3\text{-MeNH}_2\text{-HCl}$, Ag_2O , EtOH, rt, 48 h, 22%; iii) Me_2NH (33% in EtOH), EtOH, rt, 26 h, 86%; iv) $d_3\text{-Me}_2\text{NH}$, NEt_3 , MeOH, 60 °C, 20 h, 80%.

5.4.5 Synthesis of m^6t^6A

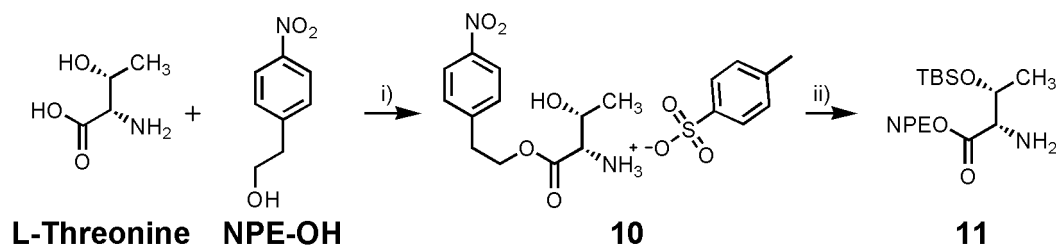
So far only one synthesis of m^6t^6A has been reported. The nucleoside m^6A was used as the intermediate and treated with the isocyanate of protected L-threonine. Attempts to methylate t^6A using methyl iodide under different conditions were not successful.^[141] Therefore, a route was utilized in this thesis by first introducing the methyl group and second attaching the threonine moiety. Nucleoside m^6A was first TBS-protected to yield compound **8**, which was treated with ethylchloroformate according to the synthetic strategy for t^6A (*Scheme 7*). Unfortunately, the reaction to compound **9** proceeded in very low yields and the subsequent substitution with L-threonine did not result in any product. The lower reactivity can be

explained by the methyl group at position 6 in comparison to good reactivity of compound **2** under the same conditions (*Scheme 1*). The isocyanate intermediate cannot be formed with the present methyl group in derivative **8** like in the base catalyzed mechanism for t^6A (*Scheme 2*). In this case the carbonyl group of the carbamate is attacked by L-threonine. No reaction was observed, because ethanolate is a bad leaving group in this reaction.



Scheme 7: First synthetic strategy towards synthesis of m^6t^6A . i) TBSCl, imidazole, DMF, rt, 18 h, 96%; ii) ethylchloroformate, pyridine, rt, 5 h, 22%.

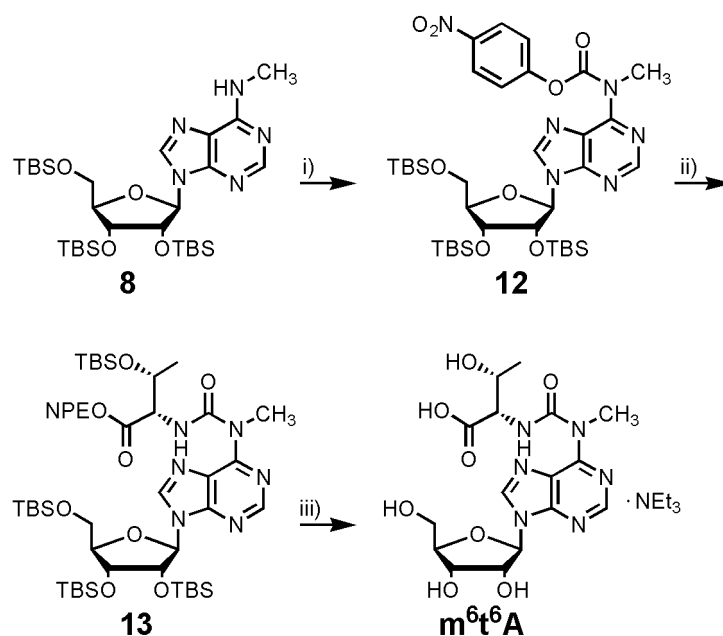
Therefore, the synthetic strategy was modified. (4-nitrophenyl)chloroformate was used as a more reactive chloroformate instead of the ethyl derivative, which additionally contains a better leaving group for substitution with L-threonine. A second difference was the protection of L-threonine, which was performed according to a literature procedure for the synthesis of t^6A .^[48] The carboxyl group was first protected in an esterification with 2-(4-nitrophenyl)ethanol (NPE-OH) to obtain the salt **10**, followed by protection of the alcohol with TBSCl to retain the free amine in **11** (*Scheme 8*). Protection of carboxylic acids with the NPE group is a commonly used in peptide chemistry, which retains stereochemistry in the deprotection step by β -elimination with a non-nucleophilic base.^[48]



Scheme 8: Protection of L-threonine. i) *p*-toluenesulfonic acid, toluene, 150 °C, 12 h, 92%; ii) TBSCl, imidazole, pyridine, rt, 18 h, 76%.

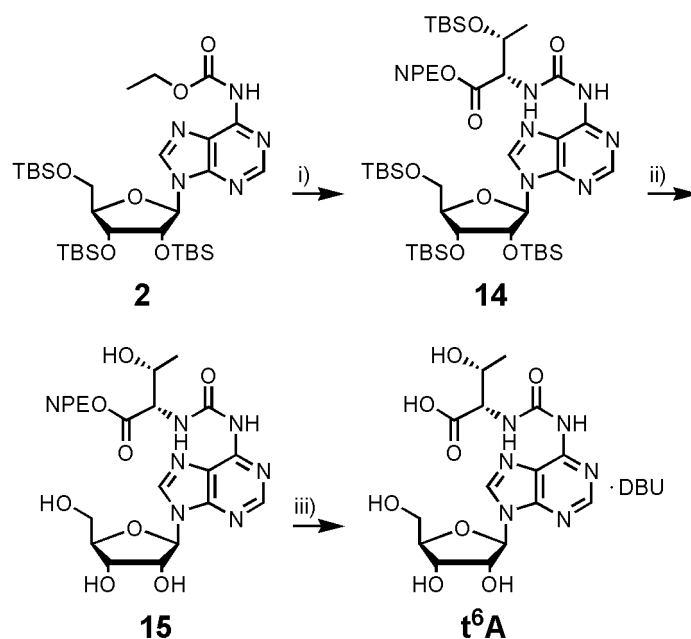
Precursor **8** reacted almost quantitatively with the electrophile (4-nitrophenyl)chloroformate. Subsequently, intermediate **12** was treated with the protected L-threonine **11** to obtain the fully protected nucleoside m^6t^6A (**13**) in good yields (*Scheme 9*). The reaction had to be carried out at rt, because we observed degradation of m^6t^6A to m^6A during heating. It is of

importance to note that also the unprotected L-threonine was used to react with **12**, but did not yield any product. After the two deprotection steps to cleave the TBS groups with $\text{NEt}_3 \cdot 3\text{HF}$ and the NPE group using DBU as a non-nucleophilic base and purification *via* HPLC the final product $\text{m}^6\text{t}^6\text{A}$ was obtained with NEt_3 as counterion due to the HPLC buffer.



Scheme 9: Synthesis of nucleoside $\text{m}^6\text{t}^6\text{A}$. i) (4-nitrophenyl)chloroformate, pyridine, 50 °C, 3 h, 80%; ii) **11**, pyridine, rt, 18 h, 84%; iii) a) $\text{NEt}_3 \cdot 3\text{HF}$, CH_2Cl_2 , rt, 24 h, 98%; b) DBU, THF, 40 °C, 3 h, 80%.

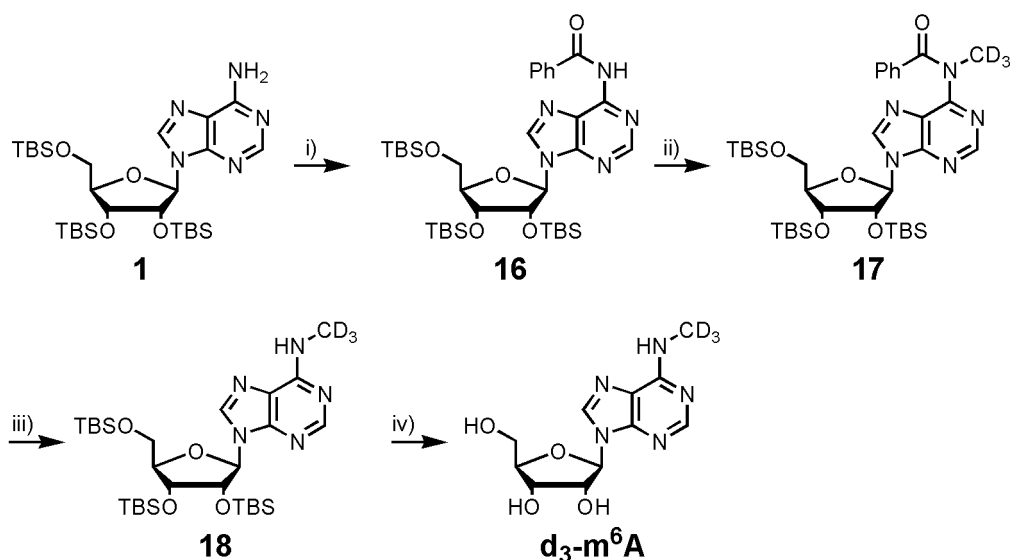
This protected amino acid **11** was also used in a second route for synthesis of nucleoside t^6A (*Scheme 10*).^[48] Intermediate **2** was treated with compound **11** to obtain the t^6A derivative **14**. The TBS groups of this compound were deprotected with $\text{NEt}_3 \cdot 3\text{HF}$ to give the carboxylic acid protected intermediate **15** in almost quantitative yield. Interestingly, this fluoride source is the only applicable reagent for deprotection of this compound and was used for all other derivatives as well. The glycosidic bond was at least partially cleaved under treatment with TBAF or $\text{py} \cdot \text{HF}$. Final deprotection of **15** with the non-nucleophilic base 1,8-diazabicyclo[5.4.0]undec-7-en (DBU) yielded t^6A in a second route (*Scheme 10*).



Scheme 10: Alternative synthesis of the modified nucleoside t^6A . i) **11**, pyridine, 125 °C, 7 h, 91%; ii) $NEt_3 \cdot 3HF$, CH_2Cl_2 , rt, 96 h, 98%; iii) DBU, THF, 40 °C, 1 h, 56%.

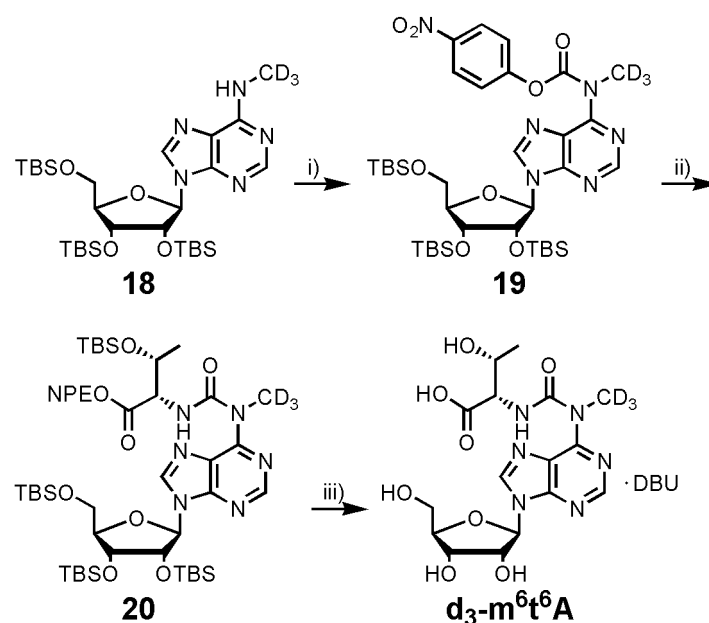
5.4.6 Synthesis of isotope-labeled m^6t^6A

Introduction of a deuterated methyl group in position 6 was chosen for introduction of an isotope-label in m^6t^6A . The intermediate d_3-m^6A had to be available in high quantities, which would be hardly realizable by the described synthesis with only 22% in the last step (*Scheme 5*). Therefore, a new synthetic strategy was chosen to obtain this intermediate in better yields. The synthesis started with TBS-protected adenosine **1**, which was treated with benzoyl chloride to obtain compound **16** in a yield of 67% (*Scheme 11*) with dibenzoylated compound as unavoidable byproduct. Afterwards the key step in this procedure was performed by inserting the deuterated methyl group with the phase transfer catalyst NBu_4Br at position 6 to yield **17** due to short reaction times.^[142] This compound was deprotected with methylamine to cleave the benzoyl group to give the sugar protected d_3-m^6A **18**. This is an intermediate in the synthesis of $d_3-m^6t^6A$ and enables a more efficient synthesis of this compound compared to the synthesis in *Scheme 5*. Additionally, compound **18** was deprotected with $NEt_3 \cdot 3HF$ to obtain d_3-m^6A in a second route. This reaction sequence was also performed with CH_3I to yield m^6A in a second route with similar yields. Synthesis is described in the Experimental Section (Chapter 5.4.6).



Scheme 11: Synthesis of TBS protected $d_3\text{-m}^6\text{A}$. i) benzoylchloride, pyridine, $-5\text{ }^\circ\text{C}$ to rt, 2 h, 67%; ii) d_3 -methyl iodide, $n\text{Bu}_4\text{NBr}$, 1M NaOH, rt, 3 h, 68%; iii) MeNH_2 (33% in EtOH), EtOH, rt, 2 h, 94%; iv) $\text{NEt}_3\cdot 3\text{HF}$, CH_2Cl_2 , rt, 16 h, 72%.

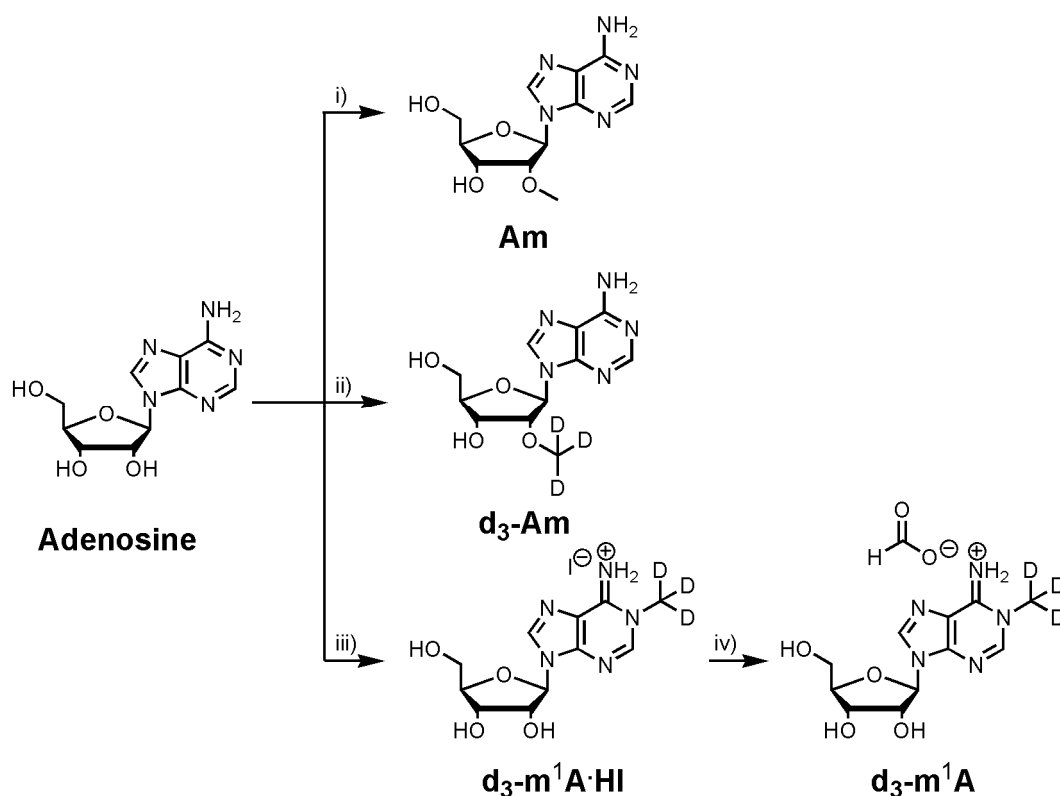
Compound **18** was treated with (4-nitrophenyl)chloroformate to obtain intermediate **19**, which was subsequently treated with protected L-threonine to substitute the 4-nitrophenol moiety and to obtain the fully protected $d_3\text{-m}^6\text{t}^6\text{A}$ (**20**) (Scheme 12). The isotope-labeled compound $d_3\text{-m}^6\text{t}^6\text{A}$ was obtained after the two deprotection steps with $\text{NEt}_3\cdot 3\text{HF}$ and DBU.



Scheme 12: Synthesis of the nucleoside $d_3\text{-m}^6\text{t}^6\text{A}$. i) (4-nitrophenoxy)chloroformate, pyridine, $50\text{ }^\circ\text{C}$, 5.5 h, 92%; ii) **11**, pyridine, rt, 15 h, 84%; iii) a) $\text{NEt}_3\cdot 3\text{HF}$, CH_2Cl_2 , rt, 48 h; b) DBU, THF, $40\text{ }^\circ\text{C}$, 5 h 25% (over 2 steps).

5.4.7 Synthesis of Am and m¹A

The synthesis was performed according to literature using a method for selective methylation at the 2' position at the free adenosine.^[143-144] The most acidic proton at the alcohol the 2' position of adenosine enabled mainly methylation in this position. A substoichiometric amount of methyl iodide and two workup steps yielded pure nucleoside Am. Again deuterated methyl iodide was used to introduce the heavy atom label to obtain the isotope-labeled nucleoside d₃-Am (Scheme 13).



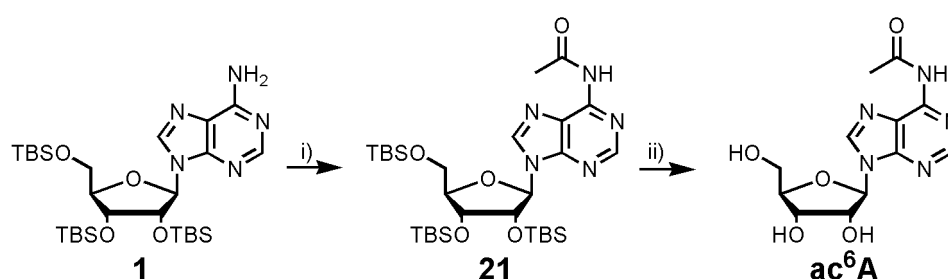
Scheme 13: Synthesis of nucleosides Am, d₃-Am, and d₃-m¹A. i) methyl iodide, NaH, DMF, 0 °C, 4 h, 16%; ii) d₃-methyl iodide, NaH, DMF, 0 °C, 4 h, 21%; iii) d₃-methyl iodide, DMA, rt, 16 h, 69%; iv) 1) conc. NH₃, 2) HCOOH.

The natural nucleoside m¹A was commercially available and used as reference compound after HPLC purification. The synthesis of the deuterated derivative d₃-m¹A was performed according to a literature procedure for m¹A.^[145] Adenosine was treated with deuterated methyl iodide without using a base, which mainly resulted in the hydroiodide of d₃-m¹A (Scheme 13). To obtain a more specific and stable counterion this nucleoside was neutralized carefully to avoid a methyl transfer to position 6. Afterwards HPLC purification under acidic conditions (HCOOH) yielded the protonated m¹A with formate as counterion.

5.4.8 Synthesis of ac⁶A

Monoacetylation at position 6 of compound **1** was obtained after reaction with acetylchloride at low temperature and short reaction time. The difficulty in this reaction is to avoid diacetylation, which finally gave **21** in a yield of 66%. The TBS-protecting groups at the sugar moiety are crucial due to cleavage under non-basic conditions with NEt₃·3HF to obtain final compound ac⁶A (*Scheme 14*).

The nucleoside ac⁶A was only detected in archaeal tRNA and we did not detect it in any of our tRNA isolates. Therefore no isotope-labeled derivative was synthesized but the presented synthesis would be applicable with the commercially available ¹³C₂-acetylchloride for synthesis of the heavy atom labeled derivative.



Scheme 14: Synthesis of the archaeal tRNA nucleosides ac⁶A. i) acetylchloride, pyridine, -5 °C to rt, 1 h, 66%; ii) NEt₃·3HF, CH₂Cl₂, rt, 15 h, 80%.

5.5 Overview

In summary, the five modified nucleosides m⁶t⁶A, t⁶A, m⁶A, m⁶₂A, and Am were synthesized together with their five corresponding heavy atom labeled derivatives (*Figure 20*). A modified synthetic strategy was developed for m⁶t⁶A. Additionally, the deuterated derivative of m¹A was synthesized as well as the tRNA modifications g⁶A and ac⁶A. The six synthesized heavy atom labeled derivatives were used as internal standard molecules in the quantification experiments.

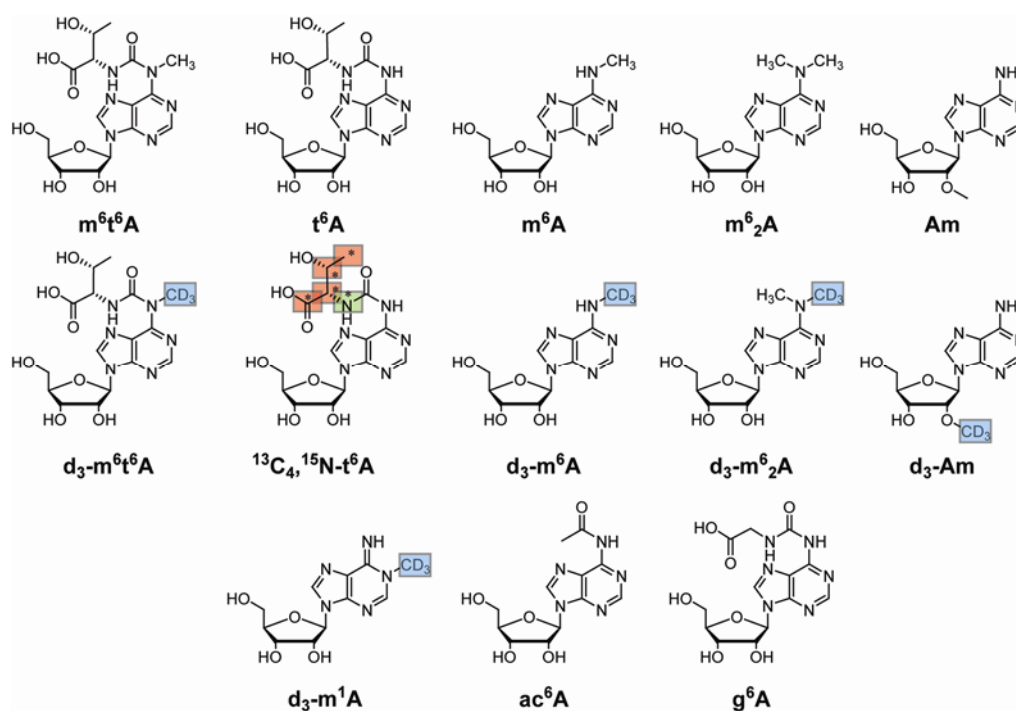


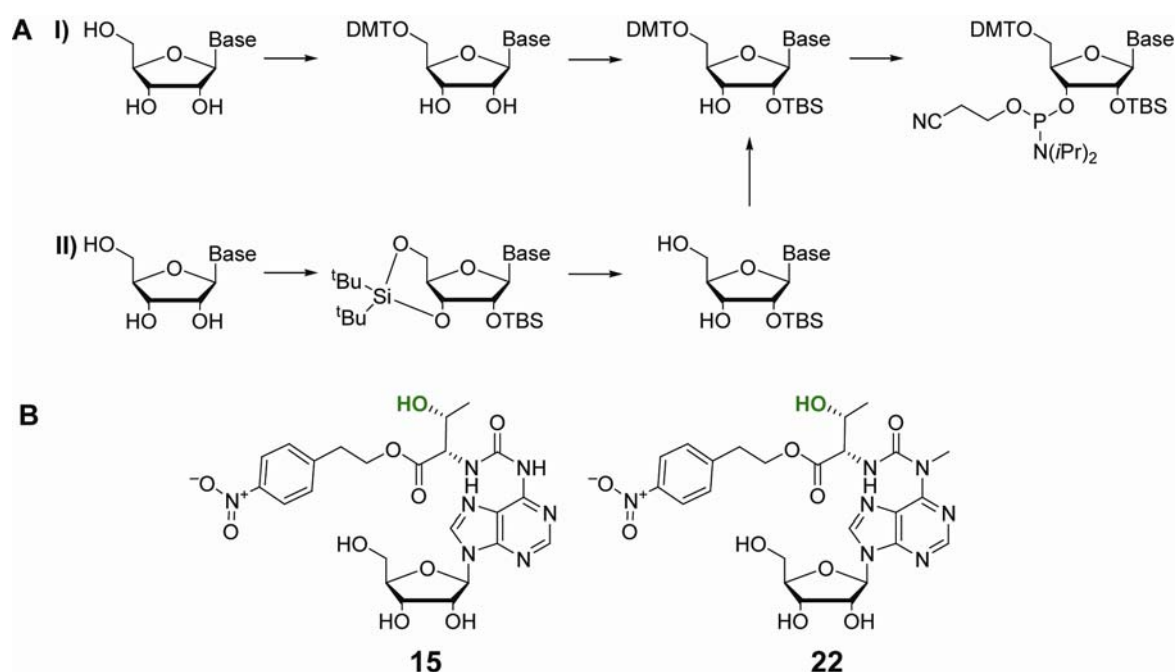
Figure 20: The synthesized 13 modified RNA nucleosides. The six isotope-labeled modifications $d_3-m^6t^6A$, $^{13}C_4, ^{15}N-t^6A$, d_3-m^6A , $d_3-m^6_2A$, d_3-Am , and d_3-m^1A were used as internal standards in quantification experiments within this Ph.D. thesis.

5.6 Building blocks for RNA synthesis

The nucleoside t^6A has been incorporated in RNA strands *via* phosphoramidite chemistry before.^[44, 48, 50] The further methylated derivative m^6t^6A has never been incorporated into RNA strands *via* phosphoramidite chemistry. Biochemical investigations would be possible to reveal the properties of the still unknown methylating enzyme, if RNA strands were available with both modifications. Influence of other modified nucleosides in the anticodon stemloop and especially at position 32 could be investigated.

To synthesize RNA strands containing modified nucleosides, RNA phosphoramidites of the desired modifications have to be available. It is very important to use a fast and high yielding protecting group strategy for phosphoramidites. They have to be present at every nucleophilic position at the base and the sugar to prevent undesired side reactions. The protecting group at the base can be attached at almost every step of the synthesis of DNA or RNA building blocks. For sugars different strategies have been described. Two protection steps are necessary for the DNA sugar, while the additional alcohol at the 2' position in RNA building blocks necessitates a different strategy. The first and most commonly applied strategy starts with protection of the primary alcohol with the acid labile DMT group (*Scheme 15A*, strategy **I**). The second step is protection of the 2' position with a TBS group and finally the

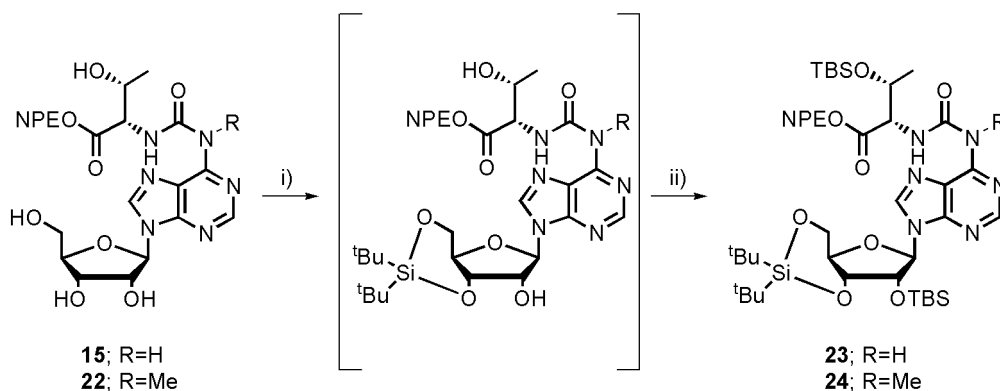
reaction of a phosphoramidite reagent with the 3' position.^[146] The disadvantage of this procedure is the side reaction of the TBS protection resulting in a 1:1 mixture of the 3' besides the 2' protected molecule, which causes low yields. An additional disadvantage of this strategy for both used intermediates for t⁶A (**15**) and m⁶t⁶A (**22**) is the unprotected hydroxygroup at the threonine moiety, which would further decrease the yield in the TBS protection step and complicate separation of all isomers (*Scheme 15B*). Therefore a second strategy (**II**) was applied in which first the 5' and 3' alcohols are protected with (tBu)₂Si(OTf)₂ under formation of a six-membered ring.^[147-148] Afterwards the 2' position is TBS protected and in case of the two t⁶A derivatives the free alcohol at the threonine moiety gets additionally protected. The next step is cleavage of the (tBu)₂Si group followed by protection of the primary alcohol with DMT.



Scheme 15: A) The two possible protecting group strategies for building block synthesis. Strategy I: DMT protection of the 5' position; TBS protection of the 2' position; phosphitylation of the 3' position. Strategy II: Simultaneous (tBu)₂Si protection of the 3' position and the 5' position and TBS protection of the 2' position; cleavage of (tBu)₂Si protecting group; DMT protection of the 5' position; phosphitylation of the 3' position. **B)** The two acid protected compounds **15** (t⁶A) and **22** (m⁶t⁶A) used as starting compounds for protecting group chemistry. The additional alcohol is colored in green.

Strategy **II** in *Scheme 15* was used for the synthesis of the t⁶A and the m⁶t⁶A building block due to the described advantages. The first step with protection of the 3' and 5' position with (tBu)₂Si(OTf)₂ followed by TBS protection of the 2' alcohols and the alcohol at the threonine moiety in a one-pot reaction had to be modified to achieve the desired intermediate (*Scheme 16*). Unfortunately, the glycosidic linkage between the modified base and the sugar

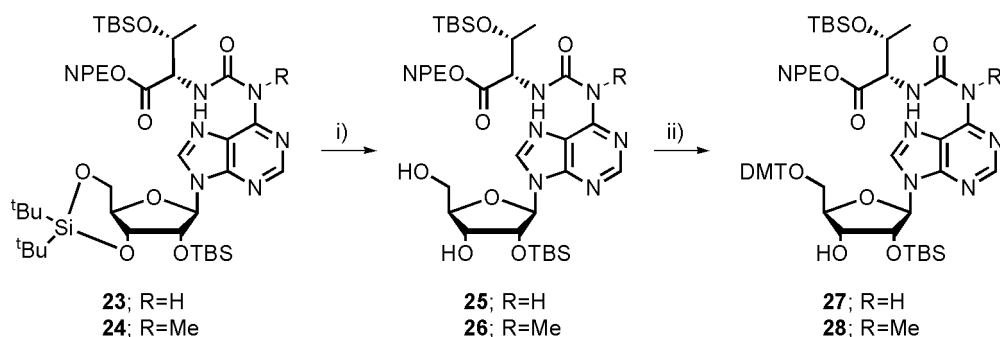
was cleaved using the conditions for protection of the four canonical nucleosides.^[147-148] Therefore the reaction conditions were optimized to yield the protected intermediates of t^6A (**23**) and m^6t^6A (**24**) in good yields of 71% and 83%, respectively.



Scheme 16: First protection step applied for t^6A and m^6t^6A . i) $(tBu)_2Si(OTf)_2$, DMF, $-5\text{ }^\circ\text{C}$ to rt, 1.5-2 h ii) imidazole, TBSCl, DMF, rt, 16 h, **23**: 71%, **24**: 83%.

Main changes were performed by increasing the time of both steps and to reduce the temperature from $60\text{ }^\circ\text{C}$ to rt. The amount of TBSCl was also increased to obtain protection of the two unprotected alcohols.

The protecting group of the 3' and the 5' position was selectively cleaved in intermediates **23** and **24** by deprotection using $py \cdot HF$ at $0\text{ }^\circ\text{C}$ to obtain **25** and **26**. Subsequent DMT protection of the primary amine at the 5' position yielded compounds **27** and **28** (Scheme 17). The last step to obtain the final building blocks for RNA synthesis was not performed in this Ph.D. thesis, because RNA synthesis was not part of this thesis work. Sufficient amounts of both t^6A and m^6t^6A DMT protected compounds were synthesized. These can be used for incorporation in synthetic RNA strands for biochemical studies.



Scheme 17: Protecting group synthesis towards incorporation in RNA of the nucleosides t^6A and m^6t^6A . i) $py \cdot HF$, pyridine, CH_2Cl_2 , $0\text{ }^\circ\text{C}$, 3-5 h, **25**: 86%, **26**: 77%; ii) DMTCl, pyridine, rt, 16-18 h, **27**: 69%, **28**: 71%.

6. Quantification method

The workflow of the developed LC-MS based method is depicted in *Figure 21*. Each step was optimized for successful and accurate quantification. Isolation and subsequent purification of a sufficient amount of bulk tRNA was optimized by Dr. T. Brückl and is important for convenient realization of the quantitative method. As part of this Ph.D. work conditions were screened to achieve quantitative enzymatic digestion of the isolated tRNA. Precise and reproducible quantification can only be achieved in case of complete hydrolysis to the nucleosides without traces of dinucleotides or 5'-monophosphates of any nucleoside. In parallel each part of the HPLC-ESI-MS method was optimized. Final analysis of the obtained mass spectrometric data yielded the quantitative values for each analyzed nucleosides.

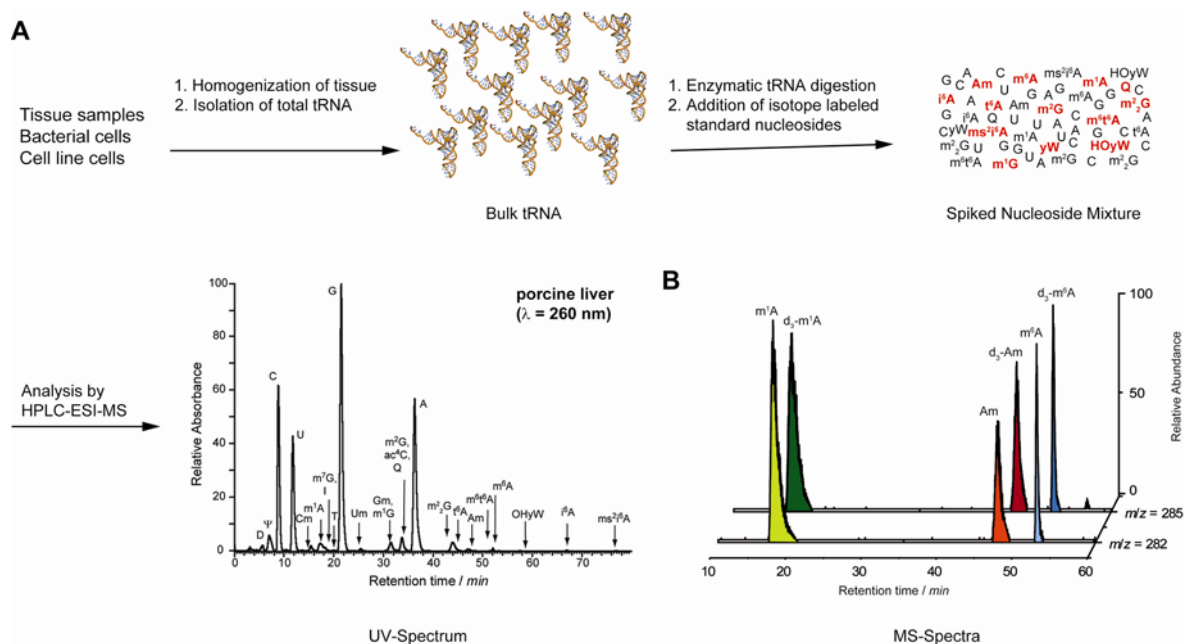


Figure 21: Workflow of the LC-MS quantification method for tRNA nucleosides. A) The first step is isolation and purification of bulk tRNA out of any cells followed by enzymatic digestion of tRNA. Then isotope-labeled nucleosides were added and the samples were subsequently analyzed with HPLC-ESI-MS. B) Representative depiction of the specific ion currents of monomethylated adenosine derivatives in parallel (front signals) and their corresponding isotope-labeled derivatives (back signals).

6.1 Extraction and purification of tRNA

6.1.1 Extraction of tRNA

For quantification of modified tRNA nucleosides, the extraction and subsequent purification of tRNA in sufficient amounts is very important. Initially we used *E. coli* cells, since it is fast growing and enables uncomplicated upscaling to test several tRNA extraction protocols. The method that finally allowed extraction of high amounts of tRNA was chosen and further modified to achieve tRNA isolation in high purity.^[94]

To this end *E. coli* cells were grown under optimal conditions, harvested by centrifugation and resuspended in our aqueous buffer supplemented with phenol. Here the phenol is used to destroy the cell walls and to extract proteins. Extraction, centrifugation, and decantation were performed in triplicate and the phenol is finally removed. The aqueous buffer contained all nucleic acids, which were separated by their different sizes in a precipitation step using 2M LiCl.^[94] While the large nucleic acids DNA, rRNA, and mRNA are precipitated, the tRNA with a lengths of only 70 to 120 nucleotides remained in the supernatant. The crude tRNA was isolated by decantation from all other nucleic acid species in the pellet.

6.1.2 Purification of tRNA

The crude extracted tRNA was further purified by anion exchange chromatography, which enables separation of differently charged molecules. For nucleic acids the separation is directly correlating with the size of the molecules due to the negatively charged phosphate backbone. Therefore, tRNA is eluting first followed by larger nucleic acids like rRNA and mRNA, which are effectively separated (*Figure 22*). In this way any remaining rRNA and mRNA impurities from the precipitation step were removed and pure tRNA was obtained.

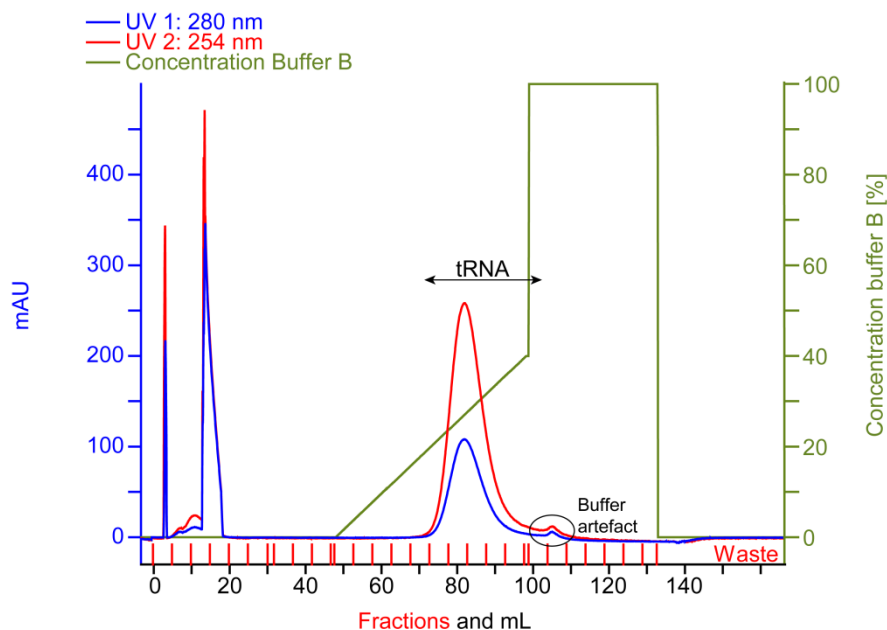


Figure 22: Representative anion exchange chromatography for purification of tRNA.

The 5S rRNA subunit consists of approximately 120 nucleotides, which is almost the same size as tRNA molecules.^[149] To the best of our knowledge, there is no procedure enabling separation of these two types of RNAs in parallel. Nevertheless, tRNAs are present in large excess in cells compared to 5S rRNA, which in addition is only rarely modified.^[150] Thus, 5S RNA does not interfere with the quantification experiments.

This established tRNA extraction method was used successfully for the isolation of tRNA from different bacterial species, yeast, plants, mammalian porcine tissue, and human cell cultures. An additional desalting step was applied for tissue samples and bacterial species experiments due to column binding problems, which caused loss of samples during purification. Therefore, this method is generally applicable for tRNA extraction from all kind of cells. tRNA extraction and purification were performed by Dr. T. Brückl and is described in more detail in his Ph.D. thesis.^[140]

As part of this thesis all further steps leading to quantification of tRNA modifications were optimized in parallel because they are dependent for each other. For clarity each part is described separately starting with preparation of enzymatic hydrolysis, combined HPLC-MS analysis, and finally calibration curve determination.

6.2 *Enzymatic hydrolysis of tRNA*

Complete enzymatic hydrolysis of the purified tRNAs to their nucleosides is essential in order to achieve accurate and precise quantification data. Previously full digestion of tRNA has been reported in two main publications by Gehrke *et al.* and an optimized procedure by Crain.^[151-152] In both cases a two-step enzymatic protocol was applied starting with hydrolysis of tRNA using nuclease P1 to yield the 5'-monophosphates of tRNA nucleosides. In the second step alkaline phosphatase and snake venom phosphodiesterase were employed to remove the residual phosphates to obtain tRNA nucleosides. This together with a method in the Carell group for DNA digestion was used as a starting point. Different enzymatic mixtures and concentrations were screened to obtain completely hydrolyzed tRNA nucleoside samples.^[153] Alkaline phosphatase was replaced with antarctic phosphatase to prevent deamination of adenosine to inosine as a side reaction. Other adenosine derivatives would also be deaminated which would cause wrong results. We replaced nuclease P1 with nuclease S1 because it is available in large amounts and is stable in the appropriate storage buffer for at least two months. Complete digestion was tested by quantifying the amount of the two modification m²A and m⁶A in *E. coli* tRNA (12 µg) and comparing with literature results obtained from 2D radioactively labeled nucleotides (*Table 1*).^[86] Each result was determined by at least two independent digests.

In the optimized protocol the tRNA was initially denatured by incubation at 100 °C for 3 min to allow efficient digestion by the enzymes which prefer single stranded RNA.^[151-152] This was followed by addition of different variations of enzyme concentrations with first applying nuclease S1 and calf spleen phosphodiesterase II followed by antarctic phosphatase and snake venom phosphodiesterase I (*Table 1*). Each enzyme digestion mixtures were incubated for 3 h at 37 °C. Calf spleen phosphodiesterase II seemed to inhibit the activity of nuclease S1, which we subsequently omitted from further digestion.

We finally obtained the enzyme mixture No9 as optimum hydrolysis protocol. Nuclease S1 (80 units) was incubated with the tRNA mixture for 3 h at 37 °C followed by addition of antarctic phosphatase (10 units) and snake venom phosphodiesterase I (0.2 units), which were again incubated for 3 h at 37 °C. This enzyme mixture yielded the same results like the reference values with perfect reproducibility and no undigested dinucleotides could be detected. These conditions were used for all our quantification experiments and a detailed procedure of conditions No9 is described in the experimental section (Chapter 10.4.4).

Table 1: Different enzymatic hydrolysis conditions tested with relative amounts of m²A and m⁶A. Values of m²A and m⁶A are obtained from at least two independent digestion experiments in ‰ of total tRNA. Standard deviations (s.d.) are shown in parentheses. ^{a)} Only one value determined; ^{b)} No s.d. available from literature values.

No	Nuclease S1 / U	Phospho- diesterase II / mU	Antarctic phosphatase / U	Phospho- diesterase I / U	‰ (m ² A) / total tRNA	‰ (m ⁶ A) / total tRNA
1	20	50	5	0.1	1.29 (37)	0.30 (30)
2	60	50	5	0.1	2.03 (3)	0.55 (1)
3	80	50	5	0.1	1.87 (9)	0.52 (1)
4	80	25	5	0.1	2.00 (3)	0.51 (7)
5	80	25	10	0.2	2.54 (19)	0.63 (17)
6	80	25	5	0.3	2.75 (14)	0.69 (15)
7	80	0	5	0.1	2.62 (2)	0.74 (-) ^a
8	60	0	5	0.1	2.34 (6)	0.64 (7)
9	80	0	10	0.2	2.75 (1)	0.69 (6)
Reference ^[86]					2.80 (-) ^b	0.70 (-) ^b
Nuclease P1 ^[151-152]					2.84 (2)	0.77 (6)
Nuclease S1 (optimized condition No 9)					2.75 (1)	0.69 (6)

6.3 HPLC-ESI-MS

HPLC-ESI-MS is a combination of chromatographic separation, followed by mass spectrometric analysis. This method is advantageous to HPLC analysis due to the higher sensitivity of the MS detector. Additionally, the distinct assignment of each nucleoside is possible with the retention time and the corresponding molecular weight. Isotope-labeled nucleosides as reference molecules were used in order to turn the MS analysis quantitative. They exhibit nearly identical physical HPLC properties like the natural occurring compounds. In addition they are comparable by their different molecular weight and are thus essential reference molecules for precise quantification.

The chromatographic conditions were thoroughly optimized to separate all tRNA nucleosides with the same molecular weight from each other. Especially monomethylated nucleosides like m²A and m⁶A have similar physical properties, which require a thorough optimization of the HPLC conditions for accurate quantification. Other modifications which possess the same

chromatographic properties can be distinguished by their molecular weight and analyzed separately. Only the two monomethylated guanosines m^1G and Gm could not be separated and we decided to quantify both together with the d_3 - m^1G reference nucleoside.

As the separation column we used a special C18 material, which is specific for separation of polar compounds like nucleosides. This column is optimized for gradients with high water concentrations over a long time range. The buffers and the flow used for adjusting the gradient were also chosen to be suitable to mass spectrometric analysis (Detailed information in the experimental section, Chapter 6.3). The optimized gradient enables separation of all present modifications and as example the two monomethylated adenosines m^2A and m^6A are shown (*Figure 23B*). The nucleoside m^2A is only present in bacterial tRNA and absent in any eukaryotic organisms. Thus a shorter gradient was used for all measurements lacking m^2A . *Figure 23A* shows as example a comparison of the HPLC chromatograms of *E. coli* containing m^2A and porcine heart.

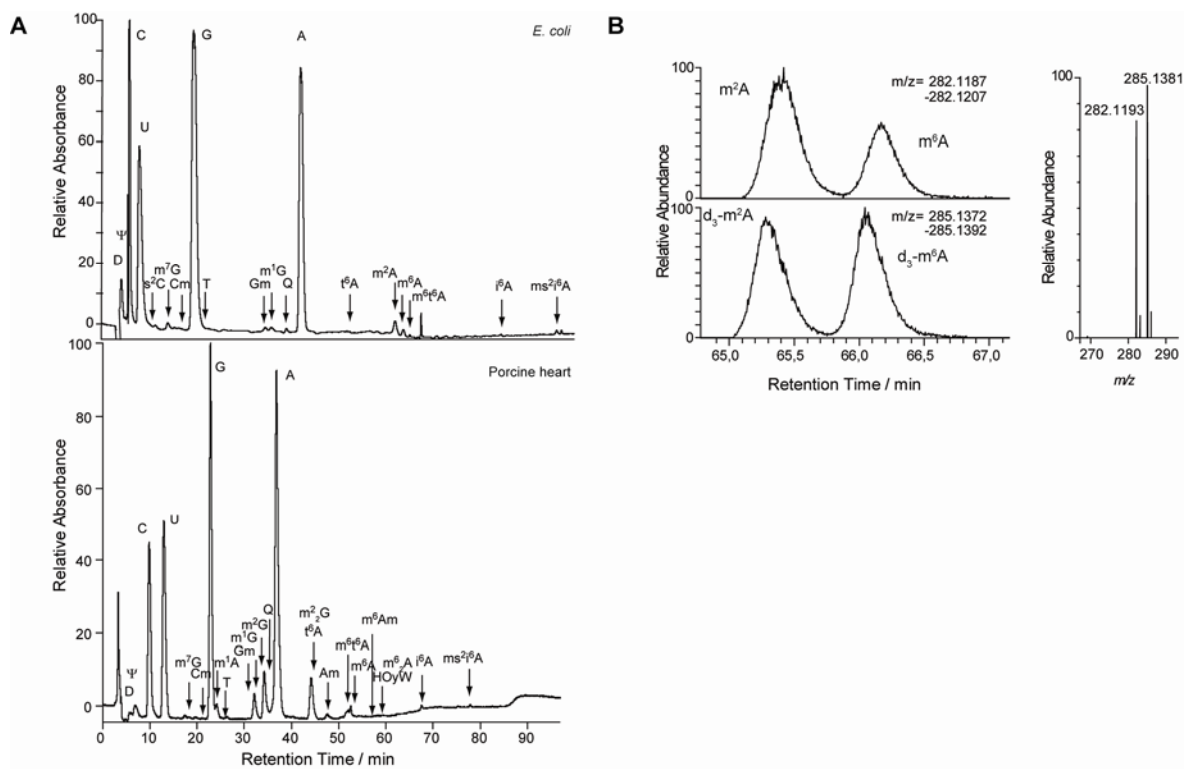


Figure 23: A) Representative HPLC chromatograms of hydrolyzed tRNA from *E. coli* and porcine heart with separation and assignments of all identified modified nucleosides. Different gradients were used for bacterial and porcine tissue tRNA. B) Positive ion traces of the protonated nucleosides m^2A and m^6A with the corresponding isotope-labeled derivatives d_3 - m^2A and d_3 - m^6A . The used m/z ranges for monomethylated adenosine and the isotope-labeled derivatives are indicated (left). Relevant high-resolution mass spectrometry peaks for unlabeled and labeled m^2A (right).

Quantitative mass spectrometric analysis was established on a LTQ-FT-ICR mass spectrometer and afterwards transferred to an Orbitrap XL from Thermo Fisher Scientific. The latter system in combination with a dedicated HPLC from Dionex was superior to the previous setup due to an increased sensitivity. Therefore, we could reduce the amount of injected sample and still enable precise quantification. Importantly, we observed the same amounts of nucleosides as for the LTQ-FT-ICR in quantification experiments, which additionally proves the general applicability and accuracy of our method.

All samples were analyzed in the positive polarity mode because higher intensities were obtained in comparison to the negative mode. The mass spectrometer values were tuned to achieve optimum conditions with freshly mixed adenosine or uridine samples, which were dissolved in the buffer used in the HPLC-MS analysis. The injecting needle of the mass spectrometer was blocked after some runs due to the high salt concentration from the hydrolyzed tRNA samples. Therefore, the first 3.5 min of every hydrolyzed sample were omitted from injection into the mass spectrometer since the salts are eluting without interacting with the C18 material. Thus, samples could be measured up to seven days without exchanging the injection needle.

Quantification was performed with parallel extraction of the high resolution mass range of each modified nucleoside and its corresponding heavy atom labeled nucleoside. These specific mass traces allow precise peak integration without background interference. This enabled us to quantify nucleosides ranging from very low to large amounts, which is shown in the results section of this Ph.D. thesis.

6.4 Stock solutions

The stock solutions were prepared by weighing out the HPLC purified and lyophilized nucleosides on a balance in a volumetric flask. For accuracy special care was taken to include all counterions from the charged nucleosides in the molecular weight calculations. To take weighing errors into account calibration curves were determined in triplicate. The weighed nucleosides were filled up to 100 mL in a volumetric flask with *ddH*₂O to receive concentration 1 of each nucleoside, followed by further dilution of 10 mL to 100 mL to obtain concentration 2, resulting in 1/10 of concentration 1. With only rare exceptions the lower concentration 2 or further diluted samples were used for quantification experiments. When a nucleoside was not soluble in *ddH*₂O, it was first dissolved in an as low as possible amount of DMSO and then filled with *ddH*₂O to 100 mL (*ms*²*i*⁶A, *m*¹A, Q, *m*²G, *m*²₂G, *io*⁶A, and

ms²io⁶A). Importantly, we took care that all four solutions of one compound (3 solutions of the unlabeled nucleoside and 1 solution of the isotope-labeled nucleosides) were dissolved in the same amount of DMSO to keep the solutions comparable. All stock solutions were stored at -20 °C and warmed up to rt prior to addition to the digestion mixture (spiking). No decomposition or byproducts were observed after several defrosting and spiking experiments.

6.5 Calibration curves

Measurements of calibration curves and assays are machine dependent and were performed for the two different mass spectrometers. Calibration curves were determined with five to seven samples, which contain different ratios of the natural nucleoside to the corresponding isotope-labeled derivative. One value represents measurements with three independent samples of the unlabeled nucleoside. For seven different ratios in total 21 samples were analyzed with the optimized HPLC gradient as shown in *Figure 23B*. The calibration curves were determined by integration of the specific mass spectrometric areas for each nucleoside separately.

The average determined area ratios from unlabeled to labeled nucleoside were plotted against the seven adjusted concentration ratios. The calibration curves with s.d. for all 16 nucleosides measured in this Ph.D. thesis are illustrated in *Figure 24* and represent perfect correlations with R² values of at least 0.999. The only exception is io⁶A with R² value of 0.990, which is still applicable for precise quantification. The shown linear equations were used for calculation of the exact nucleoside contents in bulk tRNA. Possible errors regarding preparation of standard solutions and mixing of the standard solutions are taken into account in these calibration curves due to analysis in triplicate with three independent unlabeled nucleoside solutions. Isotope-labeled compounds contain traces of unlabeled nucleosides since chemicals used in the synthesis are not labeled to 100%. These natural impurities were found to be in the range of 0.01–0.1% and are much lower than the error resulting from independent measurements. Impurities of the synthesized nucleosides can be excluded, because all nucleosides were purified *via* HPLC.

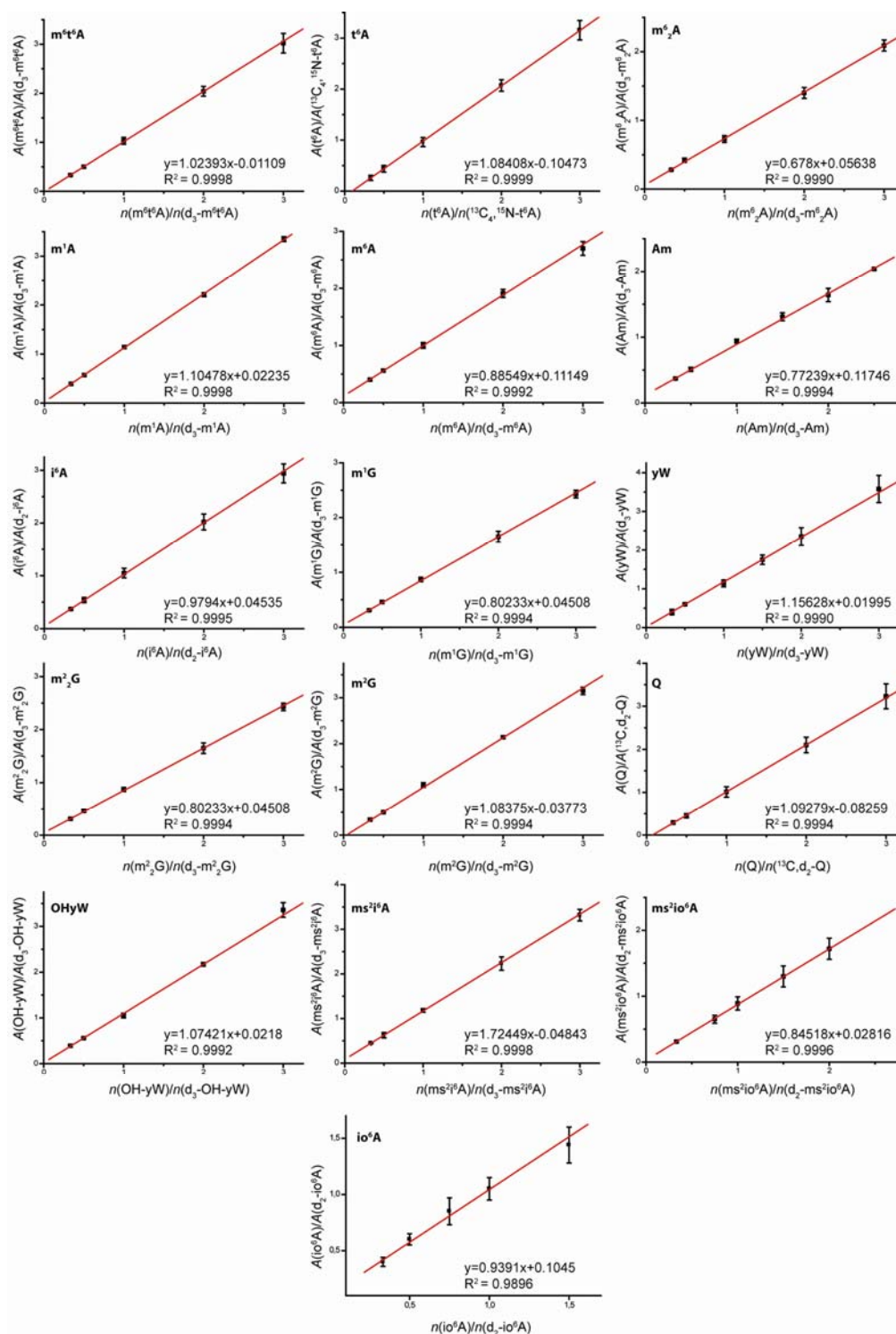


Figure 24: Calibration curves for the 16 modified RNA nucleosides determined. The first six nucleosides were synthesized as part of this thesis work. All others were synthesized by Dr. T. Brückl, I. Thoma, P. Thumbs, and A. Hienzsch.

Precise quantification was enabled by spiking the isotope-labeled modifications into hydrolyzed tRNA samples which we analyzed using the optimized HPLC-MS conditions. Calibration curves were repeated to check validity over time, and resulted in very similar equations.

6.6 Accuracy of quantification

It is extremely important to prove the reproducibility of the quantitative method in order to obtain accurate data.^[107, 154] Therefore, an intraassay and an interassay test were performed for the two nucleosides m^2A and m^6A , which were quantified in a digested tRNA sample. Here, the same amount of one sample was injected six times in a row (intraassay) and area ratios of labeled to unlabeled nucleosides were compared, showing a great reproducibility of 1.22% (N=6) for m^2A and 4.83% (N=6) for m^6A . The interassay test with injection of the same sample on five subsequent days gave an area ratio reproducibility of 2.74% (N=5) and 1.57% (N=5) for m^2A and m^6A , respectively. In contrast, large variations in the single area of labeled or unlabeled nucleoside from 18% to 28% were observed highlighting the importance of the labeled nucleosides as reference (*Table 2*). Nevertheless, this proves the stability of the sample after digestion for at least five days at room temperature. Additionally, no memory effect due to carry-over contaminations was observed during blank LC/MS experiments performed after measurements of a digested sample.

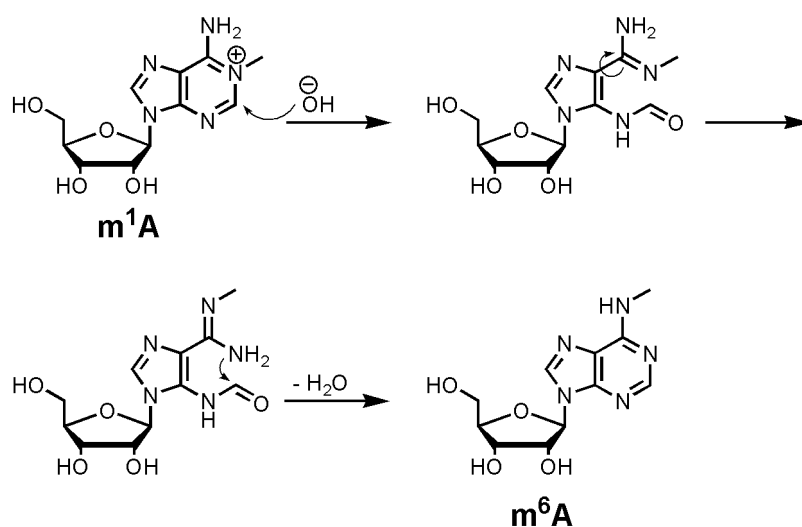
Table 2: Representative intra- and interassay test (RSD: relative standard deviation).

Intraassay	$A(m^2A)$	$A(d_3-m^2A)$	$n(m^2A)$ / pmol	$A(m^6A)$	$A(d_3-m^6A)$	$n(m^6A)$ / pmol
1	1951781	1654081	132.95	856814	1825684	27.10
2	1666684	1432034	131.21	721705	1647383	25.28
3	1469647	1266812	130.81	598778	1476839	23.37
4	1344816	1140608	132.84	584865	1339631	25.19
5	1177950	1018588	130.41	541967	1246568	25.08
6	1068219	936646	128.69	489455	1150451	24.54
Mean value	1446516	1241462	131.15	632264	1447759	25.09
RSD in %	22.51	21.61	1.22	21.26	17.59	4.83

Interassay	$A(m^2A)$	$A(d_3-m^2A)$	$n(m^2A)$ / pmol	$A(m^6A)$	$A(d_3-m^6A)$	$n(m^6A)$ / pmol
1	1068219	936646	128.69	489455	1150451	24.54
2	883523	756445	131.65	463845	1089846	24.55
3	1557891	1388066	126.74	780957	1801408	25.01
4	1545862	1288110	135.11	816523	1904931	24.73
5	1659433	1390301	134.41	854208	1935446	25.47
Mean value	1342986	1151914	131.32	680998	1576416	24.86
RSD in %	25.63	25.08	2.74	27.69	26.64	1.57

Furthermore addition of the isotope-labeled nucleosides prior or after enzymatic hydrolysis had no influence on the obtained quantitative results. Thus, we decided to add all reference nucleosides right after digestion in order to avoid a possible influence of DMSO content in stock solutions on the enzyme activity.

The stability of all nucleosides during enzymatic digestion was tested, showing that all nucleosides except the modification m^1A were stable under these conditions. The methyl group undergoes slow Dimroth rearrangement to yield m^6A under basic conditions as described before (*Scheme 18*).^[155-156] The first step of the mechanism is the attack of hydroxide at position 2 of m^1A , which leads to an opened purine ring. Afterwards the bond carrying the amidine moiety rotates, followed by nucleophilic attack of the primary amine at the formamide. The purine is formed again after release of water to yield m^6A .^[156] It is known that modified nucleosides are more stable in incorporated in RNA strands compared to single nucleosides.^[157] As all nucleosides are added after digestion, precise quantification of m^1A is possible because the reference nucleoside gets decomposed in parallel. Additionally, we excluded all m^6A values in samples with high concentration of m^1A .



Scheme 18: Mechanism of the Dimroth rearrangement. Conversion of m^1A to m^6A under basic conditions.

The intra- and interassay test for these nucleosides proved again the reproducibility of quantification values, which were performed for representative nucleosides m^1A , i^6A , $ms^{2:6}i^6A$, m^1G , and m^6A (Table 3). The intraassay after enzymatic digestion showed good reproducibility for each nucleoside (N=5) of 0.4%–2.6%. In the interassay test we obtained reproducibility (N=6) of 1.0%–4.3% for all nucleosides on six subsequent days except for m^6A with 14.3%. As described above the values differ due to the methyl group rearrangement of m^1A . Using the area ratio with the calibration curves we gained perfect reproducibility.

Table 3: Intra- and interassay of the representative nucleosides m^1A , i^6A , $ms^{2:6}i^6A$, m^1G , and m^6A (RSD: relative standard deviation).

Intraassay	m^1A /1000 tRNAs	i^6A /1000 tRNAs	$ms^{2:6}i^6A$ /1000 tRNAs	m^1G /1000 tRNAs	m^6A /1000 tRNAs
1	231.7	81.5	34.4	135.5	43.0
2	234.1	81.5	34.2	140.8	42.4
3	231.1	82.3	34.6	136.5	44.3
4	234.1	81.8	34.0	134.9	43.6
5	218.9	81.8	34.0	144.2	43.5
Mean value	230.0	81.8	34.3	138.4	43.4
RSD in %	2.5	0.4	0.7	2.6	0.6
Interassay	m^1A /1000 tRNAs	i^6A /1000 tRNAs	$ms^{2:6}i^6A$ /1000 tRNAs	m^1G /1000 tRNAs	m^6A /1000 tRNAs
1	237.9	82.0	33.7	144.6	28.4
2	232.3	83.2	34.6	128.9	34.1
3	234.4	80.4	34.3	135.5	37.4
4	234.8	82.2	35.5	132.0	40.0
5	218.9	81.8	34.0	144.2	43.5
6	222.5	81.5	35.2	139.2	44.0
Mean value	230.1	81.8	34.5	137.4	37.9
RSD in %	3.0	1.0	1.8	4.3	14.3

7. Results tRNA modifications

7.1 Differences between *E. coli*, mammalian tissue, and cell lines

We analyzed the modification pattern of different organisms using our described quantitative method. Porcine liver was selected as healthy mammalian tissue due to its similarity to humans and availability in large amounts.^[95] For comparison we decided to use the human epithelial cell lines HeLa, HCT-116, and A-375, which were derived from an adenocarcinoma of the cervix, from a colorectal tumor and from a malignant melanoma, respectively. Additionally, *E. coli* was chosen as representative bacterial organism.

The six tRNA modifications m^6A , m^2A , Am, t^6A , ms^2i^6A , and i^6A were used as reference nucleosides (Figure 25). The base modifications are present 3'-adjacent to the anticodon at position 37 and are therefore directly involved in codon-anticodon interactions.^[3-5, 7, 35] The only exception is the 2'-*O*-methylated nucleoside Am present in the amino acid acceptor stem at position 4 of eukaryotic tRNA.^[130]

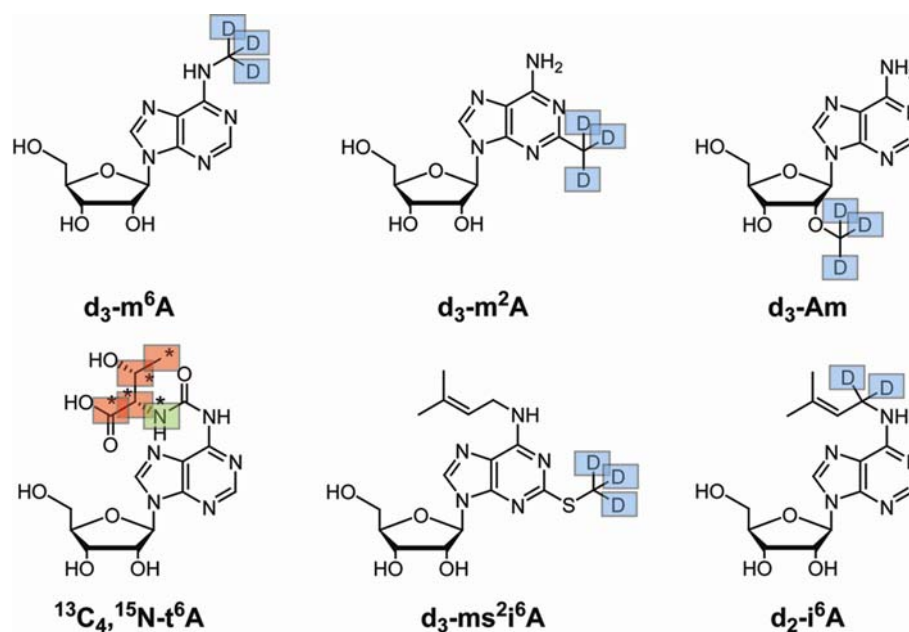


Figure 25: Isotope-labeled adenosine modifications $d_3\text{-m}^6A$, $d_3\text{-m}^2A$, $d_3\text{-Am}$, $^{13}C_4, ^{15}N\text{-t}^6A$, $d_3\text{-ms}^2i^6A$, and $d_2\text{-i}^6A$ applied as reference molecules. The isotopic labels are indicated by color, with blue for D, red for ¹³C, and green ¹⁵N.

The modification levels for the six investigated nucleosides in the five different cell types are shown in *Figure 26*. Obviously, the pattern between *E. coli* and mammalian cells show the expected differences. The bacterial modification m^2A was only present in *E. coli*, while the eukaryotic nucleoside Am was absent only in *E. coli*.^[3-5] This is a validation of our method starting with extraction of tRNA and finally yielding the quantitative data. All bars represent the average value of two independent biological replicates and workup procedures with at least three independent enzymatic digestions and LC-MS measurements. The average error margin of only 5% proves the high quality of the obtained data.

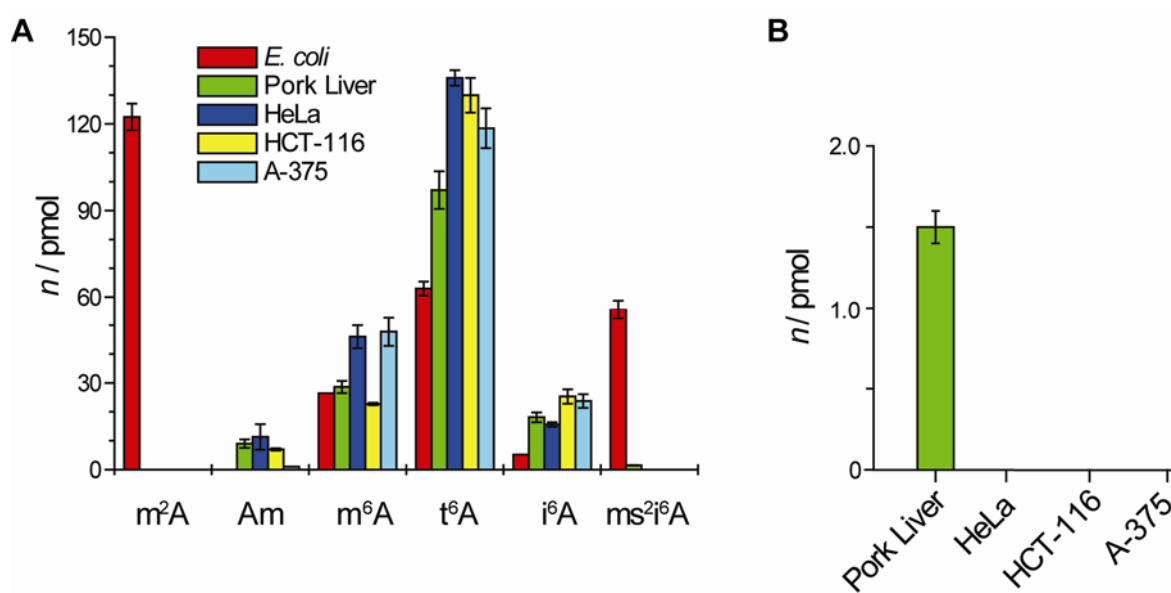


Figure 26: A) Comparison of modified tRNA nucleoside levels of *E. coli*, pork liver, HeLa, HCT-116, A-375 cell lines. B) Zoomed values of the modification ms^2i^6A in mammalian cells. Error bars represent the standard deviations calculated from multiple experiments.

Interestingly, comparison of pork liver and the three cancer cell lines reveals significant differences. The amount of the modification t^6A is significantly enhanced in all three cancer cell lines compared to the healthy tissue indicating either an up-regulated biosynthesis in cancerous cells or organism specific differences. Furthermore, we could detect significant differences for m^6A and i^6A between each cancer line with HeLa and A-375 containing twice as much m^6A than HCT-116. HeLa contains 30% less i^6A compared to the other two cell lines, which exhibit the same amount. These cell line specific modification patterns may provide a novel diagnostic tool for differentiation of cancer types by analysis of modified tRNA nucleosides.

Another highly interesting observation is that the modification ms^2i^6A is only present in healthy tissue (*Figure 26B*). We detected it in a very low but significant amount in pork liver

tissue, whereas it is completely absent in all three cancer cell lines. All other modifications were present in both tissue and cultured cells. The modification ms^2i^6A is known to be present only in mitochondrial tRNA showing the high resolution of our method.^[5, 35] Tumors have a reduced oxidative phosphorylation activity and many tumor cells derive most of their energy demand from glycolysis, which induces a reduced pH value in tumor tissue.^[158-161] The absence of ms^2i^6A provides a first indication that the impairment of mitochondrial activity in tumor cells known as Warburg effect is detectable using our isotope based quantification method.^[162] Thus, analysis of the tRNA modification ms^2i^6A could probably be installed as a tumor marker.

7.2 Strategy

Inspired by our initial results we decided to investigate a broader variety of mammalian tissues as well as cancer cell lines to further prove these observations. Additionally, a detailed analysis was performed with various bacterial species in order to test how the modification content changes between different species.

In order to obtain a higher amount of data, we increased the number of isotope-labeled nucleosides to 17, which are present at different positions in tRNAs (*Figure 27*). These reference nucleosides were applied for quantification in tRNA of the different organisms. Next to synthesis of more adenosine modifications, we also synthesized four methylated guanosine derivatives m^1G , m^2G , m^2_2G , and Gm as well as the deazaguanosine derivative Q as isotope-labeled nucleosides.^[163-167] The two tricyclic modifications OHyW and yW were additionally synthesized as isotope-labeled derivatives. Syntheses of nucleosides, which are not described in *Chapter 5.4* were performed by Dr. T. Brückl,^[140] I. Thoma, P. Thumbs, and A. Hientzsch. Details are described or will be described in their Ph.D. theses. Eleven of our reference molecules are present 3'-adjacent to the anticodon at position 37, where they are directly involved in the codon-anticodon interaction. Queuosine and Gm are present in the wobble position 34. The other methylated nucleosides are present in positions outside the anticodon stemloop. Our selection reflects the fact that the largest variety of modifications are found in the anticodon stemloop.^[3-5, 7, 35]

We performed all three studies in parallel. Dr. T. Brückl was responsible for the quantitative analysis of porcine tissues, while investigations on different bacterial species were performed as part of this thesis. M. Wagner extracted tRNA from different cancer cell lines and explained experiments of four cell lines analyzed in this thesis.

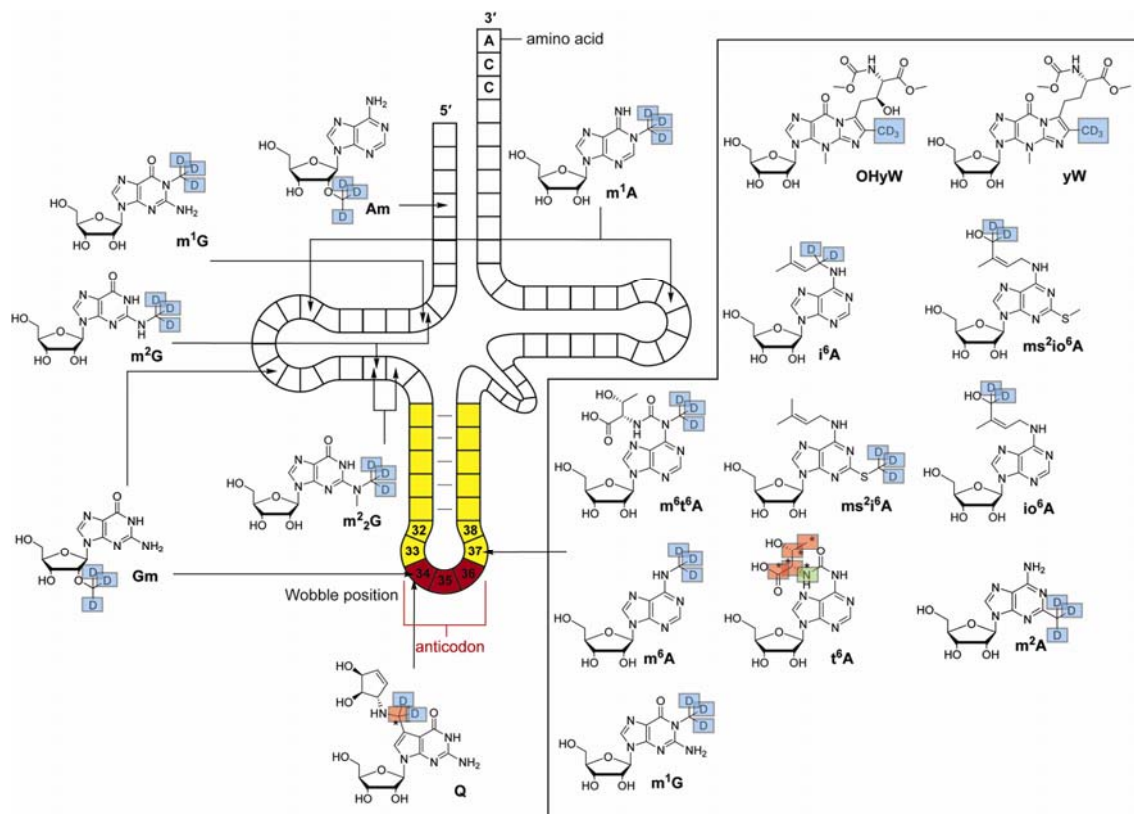


Figure 27: The seventeen synthesized modified tRNA nucleosides, which we applied for quantitative analysis during this Ph.D. thesis. The isotopic labels are indicated by color, with blue for D, red for ¹³C, and green ¹⁵N. Nucleosides are assigned to positions where they are placed in the tRNA.^[3-5, 7, 35]

7.3 Porcine tissue

The quantitative analysis of porcine tissues was performed for liver, spine marrow, spleen, kidney, lung, tongue, heart, thyroid gland, and the two brain regions cerebellum and cerebrum. Cerebrum and cerebellum were separated due to irreproducible results, which we obtained after mixing both brain regions.

We first investigated the mitochondrial modification $ms^{2i^6}A$.^[34, 168] The levels of this modification should therefore allow us to characterize the mitochondria density and activity. Indeed, we determined varying $ms^{2i^6}A$ levels in the investigated tissues (*Figure 28A*). We detected large amounts in heart, cerebellum and tongue, indicating high mitochondrial activity. Small values were found for liver, lung, and glands with up to six times less abundant than heart. To obtain a reference of mitochondrial activity, we measured cytochrome C oxidase activity for all tissues. The absolute values for cytochrome C oxidase activity (*Figure 28B*) correlate well with the $ms^{2i^6}A$ content with high significance ($P = 0.0017$, *Figure 28C*), which confirmed the previously observed correlation of mitochondrial activity with $ms^{2i^6}A$ levels. These measurements were performed by A. C. Kneuttinger.^[169]

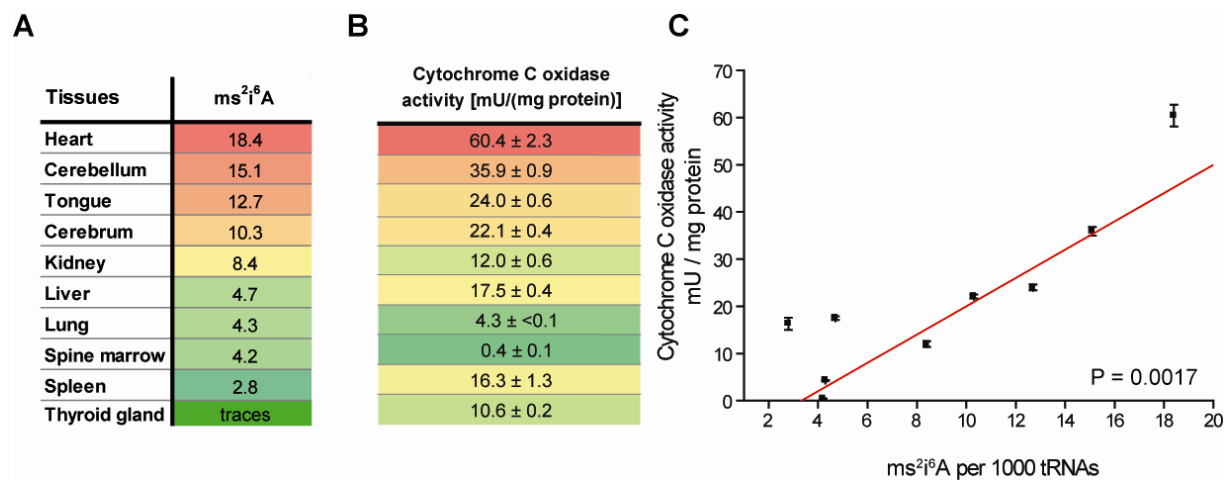


Figure 28: Tissue dependent cytochrome C oxidase activity in various tissues. Values of $ms^{2i^6}A$ are given per 1000 tRNA molecules (%); A) Levels of $ms^{2i^6}A$ in all tissues; B) Averaged cytochrome C oxidase activity data of tissues (mean ± s.d.); C) Correlation of the determined cytochrome C oxidase activity and the quantified values of $ms^{2i^6}A$ in all tissues except thyroid gland (which lacks quantitative data for $ms^{2i^6}A$; $P = 0.0017$).

In addition, we extracted mitochondria from the tissue samples before tRNA isolation.^[170] We obtained samples with enriched cytosolic tRNA as well as enriched mitochondrial tRNA and proved the purity of the preparations by measurement of cytochrome C oxidase activity as well as quantification of the mitochondrial tRNA nucleoside $ms^{2i^6}A$ (*Figure 29*). As

expected, the ms^2i^6A values follow the same trend as the cytochrome C oxidase activity. These data clearly provide evidence for a successful separation of cytosolic and mitochondrial tRNA pools. We proved this correlation for heart and liver (*Figure 29*). For all other tissues the ms^2i^6A content was used to prove depletion of mitochondria in cytosol samples.

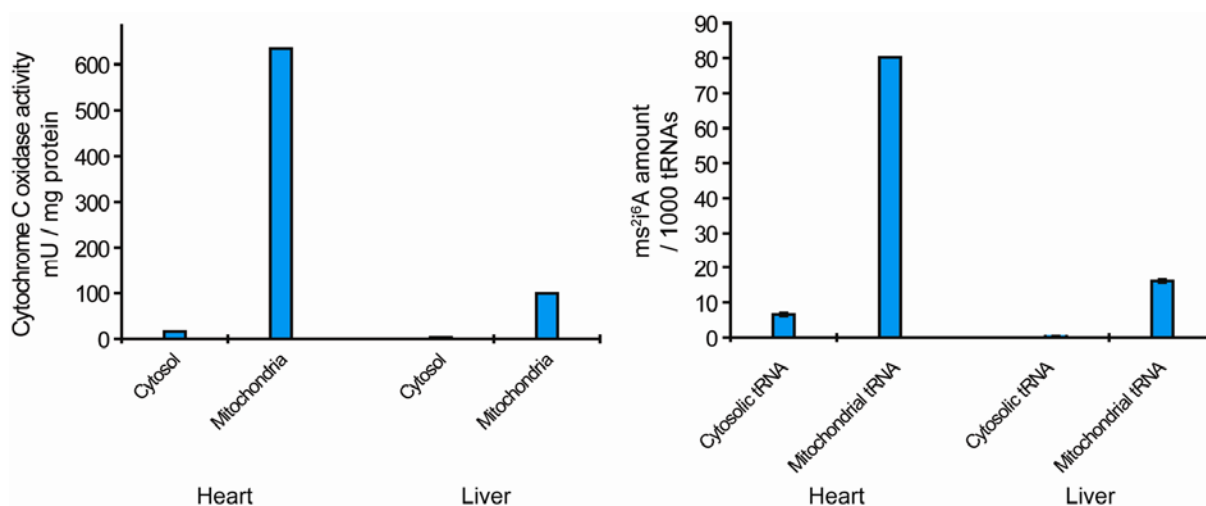


Figure 29: Cytochrome C oxidase activity and ms^2i^6A content after separation of mitochondria and cytosol. These values are increased in mitochondrial fractions and decreased in cytosolic fractions for the two representative tissues heart and liver.

Together with the absence of ms^2i^6A in cancer cell lines as described before (*Figure 26*), we proved that the method gives accurate insight into mitochondrial activity with the quantification of one modification only. A thorough literature search yielded similarly good correlations of the ms^2i^6A values to data for the ATP content,^[171] mitochondrial protein abundance,^[172] and activity^[173] with again good correlation supporting our findings (*Figure 30*).

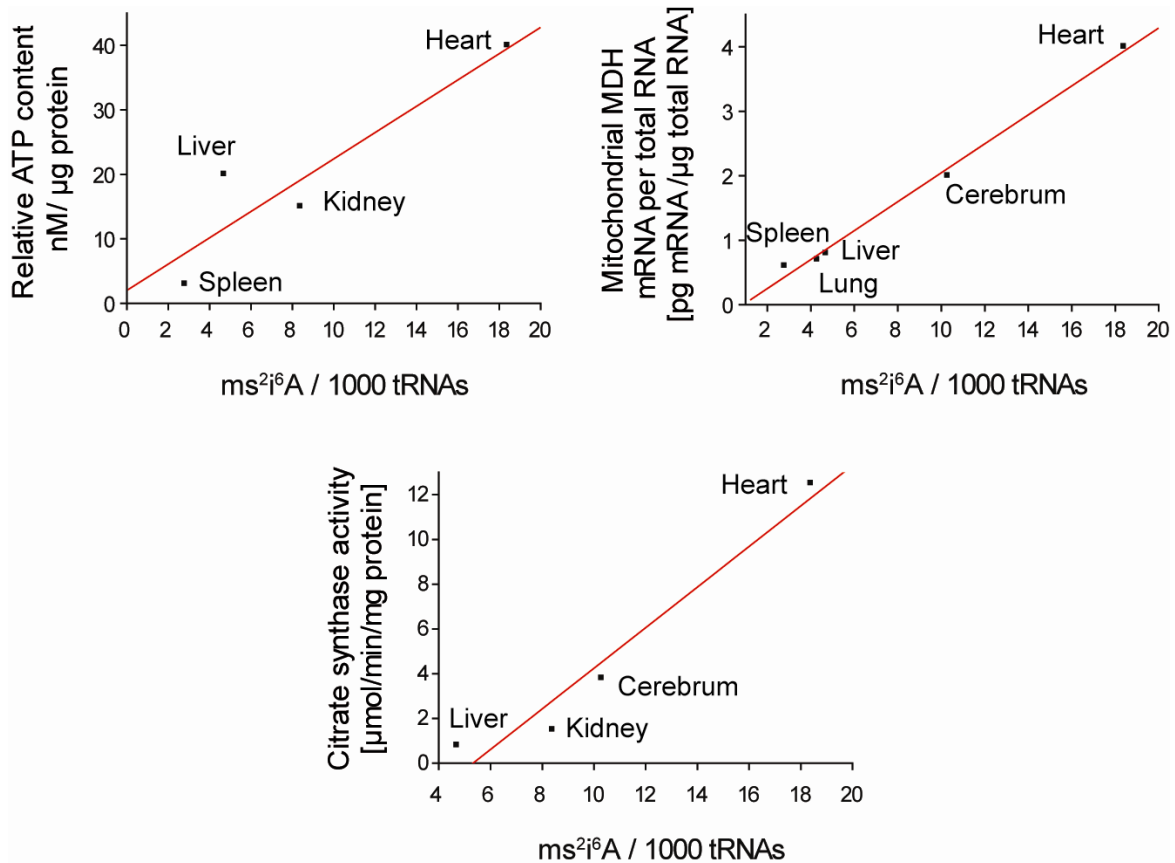


Figure 30: Correlation of ms²i⁶A content and mitochondrial specific activities in different tissues derived from literature. ATP content ($P = 0.082$),^[171] mitochondrial MDH mRNA amounts ($P = 0.0002$),^[172] and citrate synthase activity ($P = 0.025$)^[173] correlate well with the ms²i⁶A values.

The quantitative data obtained for the investigated modifications present in the tRNAs of the investigated tissues are shown color coded in *Figure 31*. The achieved %-values are normalized to the amount of tRNA present and do not represent the absolute concentration of a particular modification in a given tissue sample. Instead they indicate directly to which extent certain tRNA modifications are present at their expected position in the tRNA ensemble. Thus, the compiled data clearly shows that each tissue type tRNA ensemble is composed of different amounts of tRNA modifications, which are incorporated specifically to the demand of each tissue.

While the tRNA ensembles in liver and cerebellum tissue are modified to a large extent, those isolated from lung and kidney tissue are less modified in the specific positions. Important insights provide the data from the muscle tissues of heart and tongue. Here the modification level of the tRNA ensemble is significantly lower showing that many known modification

sites stay largely unmodified. An important fact for interpretation of these data is that the levels of these modified nucleosides do not correlate with $ms^{2:6}A$ values at all. We can conclude that high energy demands do not necessarily imply also a highly modified cytosolic tRNA ensemble.

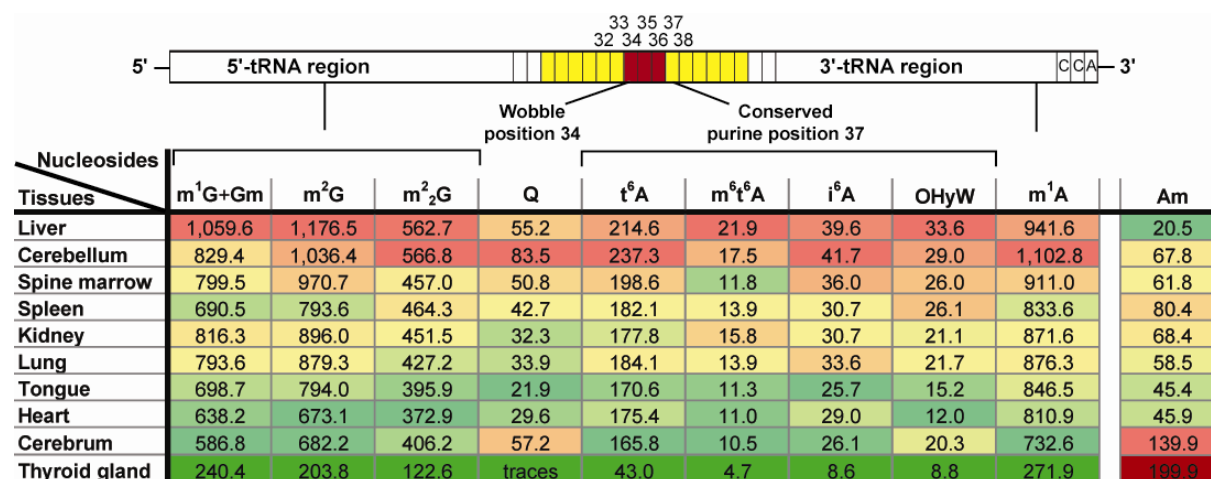


Figure 31: Quantitative data for the investigated tRNA modifications in various tissues. Data represent the amount of each modification per 1000 tRNA molecules (%). These data reveal a similar, tissue-dependent extent of modification for all investigated nucleosides except Am and $ms^{2:6}A$. Levels of Q in cerebellum and cerebrum are significantly increased relative to other modifications. The color code is based on quantile calculations; red: highest value, yellow: 50% quantile, green: lowest value, dark green (dark red): thyroid gland, for intermediate values appropriate shades of color were calculated.

A surprising observation is the different trend of Am, which seems to correlate almost inverse. Tissues which operate with a largely unmodified tRNA ensemble seem to have a high Am level, possibly to compensate for the accompanied loss in stability associated with low modification levels. The function of Am, which is present in the amino acid acceptor stem of the tRNA and which is the only known sugar methylation in a double-stranded tRNA region, has not yet been identified.^[130] However, 2'-O-methylation is generally considered to stabilize RNA and to prevent hydrolytic degradation.

Another interesting observation is the large difference measured between cerebrum and cerebellum showing impressively the high plasticity of the translational apparatus. These two modifications have an increased level of the hypermodified nucleoside queuosine, which could be worth investigating in future projects.

In order to further validate our hypothesis we decided to investigate the modification content in a sequence context, which is less sensitive to variations like dilution factors or impurities in the extracted tRNA ensemble. We therefore performed a parallel LC-MS analysis of partial tRNA RNase A digests from liver and heart which represent high and low modification levels, respectively. Additionally, these tissues have strongly deviating mitochondrial activity. The RNase A digests yield defined tRNA fragments (small oligomers) resulting from selective cleavage after C and U. We used the mammalian tRNA sequence database from the Sprinzl group^[168] to obtain sequences with potentially modified nucleosides. We then calculated the molecular weights of a representative set of modified tRNA fragments using the Mongo Oligo Mass Calculator program^[174] and identified these in the LC-MS data set. We analyzed these fragments in negative mode and mainly obtained the fragments with $m/z, z = -2$. The extent of modification of these tRNA fragments was then calculated directly from the ratio between the areas of the specific mass peaks for these oligomers carrying modifications and those for the corresponding unmodified fragments (*Figure 32*). The area ratios for heart and liver samples were compared to estimate the modification levels in a sequence context. This method is similar to a report which describes changes in the tRNA levels due to different growth conditions in *E. coli*.^[175]

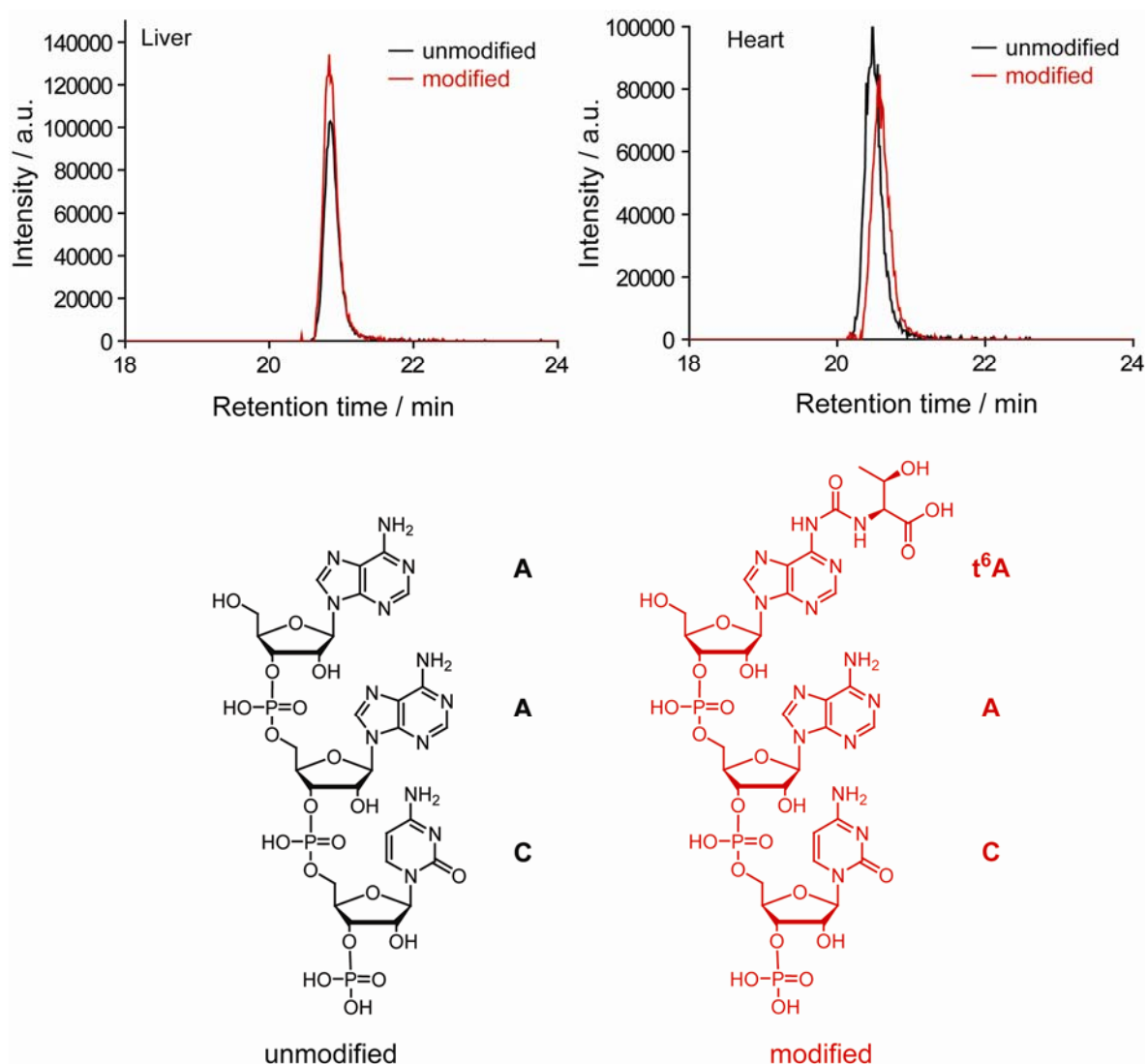


Figure 32: Representative comparison of relative amounts of unmodified RNA fragments AAC and the corresponding modified t⁶AAC in the RNase A digests of liver and heart tRNA. Overlaid LC-MS chromatograms showing ions detected at the calculated masses of the AAC ($m/z = 489.5682-489.5742$) and t⁶AAC ($m/z = 562.0863-562.0933$) fragments ($z = -2$). Structures of the modified (red) and unmodified (black) fragments.

We compared ten different fragments with the six representative modified nucleosides m¹G, m¹A, m²G, i⁶A, t⁶A, and ms²i⁶A. Also fragments with multiple modifications were investigated and combined indicate a large variety of specific sequences from the anticodon region and other parts of the tRNAs. The obtained results show that the representative fragments from liver tRNAs are indeed more modified than fragments derived from heart (*Figure 32*). The modified to unmodified area ratios of specific fragments in liver are higher than in heart or equal (*Table 4*). As expected from our quantitative values, the fragment

containing ms^2i^6A is more abundant in the investigated tRNA fragments from heart. These results support our quantitative findings that different tissues possess tRNA ensembles that vary substantially in tRNA modification levels.

Table 4: Modified tRNA fragments analyzed after RNase A digestion. The mass area ratios of modified to unmodified fragments from total tRNA of liver and heart are shown using specific mass peaks ($z = -2$). Analyzed fragments 1-7 clearly express higher modification levels in liver than in heart. Fragments 8 and 9 have similar modified to unmodified ratios. Fragment 10 represents a mitochondrial tRNA fragment containing m^2i^6A , which is present in heart and only in traces in liver. These relative non-quantitative data are in strict accordance to the quantitative values described in *Figure 32*.

Number	tRNA fragments	Liver (modified/unmodified)	Heart (modified/unmodified)
1	A- m^2G -Cp	1.00	0.62
2	G- m^2G -Up	0.49	0.41
3	m^1G - m^2G -Cp	0.59	0.35
4	t^6A -ACp	1.28	0.85
5	A- m^1A -AUp	20.3	3.69
6	G- m^1A -AACp	6.01	2.20
7	A- i^6A -ACp	1.07	0.14
8	G- m^1A -GCp	0.25	0.24
9	G- m^1A -Up	0.27	0.28
10	A- ms^2i^6A -AGCp	Traces (<0.1)	0.33

We reasoned that tissues might program their tRNA ensemble to individual translational needs by specifically inserting nucleoside modifications. So far we can conclude that tissues with a high protein synthesis demand utilize highly modified tRNAs, while cells that have a lower protein demand operate with less modified tRNAs. One can hypothesize that the modification content has a direct impact on the efficiency of translation.

In order to test this hypothesis further, we analyzed the impact of the modification content of total tRNAs extracted from the different porcine tissues on translational efficiency in an

in vitro assay.^[176] These experiments will give direct readout of the translational efficiency of different tRNA modification levels and thus will give insight in tissue specific regulation of translation.

For the determination of *in vitro* protein synthesis rates the total tRNAs from the six representative tissues liver, heart, cerebellum, cerebrum, kidney, and spleen were applied. To measure translation rates, we used an *in vitro* coupled transcription/translation reticulocyte lysate system. The original tRNAs present in the lysate were removed chromatographically with an activated ethanolamine-Sepharose column according to a previous report.^[176] Subsequently, identical amounts of the tRNA ensemble isolated from various porcine tissues were added to the tRNA depleted samples with additives to reconstitute the translation system. We used the T7 RNA polymerase and luciferase T7 control DNA to determine translational efficiency rates, which were measured by detecting the increase in luminescence accompanied with the production of the protein luciferase (*Figure 33*). Each assay mix was incubated at 30 °C and 1 µL aliquot was analyzed with the luciferase assay substrate at various time points up to 30 min.

Assays of tRNAs extracted from different tissues were analyzed in parallel with diverse tRNA-depleted lysate fractions to exclude artefact problems. A blank assay mix was measured as background to determine the activity of residual tRNAs and only fractions with low background activities were considered for analysis.

First, we used a tRNA concentration of 125 µg for each independent measurement, which is in the range as described before.^[176] The obtained *in vitro* translation curves are shown in *Figure 33A*. Progress of the luciferase synthesis was measured every third minute. Important is the lower activity of the background measurement which is starting later than fractions supplemented with tRNA. Initial synthesis rates were calculated by a linear fit of the slopes between 13-26 min and normalized to the highest value. These measurements were performed in triplicate with different tRNA-depleted lysate fractions. The obtained averaged values are shown in *Figure 33B* showing the highest values for the four tissues cerebrum, kidney, cerebellum, and spleen. Slightly lower values were obtained for liver and heart. These values do not show any differentiation between tissues and are not at all representing the correlation we obtained for the quantified tRNA modification levels (*Figure 31*).

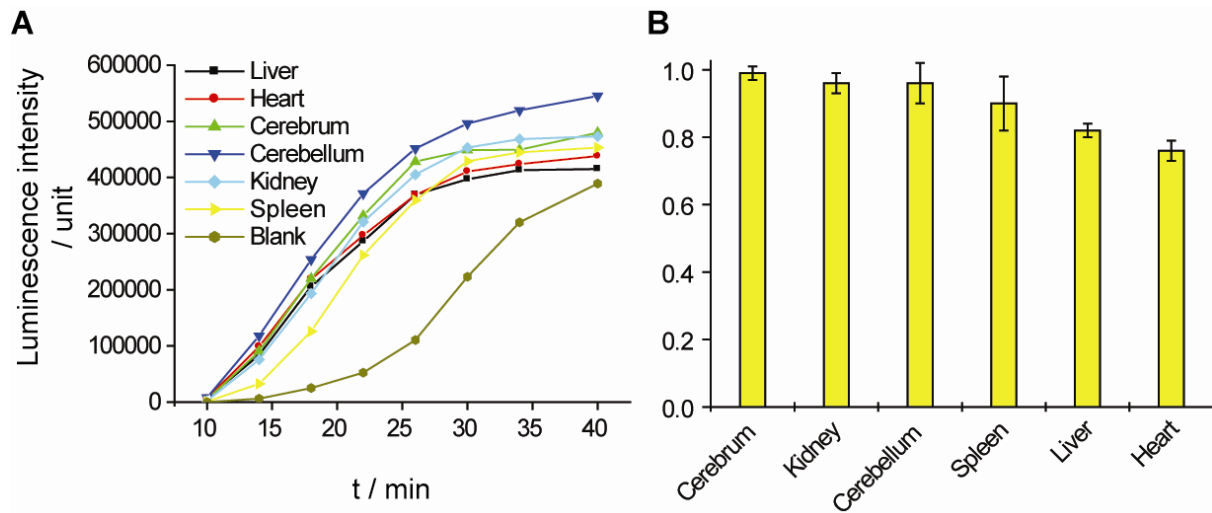


Figure 33: A) Representative *in vitro* translation experiment read out for tRNA from liver heart, cerebrum, cerebellum, kidney, spleen, and a background measurement. B) Averaged *in vitro* activities of each tissue with SD.

Two possible reasons for these unsatisfying results are discussed in more detail. First critical point could be a high impact of mixed cytosolic and mitochondrial tRNA ensembles. A second possibility could result from the fast increase of the determined curves. If the tRNA was provided in a large excess, the ribosomes would be saturated and subtle differences would disappear. We therefore reduced the amount of tRNA, because we are interested in the initial rates, which we can obtain with lower tRNA concentrations.

To address the first possibility, we decided to analyze tRNA preparations depleted of mitochondrial tRNA. For all following measurements we used 12.5 μg tRNA for each assay resulting in slower increasing curves (Figure 34). In this way the initial synthesis rates of luciferase associated to each tissue specific tRNA ensemble can be determined. Absolute values of these measurements vary substantially when using different isolated lysate fractions. However, reproducible trends were obtained after normalization of the linear fits to the highest value (liver or cerebellum). Liver tRNA was used in all measurements as reference tissue. Each correlation of liver to the other tissues was performed at least twice.

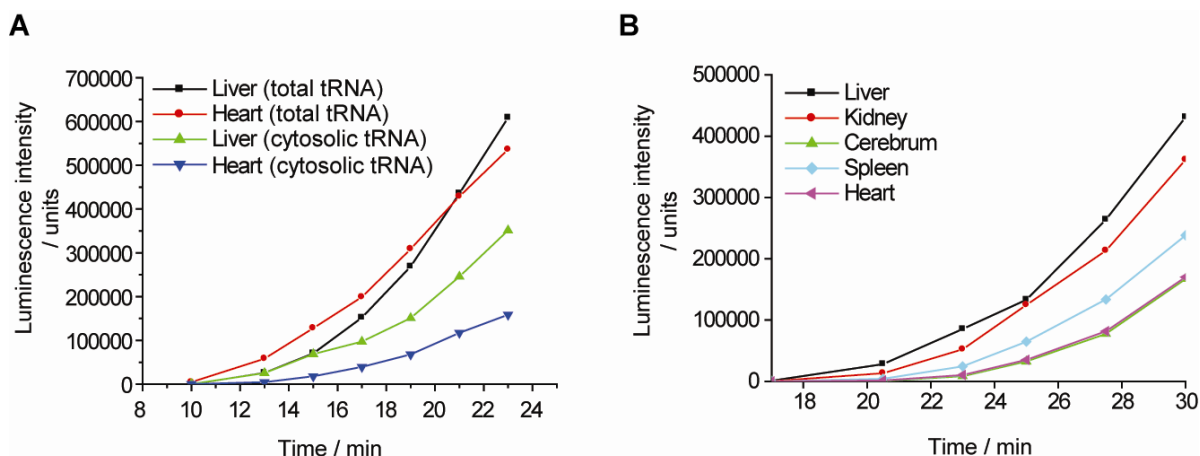


Figure 34: A) Representative *in vitro* translation experiment read out in comparison of total and cytosolic tRNA in heart and liver. These graphs clearly indicate a decreased activity of cytosolic compared to total tRNA. B) Representative *in vitro* translation experiment read out of cytosolic tRNA from the five tissues liver, kidney, cerebrum, spleen, and heart.

In order to test the impact of mitochondrial tRNAs we analyzed the rates of total and cytosolic tRNA of heart and liver. Mitochondrial tRNA from heart should have a huge impact to translational activity because of the high mitochondrial activity. Indeed, we determined higher efficiency of total tRNA compared to cytosolic tRNA and a tremendous enhanced activity of heart total tRNA. An example graph is shown in *Figure 34A*, which proved the necessity to remove mitochondria.

The results from these *in vitro* translation experiments are summarized in *Figure 35A* showing the obtained averaged data compared to a normalized measure of tRNA modification levels calculated from the LC-MS data. Normalization of our quantitative data include all nucleosides except m^2i^6A and Am .^[140] The translational efficiency of the isolated cytosolic tRNA ensembles were found to correlate with modification content ($P = 0.028$; *Figure 35B*). The high correlation coefficient shows that the modification content of cytosolic tRNA is a direct determinant of translational efficiency. We also investigated total tRNA of these six tissues and also found a strong correlation if the value from heart was excluded. This value is increased relative to the other tissues due to the high impact of the mitochondria (*Figure 35C*).

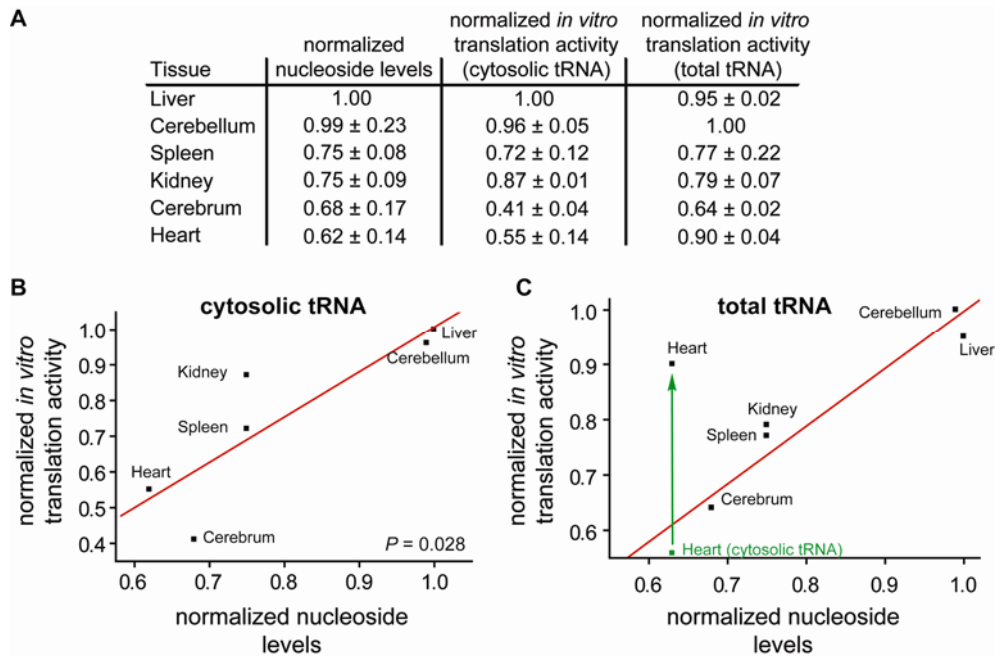


Figure 35: Translation activity of total and cytosolic tRNA originated from different tissues. A) Average normalized nucleoside levels of six tissues and relative *in vitro* translation activities of total and cytosolic tRNA. All values are normalized to the highest value and standard deviations (mean ± s.d.) are given for the other tissues. While the error values here are relatively large, these represent the variation over all modified nucleosides. The measurements for each nucleoside have low errors (~5%), and show the same relationship as the averaged set. B) Linear fit of relative *in vitro* translation activity of cytosolic tRNAs and normalized nucleoside levels showing a significant correlation ($P = 0.028$). C) Linear fit of relative *in vitro* translation activity of total tRNAs and normalized nucleoside levels showing a significant correlation for tissues except heart due to huge impact of mitochondrial tRNAs.

The obtained data support the idea that different tissues utilize varying amounts of modified tRNA in the tRNA ensembles to translate their genetic information into proteins. Further proof of this concept is a strong correlation of the quantitative tRNA modification data with *in vivo* protein synthesis rates determined by flooding dose experiments using radioactive labeled phenylalanine (Figure 36).^[177-178]

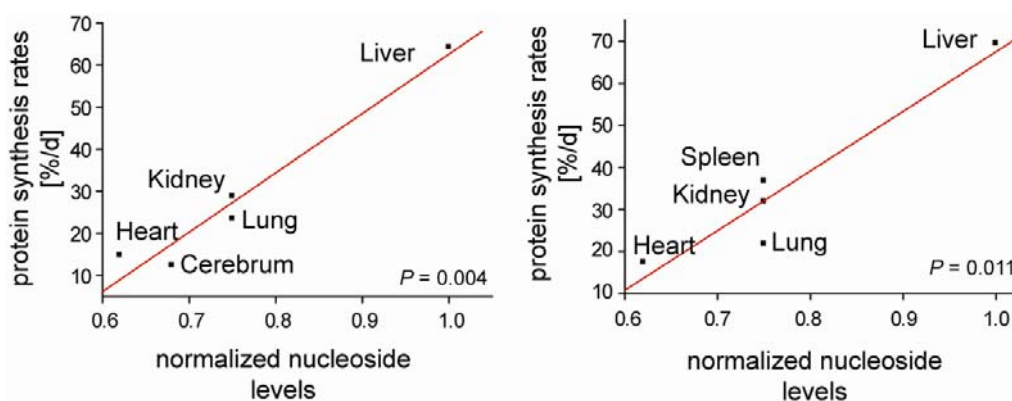


Figure 36: Correlations of *in vivo* protein synthesis rates with normalized nucleoside levels. These correlations also show high significance of $P = 0.004$ (left)^[177] and $P = 0.011$ (right)^[178].

Tissues that possess a highly modified tRNA ensemble have indeed a high protein synthesis rate. While it is known that the amounts of individual tRNA can vary between tissues,^[179-180] the fact that the quantitative data for the modifications m^1A and m^2G present in almost all tRNA species follow our correlation trend show that codon bias and tRNA composition do not affect our conclusions. A more detailed literature analysis can be found in the Ph.D. thesis of Dr. T. Brückl.^[140]

Our result can be explained by the fact that the translation rate is determined by the competition between near-cognate and cognate aminoacyl-tRNAs for binding to the ribosome^[181]. A high modification level increases the affinity of the correct tRNAs to the ribosome and thus allows faster discrimination. This reduces the ribosome step time, which in turn increases protein synthesis rate. We have now shown that this mechanism is used as a tool for regulation of the biosynthesis demand of each tissue by mammalian organisms. The tRNA modification level is hence another layer of information that programs cells regarding their translational potency.

7.4 Cancer cell lines

We further analyzed 12 cancer cell lines derived from different human tissues, which show a complete set of the investigated modified nucleosides from tRNA. This is surprising in light of the substantial chromosomal aberrations, gene mutations, and high proliferation rates that characterize cancer cells.^[182-184] Only the mitochondrial modification ms^2i^6A was absent in all cancer cell lines. This observation is supporting our previous interpretation of ms^2i^6A as a determinant of mitochondrial activity and further suggests a potential role of the nucleoside as tumor marker to differentiate between healthy and cancerous cells.^[163]

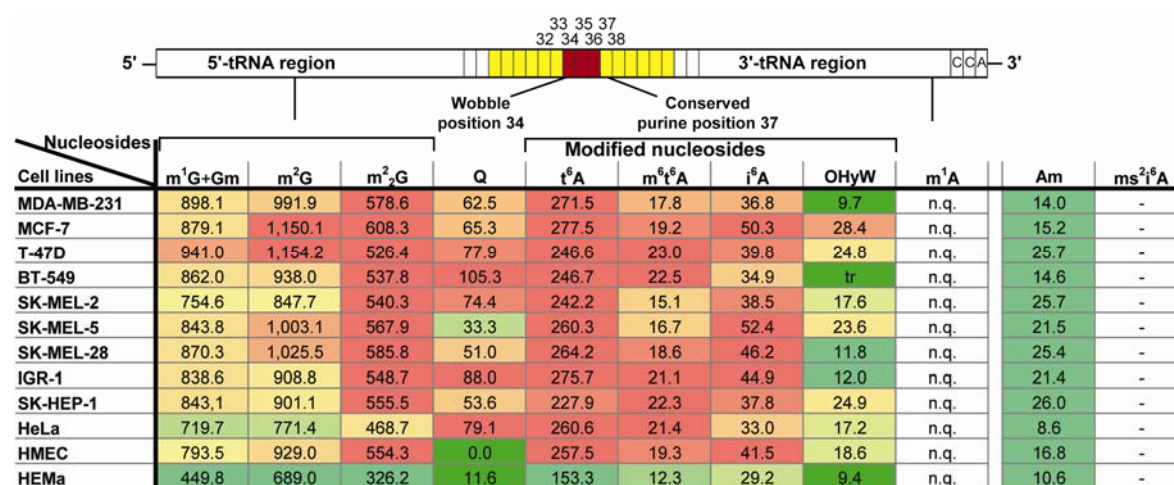


Figure 37: Quantitative data for the investigated tRNA modifications in cancer cell lines. Color code is based on the absolute coloring in *Figure 31* for better visualization of similarities to the highly modified tissue liver. n.q. = not quantifiable because m^1A LC-MS signals for cell lines overlap with G LC-MS signals. The modification ms^2i^6A could not be detected in any cancer cell line.

In addition, all cancer cell lines were found to possess largely elevated modification levels close to or even above those detected for liver tissue, which is the tissue found to maintain the most heavily modified tRNA ensemble (*Figure 37*). In line with the high protein synthesis rates shown for highly modified tRNA ensembles, these results can be explained by the high cell proliferation rates of cancer cells. This further proves the hypothesis, that highly modified tRNAs seem to be a requirement for efficient and competitive cellular growth. This is supported by the data of the primary cell line HEMa, which is only modified to a low extent. The low amount of Am found in cancer cell lines further supports the hypothesis that Am compensates for low modification levels and is thus present only in low quantities in the generally highly modified cancer cells. The two modifications Q and OHyW, which are incorporated into tRNA in complex biosynthetic routes, are the only exception to the high

modification levels. This observation hints for an impairment of the modifying system for these hypermodified nucleosides.

Furthermore, the fact that these modified nucleosides yield a modification pattern specific for each cell line allows fingerprint analysis of each cancer type. This observation could lead to diagnostic application of our method for analysis of each cancer type.

A more detailed interpretation of cell culture data will be described by M. Wagner in his upcoming Ph.D.-thesis who has grown the cell lines and extracted tRNA. The four cell line experiments were explained by him, which were analyzed in this Ph.D. thesis work.

7.5 *Phylogenetic analysis*

In an additional project we investigated the tRNA modification levels of different bacterial strains in a comparative analysis in order to investigate, if the tRNA modification patterns are conserved, random, or if the collection mirrors phylogenetic relationships. This would argue for a strong selective pressure towards fine-tuned balance of modified nucleosides in the translation machinery. Sequence similarity comparisons of the small subunit of rRNAs were performed to calculate phylogenetic trees using genomic databases which were the gold standard in the 80s and 90s.^[185-188] Horizontal gene transfer (HGT) was identified to have significant influence on the genome of bacteria.^[189] Barriers for HGT in *E. coli* for example were found to be very low under laboratory conditions and lead to the acquisition of genes different to the original developed ones.^[190] Therefore, alternative approaches were performed, which achieved phylogenetic correlation adopting protein sequence comparison of housekeeping genes,^[185, 191] homology of tRNA synthetase sequences,^[192] tRNA-dependent amidotransferases,^[193] and amino acid concentrations.^[185, 194] All these factors are present in every living organism, which is important for phylogenetic correlation calculations. tRNA modifications with their large structural diversity are perfect components, which were evolutionary developed and are of tremendous importance for survival. In addition, these are inserted by complex modifying machineries. For example, approximately 1% of the whole genome of yeast is responsible for insertion of modifications, not counting gene products involved in tRNA transcription and tRNA transport.^[195] This indicates the importance of correct modification system.

For this study we quantified 12 modified tRNA nucleosides depicted in *Figure 38*. Bacterial tRNAs are less modified compared to eukaryotic tRNA and most modifications are found in the anticodon stemloop. Most of our analyzed modifications (m^6t^6A , ms^2i^6A , io^6A , m^6A , t^6A , m^2A , m^1G , i^6A , ms^2io^6A , and Q) can be found at this position. The modification m^1A is present outside of the anticodon stemloop at position 58 in bacterial tRNAs.^[5, 7] In contrast to eukaryotic tRNA the modification m^1G is exclusively present at position 37 in bacterial tRNA. The 2'-*O*-methylated nucleoside Gm is present at the wobble position and in the DSL. We quantified it together with m^1G due to overlapping UV and mass peaks.

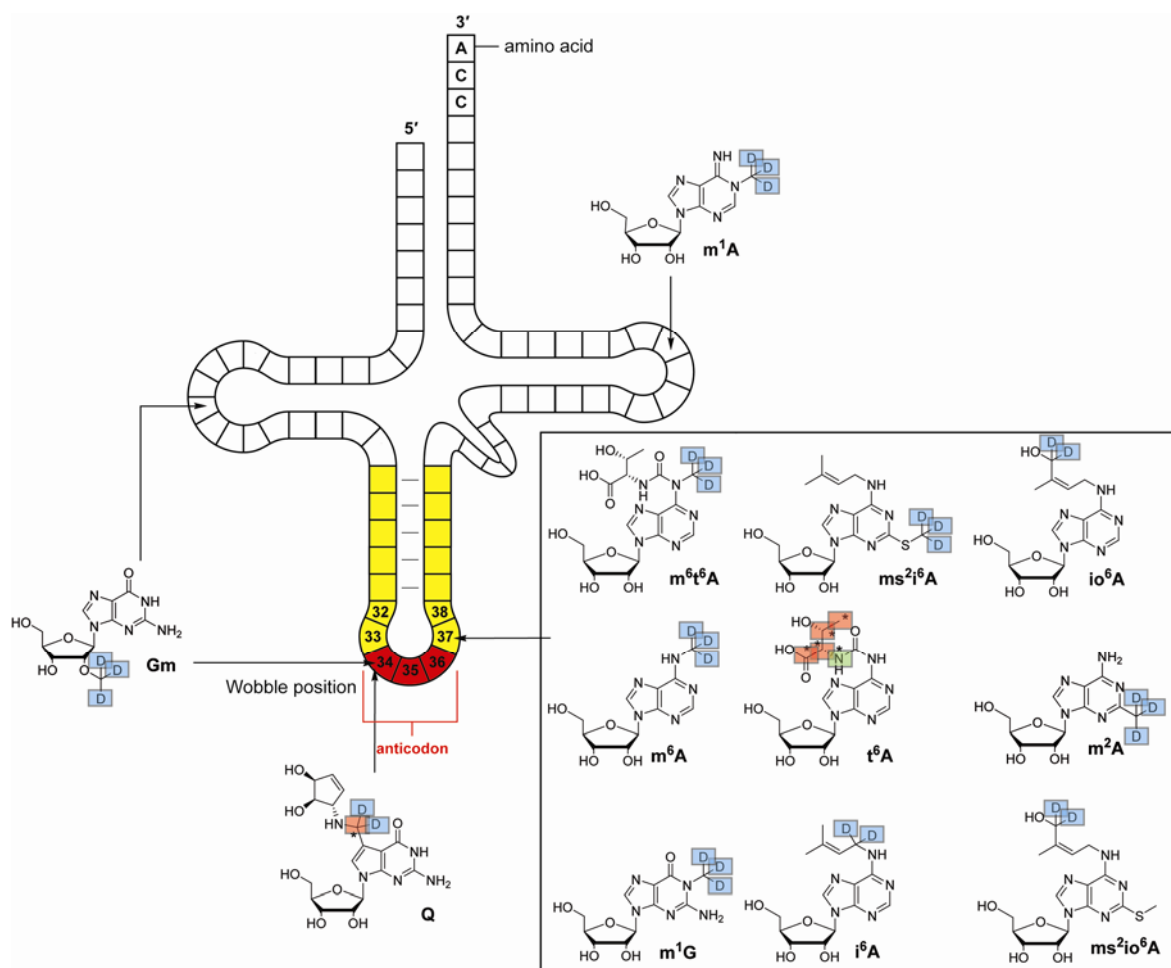


Figure 38: tRNA cloverleaf showing the investigated bacterial nucleosides. The 9 modified nucleosides m^6t^6A , ms^2i^6A , io^6A , m^6A , t^6A , m^2A , m^1G , i^6A , and ms^2io^6A are present at position 37. Q is present at the wobble position as well as Gm, which is additionally present at position 18. Modification m^1A is mainly present at position 58.^[5, 7]

With these labeled reference tRNA nucleosides in hand, we analyzed the tRNA modification pattern of five Gram-negative (*E. coli*, *Pseudomonas putida*, *Pseudomonas aeruginosa*, *Burkholderia thailandensis*, and *Burkholderia cenocepacia*) and five Gram-positive bacteria (*Bacillus subtilis*, *Listeria welshimeri*, *Listeria monocytogenes*, *Staphylococcus aureus* NCTC, and *Staphylococcus aureus* MU50) to cover several branches of the phylogenetic tree, as well as pathogenic and non-pathogenic species of the same genus.

We further analyzed the interesting bacterium *Deinococcus radiodurans*, which is controversially assigned to both Gram-groups. It is hypothesized that this bacterium as part of the genus *Deinococcus* is a possible prokaryotic intermediate in the transition from the Gram-positive to the Gram-negative bacteria.^[196] Biochemical characteristics of *D. radiodurans* from both bacterial groups support this hypothesis. This bacterium is stained like Gram-positive bacteria, but contains additional outer layers characteristic for bacteria

from the Gram-negative taxa, whereas the fatty acid profile is closer related to the Gram-negative than to Gram-positive bacteria.^[196-198] In addition, *D. radiodurans* can be assigned to either Gram-positive or Gram-negative bacteria depending on the method applied.^[196] We were interested how this bacterium with an ambiguous character would cluster in our analysis, also with respect to a described relation of *D. radiodurans* with archaea probably resulting from a horizontal gene transfer accompanied by interdomain fusion.^[199] In general, bacteria were grown under optimum conditions, followed by extraction of bulk tRNA and subsequent analysis of the nucleoside mixture resulting from tRNA digestion using our established quantitative HPLC-MS method.^[163] Bacteria were grown in collaboration with Prof. S. A. Sieber and handed to us after the first tRNA extraction step.

The results of the investigated prokaryotes are depicted in *Figure 39*. The distribution of the analyzed nucleosides shows large qualitative as well as quantitative differences over the investigated bacterial species. The five nucleosides m²A, m⁶A, m¹G, i⁶A, and t⁶A are present in all investigated organisms, but with largely varying levels ranging between 2 to more than 300 modifications per 1000 tRNAs (‰). The hypermodified nucleoside Q is unequally distributed over bacteria from different groups and is only absent in both bacteria from the genus *Listeria* and *D. radiodurans*. The modification m¹A is present in all Gram-positive bacteria and *P. putida* which is the only representative from the Gram-negative bacteria.

A first interesting observation is the presence of the two nucleosides m¹G and t⁶A in large quantities. They are known to be essential and expected to be important for the development of life.^[49] These are the only modifications, which are present in organisms of all three domains of life and must have evolved early.^[5, 7] While the amounts of m¹G do not show any systematic distribution in the investigated bacteria, t⁶A seems to be more abundant in Gram-positive than in Gram-negative bacteria. The modification m⁶A has the same tendency with values of up to 50 times more in Gram-positive bacteria, whereas values for m²A are up to 150 fold higher in Gram-negative bacteria. The hypermodified nucleoside m⁶t⁶A is only present in the γ -proteobacteria *E. coli* and both *Pseudomonas*.

The adenosine derivatives i⁶A, ms²i⁶A, io⁶A, and ms²io⁶A are nucleosides of one modification family containing an isopentenyl moiety at the exocyclic amine in position 6.^[3-4] The corresponding modifying enzymes *MiaA*, *MiaB*, and *MiaE* are modifying these adenosines at position 37 in tRNAs reading codons that start with CGN, CUN, and CCN (N stands for any canonical base).^[9, 200-201] While i⁶A is present in all investigated bacteria, ms²i⁶A is absent in *Listeria* and *P. putida*. According to literature, we found the two hydroxylated derivatives

io^6A and ms^2io^6A predominantly in the γ -proteobacteria with the genus *Pseudomonas*.^[202-203] Interestingly, *P. aeruginosa* contains all four isopentyl-derivatives, while *P. putida* lacks both 2-methylthiolated derivatives, which is somehow compensated by up to 12 times higher values of i^6A and io^6A . Furthermore, we detected the modified nucleoside ms^2io^6A in both β -proteobacteria *Burkholderia* as well as traces in *D. radiodurans* although the sequence of the modifying enzyme *MiaE* was not detected during genomic analysis.^[201] These data are indicating that the functionalities for the last hydroxylation step have evolved independently.

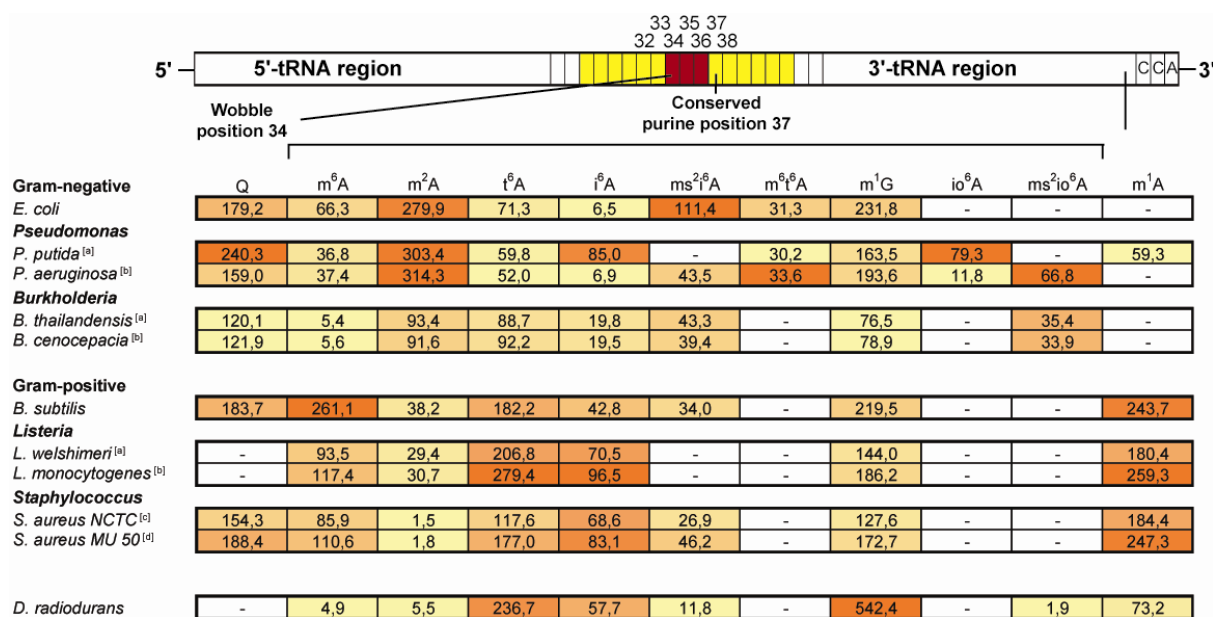


Figure 39: tRNA modification pattern of the investigated bacteria. tRNA modification levels are presented as nucleosides per 1000 tRNAs as average values of at least two independent growths with an average standard deviation of 7%. Listed are the five Gram-negative, then the five Gram-positive bacteria and at the end *D. radiodurans*. Each modification was color-coded independently (Red: Highest value; Yellow: Lowest value). ^{a)} non-pathogenic bacteria; ^{b)} pathogenic bacteria; ^{c)} non-resistant bacterium; ^{d)} methicillin-resistant bacterium.

Our data clearly indicate that the bacterium *D. radiodurans* exhibits a special character also in regard of the tRNA modification pattern. Interestingly, the two modifications m^1G and t^6A represent about 90% of all investigated modifications at position 37 of *Deinococcus* tRNAs. This ratio is about 50% in all other investigated bacteria. We also found the four bacterial modifications m^6A , m^2A , ms^2i^6A , and ms^2io^6A to be less abundant, while i^6A is present in similar quantities like in the other genera. In addition, this bacterium is lacking Q and contains m^1A . Combined, these findings confirm the special character of *D. radiodurans* also at the tRNA modification level as described before for other biosynthetic processes^[196] and are of high interest from an evolutionary point of view. This tRNA modification pattern with

signatures from both Gram-types indicates that this bacterium is an intermediate between Gram-positive and Gram-negative bacteria.

In addition, the two predominately modified nucleosides t⁶A and m¹G of *D. radiodurans* are exclusively present at position 37 in archaeal tRNA.^[5, 7] This is in line with the observation of horizontal gene transfer from archaea to *D. radiodurans*,^[199] and further supports the interdomain fusion hypothesis that *D. radiodurans* is a possible hybrid organism of archaea and bacteria. These data demonstrate the high importance of these two modifications for organisms, which may be considered as a minimal set of modified tRNA nucleosides at position 37 for unicellular organisms. As reported before, they could be possible nucleosides of the last universal common ancestor (LUCA) due to their abundance in all domains and therefore had to develop early during the evolution of life.^[61]

Inspired from these differences between each species as well as the two different Gram-groups we applied a hierarchical clustering algorithm using the programs *Cluster* and *Treeview* for homology analysis.^[204-205] We used the Euclidean distance correlation for a measure of similarity, because in our opinion this is the most suitable calculation possibility for our data sets. We included the quantitative data of liver, kidney, spleen, and heart, which represent four porcine tissues with high, medium, and low protein synthesis rates. Additionally, the data of mitochondria and cytosolic tRNA from heart and liver were incorporated in our analysis. We added the two yeast strains *S. cerevisiae* and *S. pombe* as unicellular eukaryotes as well, which were extracted and quantified by A. Hienzsch. In total, we applied 17 different modified tRNA nucleosides as well as 16 different organisms and with all tissues from *S. scrofa domestica* we clustered 24 different data sets in total.

To the best of our knowledge, no quantitative data of tRNA modifications has been applied for homology comparison yet. Only one report claims phylogenetic correlations based on the presence of conserved modifications in archaeal, which are compared with the phylogenetic tree.^[90]

Indeed, this *Cluster* analysis of modified tRNA nucleosides resembles the phylogenetic tree with distinct differentiation of eukaryotic and prokaryotic organisms (*Figure 40*). The eukaryotic organisms are separated from each other with very close correlation of both yeast strains and a correlation of 70% to the different porcine tissues. These are clustered in tissues according to their average amount of tRNA modification levels. Obviously, Gram-negative and Gram-positive bacteria are clearly separated. Even very closely related bacterial classes

like γ -proteobacteria (*E. coli* and both *Pseudomonas*) and β -proteobacteria (both *Burkholderia*) are distinguishable. Distinct differentiation of the three Gram-positive bacteria from the phylum *Firmicutes* proves the high resolution of our analysis. Interestingly, *D. radiodurans* indicates the ambiguous character in our Cluster analysis as well. This bacterium is identically well correlated with Gram-positive and Gram-negative bacteria. This can be explained by an impact of both Gram-groups in biosynthetic processes,^[197] and could hint for *D. radiodurans* as an evolutionary intermediate of both bacterial groups.^[206]

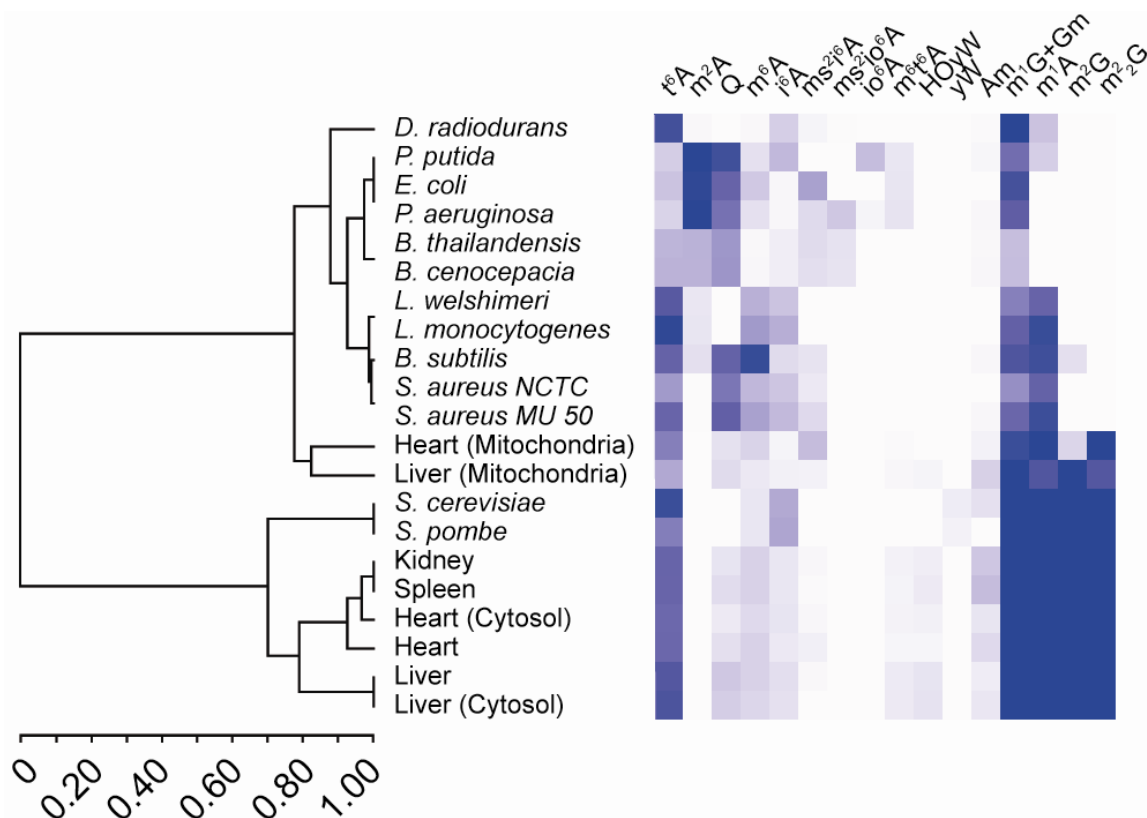


Figure 40: Cluster analysis using quantitative data of analyzed modified tRNA nucleosides of bacteria, two yeast strains, four selected tissue from *S. scrofa domestica*, and mitochondrial and cytosolic tRNA from heart and liver. Clustering was performed using the programs *Cluster* and *TreeView* correlation of the measured values with average linkage clustering using the Euclidean distance correlation as the measure of similarity.^[204-205] Blue color scale intensities represent the relative tRNA nucleoside amounts. The scale bar represents relative similarity of organisms between a factor of 0.0 to 1.0.

Whereas mitochondrial data sets of liver and heart are related to prokaryotic organisms the corresponding cytosolic data sets are clustering with the other eukaryotic organisms. This interesting observation is in line with the fact that mitochondria originate from prokaryotes. This correlation is certainly shown by our analysis. However, this is a surprising fact, because mitochondrial tRNAs contain modifications from eukaryotes and prokaryotes. Furthermore, the data indicate the higher impact of mitochondrial tRNA in heart compared to liver. Total

tRNA of liver and the corresponding cytosolic tRNA show higher similarity compared to total tRNA from heart with its cytosolic values. This result is according to the *in vitro* translation experiments (Figure 35). Both unicellular yeast strains cluster with eukaryotes and are additionally distinct separated from all porcine tissues. This shows the difference between mammals and unicellular organisms. *S. cerevisiae* and *S. pombe* are correlated perfectly with each other.

Analysis of phylogenetic correlations for only prokaryotes revealed the high resolution of our method (Figure 41). The more detailed analysis indicates the close relation of bacteria from one genus with an excellent correlation factor of 0.94. *P. aeruginosa* is clustered in closer relation to *E. coli* with a factor of 0.94 than *P. putida* with a similarity of only 0.88, although they are bacteria from the same genus. A possible reason could be the different biochemical properties of members from the genus *Pseudomonas* which are further subdivided in several main groups.^[207] *P. aeruginosa* and *P. putida* are representatives of two subgroups which exhibit different biological properties.^[208] High levels of horizontal gene transfer could be a reason for the different modification levels in the two investigated *Pseudomonas* by a possible early diverse gene development of each species.^[209] Horizontal gene transfer was proven for aminoacyl-tRNA genes and could influence the development of tRNA modifications as well.^[210-212]

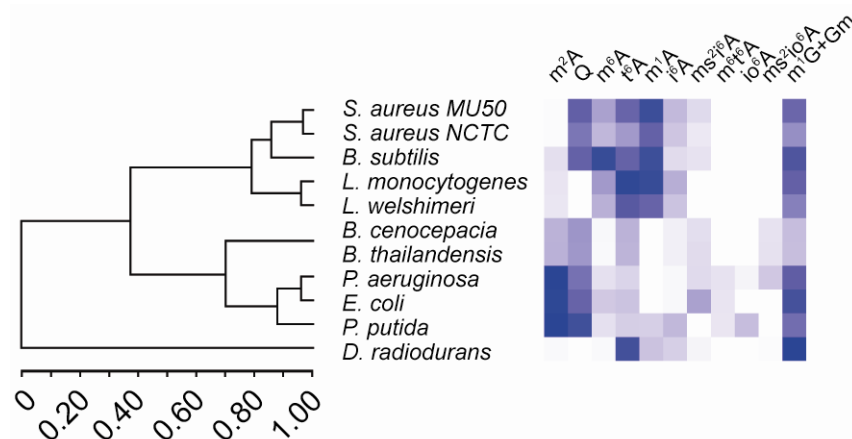


Figure 41: Cluster analysis using quantitative data of analyzed modified tRNA nucleosides of all investigated bacteria. Clustering was performed using the programs *Cluster* and *TreeView* correlation of the measured values with average linkage clustering using the Euclidean distance correlation as the measure of similarity.^[204-205] Blue color scale intensities represent the relative tRNA nucleoside amounts. The scale bars represent relative similarity of organisms between a factor of 0.0 to 1.0.

The exceptionally high resolution of our quantitative tRNA modification data represents the phylogenetic tree, which is comparable to other described correlations.^[185, 191] Furthermore,

we were even able to prove the correlation of mitochondrial tRNA from pork with prokaryotes. These largely varying quantitative results paired with the phylogenetic correlation indicate the different development of modified nucleosides for optimum viability of each bacterial species. All these observations indicate optimization of modified tRNA nucleosides resulting in an evolutionary controlled distribution and the Darwinian fitness in order to adapt to their specific environment. The fact that we have mainly analyzed modified nucleosides present at position 37 is supporting the extended anticodon hypothesis. In this theory, almost the whole anticodon stemloop is responsible for correct codon anticodon interaction.^[10, 29, 213] Therefore, modifications have to be evolutionary adapted in parallel to the genetic code. Our data additionally hint for a high impact of horizontal gene transfer especially for the bacterium *D. radiodurans* with most modifications known to be present in archaeal tRNAs.^[199, 209-212]

7.6 Pathogenic bacteria

Another possible application of our method is the differentiation of pathogenic from non-pathogenic bacteria. Bacterial infections are the primary cause of death in the intensive-care units of hospitals worldwide and represent a highly important challenge.^[214] Antibiotic resistance and biofilm formation as defense strategy are increasing the threat of bacteria to humans,^[215-216] which is fueling investigations to target bacteria with novel tools.^[217-220] Specific and fast treatment of each pathogen requires methods for distinct differentiation. In the last decade PCR analysis was established as the method of choice.^[221-223] Our method could be applied as further analytical tool to distinguish bacteria. Therefore, we compared three pathogenic and non-pathogenic bacteria pairs from the genera *Pseudomonas*, *Burkholderia*, *Listeria* and one methicillin-resistant and non-resistant pair from the genus *S. aureus* (Figure 39). These bacteria represent a selection of the most dangerous clinical pathogens, which are responsible for many death incidents.

We are able to distinguish between Gram-positive and Gram-negative bacteria by their different tRNA modification pattern.^[224] For example, we are able to assign the Gram-group to a bacterium by the amounts of m⁶A, m²A, and t⁶A, which have varying values in the two Gram-types (Figure 39). If we take the other modifications into account, we are even able to assign the genus of a bacterium. The content and absence of a modified nucleoside leads to a fingerprint for bacteria and enables fast differentiation. In the case of *Pseudomonas*, *Listeria*, and *Staphylococcus* the pathogenic and resistant species can be distinguished from their

non-harmful counterpart, which probably indicates the different enzyme requirements like for the genus *Pseudomonas*.^[207-208] While the modification content was considerably higher for the pathogenic and the resistant species in *Listeria* and *Staphylococcus*, respectively, the two *Pseudomonas* species even contain a different modified tRNA nucleoside set. While the pathogenic species *P. aeruginosa* contains all four derivatives i⁶A, ms²i⁶A, io⁶A and ms²io⁶A, the non-pathogenic species *P. putida* contains only i⁶A and io⁶A lacking the methylthio group at position 2. Interestingly, the presence of the methylthio moiety is important for synthesis of virulence protein *VirF* in *Shigella flexneri*.^[76] Inhibition of the biosynthesis of this modification could be a possible drug-target to inhibit virulence. On the other hand, nucleoside m¹A is only present in the non-pathogenic species *P. putida*.

Both *Burkholderia* species showed almost no difference and are therefore hardly distinguishable by their modification pattern. This is known also for other methods, that bacteria from this genus are very closely related and distinguishable only using special methods.^[225-226] In our case, differentiation of these two species may be possible with an increased number of modified nucleosides like cytidine and uridine derivatives even though we quantified the most frequent modifications. However, our method provides a novel possibility for differentiation between pathogenic and non-pathogenic bacteria.

The ability to characterize bacteria based on tRNA modification pattern may be clinically useful. Each bacterial genus can be designated by the modification pattern and even pathogenic and non-pathogenic bacteria can be discriminated using our method. It would be possible to use the obtained data in this Ph.D. thesis as reference values for pathogenic isolates in the clinic.

7.7 *Stress response*

The obtained differences between cancer cell lines, healthy tissue and between the investigated prokaryotes led us to the question if cells regulate their modification pattern in response to environmental changes. We have chosen the easy available model organism *E. coli* which is one of the most studied organisms. Changes in the tRNA composition and proteomic analyses were shown after application of several stress conditions like osmotic stress,^[227-228] thermal stress,^[229] nutrients depletion,^[230] and oxidative stress^[231-232] for different unicellular organisms. So far, no data are reported, which include quantification of modified nucleosides in response to these applied stress conditions.

We analyzed the amounts of the two modifications m^2A and m^6A , which are present 3'-adjacent to the anticodon at position 37. Important is the fact that these two modifications are synthesized by two different enzymes resulting in independent responses to external stimuli. Additionally, the nucleoside m^6A is only present in tRNA^{Val}, while m^2A is present in six different tRNA species.^[3] Nucleoside m^6A carries a methyl group at the exocyclic nitrogen, while m^2A is assembled by a rarely present carbon-carbon bond formation in purines (*Figure 42*).

We determined reference values for m^2A (121.4 pmol) and m^6A (29.3 pmol) in 12 ng of total *E. coli* tRNA under optimum growth conditions at 37 °C in LB medium. All presented data points are average values of two independent cultivations and at least three independent digestion experiments. We strictly applied stress initiation at OD = 1.0 after we observed an dependence on culture density.^[140]

We first varied the pH value to three different values of acidic stress (addition of 4M H₃PO₄) and three different values of alkaline stress (addition of 2M NaOH) compared to normal medium at pH = 6.5. For m^2A the determined values decreased significantly for all deviations from the normal pH-value ranging from 20–40% with one extreme reduced value of 75% at pH = 9.5 (*Figure 42A*). All changes of nucleoside levels were reproducible with high accuracy. In the case of m^6A no changes were detected for the pH-range of 5.5 to 8.6. For acidic conditions lower than 5.5 and basic conditions decreased values of 25–30% were detected. These results probably indicate an individual down-regulation of the modified tRNA nucleoside level to external stimulation independent for each modified nucleoside m^2A and m^6A .

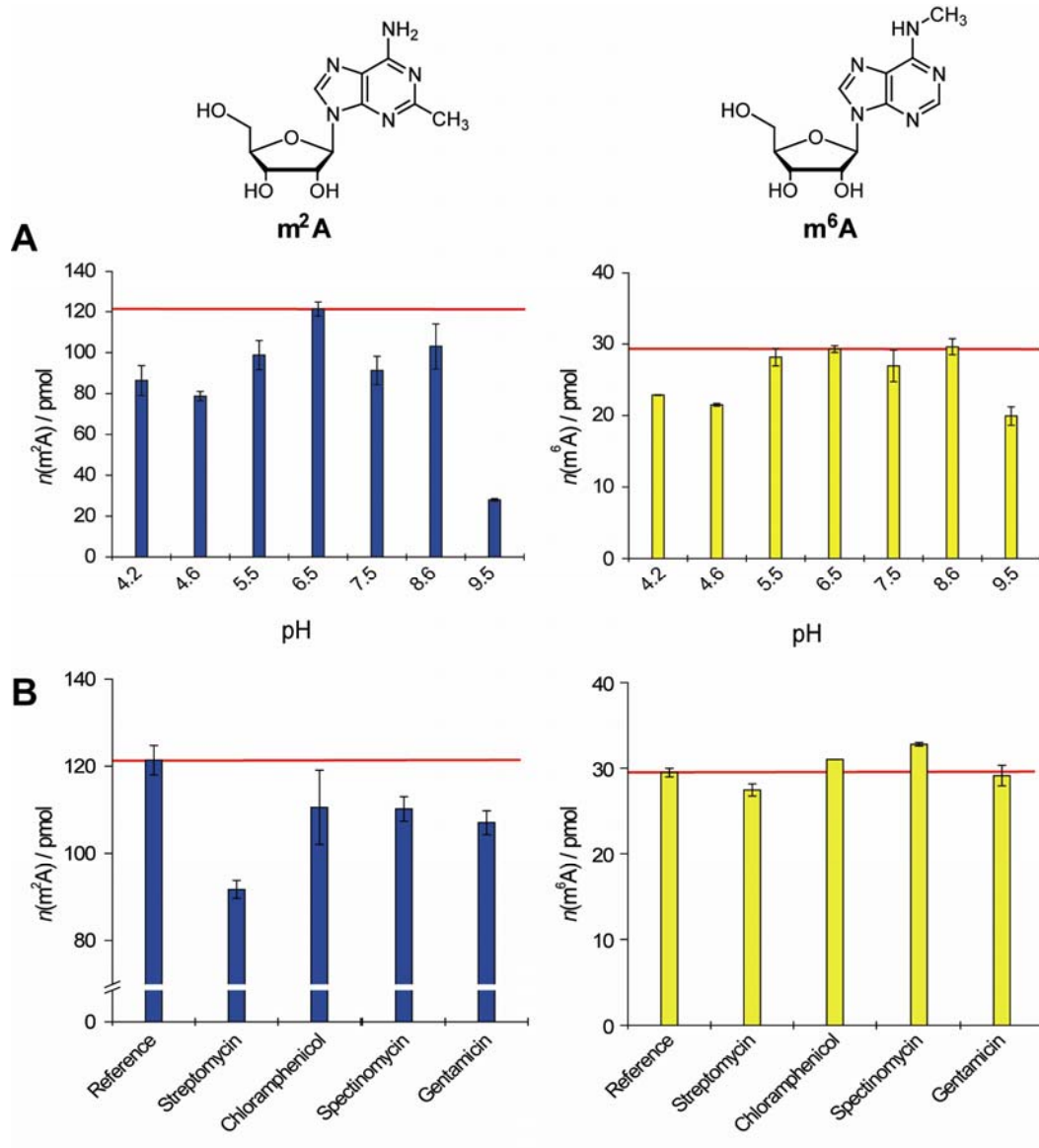


Figure 42: Influence of different pH-values and antibiotics on the nucleoside levels of m²A (blue) and m⁶A (yellow) in *E. coli*. In total, 12 µg of total tRNA were analyzed and the bars represent average values with standard deviation.

In addition to these results we were interested to study the influence of antibiotics to the tRNA nucleoside level. We applied four different ribosome-binding antibiotics at non-lethal concentrations, which are directly influencing the bacterial translation process. We used the three aminoglycosides Streptomycin, Spectinomycin, Gentamicin, and the broad-spectrum antibiotic Chloramphenicol. Aminoglycosides antibiotics are known to bind tRNAs, which hinder aminoacylation of the affected tRNA.^[233-236]

After exposure of *E. coli* to antibiotics we detected again a strong antibiotic-dependent reduction of m²A. While for Chloramphenicol, Spectinomycin and Gentamicin the amount of m²A is decreased by 5–12%, the impact of Streptomycin on the m²A level is 25%. For the

modified nucleoside m⁶A we detected a different pattern. It is only reduced after Streptomycin application, while the m⁶A level is raised after Chloramphenicol and Spectinomycin treatment. A constant level was observed after application with Gentamicin compared to the reference data. The changes of nucleoside m⁶A range from 6–12%. Streptomycin has a clearly different impact compared to the other investigated antibiotics. It induces an at least two fold higher reduction of m²A and a unique decrease for m⁶A. These results indicate that antibiotics can influence the tRNA modification level.

These reproducible changes imply directed nucleoside level variations as a reaction to external stimulation and lead to a directed quantitative response of the modified tRNA nucleoside level in *E. coli*. Interestingly, the low variations of m⁶A are in line with a recent report, that m⁶A enhances cellular survival during osmotic and oxidative stress.^[228]

Furthermore, we investigated the influence of provided nutrients on varying nucleoside levels. We grew *E. coli* in minimum MOPS medium and found the same amounts of m²A and m⁶A like for the reference data.^[237] But, we observed in these experiments the appearance of the modified nucleoside epoxyqueuoosine (oQ), which is the precursor of Q. It is known, that this last biosynthetic step is a vitamin B12-dependent reduction, even though the modifying enzyme is not identified yet.^[238-240] We detected oQ in tRNA of *E. coli* grown in MOPS medium because it is lacking vitamin B12. Our constant values indicate no influence on the levels of m²A and m⁶A by presence of the precursor oQ instead of Q. These results prove the importance of sufficient nutrients for an organism to maintain the optimum biosynthetic machinery.

We used these tRNA extracts for identification of the modified nucleoside oQ, which was synthesized by I. Thoma. After enzymatic digestion of bulk tRNA containing the natural oQ, we spiked the synthesized nucleoside in a 1:1 ratio and analyzed this mixture using HPLC-MS (*Figure 43*). The resulting single mass peak without a second peak indicates the correct stereoisomerism of the synthetic nucleoside.

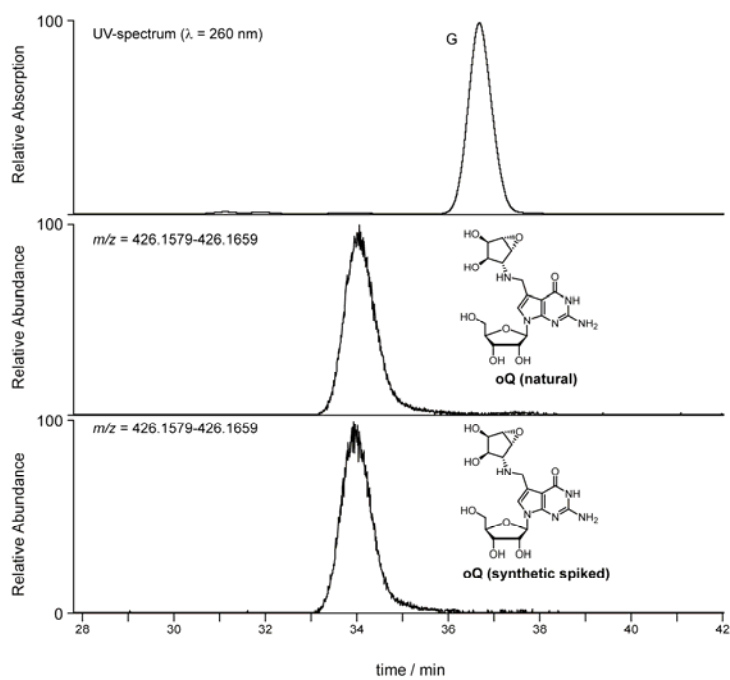


Figure 43: HPLC-MS analysis of oQ. The specific mass range for the natural and the spiked synthetic oQ indicate the correct stereoisomerism of the synthetic nucleoside.

8. Modified nucleosides in DNA

8.1 5-Hydroxymethylcytosine

Next to the four canonical bases A, C, G, and T natural modifications also exist in genomic DNA (*Figure 44*).^[241] The epigenetic modified base 5-methylcytosine (mC) is the most abundant modification in mammalian DNA, which is present in promoter elements (CpG sequences) and is responsible for repression of gene transcription.^[13-14] This modification was first identified as DNA constituent in the early 50s^[242] and since then huge efforts were made to elucidate the role of mC.^[13, 15, 243-244] In 2009, the modification 5-hydroxymethylcytosine (hmC) was detected in purkinje neurons in the cerebellum of mammalian tissue indicating a potential role in neuronal function.^[20] The hydroxylating α -ketoglutarate and Fe(II)-dependent Tet protein family was identified to convert mC to hmC in embryonic stem cells (ES cells) and hmC appears to play an important epigenetic role in mammalian cells.^[21, 245] Previously, hmC was reported to be present in high amounts in rat liver,^[246] but these results could not be verified by others.^[247] Moreover, this modified base was identified in T-even bacteriophage DNA, where it is further glycosylated by specific transferases to protect the phage DNA from cleavage by host nucleases.^[248-249] However, the role of the new sixth base in mammalian DNA has not been elucidated yet. To shed light onto the function of hmC, we adopted our HPLC-ESI-MS based method developed for tRNA nucleosides to quantify mC and hmC contents in mammalian tissue.

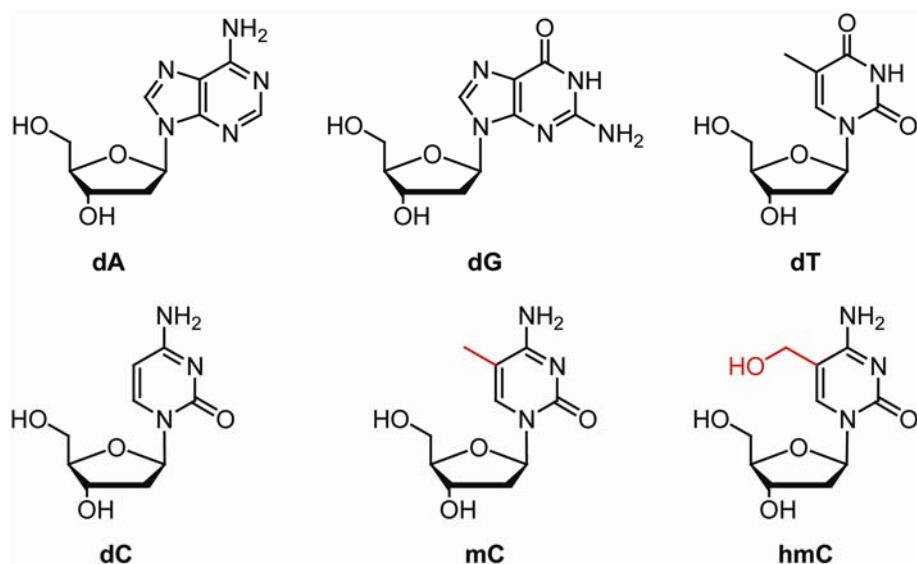


Figure 44: The canonical DNA nucleosides with the two mammalian epigenetic modifications mC and hmC. Alterations to C are shown in red.

8.2 Quantification of hmC by HPLC-ESI-MS

With the knowledge of the described tRNA projects, we were able to rapidly modify the method to quantify these two DNA modifications in mammalian tissue (*Figure 45*). Quantification using HPLC analysis as described before for mC^[247, 250-251] is not possible for hmC due to the low amounts present in genomic DNA. The signal is therefore mainly hidden in the baseline of the HPLC chromatogram. The more sensitive coupled HPLC-MS method with the specific high resolution mass range allowed us to quantify hmC.^[154, 252]

In the first step tissues were homogenized to extract genomic DNA. This procedure was developed by Dr. T. Brückl and Dr. M. Müller using porcine tissue and is based on the phenol extraction which is a key step also in the tRNA isolation procedure. Enriched samples of DNA were obtained after two RNase digestion steps.^[140] After optimization of the extraction method sufficient amounts of DNA from tissues were extracted to enable precise quantification. Enzymatic hydrolysis was performed with the same method like for tRNA digestion to also achieve complete DNA hydrolysis. We used the same HPLC gradient as previously applied for synthetic DNA hydrolysis experiments in the Carell group, because it facilitates separation of the canonical bases and the two modified nucleosides mC and hmC. The isotope-labeled nucleosides d₃-mC and two different isotope-labeled nucleosides ¹⁸O-hmC and d₂-hmC were used as reference compounds for quantification. These compounds were synthesized by M. Münzel and will be described in his upcoming Ph.D. thesis. In the course of this Ph.D. thesis these nucleosides were applied to determine

calibration curves, which resulted in excellent R^2 values of at least 0.998 (Figure 47). The isotope-labeled nucleosides were thereafter applied as isotope-labeled reference compounds in the quantification experiments.

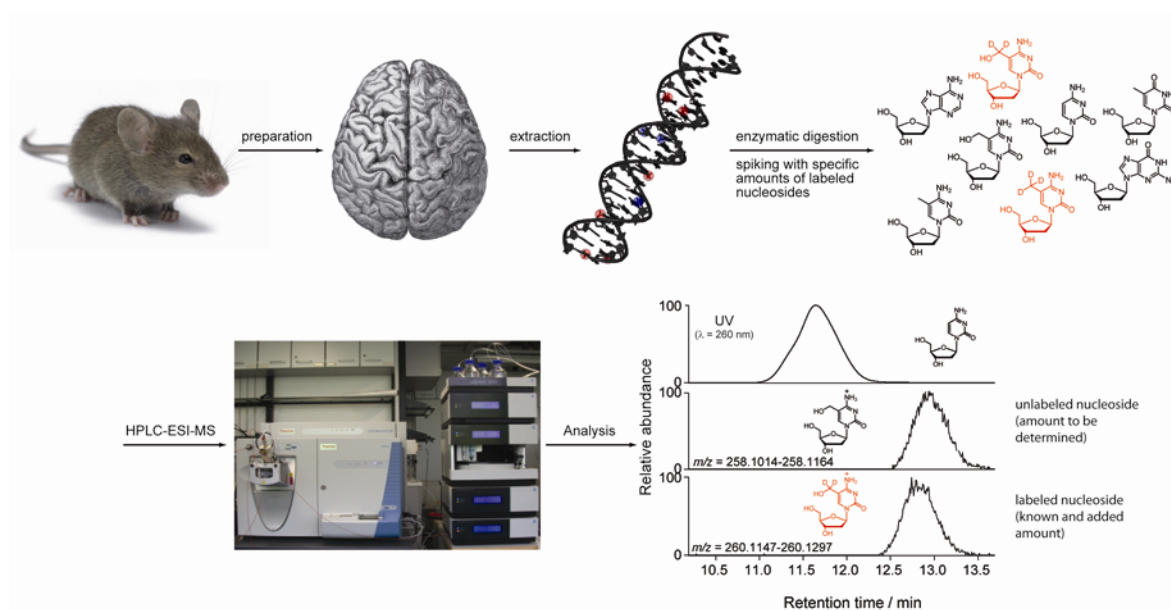


Figure 45: Depiction of the method used for quantification of 5-hydroxymethylcytosine in genomic DNA. After extraction of DNA from different mouse tissues, the DNA was enzymatically digested. Afterwards the nucleoside mixture was spiked with synthesized isotope-labeled nucleosides and analyzed *via* HPLC-ESI-MS.

The first generation reference nucleoside was ^{18}O -hmC with a content of 30% unlabeled hmC due to unavailable pure H_2^{18}O , which was used during the synthesis (Figure 46A). This nucleoside allows precise quantification of sufficient amounts of hmC using the corresponding calibration curve. Small amounts of hmC can only be quantified in high accuracy without background signals of the natural nucleoside. Therefore, we synthesized a second labeled derivative d_2 -hmC which was labeled to above $>99\%$ (Figure 46B). Importantly, both standard molecules yielded the same data from tissues with levels higher than 0.3% hmC of dG.

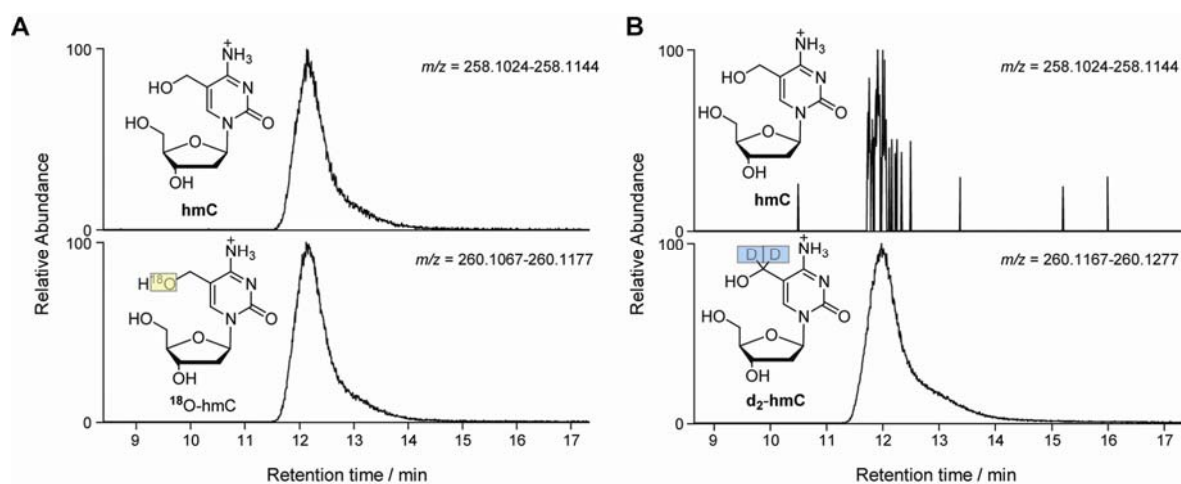


Figure 46: HPLC-ESI-MS ion currents of the two different isotope-labeled nucleosides ^{18}O -hmC and d_2 -hmC. A) The first generation reference nucleoside ^{18}O -hmC contains 30% of the natural nucleoside, while B) the second nucleoside d_2 -hmC contains only traces of the natural nucleoside (approx. 0.06%) and allows precise quantification of low amounts of hmC.

In order to avoid that the results are influenced by possible RNA contaminations in the extracted DNA samples, dG was quantified as an internal standard in the UV trace of the HPLC-chromatogram. We chose dG, because it is pairing with all cytosine derivatives and the HPLC peak of dG is not overlapping with any canonical RNA nucleoside contamination. The calibration curve for dG was determined with two different dG concentrations, which were measured in duplicate. A R^2 value of 0.998 was obtained. The amounts of hmC and mC were determined in pmol and calculated in % relative to the internal standard dG. Thus, the quantification of hmC and mC is independent of the total amount of DNA used. However, best results were obtained when 6-10 μg DNA were analyzed.

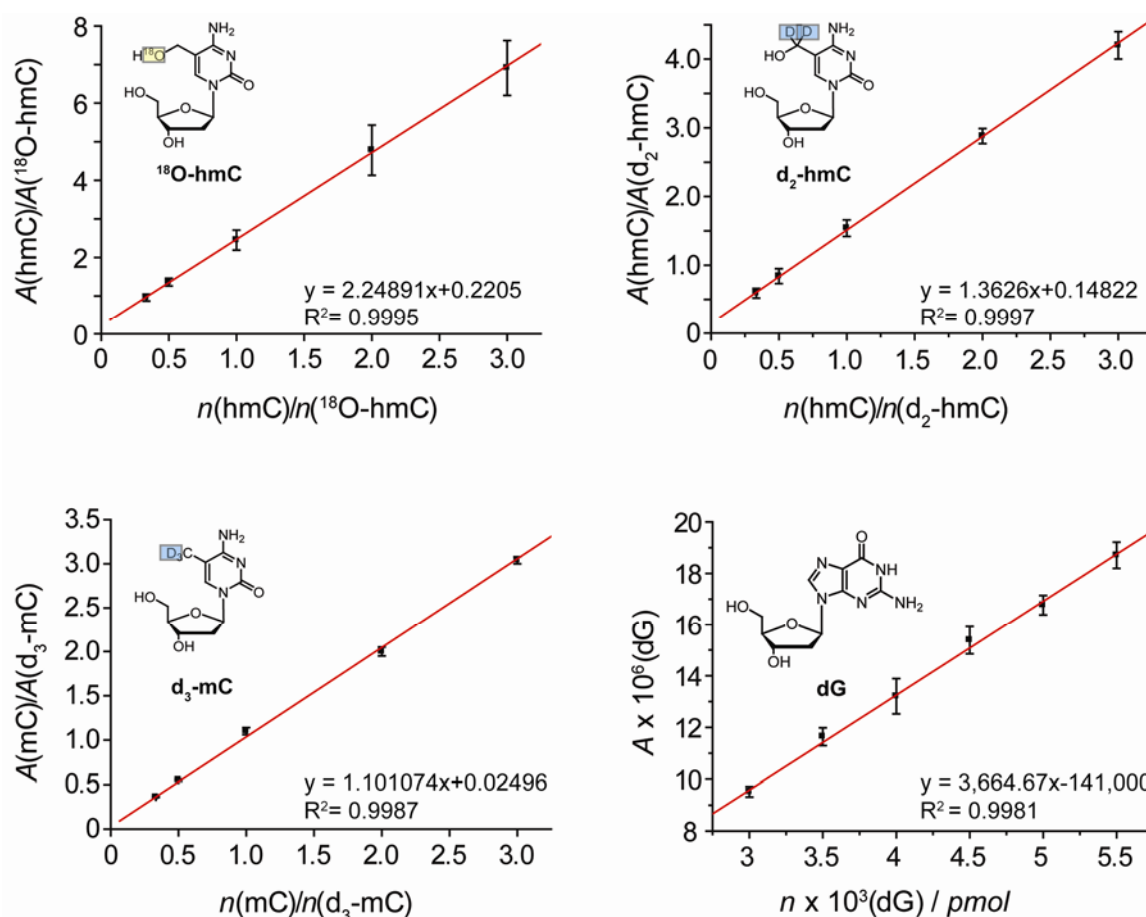


Figure 47: Mass calibration curves of the labeled nucleosides ^{18}O -hmC, d_2 -hmC, and d_3 -mC and HPLC calibration curve of dG. All mass spectrometric data represent averaged values of three different stock solution concentrations of the unlabeled derivative versus one labeled reference nucleoside concentration. The HPLC data points represent two different dG concentrations, which were measured in duplicate. Error bars represent standard deviations.

8.3 Distribution of hmC in mammalian tissue

Since hmC was initially found in the cerebellum,^[20] we were interested to study how hmC would be distributed in the whole mammalian body. Therefore, DNA was extracted from various tissues of three to four different mice (in collaboration with Dr. S. Michalakis, group of Prof. M. Biel, Department of Pharmacy). The respective hmC and mC contents were determined at least twice, independently.

We quantified hmC and mC in tissues from the central nervous system (CNS), muscle tissue, different organs, and glands. The methylated cytosine mC was used as a reference, which should provide constant values in all tissues.^[250, 253] Indeed, the mC values were found to be constant, which proves the applicability of our method with a relative standard deviation of

only 7% (*Figure 48*). Only the level of nasal epithelia deviated from the average values of 4.26% mC of dG.

The first interesting result is the presence of hmC in all tissues, which clearly establishes hmC as a new post-replicatively formed nucleoside in mammalian organisms. Even more important is the fact that the hmC value varies significantly between tissues. We identified three different classes of hmC values with tissues of the central nervous system (CNS) as the class with the highest hmC content. The values are in the range of 0.33%–0.65% hmC over dG. The tissues kidney, nasal epithelium, bladder, heart, skeletal muscle, and lung have medium hmC values from 0.15%–0.17% and built the second class of tissues. The last class contains liver, spleen, and endocrine glands (testes and pituitary gland), which possess the lowest amounts of hmC, ranging from 0.03%–0.06%. The determined levels of hmC vary between 0.03%–0.65%. They are up to 20-fold higher in the cerebral cortex than in spleen or testes. Interestingly, pituitary gland, which is located in the brain, has a low hmC value of only 0.06%, supporting the hypothesis that high hmC content is related to neuronal function. Our method provides data with standard deviations of $SD = 8\%$ for values >0.1 and $SD = 23\%$ for values <0.1 . In summary, these tissue specific varying amounts of hmC compared to the constant amounts mC level, indicate a tissue specific epigenetic role of the sixth DNA base hmC, independent of mC. The six base hmC might be as important in gene regulation as the more abundant base mC, albeit the exact hmC function remains unknown at this point.

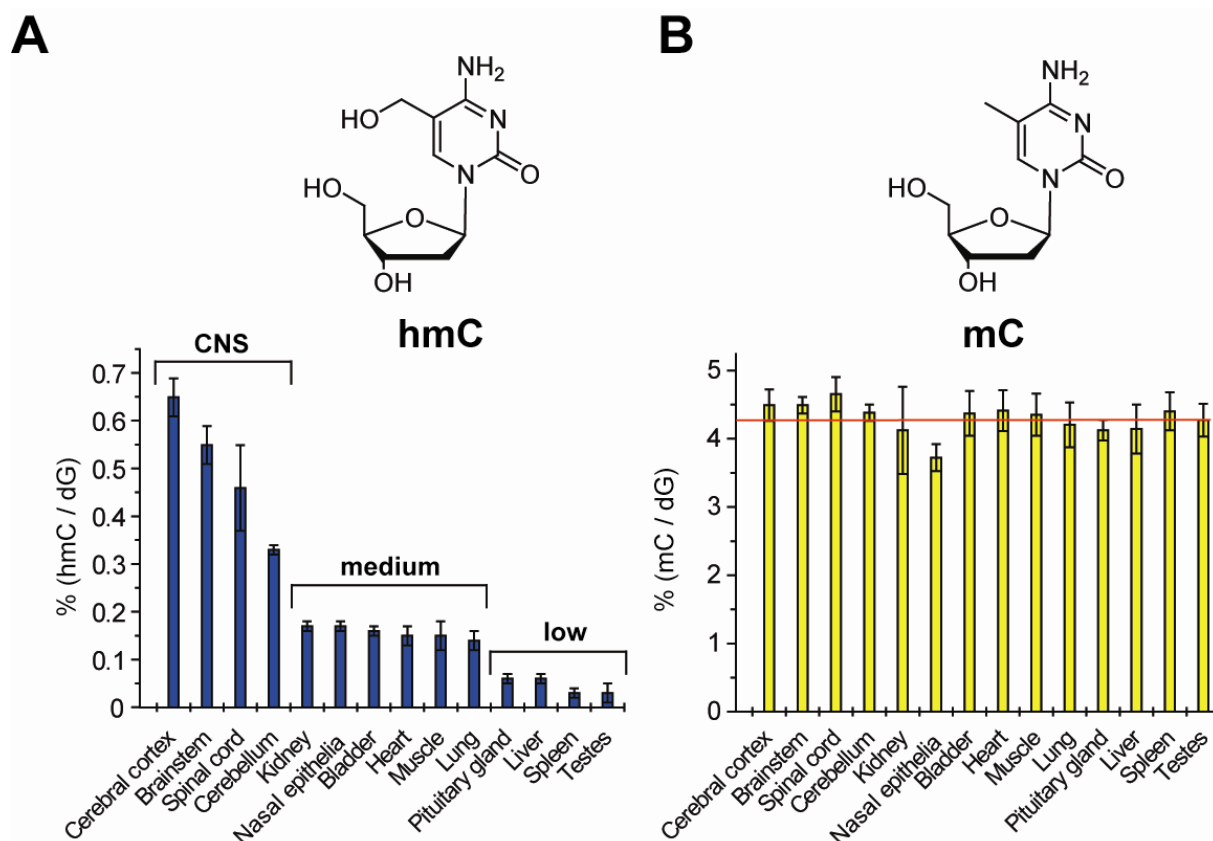


Figure 48: Distribution of hmC and mC in the mammalian body. Measured values of hmC and mC in % over dG shown in blue and yellow, respectively. Data represent values for each tissue of at least two mice with standard deviation (s.d.) and are arranged according to hmC values. The red line indicates the average mC value of all tissues.^[254]

Since hmC was predominately found in tissues from the CNS, its distribution in the mammalian brain was analyzed in more detail. Therefore the hmC and mC content in the hypothalamus, hippocampus, olfactory bulb, and retina of in total four 90 days old mice was determined (*Figure 49A*). These brain areas contain hmC in different amounts, while the mC values were found to be stable at around 4.5% of dG in accordance with literature. The standard deviation is approximately 5%. Between 0.3% and 0.7% of all dC nucleosides are hydroxymethylated in the brain. As reported previously hmC was predominately observed in purkinje neurons,^[20] which are present in the cerebellum. Nevertheless, our data show that the amount of the base is even larger in the cerebral cortex and hippocampus, where purkinje cells are not present.

Following our data we can roughly divide the mouse brain into three different areas (*Figure 49B*). Most hmC is found in hippocampus and cortex (I), which are brain areas with higher cognitive functions. Brainstem and olfactory bulb form a second category, which possess intermediate hmC levels (II). Cerebellum and retina finally contain the lowest

amounts of hmC and form group III. In addition, the hypothalamus, which is part of the endocrine system that controls hormone based processes, shows a relatively high level of hmC as well.

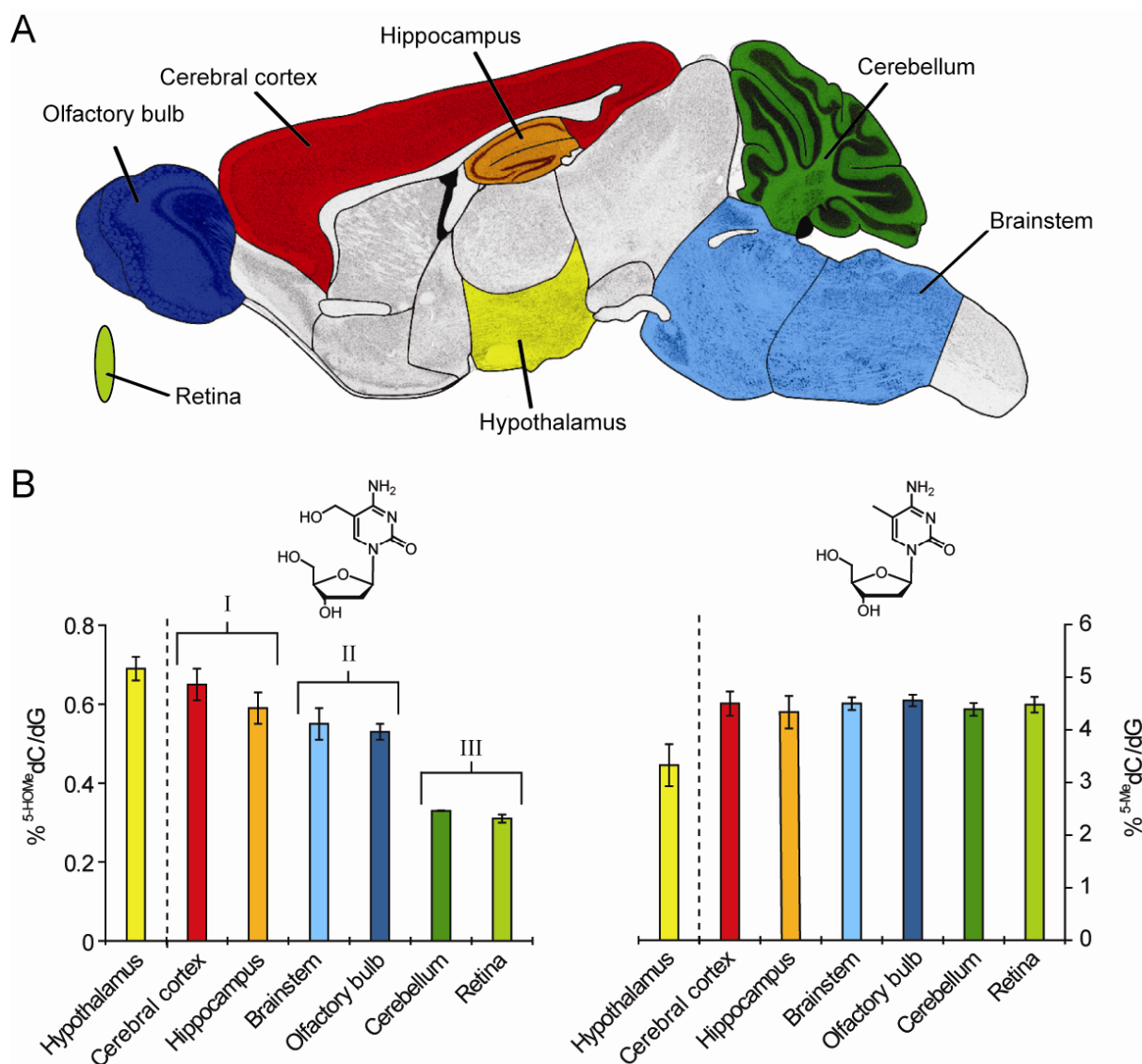


Figure 49: A) Depiction of a sagittal section of the mouse brain. Brain areas highlighted in color were analyzed. B) Ratio of hmC and mC to dG in different brain tissues in percent. dG was chosen as a reference, because it forms base pairs with dC, hmC and mC in DNA.

After we could prove the presence of hmC in the whole mammalian body, immunostaining experiments were carried out. We used a commercially available hmC-specific antibody to determine the exact location of hmC more precisely in the various tissues. The high specificity of the antibody for hmC was shown by Dot Blot analysis performed by Dr. M. Müller (*Figure 50*). Neither extracted total RNA nor a DNA strand containing 5-mC were stained with this antibody. This indicates the specificity of this commercial antibody, which was further confirmed by a second report.^[245, 255]

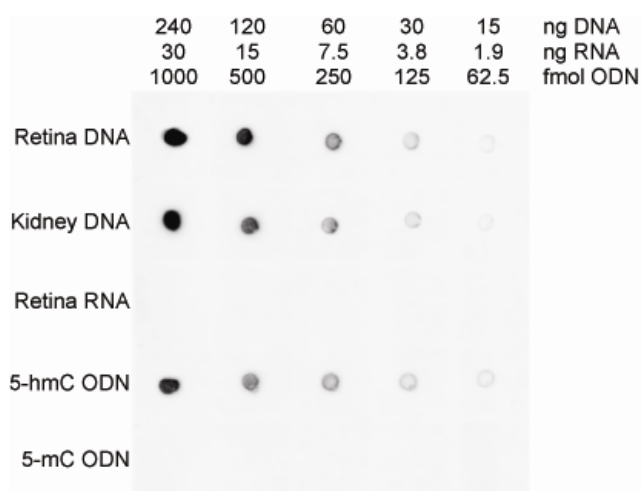


Figure 50: Dot Blot analysis indicate the high specificity of the used hmC antibody.^[255]

For the immunostaining experiments hippocampus, kidney, and liver as representative tissues from the three groups with high, medium and low hmC content were chosen (*Figure 48*). These experiments were performed by Dr. S. Michalakakis und S. Koch from the pharmacy department (Group of Prof. M. Biel). The DNA specific dye Hoechst 33342 was used for nuclear staining showing that virtually all cells contain hmC. The pictures show that hmC is located in the cell nuclei as expected (*Figure 51*). An important observation is the fact that all cells contain hmC. Furthermore, it is clearly evident that the highest intensity for hmC is present in the nuclei of the hippocampus. Kidney is stained with a distinct higher intensity than liver, which supports our HPLC-MS results. (*Figure 51*). To further prove the specificity of the antibody, the anti-hmC staining signal was competed out by addition of 2 μ M DNA containing hmC. These experiments are not depicted here.^[254-255]

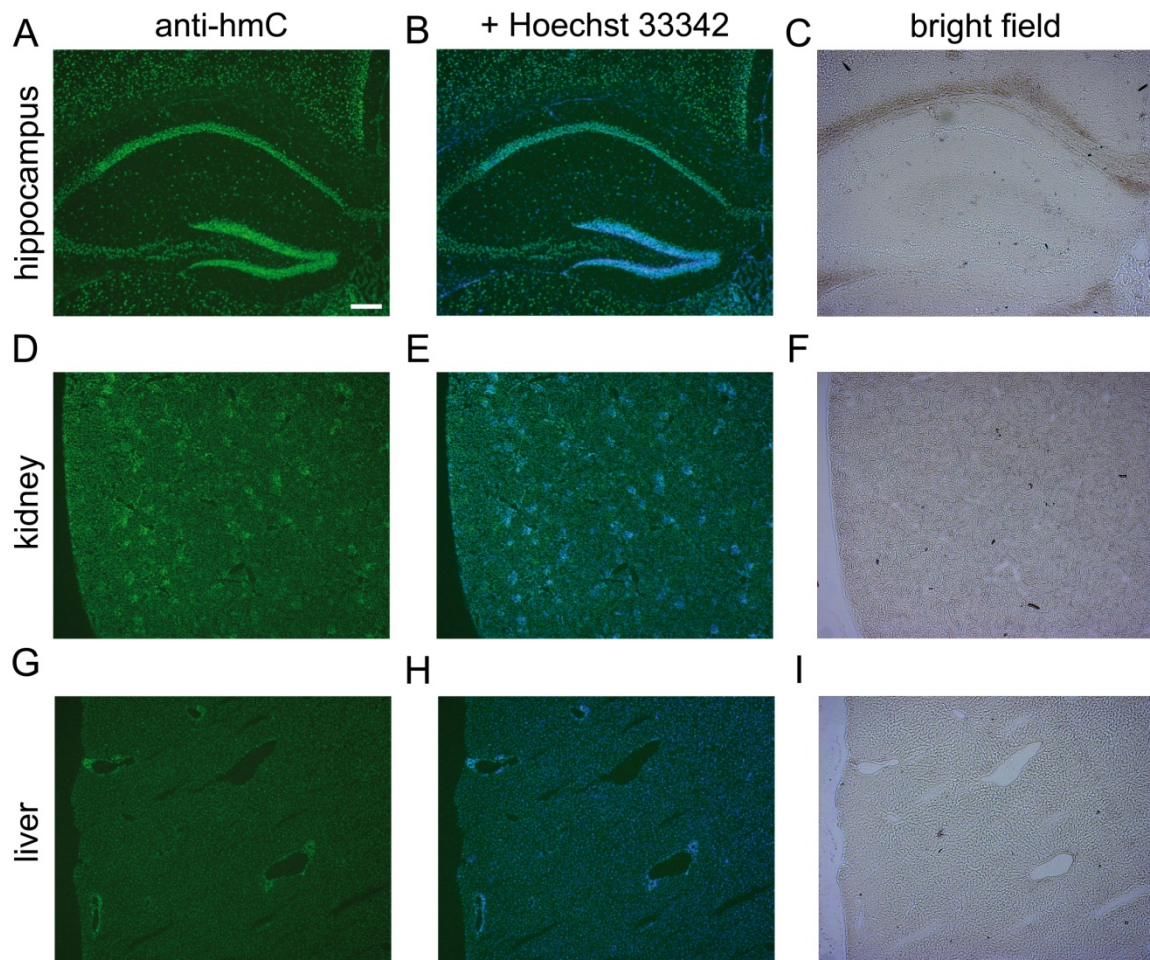


Figure 51: Immunolocalization of hmC in mouse hippocampus, kidney, and liver. Scale bar: 200 μ M. Left column: mouse tissues stained with anti-hmC (green). Middle column: mouse tissues stained with anti-hmC (green) and Hoechst 33342 (blue) for nuclear staining. Right column: Bright field pictures of corresponding tissue.

Interestingly, whereas hmC is equally distributed in liver and kidney, its location in the hippocampus is very diverse. We identified the most intensive signals in the fully differentiated neurons of the dentate gyrus (DG). Cells located in the subgranular zone between DG and hilus show clearly reduced staining in line with reduced hmC levels (*Figure 52*). This area is especially rich in stem cells associated with neurogenesis.^[256-257]

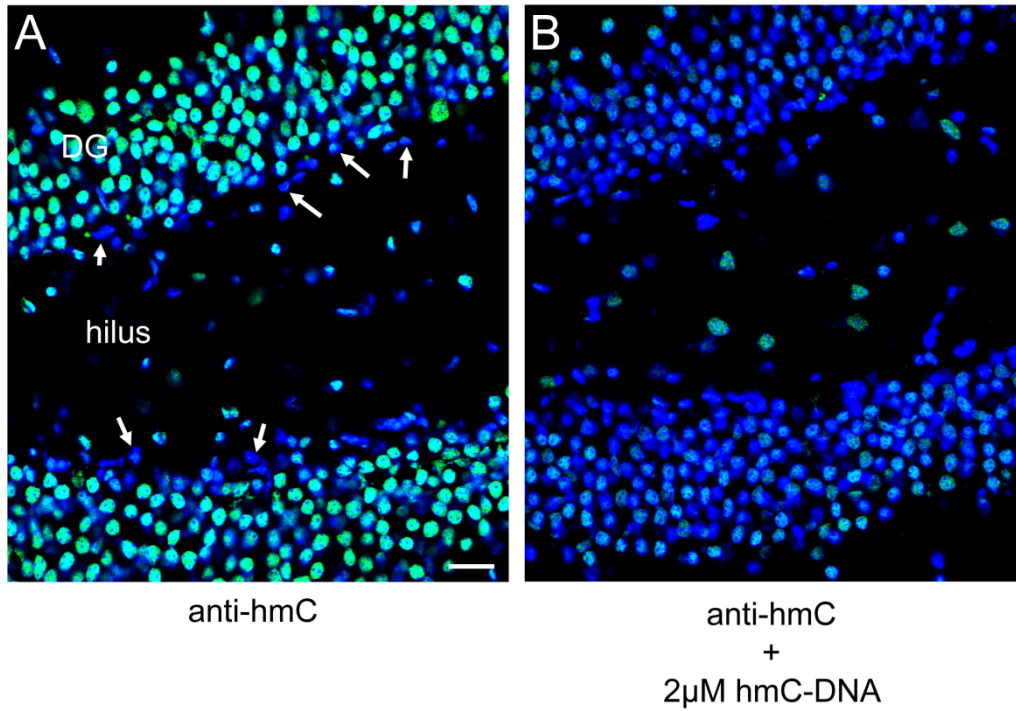


Figure 52: Immunolocalization of hmC in mouse hippocampus. Scale bar: 20 μm . Depiction of the dentate gyrus (DG) and the hilus. A) Mouse tissues stained with anti-hmC (green) and Hoechst 33342 nuclear staining is shown in blue. B) Addition of 2 μM hmC-DNA.

We were also interested if the levels of mC and hmC are age dependent and analyzed the hippocampus tissue of a one-day old mouse (*Figure 53*). Interestingly, significantly reduced levels of mC and hmC were detected in a young mouse that we also studied. The mC value increases with age from $3.5\pm 0.1\%$ to $4.3\pm 0.3\%$ and the hmC value is raised in 90 day old mice to almost double amount from $0.34\pm 0.02\%$ to $0.59\pm 0.04\%$. These values show age dependent hmC changes and will be further investigated in future projects. The same hmC age dependent trend was shown in a recent publication for cerebellum with lower hmC values in young mice.^[258]

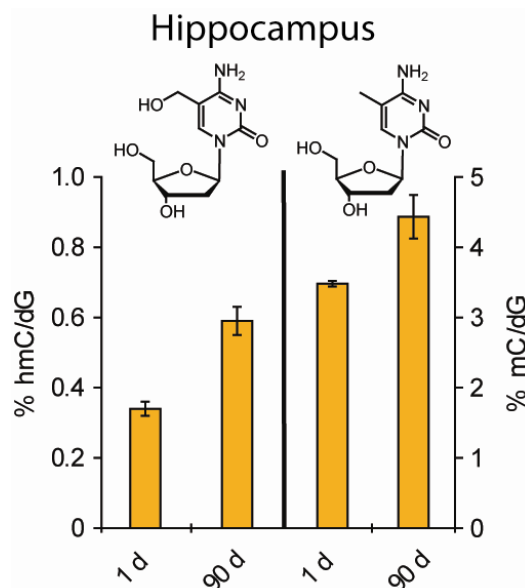


Figure 53: Ratio of hmC and mC to dG in the hippocampus of 1 day and 90 days old mice in percent.

8.4 *hmC as a putative intermediate in the demethylation process?*

There are several possibilities of the potential role of hmC. It has been described that methyl-CpG binding protein 2 (MeCP2) is unable to bind to the corresponding sequences when mCs were converted to hmCs in CpG sequences.^[259] Here the question arises, if hmC is an intermediate in the active demethylation process. A recent study has shown that MTases are able to deformylate hmC in *in vitro* experiments.^[260] Oxidation of the hydroxymethyl group to a formyl group would yield 5-formylcytosine (fC) which could expel formic acid and react to dC. Another possibility would be further oxidation of hmC or fC to yield 5-carboxylcytosine (caC) which possesses a carboxy group and would enable quick decarboxylation to regenerate dC (*Figure 54*)^[261] Nature's most proficient enzyme orotate decarboxylase catalyzes a similar reaction in which orotate (6-carboxyuracil) is decarboxylated to uracil.^[262-263] Similar oxidation and decarboxylation reactions are known for thymine in the pyrimidine salvage pathway of certain eukaryotes.^[263-265] Another potential active demethylation pathway is the excision of hmC by DNA glycosylases.^[266] hmC could be converted by deamination with an activation-induced deaminase (AID) analog to yield the uracil derivative hmU.^[18] This uridine derivative is known to be a substrate for the base excision repair (BER) enzyme SMUG1.^[267-268] The deoxynucleotide hmC might be a possible intermediate in BER as well, because *in vitro* experiments in extracts from calf thymus have shown BER activity for hmC.^[269]

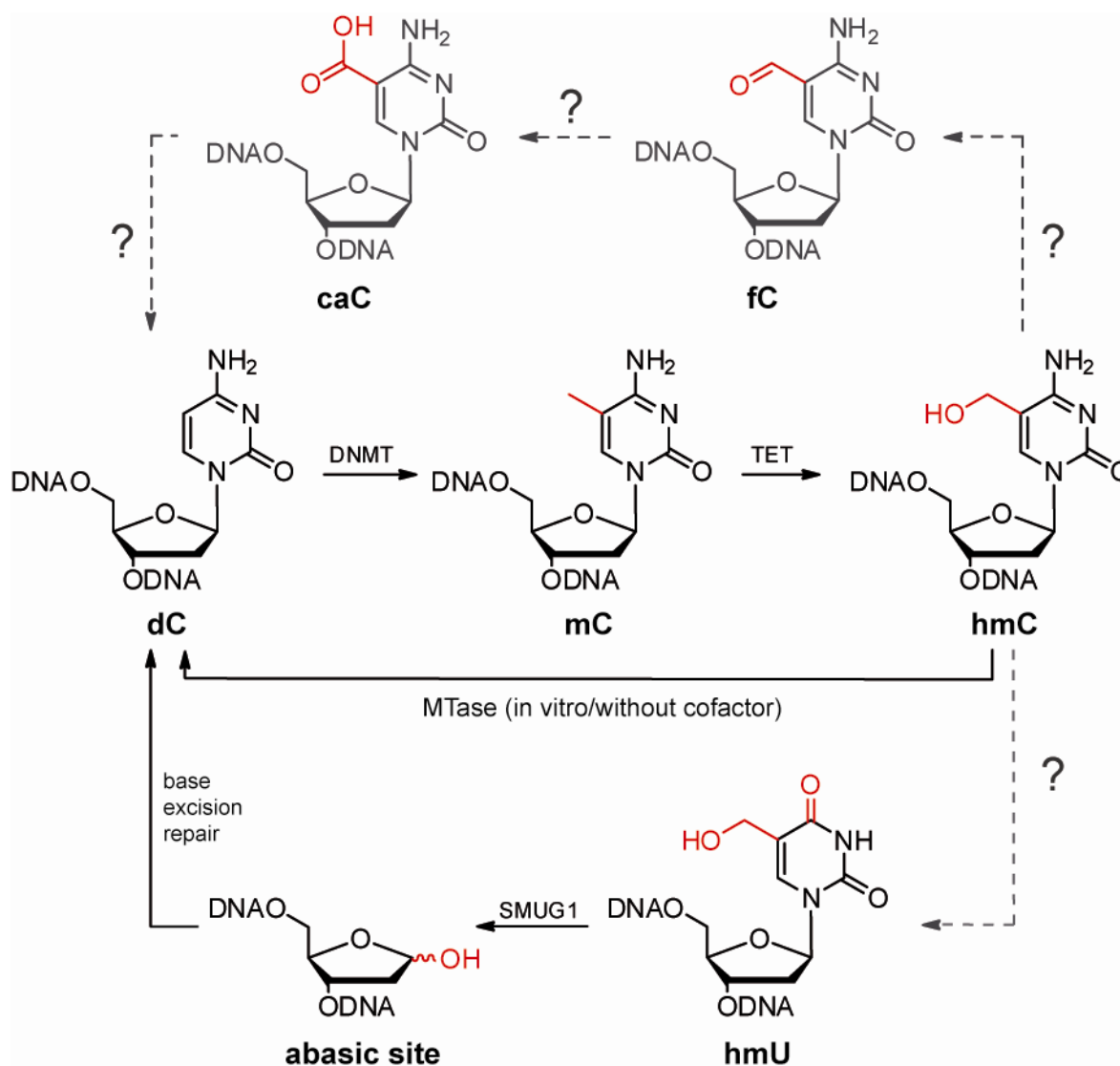


Figure 54: Depiction of the known cytosine modifications mC and hmC and the putative oxidative “demethylation” intermediates fC and caC. The base excision repair (BER) pathway is a second possible demethylation pathway *via* the intermediate hmU.

In order to test the idea that hmC is an intermediate of a possible oxidative demethylation pathway, we used our HPLC-MS method to detect the presence of fC, caC, and hmU in different tissues. The three putative intermediates were synthesized by M. Münzel and used in this thesis to determine their chromatographic and mass spectrometric properties. Therefore, the same HPLC gradient used for hmC quantification was employed, which already provides ideal separation of all five modified DNA nucleosides (*Figure 55*). The difference of each modified nucleoside also allows unambiguously assignments by their different molecular weights (*Figure 55*).

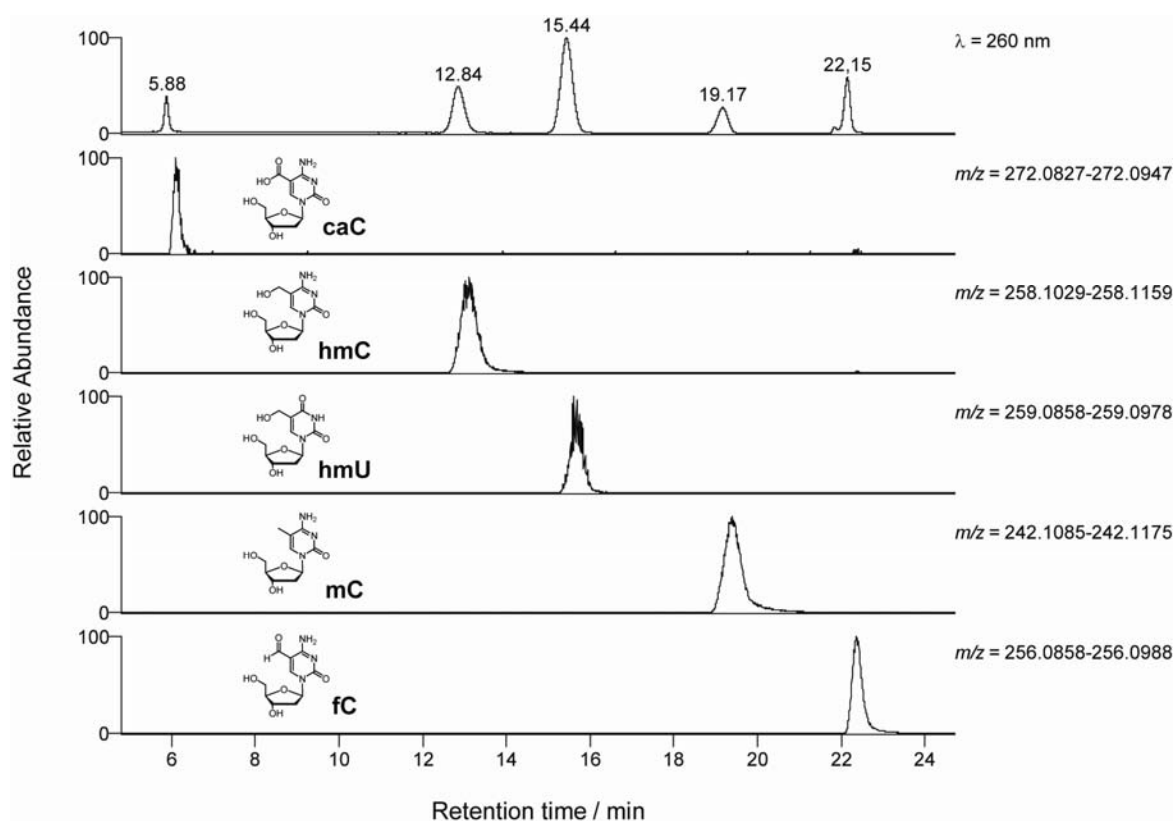


Figure 55: HPLC chromatogram and nucleoside specific mass spectra of the modified DNA nucleosides hmC, and mC with the putative demethylation intermediates caC, hmU, and fC. Nucleosides are ordered to their retention time.

Knowing the retention times of the putative nucleosides all previous recorded LC-MS data were screened for these nucleosides. We could however not detect any caC, hmU or fC in the quantification experiments described above, in which we used 10 μg DNA (Figure 48 and Figure 49). Therefore, the amount of hydrolyzed DNA was enriched up to 16 times. We hydrolyzed 7–16 samples of one tissue in parallel to ensure quantitative digestion and combined all samples afterwards which contain in total 70–160 μg DNA. The nucleoside mixture was taken up in 100 μL $d_2\text{H}_2\text{O}$, $d_2\text{-hmC}$ was spiked and the sample analyzed *via* HPLC-MS. Importantly, the column was not overload or the entrance of the mass spectrometer capped. Thus, highly accurate mass spectrometric data were obtained. Also no memory effect was observed in blank runs after these LC-MS measurements.

As representative tissues for high, average, and low hmC content, olfactory bulb, retina, cerebellum, kidney, and liver were chosen. Despite higher DNA concentrations, we could not detect any of the three putative intermediates fC, caC, or hmU. The exact concentration of hmC in the analyzed samples was determined and even in the olfactory bulb with 342 pmol hmC non of these three nucleosides was detected. The detection limit was found to be in the

low picomolar range (*Figure 56*) and all investigated compounds proved to be stable during enzymatic hydrolysis, with minor instability of caC. Nevertheless, if these nucleosides were present, we would be able to detect these derivatives even in traces 350–700 times less abundant than hmC. Thus if present, fC does not reach levels above $7 \cdot 10^{-4}\%$ of all nucleosides or 0.3% of all hmC. With other words our results exclude that caC is present in genomic DNA with more than 3.5 caCs in 10^5 nucleosides.

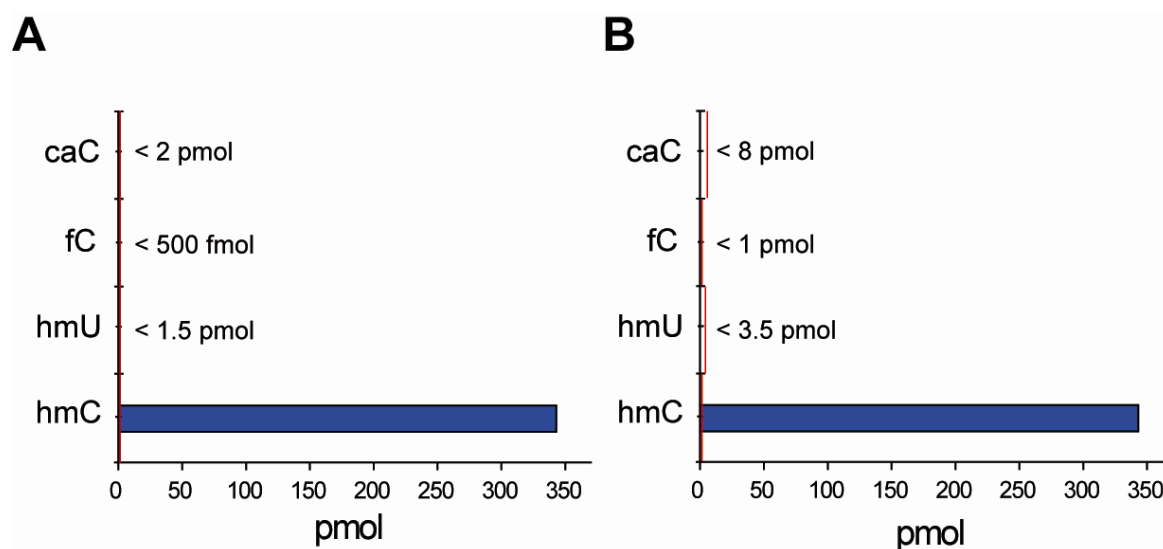


Figure 56: Detected values of the potential hmC demethylation intermediates in olfactory bulb as an example. A) Detection limits determined with synthetic nucleoside samples. B) Detection limits in digested DNA nucleoside samples. The red line indicates the detection limits of the modified nucleosides. The detection limit for hmC is 1.5 pmol.

The data presented in this thesis provide new insights into the distribution of the modification hmC in mammalian tissue. We showed that hmC is present in every cell type in the mammalian body and its distribution is tissue dependent, ranging from from 0.03%–0.7%. This allowed us to classify tissues in three different groups with tissues from the CNS containing the highest amounts of hmC with up to 20-fold more compared to other tissues. Additionally, substantial further oxidation of hmC to fC or to caC or deamination of hmC to give hmU can be excluded. Nevertheless, the absence of these two putative pathways cannot fully be ruled out, but the data indicate that the unavoidable intermediates do not accumulate to any significant level. Either these reactions do not occur on large scale or the investigated intermediates are so short lived that they are not released from the enzymatic complex.^[254]

8.5 hmC in cancer cell lines

Additionally, the hmC and mC content in different cancer cell lines as well as in one primary cell culture was investigated. Cell lines do not contain hmC as described previously, while low amounts are present in ES cells.^[20-21] In this work the hmC content in DNA was analyzed from the breast cell line MCF-7 originated from mammary gland adenocarcinoma, the primary cell culture HMEC originated from primary mammary epithelial cells as well as the brain derived cancer cell lines U-87 MG (glial) and Neuro-2a (neuroblastoma) due to high quantities of hmC in tissues from the CNS (*Figure 48*). Moreover the cell line P19 (teratocarcinoma) was also investigated, which is related to ES cells. Values of 4.2–4.7% mC of dG were determined in HMEC, MCF-7, and P19 cells, while the values for the cell lines originated from the two nerve cells are reduced to 3.1% of dG. Nevertheless, we could not detect hmC in any of the cell lines, even though they are originated from different cell types. Cell lines were grown and DNA was extracted by M. Wagner.

Traces of hmC of less than 0.01% of dG were found when the amount of enzymatic hydrolyzed DNA obtained from the cell line P19 was increased up to 10 times. In an ongoing project, we are trying to get exact values of hmC in the investigated cell lines.

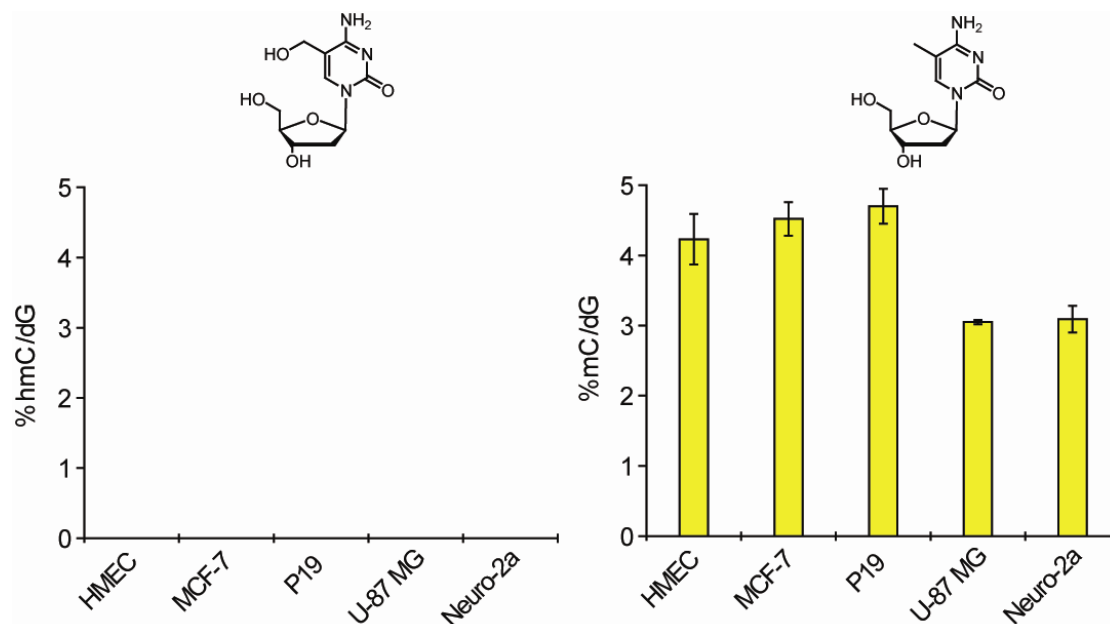


Figure 57: Ratio of hmC and mC to dG in the investigated cell lines in percent.

In summary, the method for quantification of modified tRNA nucleosides could successfully be transferred to modified DNA nucleosides. Previously hmC was detected in purkinje neurons of the cerebellum. Results in this thesis reveal the presence of hmC in all cells

throughout the body but with tissue dependent amounts. Highest amounts were detected in tissues from the CNS especially in those tissues associated with high cognate functions. Furthermore, an age dependent concentration of hmC was detected in the cerebellum.

hmC could be part of the active demethylation process but no putative intermediate could be detected even though the detection limit was strongly reduced. Furthermore, only traces of hmC were detected in cell lines derived from brain tissues.

9. Outlook

The results described in this thesis suggest biological roles of modified tRNA nucleoside that are beyond of what was reported before. The quantification of these modifications furnished new insights into biological processes like the tissue dependent correlation of high tRNA modification levels with high protein synthesis activities. Also, cancer cell lines were found to have high tRNA modification levels suggesting a correlation with high proliferation rates. Inhibition or down-regulation of the modification machinery in cancer cell lines could lead to slower cancer cell growth. This could be tested for specific modifications with siRNA experiments.

The mitochondrial modification $\text{ms}^2\text{i}^6\text{A}$ is absent in cancer cell lines and is therefore a possible marker to differentiate between healthy and tumor tissues. Analysis of cancer tissues from mammals could be performed in order to evaluate potential clinical applicability.

Phylogenetic correlations of the tRNA modifications were shown to occur for eukaryotic and prokaryotic organisms. The high resolution of the performed cluster analysis enabled even differentiation of bacteria from the same genus. These analyses should be extended with archaea and with additional bacterial organisms particularly in order to elucidate the relative clustering of *D. radiodurans*, which is expected to be a hybrid between archaea and bacteria. In addition, pathogenic and non-pathogenic bacteria can be distinguished by their tRNA modification pattern, which leads to possible further clinical application. This quantification method could also be further optimized to allow faster extraction of tRNA as well as analysis of lower amounts of tRNA. Another possibility is the quantification of total RNA to reduce extraction time.

The influence of external stimulation to the tRNA modification level in *E. coli* was shown for two modifications. This study should be repeated with an extended number of modifications and also should be performed for a yeast strain to elucidate the variability of the tRNA modifications pattern in eukaryotes.

The results of this Ph.D. work were obtained with almost all modified purines and queuosine as representative wobble modification. Modified pyrimidine nucleosides should be synthesized to extend the nucleoside library and to further enhance the resolution of our analyses. Now, with the available quantification method and reference modifications further

projects could lead to new insights in organism development and regulation of biological processes.

The distribution of 5-hydroxymethylcytosine (hmC) in the whole mammalian body indicates an epigenetic function of this modification. Our results have additionally shown high levels in tissues from the central nervous system (CNS) leading to the assumption that it has a neuronal function. Therefore learning experiments with mice could elucidate, if hmC is involved in learning and memory formation.

The absence in high quantities of the putative demethylation intermediates indicates that they do not accumulate to any significant level in mammalian tissue. Antibodies against these nucleosides would enhance the sensitivity and could be used in immunohistology experiments to search for these nucleosides.

Cancer cell lines contain only a very low amount of hmC. Therefore, differentiation experiments could be performed with ES cells related cell lines to show, if the hmC level is varying in this process. If hmC is related to diseases, the modifying enzymes would be an interesting therapeutic target. Analysis of mammalian cancer tissues and tissues related to diseases of the CNS could lead to target validation.

The method was successfully developed for quantification of tRNA and DNA modifications. In addition, the method can be modified for quantification of modifications in rRNA and mRNA.

10. Experimental Section

10.1 *General chemical materials and methods*

Chemicals and solvents were purchased from ABCR, Alfa Aesar, Acros, Fluka, Sigma-Aldrich or TCI in the qualities puriss, p.a. or purum, unless stated otherwise. For all solutions injected into the mass spectrometer MilliQ water and mass spectrometry grade solvents and reagents were used. Dry solvents (< 50 ppm H₂O) were obtained from Fluka and Acros. All non-aqueous reactions were performed using flame- or oven-dried glassware under an atmosphere of dry nitrogen or argon. Non-aqueous reagents were transferred under nitrogen with a syringe or cannula. Technical grade solvents were distilled prior to use for column chromatography and liquid-liquid extractions on a rotary evaporator (Heidolph Laborota 4000). Reaction products were dried at high vacuum (10 mbar). Aqueous solutions were dried on a SpeedVac plus CS110A or SPD 111V from Savant or lyophilized (Christ ALPHA 2-4).

Column chromatography was performed with Si 60 (40-63 μM) silica gel from Merck.

Thin layer chromatography (TLC) was performed on Merck 60 aluminum plates (silica gel 60 F₂₅₄). Substances were visualized by illumination with UV-light ($\lambda = 254$ nm) or by staining with subsequent heating. The staining was performed using potassium permanganate solution (1.0 g KMnO₄ in 100 mL H₂O), anisaldehyde solution (2.2 g anisaldehyde, 2.0 mL conc. H₂SO₄, in 100 mL acetic acid), ninhydrin solution (20 g ninhydrin in 600 mL ethanol), or molybdato-phosphoric acid solution (10 g Ce(SO₄)₂·H₂O, 25 g molybdato-phosphoric acid, and 60 mL H₂SO₄ in 940 mL H₂O).

HPLC purification was performed on a Merck-Hitachi system (L-7400 UV detector, L-7480 fluorescence detector, L-7100 pump), on a Waters system (alliance 2695 with PDA 2996 or 996 and fluorescence detector 2475; preparative HPLC: 1525EF with 2484 UV detector. As columns VP 250/32 Nucleosil 100-7 C18, VP 250/10 Nucleosil 100-7 C18, CC 250/4 Nucleosil 120-3 C18, VP 250/10 Nucleodur 100-5 C18 ec, VP 250/4 Nucleodur 100-5 C18 ec, and CC 250/4 Nucleodur 120-3 C18 ec columns from Macherey-Nagel and Uptisphere120-3HDO columns from Interchim were used.

Mass spectrometry data for ESI-MS was performed on a Finnigan LTQ FT-ICR. MALDI-TOF was performed on a Bruker Autoflex II spectrometer with 6-aza-2-thiothymine (ATT) as matrix (10 mg ATT in 1 mL H₂O).

HPLC-MS purification was performed on a on a Finnigan LTQ FT-ICR on a Surveyor system and on a Thermo Finnigan LTQ Orbitrap XL on a Dionex system (Ultimate 3000 HPLC). The Uptisphere120-3HDO column from Interchim was used.

Melting points were measured with a Büchi Melting Point B-540.

Infrared spectroscopy was IR measurements were performed on n *Perkin Elmer Spectrum BX FT-IR* spectrometer (Perkin Elmer) with a diamond-ATR (Attenuated Total Reflection) setup. The detection ranged from 400 to 4000 cm^{-1} . The following abbreviations were used for the characterization of the bands: *s* (*strong*), *m* (*medium*), *w* (*weak*).

NMR spectra were recorded on the following spectrometers: *Varian Oxford 200*, *Bruker AC 300*, *Varian XL 400* and *Bruker AMX 600*. The chemical shifts (δ) are given in ppm, the coupling constants (*J*) in Hz. Multiplicities are abbreviated as follows: s = singlet, d = doublet, t = triplet, q = quartet, m = multiplet.

10.2 Tissue samples, bacterial strains, and cell culture

Pork tissue samples were obtained from the local slaughterhouse (Schweineschlachtung München GmbH) right after sacrifice. All samples were processed within 4 hours after sacrifice.

Bacterial strains except *E. coli* and *B. subtilis* were grown and harvested in the laboratory of Prof. S. A. Sieber.

Mouse tissues from three male mice (C57BL/6N) obtained from the group of Prof. M. Biel and were frozen in liquid nitrogen right after sacrifice. Depending on the tissue type each mouse supplied enough DNA for up to 4 measurements.

Cell culture experiments for tRNA and DNA quantification were mainly performed by Mirko Wagner. Experiments for tRNA quantification of four cell lines were performed in course of this Ph.D. thesis. All cell lines were grown to 80 to 90% confluence at 37 °C and 5% CO₂ in RPMI 1640 medium containing L-glutamine (Invitrogen GmbH, Karlsruhe, Germany). RPMI 1640 was supplemented with 10% (v/v) fetal bovine serum and penicillin (10 mg/L) / streptomycin (0.025 mg/L).

10.3 Biochemical materials

10.3.1 Equipment

Equipment	Supplier
Äkta purifier chromatography system	GE, Munich
Agarose gel electrophoresis chamber	Biorad, Munich
Autoclave Vakulab S3000	Systec, Gießen
Biofuge pico	Heraeus, Hanau
BioPhotometer 6131	Eppendorf, Hamburg
Blender, Waring, 37-110 mL	VWR, Darmstadt
Centrifuge 5810R	Eppendorf, Hamburg
Fermenter Minifors	Infors AG, Bottingen
French pressure cell press	Thermo, Dreieich
Elisa Reader, FP Spectrometer	Tecan, Crailsheim
Gel scanner IDA	Raytest, Straubenhardt
Gel documentation device LAS3000	Raytest, Straubenhardt
Inkubator 1S	Noctua, Wiesloch
Inkubator 44R	New Brunswick
Microplate Reader Genios Pro	Tecan, Crailsheim
Mini Protean 3 Cell	Biorad, Munich
Multicaster	Biorad, Munich
Nanodrop UV-spectrometer	Peqlab, Erlangen
pH meter MP220	Mettler Toledo, Gießen
Sorvall centrifuge, Evolution RC	Kendro, Dreieich
Spectrophotometer V-650	Jasco, Groß-Umstadt
Thermomixer Comfort	Eppendorf, Hamburg
Tissue grind tube, SZ 24	VWR, Darmstadt
TissueLyser	Qiagen, Hilden
Deep-freezer	Sanyo, Bad Nenndorf
Desktop centrifuge 5415R	Eppendorf, Hamburg
Ultrasonic bath	Bandelin, Berlin
Vortexer	VWR, Darmstadt
Water bath	Labora, Mannheim
Waters Millipore System	Millipore, Schwalbach

10.3.2 Bacterial strains and cell lines

Strain Cancer cell line	Supplier
A-375	Cell Lines Service, Eppelheim
BT-549	Cell Lines Service, Eppelheim
<i>E. coli</i> K12	DSMZ, Braunschweig
HCT-116	Cell Lines Service, Eppelheim
HeLa	Cell Lines Service, Eppelheim
HEMA	Cell Lines Service, Eppelheim
HMEC	Cell Lines Service, Eppelheim
IGR-1	Cell Lines Service, Eppelheim
MCF 7	Cell Lines Service, Eppelheim
MDA-MB-231	Cell Lines Service, Eppelheim
Neuro-2a	Cell Lines Service, Eppelheim
P19	Cell Lines Service, Eppelheim
SK-HEP-1	Cell Lines Service, Eppelheim
SK-MEL-2	Cell Lines Service, Eppelheim
SK-MEL-5	Cell Lines Service, Eppelheim
SK-MEL-28	Cell Lines Service, Eppelheim
T-47D	Cell Lines Service, Eppelheim
U-87 MG	Cell Lines Service, Eppelheim

10.4 Biochemical methods

10.4.1 Bacterial strains and growth conditions

Bacteria were stored as glycerol stocks at -80 °C before usage. During the studies they were kept on LB agar at 4 °C and transferred to a new agar plate every second week. Inocula (50 mL) were grown over night at 37 °C shaking at 240 rpm in the medium, in which the later experiment was performed.

E. coli cultures (1 L) were inoculated with an overnight culture (5 to 8 mL) and shaken at 240 rpm at 37 °C until OD 1 (600 nm) was reached, unless stated otherwise. To gain reference modification levels samples were taken at this point. For stress response studies the stress factor was introduced at this point and the culture was shaken at 240 rpm at 37 °C, unless stated otherwise. Detailed experimental procedures are described in the Ph.D. thesis of Dr. T. Brückl.^[140]

Bacteria for phylogenetic analysis were grown and harvested by the group of Prof. S. A. Sieber. *B. subtilis* was grown by Dr. D. Pearson. The OD values at which the bacteria were harvested is shown in *Table 5*.

Table 5: OD values at which the bacteria were harvested

Bacterium	OD	Bacterium	OD
<i>E. coli</i>	1.0	<i>L. monocytogenes</i>	1.9
<i>P. putida</i>	1.1	<i>L. welshimeri</i>	1.9
<i>P. aeruginosa</i>	1.2	<i>B. thailandensis</i>	1.0
<i>B. subtilis</i>	1.0	<i>B. cenocepacia</i>	1.1
<i>S. aureus</i> MU 50	4.1	<i>D. radiodurans</i>	1.0
<i>S. aureus</i> NCTC	3.6		

Each bacterium was grown in its optimum media (*Table 6*):

- 1) LB: 1% Pepton, 0.5% NaCl, 0.5% Yeast extract (pH 7.5)
- 2) BHB: 37 g Brain Heart Broth (Fluka 53286) in 1L H₂O
- 3) CASO: 30 g CASO Broth (Fluka 22098) in 1L H₂O
- 4) TGY: 0.5% Trypton, 0.1% Glucose, 0.3% Yeast extract (pH 7,2)

Table 6: Bacterial media

Medium	Bacteria
LB	<i>E. coli</i> , <i>P. putida</i> , <i>P. aeruginosa</i> , <i>B. subtilis</i>
BHB	<i>S. aureus</i> MU 50, <i>S. aureus</i> NCTC, <i>L. monocytogenes</i> , <i>L. welshimeri</i>
CASO	<i>B. thailandensis</i> , <i>B. cenocepacia</i>
TGY	<i>D. radiodurans</i>

After completion of growth the culture was quickly transferred to two precooled 500 mL centrifugal tubes equipped with ice. After centrifugation (8 min, 10816 g, 4 °C) the supernatants were discarded. The pellets were suspended in buffer 1 (10 mL, 0.01 M Mg(OAc)₂, 0.05 M NaOAc, 0.15 M NaCl, pH 4.5). The suspensions were combined in a 50 mL Falcon tube and centrifuged (30 min, 3220 g, 4 °C). The supernatant was discarded and the pellet was stored at -80 °C until further use.

10.4.2 tRNA purification

10.4.2.1 tRNA extraction

Tissue samples were cut out from inside the organ omitting surface areas, inhomogeneous areas, and vessels. For brain samples meninges and surface blood vessels were removed before processing, because for these samples surface areas could not be omitted.

All extraction steps were performed on ice or at 4 °C. A Waring Blender was equipped with pork tissue (5 g), buffer 1 (15 mL) and ice. The mixture was blended until a homogenous suspension was obtained and transferred to a 50 mL Falcon tube. After addition of 80% aq. phenol (15 mL) the suspension was shaken vigorously for 30 min. The mixture was centrifuged (30 min, 3220 g). The aq. layer was collected and treated again with 80% aq. phenol (20 mL). The suspension was shaken vigorously for 1 min, centrifuged (30 min, 3220 g) and the layers were separated. The second phenol layer was extracted with buffer 1 (5 mL). The aq. layer was collected, all aq. layers were combined and extracted with 80% aq. phenol (5 mL). The aq. layer was collected and extracted with chloroform (5 mL) twice. The aq. layer was collected and 20% KOAc, pH 4.5 (0.1 vol) and 12 M LiCl were added to a 2.0 M final LiCl concentration. DNA and long RNAs were precipitated on ice for 4 h and pelleted by centrifugation afterwards (20 min, 38724 g). The supernatant was added to abs.

EtOH (3.0 vol) in a 500 mL centrifugal tube and kept at -20 °C over night. After centrifugation (60 min, 24336 g) the supernatant was discarded and the pellet was dried.

The cell pellet of bacteria, yeast strains and cell culture were allowed to thaw on ice and suspended in buffer 1 (15 mL) and 80% aq. phenol (15 mL) was added. Further tRNA isolation was performed as described for pork tissue. Desalting was not necessary for tRNAs isolated from yeast and cancer cell lines. The obtained tRNA pellet was kept at -80 °C until anion exchange chromatography was performed.

10.4.2.2 tRNA purification

A PD10 column (GE health care) was preequilibrated with buffer A (25 mL, 0.10 M Tris-HCl, pH 7.5, 0.01 M MgCl₂). The tRNA pellets obtained from bacteria and pork tissue were dissolved in buffer A (2.5 mL) and applied on the PD10 column. The suspension containing the crude tRNA was allowed to enter the column and the flow-through was discarded. The crude tRNA was eluted with buffer A (10 to 15 mL) until the eluant showed no UV absorbance any more. The obtained solution containing crude tRNA was kept at -80 °C until subjection to anion exchange chromatography. The utilized PD10 column was reequilibrated with buffer A (25 mL) and reused up to ten times. For storage PD10 columns were equilibrated with 20/80 ethanol/water (25 mL).

The isolated tRNA was further purified by anion exchange chromatography. All associated steps were performed on ice or at 4 °C. The tRNA pellet from bacteria, yeast, and cell culture cells were dissolved in buffer A (10 mL). Crude tRNA from pork liver tissue entered this purification phase already in solution. Remaining impurities were removed from the tRNA samples by weak anion exchange chromatography (DEAE Sepharose Fast Flow 5 mL, column volume (CV): 5 mL) utilizing an ÄKTA purifier. The gradient was 5 CV, 0% buffer B (25 mL, 0.10 M Tris-HCl, pH 7.5, 0.01 M MgCl₂, 1.0 M NaCl); 10 CV, 0% → 40% buffer B; 5 CV, 100% buffer B; 3 CV, 0% buffer B. The fractions eluting at about 20% to 40% buffer B and showing approximately a 2:1 ration for the absorption at 254 nm and 280 nm were collected. To the combined fractions abs. EtOH (3.0 vol) was added and the mixture was kept at -20 °C over night. After centrifugation (60 min, 24366 g) the supernatant was discarded and the pellet was dissolved in MilliQ water (2 x 1.0 mL). In case the resulting tRNA concentration proved to be too low for the subsequent digestion (< 140 ng/μl) another EtOH precipitation step was conducted.

10.4.3 DNA isolation from tissue samples and cancer cell lines

DNA isolation was performed on the basis of the QIAamp DNA Mini Kit. Instead of column purification phenol extraction was performed as outlined in the next paragraph. The RNA digest was executed twice. All other steps were performed as described by the manufacturer. For samples with more than 25 mg weight the quantities of the reagents were increased accordingly. Tissue samples were homogenized with PBS and a stainless steel bead in a TissueLyser (Qiagen, 30 Hz, 2 min). Buffer ATL and proteinase K were added and the solution was incubated. DNase-free RNase A (4 mL, 100 mg/mL) was added. After mixing the sample was incubated and shaken (600 rpm) at rt for 5 min. A second portion of DNasefree RNase A (4 mL, 100 mg/mL) was added and the mixture was again incubated and shaken (600 rpm) at rt for 5 min. The tube was centrifuged briefly and buffer AL was added. The sample was mixed and incubated. Following this step the sample was no longer processed on the basis of the QIAamp DNA Mini Kit. The sample was distributed equally to two 2 mL reaction tubes, if necessary. A 1/1 mixture of RotiHPhenol/chloroform (1 vol.) was added and the tube was shaken vigorously at rt for 5 min. The tube was centrifuged (12100 g, 15 min) and the aq. layer was collected. This procedure was repeated once. To the obtained aq. layer chloroform (1 vol.) was added and the tube was shaken at rt for 1 min. After centrifugation (12100 g, 5 min) the aq. layer was collected. During collection of the aq. layers special care was taken to include the interphase. The sample was distributed equally to two 2 mL reaction tubes, if necessary. Ethanol (3 vol.) was added. The sample was left to stand at rt for approximately 2 h. After precipitation of the DNA the tube was centrifuged (12100 g, 30 min). The supernatant was discarded and the pellet was dried. Subsequently, it was dissolved in water (100–400 mL). The solution was centrifuged (12100 g, 30 min) and the supernatant was collected.

10.4.4 Enzymatic digestion of tRNA

Solutions of bulk tRNA from all samples in water (12 µg in 100 µL final volume) were heated to 100 °C for 3 min to denature tRNA and then rapidly cooled on ice. After addition of buffer 2 (10 µL, 300 mM ammonium acetate, 100 mM CaCl₂, 1 mM ZnSO₄, pH 5.7) and nuclease S1 (80 units, *Aspergillus oryzae*) the mixture was incubated for 3 h at 37 °C. Addition of buffer 3 (12 µL, 500 mM Tris-HCl, 1 mM EDTA, pH 8.0), antarctic phosphatase (10 units), snake venom phosphodiesterase I (0.2 units, *Crotalus adamanteus venom*) and incubation for further 3 h at 37 °C completed the digestion. All labeled nucleosides of interest were added. Then the sample was centrifuged (12100 g, 15 min). The supernatant was

removed and lyophilized to a total volume of 105 μL . Each digestion and HPLC-ESI-MS measurement was performed at least in triplicate with three independent concentrations of the appropriate labeled nucleosides. The concentrations of standard solutions were chosen to be in the expected range of the sample nucleoside concentration.

10.4.5 Enzymatic digestion of DNA

DNA mixtures (4 to 10 mg in a final volume of 100 μL H₂O) were heated to 100 °C for 5 min to denature the DNA and rapidly cooled on ice. Buffer 2 (10 mL, 300 mM ammonium acetate, 100 mM CaCl₂, 1 mM ZnSO₄, pH 5.7) and nuclease S1 (80 units, *Aspergillus oryzae*) were added to the mixture and incubated for 3 h at 37 °C. Addition of buffer 3 (12 mL, 500 mM Tris-HCl, 1 mM EDTA), antarctic phosphatase (10 units), snake venom phosphodiesterase I (0.2 units, *Crotalus adamanteus* venom) and incubation for further 3 h at 37 °C completed the digestion. Labeled nucleosides were added, followed by centrifugation of the sample (12100 g, 15 min). The supernatant was removed, the volume reduced to 100 μL and measured with HPLC-ESI-MS. Each sample was analyzed at least in duplicate with independent concentrations of the two labeled nucleosides. The concentrations of standard solutions were chosen to be in the expected range of the sample nucleoside concentration.

10.4.6 HPLC-ESI-MS

The samples (100 mL injection volume) were analyzed by HPLC-ESI-MS on a Thermo Finnigan LTQ Orbitrap XL and chromatographed by a Dionex Ultimate 3000 HPLC system with a flow of 0.15 mL/min over an Uptisphere120-3HDO column from Interchim. The column temperature was maintained at 30 °C. The chromatographic eluent was directly injected into the ion source without prior splitting. Ions were scanned by use of a positive polarity mode over a full-scan range of m/z 200–1000 with a resolution of 30.000. Parameters of the mass spectrometer were tuned with a freshly mixed solution of adenosine (5 mM) in buffer C. The parameters used in this section were sheath gas flow rate, 16 arb; auxiliary gas flow rate, 11 arb; sweep gas flow rate, 4 arb; spray voltage, 5.0 kV; capillary temperature, 200°C; capillary voltage, 12 V, tube lens 60 V.

Eluting buffers were buffer C (2 mM HCOONH₄ in H₂O (pH 5.5)) and buffer D (2 mM HCOONH₄ in H₂O/MeCN 20/80 (pH 5.5)). The elution was monitored in all cases at 260 nm (Dionex Ultimate 3000 Diode Array Detector).

The gradient for tRNA (with m²A): 0 → 41.25 min; 0% → 6% buffer D; 41.25 → 80 min; 6% → 60% buffer D; 80 → 82 min; 60% → 100% buffer D; 82 → 100 min; 100% buffer D; 100 → 105 min; 100 → 0% buffer D; 105 → 115 min; 0% buffer D.

The gradient for tRNA (without m²A) was 0 → 12 min; 0% → 3% buffer D; 12 → 60 min; 3% → 60% buffer D; 60 → 62 min; 60% → 100% buffer D; 62 → 70 min; 100% buffer D; 70 → 85 min; 100 → 0% buffer D; 85 → 95 min; 0% buffer D. The elution was monitored at 260 nm (Dionex Ultimate 3000 Diode Array Detector).

The gradient for DNA was 0 → 12 min; 0% → 3% buffer D; 12 → 60 min; 3% → 60% buffer D; 60 → 62 min; 60% → 100% buffer D; 62 → 70 min; 100% buffer D; 70 → 85 min; 100 → 0% buffer D; 85 → 95 min; 0% buffer D. The elution was monitored at 260 nm (Dionex Ultimate 3000 Diode Array Detector).

10.4.6.1 Mass filter

The areas of labeled and unlabeled nucleosides from LC-MS measurements were determined using the *Qualbrowser* program by extraction of the accurate mass range with a mass filter (*Table 7*) from the total ion current (TIC).

Table 7: High resolution mass ranges of natural and corresponding labeled nucleosides used for quantification.

Nucleoside	Nucleosides mass range m/z	Labeled nucleosides mass range m/z
Am, m ⁶ A, m ¹ A, m ² A	282.1142-282.1262	285.1335-285.1435
t ⁶ A	413.1315-413.1475	418.1420-418.1580
i ⁶ A	336.1606-336.1716	338.1740-338.1840
ms ² i ⁶ A	382.1484-382.1594	385.1679-385.1789
m ² ₂ G	312.1248-312.1368	315.1441-315.1561
m ² G, m ¹ G, Gm	298.1076-298.1196	301.1276-301.1396
Q	410.1640-410.1730	413.1778-413.1898
m ⁶ t ⁶ A	427.1532-427.1622	430.1707-430.1807
OHyW	525.1879-525.2029	528.2065-528.2195
yW	509.1937-509.2037	512.2138-512.2238
io ⁶ A	352.0915-352.2315	354.1041-354.2441
ms ² io ⁶ A	398.1423-398.1563	400.0918-400.2318
m ⁶ ₂ A	296.1233-296.1413	299.1488-299.1608
hmC	258.1024-258.1144	260.1167-260.1277 (d ₂ -hmC) 260.1067-260.1177 (¹⁸ O-hmC)
mC	242.1075-242.1195	245.1261-245.1381
caC	272.0827-272.0947	-
fC	256.0858-256.0988	-
hmC	259.0858-259.0978	-

10.4.6.2 Calibration curves

Mass calibration curves of the labelled and corresponding unlabelled synthesized nucleosides were obtained at five different concentration ratios. For each concentration an average value of three independent measurements was determined (*Figure 24*). Each labelled nucleoside solution was mixed with three different concentrations of the corresponding unlabelled nucleosides. The areas of labelled and unlabelled nucleosides from LC-MS measurements

were determined using the *Qualbrowser* program by extraction of the accurate mass range with a mass filter (*Table 1*) from the total ion current (TIC). The linear fits of the determined area ratios with the amount ratios gave R^2 -values of minimum 0.9992. The linear fit equations were used for calculation of the exact nucleoside contents in bulk tRNA samples. Synthetic labelled nucleosides were added to the digest solutions and the areas of labelled and unlabelled nucleosides were determined as described above. The amount of each nucleoside was calculated from the obtained area ratios and the linear fit equations of the calibration curves.

10.4.7 Separation of mitochondria and cytosol

These experiments were performed by A. C. Kneuttinger and Cytochrome C oxidase experiments are described in her Masterthesis.^[169] 10-20 g tissue samples were sliced and washed on ice with ice-cold buffers as described in the manual. The preparations of liver, kidney, spleen, cerebellum and cerebrum (“soft” tissues) were washed twice in 2 volumes of extraction buffer E (10 mM HEPES, pH 7.5, containing 0.2 M mannitol, 70 mM sucrose, and 1 mM EGTA). Subsequent homogenization was performed in 10 volumes of 2 mg/mL albumin in buffer E using a commercial blender and a potter homogenizer for large amounts of tissue. Heart preparations (“hard” tissue) required pretreatment with trypsin to promote breakdown of the cellular structure. The samples were washed once briefly in 2 volumes of buffer E, 3 min in 10 volumes of 0.25 mg/mL trypsin in buffer E and 20 min in 8 volumes of 0.25 mg/mL trypsin in buffer E. To quench the proteolytic reaction, albumin solution was added to a final concentration of 10 mg/mL. After one additional washing step with 8 volumes of buffer E, the preparations were homogenized in 8 volumes of buffer E as described above. The centrifugation steps for fractionation of the cellular components were adopted from literature^[170] to avoid simultaneous enrichment of lysosomes and peroxisomes in the mitochondria pellet. Low-speed centrifugation was carried out at 4 °C and 600 g for 15 min and high-speed centrifugation of the previous supernatant at 4 °C and 7,000 g for 15 min. The mitochondria pellets and the supernatant, which contained components of the cytosol, were subsequently assayed for purity by a commercial cytochrome C oxidase assay (Sigma-Aldrich) and the tRNA was isolated for further analysis. Extraction of mitochondrial and cytosolic tRNA was performed as described for whole tissue samples.

10.4.8 *In vitro* translation assay

We used the non-radioactive luciferase control reaction with TNT RNA Polymerase T7 and Luciferase control DNA as described in the Promega Kit with minor changes. Each assay contained TNT reaction buffer (0.5 μ L), T7 TNT RNA Polymerase (0.25 μ L), amino acid mixture minus leucine (1 mM), amino acid mixture minus methionine (1 mM), RNasin ribonuclease inhibitor (10 U), Luciferase T7 control DNA (0.25 μ g). Afterwards the appropriate tRNA (12.5 ng) and RNase-free water were added to a total assay volume of 6.25 μ L, followed by addition of tRNA-depleted lysate (6.25 μ L).

These translation reactions were incubated at 30 °C and a 1 μ L aliquot was removed every 2-3 min from each fraction starting at 12 min. This sample was transferred into a 96 well plate, mixed well with 25 μ L of Luciferase Assay substrate and analyzed immediately. Luminescence was measured with a TECAN Microplate Reader Genios Pro in 10 cycles for 100 ms each cycle. Reproducible luminescence slopes were obtained after normalization to the liver value and the results are shown in Fig 2. The data were averaged and plotted against time. A linear fit of each initial slope was performed and normalized to the highest value (usually liver). Every measurement was repeated at least in triplicate and every value represents mean value with s.d. Care was taken to use different tRNA-depleted fractions.

10.4.9 Immunohistochemistry

Immunohistochemistry was performed by Dr. S. Michalakis and S. Koch from the group of Prof. M. Biel. Coronal cryosections (12 μ m) from 12 week old C57-BL6/N mice were rehydrated in phosphate buffered saline (PBS), fixed (10 min, 4% paraformaldehyde in PBS, pH 7.4), treated with 2N HCl in PBS (20 min) and incubated for 16 hours (4°C) with primary antibodies in 5% chemiblocker (Millipore, Germany) and 0.3% Triton X-100 in PBS. The primary antibody used was: rabbit anti-5-hydroxymethylcytosine (hmC, 1:500, Active Motif, Belgium). For secondary detection we used goat Alexa488 anti-rabbit (1:800, Cell Signaling Technologies, Germany). Cell nuclei were counterstained with Hoechst 33342 (5 mg/mL, Sigma, Germany) and sections were mounted with aqueous mounting medium (PermaFluor, Beckman-Coulter, USA). Tissues were analyzed using a Zeiss Axioscope epifluorescence microscope equipped with a HBO 100 mercury arc lamp, appropriate filters equipped with an MRc ccd camera (Zeiss, Germany). Laser scanning confocal micrographs were collected using a LSM 510 meta microscope (Carl Zeiss, Germany).

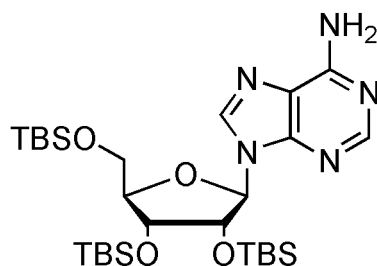
10.5 Phylogenetic analysis

For phylogenetic analysis the programs *Cluster 3.0* and *Java Treeview* were used.^[204-205] Hierarchical clustering was performed with the euclidean distance algorithm of the averaged quantitative raw data. Average linkage yielded the clustered data, which were visualized with *Java Treeview*. Correlation factors were used as labeled in this program.

10.6 Syntheses

10.6.1 Synthesis of t⁶A

2',3',5'-Tri-*O*-(*tert*-butyldimethylsilyl)adenosine (1)



Adenosine (15.0 g, 56.1 mmol), imidazole (34.4 g, 0.51 mol), and TBSCl (29.5 g, 196 mmol) were suspended in dry DMF (60 mL) and stirred for 19 h at rt. The reaction mixture was stopped with H₂O and extracted with CH₂Cl₂ (3 × 200 mL). The combined organic phase was dried over MgSO₄, the solvent removed *in vacuo* and purified *via* column chromatography (EtOAc/cyclohexane = 20:80 → 50:50). Compound **1** (27.7 g, 45.4 mmol) was obtained as colorless foam with 81%.

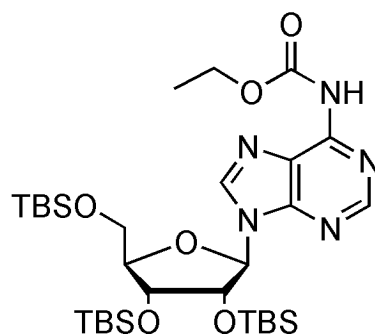
R_f = 0.39 (EtOAc/cyclohexane = 1:1). M.p.: 144 °C.

¹H NMR (CDCl₃, 600 MHz) δ (ppm) = 8.31 (s, 1H, C2H), 8.16 (s, 1H, C8H), 6.01 (d, ³J=5.2 Hz, 1H, C1H), 5.96 (s, 2H, NH₂), 4.65 (t, ³J=4.7 Hz, 1H, C2H), 4.29 (t, ³J=3.9 Hz, 1H, C3H), 4.11 (dd, ³J=3.7 Hz, ³J=6.7 Hz, 1H, C4H), 4.01 (dd, ³J=4.1 Hz, ²J=11.3 Hz, 1H, C5H_a), 3.77 (dd, ³J=2.8 Hz, ²J=11.3 Hz, 1H, C5H_b), 0.12 – 0.08 (3s, 27H, SiC(CH₃)₃), 0.12 – (-0.25) (6s, 18H, Si(CH₃)₂).

¹³C NMR (CDCl₃, 151 MHz) δ (ppm) = 155.2, 152.3, 150.1, 140.1, 120.2, 88.6, 85.7, 76.1, 72.2, 62.7, 26.3, 26.1, 25.9, 18.7, 18.3, 18.1, -4.2, -4.5, -4.5, -4.9, -5.1, -5.2.

HRMS (ESI⁺): calcd. for C₂₈H₅₅N₅O₄Si₃ [M+H]⁺: 610.3635, found: 610.3645.

IR: $\tilde{\nu}$ (cm⁻¹) = 3317 w, 3151 w, 2953 s, 2929 s, 2897 m, 2857 s, 1658 m, 1643 m, 1597 m, 1552 w, 1472 m, 1416 w, 1361 m, 1329 m, 1297 m, 1253 s, 1156 m, 1128 m, 1072 m, 1043 m, 999 m, 968 m, 939 m, 831 s, 776 s, 669 w.

***N*⁶-Ethoxycarbonyl-2',3',5'-tri-*O*-(*tert*-butyldimethyl-silyl)adenosine (**2**)^[50, 137]**

Compound **1** (27.7 g, 45.4 mmol) was dissolved in dry pyridine (300 mL), followed by slow addition of ethylchloroformate (15.2 mL, 159 mmol) at 0 °C. The yellow reaction mixture was stirred for 5 h at rt, then H₂O (500 mL) was added to stop the reaction and afterwards extracted with CH₂Cl₂ (3 × 350 mL). The combined organic phases were dried over MgSO₄ and the solvent removed *in vacuo*. Afterwards the crude material was purified *via* column chromatography (EtOAc/cyclohexane = 20:80 → 50:50) to obtain compound **2** (22.2 g, 32.5 mmol, 72%) as a colorless foam.

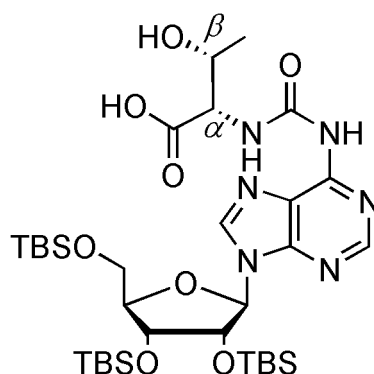
R_f = 0.70 (EtOAc/cyclohexane = 1:1). M.p.: 114 °C.

¹H NMR (CDCl₃, 600 MHz) δ (ppm) = 8.74 (s, 1H, C2H), 8.39 (s, 2H, C8H, NH), 6.07 (d, ³J=5.0 Hz, 1H, C1'H), 4.62 (t, ³J=4.6 Hz, 1H, C2'H), 4.31 (q, ³J=7.1 Hz, 2H, CH₂CH₃), 4.27 (t, ³J=4.0 Hz, 1H, C3'H), 4.13 (dd, ³J=3.6 Hz, ³J=6.4 Hz, 1H, C4'H), 4.01 (dd, ³J=3.9 Hz, ²J=11.4 Hz, 1H, C5'H_a), 3.79 (dd, ³J=2.6 Hz, ²J=11.4 Hz, 1H, C5'H_b), 1.33 (t, ³J=7.1 Hz, 3H, CH₂CH₃), 0.94 – 0.77 (3s, 27H, SiC(CH₃)₃) 0.12 – (-0.27) (6s, 18H, Si(CH₃)₂).

¹³C NMR (CDCl₃, 151 MHz) δ (ppm) = 153.1, 151.1, 149.5, 141.6, 121.8, 88.7, 85.9, 76.3, 72.0, 62.6, 62.4, 27.1, 27.1, 27.1, 26.3, 26.0, 25.9, 18.8, 18.3, 18.1, 14.6, -4.2, -4.5, -4.5, -4.8, -5.1, -5.2.

HRMS (ESI⁺): calcd. for C₃₁H₅₉N₅O₆Si₃ [M+H]⁺: 682.3846, found: 682.3865.

IR: $\tilde{\nu}$ (cm⁻¹) = 2953 w, 2930 w, 2857 w, 2360 w, 1751 m, 1734 m, 1613 m, 1586 m, 1521 w, 1464 m, 1252 m, 1211 m, 1154 s, 1072 m, 1022 w, 834 s, 774 s, 670 m, 644 m.

2',3',5'-Tri-*O*-(*tert*-butyldimethylsilyl)-*N*⁶-threonylcarbamoyladenosine (3)^[50, 137]

Compound **2** (1.00 g, 1.46 mmol) and L-threonine (0.26 g, 2.21 mmol) were dissolved in dry pyridine (20 mL) and refluxed at 125 °C for 6.5 h. Then another portion of L-threonine (0.09 g, 0.73 mmol) was added and the reaction was refluxed for another 2 h. The solvent was then removed *in vacuo*, followed by purification *via* column chromatography (MeOH/CH₂Cl₂ = 0:100 → 10:90) of the crude product. Compound **3** (0.88 g, 1.16 mmol, 80%) was obtained as a colorless solid.

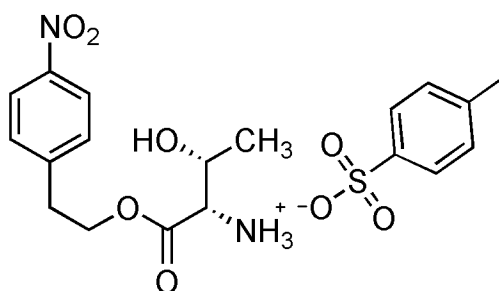
R_f = 0.10 (CH₂Cl₂/MeOH = 10:1). M.p.: 183 °C.

¹H NMR (d₆-DMSO, 400 MHz) δ (ppm) = 9.62 (d, ³J=6.4 Hz, 1H, C₆NH), 9.45 (s, 1H, C_αNH), 8.60 (s, 1H, C₈H), 8.51 (s, 1H, C₂H), 6.01 (d, ³J=6.4 Hz, 1H, C₁H), 4.94 (dd, ³J=4.5 Hz, ³J=6.1, 1H, C₂H), 4.35 (d, ³J=4.2 Hz, 1H, C₃H), 4.15 – 3.93 (m, 3H, C₄H, C_αH, C_βH), 3.80 – 3.70 (m, 2H, C₅H₂), 1.02 (d, ³J=6.3 Hz, 3H, β-CH₃), 0.95 – 0.64 (3s, 27H, SiC(CH₃)₃), 0.19 – (-0.45) (6s, 18H, Si(CH₃)₂).

¹³C NMR (d₆-DMSO, 101 MHz) δ (ppm) = 173.5, 152.7, 151.0, 150.4, 150.2, 120.3, 87.1, 85.5, 74.2, 72.2, 66.3, 62.4, 58.7, 54.9, 25.8, 25.7, 25.4, 19.3, 18.0, 17.8, 17.5, -4.7, -4.8, -4.8, -5.5, -5.5.

HRMS (ESI⁻), calcd. for C₃₃H₆₂N₆O₈Si₃ [M-H]⁻: 753.3864, found: 753.3864.

IR: $\tilde{\nu}$ (cm⁻¹) = 2953 w, 2930 w, 2857 w, 2361 m, 2320 m, 1726 w, 1612 m, 1548 w, 1530 w, 1469 m, 1254 m, 1073 m, 834 s, 777 s, 668 m, 582 m.

L-Threonine-[2-(4-nitrophenyl)ethyl]ester-mono(para-toluol-sulfonate)salt (10**)**^[48]

Para-toluenesulfonic acid (22.2 g, 118 mmol) and 2-(4-nitrophenyl)ethanol (19.6 g, 118 mmol) were added to a mixture of L-threonine (7.00 g, 58.8 mmol) in toluene (350 mL). The reaction mixture was refluxed under *Dean Stark* conditions at 150 °C for 12 h. Diethylether (120 mL) was added to the brown two phase mixture and the upper layer was decanted. After a second addition of diethylether (120 mL) and the residual solvent was removed *in vacuo* after decantation of the upper layer. The brown oil was dissolved while heating in MeOH (60 mL) and diethylether (220 mL) added to crystallize the product at 4 °C for 24 h. The brown crystals were washed with cold MeOH and dried *in vacuo* to yield compound **10** (23.9 g, 54.4 mmol, 92%) as brown crystals.

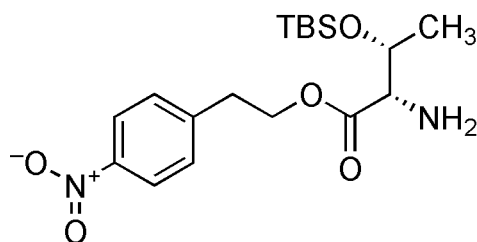
M.p.: 192–194 °C.

¹H NMR (d₆-DMSO, 400 MHz) δ (ppm) = 8.23 (s, 3H, NH₃⁺), 8.17 [d, ³J=8.8 Hz, 2H, H_{Npe}(o-NO₂)], 7.58 [d, ³J=8.8 Hz, 2H, H_{Npe}(m-NO₂)], 7.49 [d, ³J=8.0 Hz, 2H, H_{Tos}(m-CH₃)], 7.11 [d, ³J=7.8 Hz, 2H, H_{Tos}(o-CH₃)], 4.52 – 4.36 (m, 2H, CH₂CH₂O), 4.11 – 4.00 (m, 1H, C _{β} H), 3.90 (s, 1H, C _{α} H), 3.10 (t, ³J=6.4 Hz, 2H, CH₂CH₂O), 2.28 (s, 3H, Tos-CH₃), 1.14 (d, ³J=6.5 Hz, 3H, β -CH₃).

¹³C NMR (d₆-DMSO, 101 MHz) δ (ppm) = 168.1, 146.3, 146.2, 145.6, 137.7, 130.3, 128.0, 125.5, 123.4, 65.4, 64.9, 57.8, 33.8, 20.8, 20.0.

HRMS (ESI⁺): calcd. for C₁₂H₁₆N₂O₅ [M+H]⁺: 269.1132, found: 269.1134.

IR: $\tilde{\nu}$ (cm⁻¹) = 3395 *m*, 3197 *m*, 2895 *s*, 2793 *m*, 2693 *w*, 1733 *s*, 1608 *m*, 1600 *m*, 1524 *s*, 1480 *w*, 1396 *w*, 1345 *m*, 1297 *m*, 1227 *s*, 1168 *s*, 1116 *s*, 1083 *s*, 920 *w*, 677 *w*, 634 *w*, 563 *s*.

***O*-(*tert*-Butyldimethylsilyl)-L-threonine-[2-(4-nitrophenyl)-ethyl]ester (**11**)^[48]**

Compound **10** (23.9 g, 54.4 mmol), imidazole (18.5 g, 272 mmol) and TBSCl (16.4 g, 109 mmol) were dissolved in dry pyridine (400 mL). The reaction mixture was stirred at rt for 18 h, followed by evaporation of the solvent *in vacuo*. To the orange oil H₂O (200 mL) was added, extracted with CH₂Cl₂ (150 mL) and washed three times with H₂O (3 × 200 mL). The combined organic layers were dried over MgSO₄, the solvent removed *in vacuo* and the crude product purified by column chromatography (CH₂Cl₂/MeOH = 20:1). Pure compound **11** (15.9 g, 41.5 mmol, 76%) was obtained as an orange oil.

R_f = 0.73 (CH₂Cl₂/MeOH = 10:1).

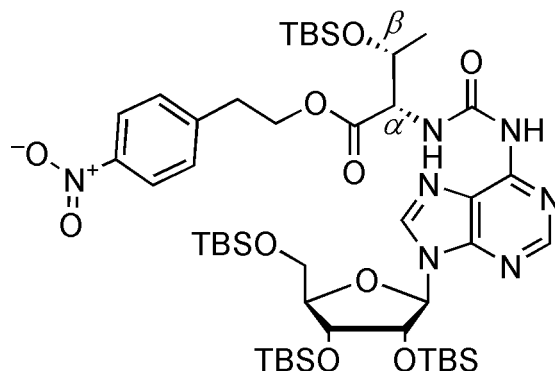
¹H NMR (CDCl₃, 200 MHz) δ (ppm) = 8.25 – 8.07 [m, ³J = 8.8 Hz, 2H, H_{Npe}(o-NO₂)], 7.45 – 7.31 [m, ³J = 8.8 Hz, 2H, H_{Npe}(m-NO₂)], 4.63 – 4.04 (m, 3H, CH₂CH₂O, C_βH), 3.23 (d, ³J = 2.8 Hz, 1H, C_αH), 3.05 (t, ³J = 6.8 Hz, 2H, CH₂CH₂O), 1.55 (s, br, 2H, NH₂), 1.19 (d, ³J = 6.3 Hz, 3H, CH₃), 0.80 (s, 9H, SiC(CH₃)₃), -0.01 – (-0.10) (2s, 6H, Si(CH₃)₂).

¹³C NMR (CDCl₃, 75 MHz) δ (ppm) = 174.2, 147.2, 145.6, 130.0, 124.0, 69.8, 64.7, 61.0, 35.1, 25.8, 21.1, 18.1, -4.1, -5.0.

HRMS (ESI⁺): calcd. for C₁₈H₃₀N₂O₅Si [M+H]⁺: 383.1997, found: 383.2004.

IR: $\tilde{\nu}$ (cm⁻¹) = 3588 w, 2955 m, 2930 m, 2896 m, 2857 m, 1739 s, 1679 m, 1600 w, 1519 s, 1472 w, 1472 m, 1345 s, 1320 w, 1251 s, 1154 s, 1110 m, 1075 m, 1039 w, 1006 m, 968 m, 939 w, 835 s, 807 s, 775 s, 697 m, 632 w, 616 w.

2',3',5'-Tri-*O*-(*Tert*-butyldimethylsilyl)-*N*⁶-{[(1*S*,2*R*)-2-[[*tert*-butyl]dimethyl]silyloxy]-1-[[2-(4-nitrophenyl)ethoxy]carbonyl]propyl]amino}carbonyl}adenosine (14**)**



O-(*tert*-Butyldimethylsilyl)-*L*-threonine-[2-(4-nitrophenyl) ethyl]ester (**11**, 2.10 g, 5.46 mmol) and compound **2** (3.10 g, 4.55 mmol) were dissolved in dry pyridine (35 mL). The reaction mixture was refluxed for 7 h at 125 °C and subsequently CH₂Cl₂ (200 mL) was added. Afterwards the organic layer was washed with H₂O (3 × 150 mL), dried over MgSO₄ and filtrated. After evaporation of the solvent *in vacuo* the raw product was purified *via* column chromatography (EtOAc/cyclohexane = 20:80). Pure compound **14** (3.53 g, 4.14 mmol, 91%) was obtained as colorless foam after drying *in vacuo*.

R_f = 0.65 (EtOAc/cyclohexane = 1:1).

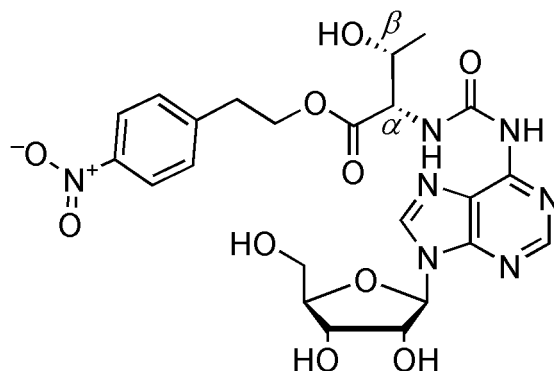
¹H NMR (CDCl₃, 400 MHz) δ (ppm) = 9.90 (d, ³J=9.1 Hz, 2H, C_αNH), 8.46 (s, 1H, C2H), 8.43 (s, 1H, C8H), 8.17 (s, br, 1H, C₆NH) 7.99 [d, ³J=8.8 Hz, 2H, H_{Npe(o-NO₂)}], 7.32 [d, ³J=8.7 Hz, 2H, H_{Npe(m-NO₂)}], 6.08 (d, ³J=4.6 Hz, 1H, C₁H), 4.62 (t, ³J=4.4 Hz, 1H, C₂H), 4.55 (dd, ³J=1.6 Hz, ³J=9.1 Hz, 1H, C_βH), 4.50 (qd, ³J=1.6 Hz, ³J=9.2 Hz, 1H, C_αH), 4.43 – 4.29 (m, 3H, C₃H, CH₂CH₂O), 4.15 (dd, ³J=3.7 Hz, ³J=6.5 Hz, 1H, C₄H), 4.04 (dd, ³J=3.7 Hz, ²J=11.5 Hz, 1H, C₅H_a), 3.79 (dd, ³J=2.5 Hz, ²J=11.5 Hz, 1H, C₅H_b), 3.02 (t, ³J=6.5 Hz, 2H, CH₂CH₂O), 1.24 (d, ³J=6.3 Hz, 3H, C_βCH₃), 0.95 – 0.81 (4s, 36H, SiC(CH₃)₃), 0.14 – (-0.17) (8s, 24H, Si(CH₃)₂).

¹³C NMR (CDCl₃, 101 MHz) δ (ppm) = 171.1, 154.3, 150.3, 150.1, 147.0, 145.7, 141.5, 130.0, 123.8, 120.3, 88.9, 85.6, 77.4, 76.4, 71.8, 68.9, 64.9, 62.5, 59.8, 35.0, 26.3, 26.1, 25.9, 25.7, 21.3, 18.8, 18.3, 18.1, 18.0, -4.1, -4.1, -4.5, -4.5, -4.7, -5.1, -5.2.

HRMS (ESI⁺): calcd. for C₄₇H₈₃N₇O₁₀Si₄ [M+H]⁺: 1018.5351, found: 1018.5428.

IR: $\tilde{\nu}$ (cm^{-1}) = 3238 *w*, 2954 *m*, 2930 *m*, 2857 *m*, 1735 *w*, 1701 *m*, 1610 *m*, 1587 *m*, 1522 *s*, 1471 *m*, 1345 *w*, 1311 *w*, 1250 *s*, 1162 *w*, 1127 *w*, 1096 *m*, 1069 *w*, 998 *m*, 968 *w*, 940 *w*, 833 *s*, 745 *s*, 671 *m*.

***N*⁶-{[(1*S*,2*R*)-2-hydroxy-1-[[2-(4-nitrophenyl)ethoxy]carbonyl]propyl]amino}carbonyl}adenosine (**15**)**



Compound **14** (3.53 g, 4.14 mmol) was dissolved in CH₂Cl₂ (3 mL) and afterwards NEt₃·3HF (4.53 g, 28.1 mmol) added. The reaction mixture was stirred for 24 h at rt and afterwards stopped with methoxytrimethylsilane (30 mL, 0.22 mol). After stirring for another hour the solvent was removed *in vacuo* and the crude material purified *via* column chromatography (CH₂Cl₂/MeOH = 50:1 → 10:1). Pure product **15** (1.62 g, 4.09 mmol, 98%) was obtained as a colorless foam after removing the solvent *in vacuo*.

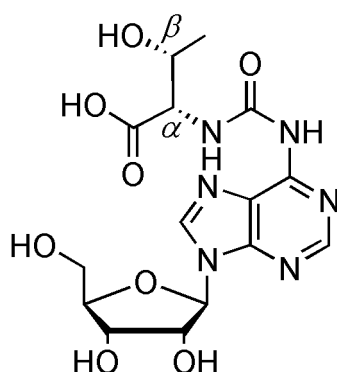
R_f = 0.15 (CH₂Cl₂/MeOH = 10:1).

¹H NMR (d₆-DMSO, 400 MHz) δ (ppm) = 9.88 (s, 1H, C₆NH), 9.80 (d, ³J=8.3 Hz, 1H, C_αNH), 8.69 (s, 1H, C₈H), 8.52 (s, 1H, C₂H), 8.08 [d, ³J=8.8 Hz, 2H, H_{Npe(o-NO₂)}], 7.54 [d, ³J=8.7 Hz, 2H, H_{Npe(m-NO₂)}], 6.00 (d, ³J=5.4 Hz, 1H, C₁H), 5.52 (d, ³J=5.9 Hz, 1H, C₂OH), 5.21 (dd, ³J=2.4 Hz, ³J=4.7 Hz, C₃OH, C_βOH), 5.12 (t, ³J=5.6 Hz, 1H, C₅OH), 4.59 (dd, ³J=5.4 Hz, 10.8 Hz, 1H, C₂H), 4.45 – 4.25 (m, 3H, C_αH, CH₂CH₂O), 4.19 (dd, ³J=4.8 Hz, ³J=8.8 Hz, 2H, C₃H, C_βH), 3.98 (dd, ³J=3.8 Hz, ³J=7.8 Hz, 1H, C₄H), 3.76 – 3.65 (m, 1H, C₅H_a), 3.59 (m, 1H, C₅H_b), 3.05 (t, ³J=6.4 Hz, 2H, CH₂CH₂O), 1.12 (d, ³J=6.3 Hz, 3H, β-CH₃).

¹³C NMR (d₆-DMSO, 101 MHz) δ (ppm) = 170.8, 153.7, 150.7, 150.3, 150.2, 146.6, 146.2, 142.2, 130.2, 123.3, 120.4, 87.8, 85.6, 73.9, 70.2, 66.2, 64.3, 61.2, 58.9, 34.0, 20.5.

HRMS (ESI⁺): *m/z* for C₂₃H₂₇N₇O₁₀ [M+H]⁺: calcd. 562.1892, found: 562.1902.

IR: $\tilde{\nu}$ (cm⁻¹) = 3228 *m*, 2926 *m*, 1736 *m*, 1684 *s*, 1615 *m*, 1590 *m*, 1516 *s*, 1469 *m*, 1397 *w*, 1343 *s*, 1297 *m*, 1236 *m*, 1108 *m*, 1079 *s*, 1017 *m*, 896 *w*, 856 *w*, 796 *w*, 736 *w*, 696 *w*, 642 *w*.

***N*⁶-Threonylcarbamoyladenine (t⁶A)**

Method A: Compound **3** (0.44 g, 0.58 mmol) and NEt₃·3HF (0.91 mL, 5.55 mmol) were dissolved in CH₂Cl₂ (3 mL) and stirred at rt for 20 h. Afterwards methoxytrimethylsilane (10 mL, 0.73 mol) was added to stop the reaction and stirred for additional 30 min. After removing the solvent *in vacuo* the crude material was dissolved in EtOH while heating, filtrated and the solvent was again removed *in vacuo*. The crude product was purified *via* RP-HPLC (eluent A: H₂O, eluent B: MeCN, gradient: 100% A, 0% B → 0% A, 100% B in 45 min, retention time = 18.5 min) to yield nucleoside t⁶A (174 mg, 0.38 mmol, 65%) as a colorless hygroscopic salt with NEt₃ as counterion (ratio of 1.5:1).

Method B: 50.0 mg (89.0 μmol) of compound **15** were dissolved in 900 μL THF and treated with 100 μL (660 μmol) 1,8-Diaza-bicyclo[5.4.0]undec-7-en. Afterwards the reaction mixture was shaken for 2 h at 45 °C at 700 rpm. The solvent was removed and crude product was purified *via* RP-HPLC (eluent A: H₂O, eluent B: MeCN, gradient: 100% A, 0% B → 0% A, 100% B in 45 min, retention time = 18.5 min) to yield t⁶A (23.0 mg, 49.7 μmol, 56%).

¹H NMR (CD₃OD, 400 MHz) δ (ppm) = 8.59 (s, 1H, C₈H), 8.51 (s, 1H, C₂H), 6.07 (d, ³J=5.9 Hz, 1H, C₁H), 4.77 – 4.72 (m, 1H, C₂H), 4.39 – 4.31 (m, 3H, C₃H, C_αH, C_βH), 4.17 (q, ³J=3.0 Hz, 1H, C₄H), 3.89 (dd, ³J=2.8 Hz, ²J=12.4 Hz, 1H, C₅H_a), 3.77 (dd, ³J=3.1 Hz, ²J=12.4 Hz, 1H, C₅H_b), 3.19 (q, ³J=7.3 Hz, 4H, N(CH₂CH₃)₃), 1.30 (t, ³J=7.3 Hz, 6H, N(CH₂CH₃)₃), 1.26 (d, ³J=6.3 Hz, 3H, β-CH₃).

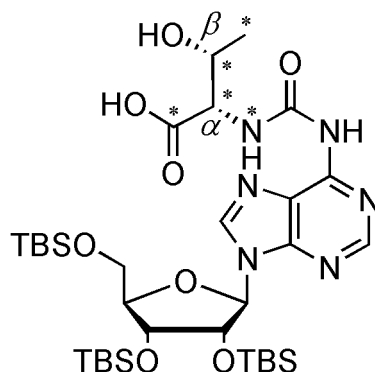
¹³C NMR (CD₃OD, 101 MHz) δ (ppm) = 175.4, 154.6, 150.9, 150.5, 149.8, 142.4, 120.6, 89.6, 86.4, 74.2, 70.9, 67.7, 61.8, 60.2, 46.3 (NEt₃), 18.9, 7.7 (NEt₃).

HRMS (ESI), calcd. for C₁₅H₂₀N₆O₈ [M-H]⁻:411.1270, found: 411.1264.

IR: $\tilde{\nu}$ (cm⁻¹) = 3234 *m*, 2929 *w*, 2360 *w*, 2341 *w*, 1681 *s*, 1607 *s*, 1589 *s*, 1531 *s*, 1467 *s*, 1391 *s*, 1359 *m*, 1331 *m*, 1298 *m*, 1252 *s*, 1081 *s*, 1055 *s*, 984 *m*, 895 *m*, 838 *m*, 796 *s*, 642 *s*.

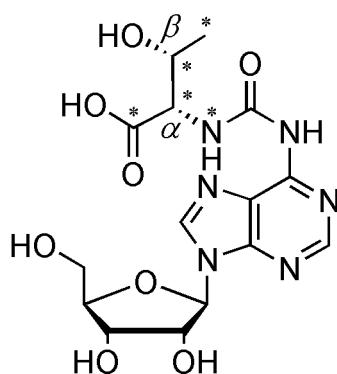
10.6.2 Synthesis of $^{13}\text{C}_4, ^{15}\text{N-t}^6\text{A}$

$^{13}\text{C}_4, ^{15}\text{N-2',3',5'}$ -Tri-*O*-(*tert*-butyldimethylsilyl)-*N*⁶-threonylcarbamoyladenosine (**4**)



Compound **2** (183 mg, 269 μmol) and $^{13}\text{C}_4, ^{15}\text{N}$ -L-threonine (50.0 mg, 403 μmol) were dissolved in dry pyridine (4.0 mL) and refluxed at 125 $^\circ\text{C}$ for 6.5 h. Afterwards the solvent was removed *in vacuo* and the raw product purified *via* column chromatography (MeOH/ CH_2Cl_2 = 0:100 \rightarrow 10:90). Compound **4** was obtained as a colorless solid and used in the following reaction.

HRMS (ESI), calcd. for $\text{C}_{29}^{13}\text{C}_4\text{H}_{62}\text{N}_5^{15}\text{NO}_8\text{Si}_3$ $[\text{M-H}]^-$: 758.3969, found: 758.3980.

$^{13}\text{C}_4,^{15}\text{N}-N^6$ -Threonylcarbamoyladenine ($^{13}\text{C}_4,^{15}\text{N}-t^6\text{A}$)

The isotope-labeled compound **4** (133 mg, 175 μmol) and $\text{NEt}_3 \cdot 3\text{HF}$ (142 μL , 875 μmol) were dissolved in CH_2Cl_2 (3 mL) and stirred at rt for 72 h. Afterwards methoxytrimethylsilane (1.50 mL, 4.84 mmol) was added to stop the reaction and stirred for additional 30 min. After removing the solvent *in vacuo* the colorless crude material was dissolved in EtOH while heating, filtrated and the solvent was again removed *in vacuo*. The crude product was purified *via* RP-HPLC (eluent A: H_2O , eluent B: MeCN, gradient: 100% A, 0% B \rightarrow 0% A, 100% B in 45 min, retention time = 18.5 min) to yield nucleoside $^{13}\text{C}_4,^{15}\text{N}-t^6\text{A}$ (57.0 mg, 122 μmol , 45% over two steps) as a colorless oil with NEt_3 (ratio of 1.5:1).

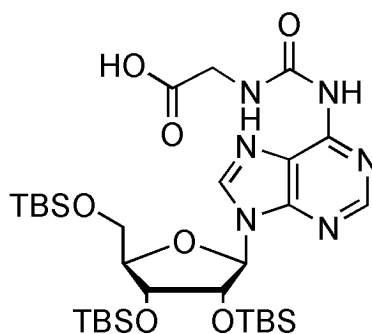
^1H NMR (CD_3OD , 400 MHz) δ (ppm) = 8.58 (s, 1H, C8H), 8.52 (s, 1H, C2H), 6.07 (d, $^3J=5.9$ Hz, 1H, C1H), 4.77 – 4.71 (m, 1H, C2'H), 4.34 (s, $^1J=140$ Hz, 2H, C $_{\alpha}$ H, C $_{\beta}$ H), 4.37 (dd, $^3J=3.3$ Hz, $^3J=5.1$ Hz, 1H, C3'H), 4.17 (dd, $^3J=3.0$ Hz, $^3J=6.1$ Hz, 1H, C4'H), 3.89 (dd, $^3J=2.8$ Hz, $^2J=12.4$ Hz, 1H, C5'H_a), 3.77 (dd, $^3J=3.1$ Hz, $^2J=12.4$ Hz, 1H, C5'H_b), 3.18 (q, $^3J=7.3$ Hz, 4H, N(CH₂CH₃)₃), 1.29 (t, $^3J=7.3$ Hz, 6H, N(CH₂CH₃)₃), 1.25 (dd, 3H, $^3J=5.9$ Hz, $^2J=8.4$ Hz, $^1J=124$ Hz).

^{13}C NMR (CD_3OD , 101 MHz) δ (ppm) = 177.3 (d, $^1J=53$ Hz, ^{13}CO), 156.1 (d, $^1J=22$ Hz, ^{15}N CO) 152.5, 152.0, 151.4, 144.0, 122.1, 91.1, 88.0, 75.8, 72.5, 69.3 (t, $^1J=39$ Hz, β - ^{13}CH), 63.3, 61.9 (t, $^1J=44$ Hz, α - ^{13}CH), 47.8 (NEt_3), 20.6 (d, $^1J=38$ Hz, β - $^{13}\text{CH}_3$), 9.3 (NEt_3).

HRMS (ESI), calcd. for $\text{C}_{11}^{13}\text{C}_4\text{H}_{20}\text{N}_5^{15}\text{NO}_8$ [$\text{M}-\text{H}$] $^-$: 416.1374, found: 416.1367.

10.6.3 Synthesis of g⁶A

2',3',5'-Tri-*O*-(*tert*-butyldimethylsilyl)-*N*⁶-glycinylicarbamoyladenosine (**5**)^[137]



Compound **2** (500 mg, 0.79 mmol) and glycine (110 mg, 1.47 mmol) were dissolved in dry pyridine (12.5 mL) and refluxed at 125 °C for 7 h. Afterwards the solvent was removed *in vacuo*, followed by purification *via* column chromatography (CH₂Cl₂/MeOH = 10:1) of the crude product. Compound **5** (389 mg, 0.55 mmol, 69%) was obtained as a colorless solid.

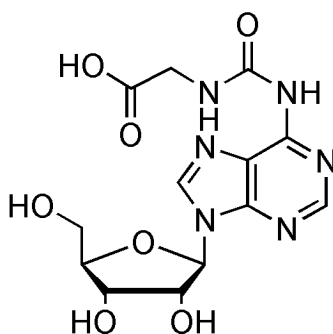
R_f = 0.07 (CH₂Cl₂/MeOH = 10:1). M.p.: 209 °C.

¹H NMR (d₆-DMSO 400 MHz): δ (ppm) = 9.52 – 9.40 (m, 2H, C₆-NH, C_α-NH), 8.60 (s, 1H, C2H), 8.52 (s, 1H, C8H), 6.02 (d, ³J=6.4 Hz, 1H, C₁H), 4.92 (dd, ³J=4.4 Hz, ³J=6.4 Hz, 1H, C₂H), 4.34 (dd, ³J=1.8 Hz, ³J=4.3 Hz, 1H, C₃H), 4.04 – 3.97 (m, 2H, C₄H, C₅H_a), 3.77 (dd, ³J=3.2 Hz, ²J=10.2 Hz, 1H, C₅H_b), 3.72 (d, ³J=4.6 Hz, 2H, CH₂), 0.93 – 0.70 (3s, 27H, 3 SiC(CH₃)₃), 0.14 – (-0.39) (6s, 18H, 3 Si(CH₃)₂).

¹³C NMR (d₆-DMSO, 101 MHz) δ (ppm) = 171.7, 153.2, 150.9, 150.3, 150.3, 142.1, 120.3, 87.0, 85.5, 74.3, 72.2, 62.4, 45.4, 25.8, 25.7, 25.4, 18.0, 17.8, 17.4, -4.7, -4.8, -4.9, -5.5, -5.5, -5.5.

HRMS (ESI): calcd. for C₃₁H₅₈N₆O₇Si₃ [M-H]⁻: 709.3602, found: 709.3596.

IR: $\tilde{\nu}$ (cm⁻¹) = 2945 w, 2929 m, 2857 w, 1696 m, 1612 m, 1591 m, 1542 m, 1472 m, 1403 w, 1360 w, 1252 s, 1159 m, 1098 m, 1072 m, 1005 w, 966 w, 940 w, 835 s, 776 s, 671 w.

N⁶-Glycylcarbamoyladenosine (g⁶A)^[137]

Compound **5** (160 mg, 0.23 mmol) and $\text{NEt}_3 \cdot 3\text{HF}$ (110 μL , 0.68 mmol) were dissolved in CH_2Cl_2 (5 mL) and stirred at rt for 48 h. Afterwards methoxytrimethylsilane (1 mL, 7.52 mmol) was added to stop the reaction and stirred for additional 1 h. After removing the solvent *in vacuo* the colorless crude material was dissolved in EtOH while heating, filtrated and the solvent was again removed *in vacuo*. The crude product was purified *via* RP-HPLC (eluent A: H_2O , eluent B: MeCN, gradient: 100% A, 0% B \rightarrow 0% A, 100% B in 45 min, retention time = 17.8 min) to yield nucleoside **g⁶A** (5.00 mg, 13.58 μmol , 6%) as a colorless hygroscopic salt with NEt_3 as counterion (ratio 1.5:1).

^1H NMR (CD_3OD , 200 MHz) δ (ppm) = 8.59 (s, 1H, C2H), 8.51 (s, 1H, C8H), 6.06 (d, $^3J=5.9$ Hz, 1H, C1'H), 4.74 (t, $^3J=5.5$ Hz, 1H, C2'H), 4.36 (dd, $^3J=3.3$ Hz, $^3J=5.0$ Hz, 1H, C3'H), 4.17 (dd, $^3J=2.7$ Hz, $^3J=5.6$ Hz, 1H, C4'H), 3.99 (s, 2H, CH_2), 3.83 (dd, $^3J=2.8$ Hz, $^2J=12.4$ Hz, 2H, C_5H_2), 3.20 (q, $^3J=7.3$ Hz, 4H, $\text{N}(\text{CH}_2\text{CH}_3)_3$), 1.31 (t, $^3J=7.3$ Hz, 6H, $\text{N}(\text{CH}_2\text{CH}_3)_3$).

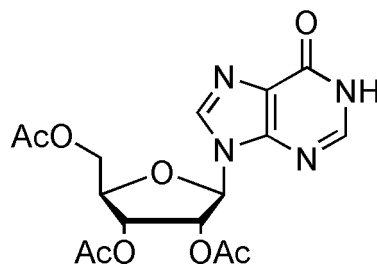
^{13}C NMR (CD_3OD , 101 MHz) δ (ppm) = 176.5, 155.9, 152.5, 152.4, 151.1, 143.9, 122.1, 91.2, 88.0, 75.8, 72.5, 63.3, 47.8 (NEt_3), 45.6, 9.5 (NEt_3).

HRMS (ESI), calcd. for $\text{C}_{13}\text{H}_{16}\text{N}_6\text{O}_7$ [$\text{M}-\text{H}$] $^-$: 367.1008, found: 367.1005.

IR: $\tilde{\nu}$ (cm^{-1}) = 3334 w, 3146 m, 2924 w, 2362 w, 2338 w, 1718 w, 1633 s, 1593 m, 1543 w, 1448 m, 1404 m, 1333 m, 1308 m, 1221 s, 1190 m, 1101 s, 1081 m, 1054 s, 985 m, 947 w, 863 m, 758 s, 668 w, 639 w, 625 w.

10.6.4 Synthesis of m^6A , $d_3\text{-}m^6A$, m^6_2A , and $d_3\text{-}m^6_2A$

2',3',5'-Tri-*O*-acetylinosine (**6**)^[139]



Inosine (5.00 g, 18.6 mmol) was dissolved in dry DMF (12 mL), followed by addition of dry pyridine (5 mL) and acetic anhydride (10 mL, 106 mmol). The reaction mixture was refluxed at 75 °C for 30 min. Afterwards the solvent was removed *in vacuo* and the crude product recrystallized from *iso*-propanol. The obtained crystals were filtered off and washed twice with *iso*-propanol to obtain product **6** (6.38 g, 16.2 mmol, 87%) as a colorless solid.

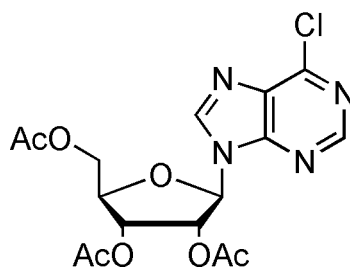
$R_f = 0.12$ ($\text{CH}_2\text{Cl}_2/\text{MeOH}$ 20:1). M.p.: 243 °C.

^1H NMR (d_6 -DMSO, 400 MHz): δ (ppm) = 12.48 (s, 1H, NH), 8.31 (s, 1H, C8H), 8.10 (s, 1H, C2H), 6.19 (d, $^3J = 5.7$ Hz, 1H, C1'H), 5.91 (t, $^3J = 5.7$ Hz, 1H, C2'H), 5.55 (t, $^3J = 5.8$ Hz, 1H, C3'H), 4.41 – 4.22 (m, 3H, C4'H, C5'H₂), 2.11 – 2.02 (3s, 9H, COCH₃).

^{13}C NMR (d_6 -DMSO, 101 MHz) δ (ppm) = 170.0, 169.4, 169.2, 156.4, 147.9, 146.3, 139.3, 124.8, 85.6, 79.5, 72.2, 70.0, 62.8, 20.5, 20.3, 20.2.

HRMS (ESI⁺): calcd. for $\text{C}_{16}\text{H}_{18}\text{N}_4\text{O}_8$ $[\text{M}+\text{H}]^+$: 395.1197, found: 395.1203.

IR: $\tilde{\nu}$ (cm^{-1}) = 3564 w, 3052 w, 3008 w, 2808 w, 1758 m, 1740 m, 1728 m, 1703 s, 1592 w, 1553 w, 1512 w, 1370 m, 1344 w, 1228 s, 1199 s, 1114 m, 1092 m, 1053 w, 1019 m, 960 w, 920 m, 862 w, 636 w.

2',3',5'-Tri-*O*-acetyl-6-chlorinosine (7)^[139]

(Chloromethylen)dimethyliminiumchloride (20.1 g, 157.1 mmol) was dissolved in dry CH_2Cl_2 (130 mL), followed by addition of 2',3',5'-tri-*O*-acetylinosine (**6**, 31.0 g, 78.6 mmol). The yellow suspension was refluxed at 40 °C for 24 h and afterwards slowly poured into 1 L of half concentrated NaHCO_3 solution in 50% water (300 mL). Then the solution was extracted with CH_2Cl_2 (3×100 mL), the combined organic layers were dried over MgSO_4 and the solvent removed *in vacuo*. Purification *via* column chromatography ($\text{CH}_2\text{Cl}_2/\text{MeOH} = 40:1$) of the crude material obtained product **7** (30.0 g, 72.7 mmol, 93%) as a yellow oil.

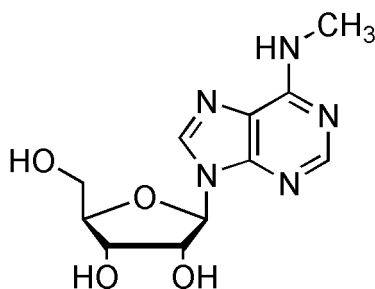
$R_f = 0.77$ ($\text{CH}_2\text{Cl}_2/\text{MeOH} = 10:1$).

^1H NMR (CDCl_3 , 300 MHz) δ (ppm) = 8.74 (s, 1H, C2H), 8.27 (s, 1H, C8H), 6.20 (d, $^3J=5.1$ Hz, 1H, C1'H), 5.91 (t, $^3J=5.3$ Hz, 1H, C2'H), 5.61 (t, $^3J=5.2$ Hz, 1H, C3'H), 4.50 – 4.29 (m, 3H, C4'H, C5'H₂), 2.17 – 1.99 (3s, 9H, COCH_3).

^{13}C NMR (CDCl_3 , 75 MHz) δ (ppm) = 170.4, 169.7, 169.5, 152.5, 151.9, 151.5, 143.8, 132.6, 87.1, 80.8, 73.3, 70.7, 63.1, 21.0, 20.7, 20.6.

HRMS (ESI⁺): calcd. for $\text{C}_{16}\text{H}_{17}\text{ClN}_4\text{O}_7$ $[\text{M}+\text{H}]^+$: 413.0859, found: 413.0869.

IR: $\tilde{\nu}$ (cm^{-1}) = 3611 w, 2960 w, 1741 s, 1673 m, 1592 m, 1561 m, 1493 w, 1425 w, 1369 m, 1340 m, 1200 s, 1147 m, 1042 s, 958 w, 924 m, 901 m, 860 w, 635 w.

***N*⁶-Methyladenosine (**m⁶A**)^[139]**

Compound **7** (30.0 g, 72.7 mmol) was dissolved in 500 mL ethanol and treated with ethanolic methylamine solution (33%, 43.0 mL) and stirred for 18 h at rt. The solvent was removed *in vacuo*, washed with ethanol and the resulted solid was recrystallized twice from methanol. After washing with methanol and drying *in vacuo*, the pure nucleoside **m⁶A** (19.1 g, 67.7 mmol, 93%) was obtained as a white solid.

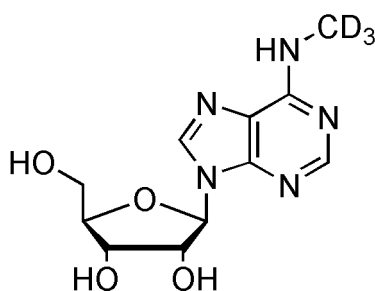
$R_f = 0.18$ ($\text{CH}_2\text{Cl}_2/\text{MeOH} = 10:1$). M.p.: 146 °C.

¹H NMR (d_6 -DMSO, 400 MHz) δ (ppm) = 8.33 (s, 1H, C2H), 8.22 (s, 1H, C8H), 7.79 (s, br, 1H, HNCH₃), 5.88 (d, ³ $J=6.2$ Hz, 1H, C₁H), 5.42 (dd, 2H, ³ $J=4.6$ Hz, ³ $J=6.8$ Hz, C₂OH, C₅OH), 5.17 (d, ³ $J=4.6$ Hz, 1H, C₃OH), 4.60 (dd, ³ $J=6.2$ Hz, ³ $J=11.3$ Hz, 1H, C₂H), 4.15 (td, ³ $J=3.1$ Hz, ³ $J=4.8$ Hz, 1H, C₃H), 3.97 (q, ³ $J=3.5$ Hz, 1H, C₄H), 3.72 – 3.63 (m, 1H, C₅H_{2a}), 3.55 (ddd, ³ $J=3.6$ Hz, ³ $J=7.3$ Hz, ² $J=12.1$ Hz, 1H, C₅H_{2b}), 2.96 (s, 3H, NCH₃).

¹³C NMR (d_6 -DMSO, 101 MHz): δ (ppm) = 155.1, 152.4, 148.1, 139.6, 119.9, 87.9, 85.9, 73.5, 70.7, 61.7, 27.0 ppm.

HRMS (ESI⁺): calcd. for C₁₁H₁₅N₅O₄ [M+H]⁺: 282.1197, found: 282.1201.

IR: $\tilde{\nu}$ (cm⁻¹) = 3332 w, 3146 w, 2922 w, 1686 w, 1634 s, 1593 m, 1500 m, 1404 m, 1381 m, 1333 m, 1309 s, 1222 m, 1190 m, 1134 m, 1101 m, 1082 m, 1056 s, 1031 m, 986 m, 947 w, 864 m, 822 w, 794 w, 759 m, 669 w, 625 w.

d₃-N⁶-Methyladenosine (d₃-m⁶A)

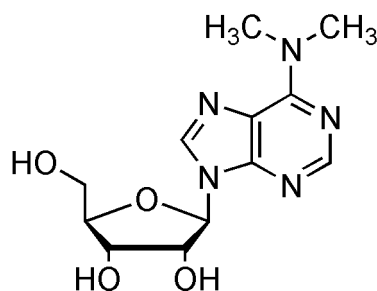
Method A: Ag₂O (1.35 g, 5.82 mmol) was added to a solution d₃-methylamine hydrochloride (0.34 g, 4.85 mmol) in 6 mL EtOH. After 30 min stirring at rt, the precipitate was filtered off and 2',3',5'-tri-*O*-acetyl-6-chloroinosine (**7**, 0.20 g, 0.49 mmol) was added to the filtrate and stirred for 48 h at rt. The reaction mixture was filtrated afterwards and the solvent of the filtrate was removed *in vacuo*. Afterwards the crude product was purified *via* RP-HPLC (eluent A: H₂O, eluent B: MeCN, gradient: 100% A, 0% B → 40% A, 100% B in 45 min, retention time = 20.8 min) to yield pure nucleoside **d₃-m⁶A** (30.0 mg, 0.11 mmol, 22%) as a colorless solid.

Method B: Compound **17** (34.0 mg, 54.0 μmol) were dissolved in 2 mL CH₂Cl₂ with subsequent addition of NEt₃·3HF (35 μL, 217 μmol) and stirred at rt for 16 h. The reaction was stopped with methoxytrimethylsilane (300 μL), stirred for another 30 min and then the solvent was removed *in vacuo*. Afterwards the crude product was purified *via* RP-HPLC (eluent A: H₂O, eluent B: MeCN, gradient: 100% A, 0% B → 40% A, 100% B in 45 min, retention time = 20.8 min) to yield pure nucleoside **d₃-m⁶A** (11.0 mg, 39.0 μmol, 72%) as a colorless solid.

¹H NMR (CD₃OD, 400 MHz) δ (ppm) = 8.23 (s, 2H, C2H, C8H), 5.95 (d, ³J=6.5 Hz, 1H, C1'H), 4.74 (dd, ³J=5.2 Hz, ³J=6.4 Hz, 1H, C2'H), 4.32 (dd, ³J=2.5 Hz, ³J=5.1 Hz, 1H, C3'H), 4.17 (q, ³J=2.5 Hz, 1H, C4'H), 3.89 (dd, ³J=2.5 Hz, ²J=12.6 Hz, 1H, C5'H_a), 3.74 (dd, ³J=2.6 Hz, ²J=12.5 Hz, 1H, C5'H_b).

¹³C NMR (CD₃OD, 101 MHz) δ (ppm) = 155.5, 152.0, 146.5, 140.0, 120.1, 89.9, 86.8, 74.0, 71.3, 62.1.

HRMS (ESI⁺): calcd. for C₁₁H₁₂D₃N₅O₄ [M+H]⁺: 285.1382, found: 285.1387.

***N*⁶,*N*⁶-Dimethyladenosine (**m**⁶₂**A**)**^[139]

Compound **7** (1.00 g, 2.43 mmol) was dissolved in 22 mL ethanol, treated with ethanolic dimethylamine solution (33%, 5.00 mL) and stirred at rt. After 18 h another portion of ethanolic dimethylamine solution (33%, 2.00 mL) was added, the solution stirred for another 8 h and the solvent was removed afterwards *in vacuo*. CH₂Cl₂ was added and stirred for 30 min. The precipitated white solid was filtered off, washed with CH₂Cl₂ and dried *in vacuo* to obtain pure nucleoside **m**⁶₂**A** (0.62 g, 2.10 mmol, 86%) as a white solid.

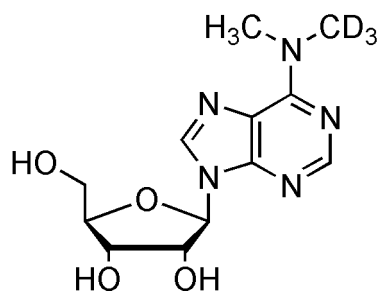
R_f = 0.31 (CH₂Cl₂/MeOH = 10:1). M.p.: 153 °C.

¹H NMR (d₆-DMSO, 200 MHz) δ (ppm) = 8.35 (s, 1H, C2H), 8.19 (s, 1H, C8H), 5.89 (d, ³J=6.1 Hz, 1H, C1'H), 5.44 (d, ³J=6.2 Hz, 1H, C2'OH), 5.36 (dd, ³J=4.7 Hz, ³J=6.9 Hz, 1H, C5'OH), 5.18 (d, ³J=4.7 Hz, 1H, C3'OH), 4.55 (dd, ³J=5.9 Hz, ³J=11.1 Hz, 1H, C2'H), 4.12 (dd, ³J=4.8 Hz, ³J=8.1 Hz, 1H, C3'H), 3.94 (dd, ³J=3.5 Hz, 1H, C4'H), 3.73 – 3.35 (m, 8H, C5'H₂, N(CH₃)₂).

¹³C NMR (d₆-DMSO, 101 MHz) δ (ppm) = 155.0, 152.4, 150.6, 139.3, 120.5, 88.4, 86.4, 74.2, 71.2, 62.2, 45.0.

HRMS (ESI⁺): calcd. for C₁₂H₁₇N₅O₄ [M+H]⁺: 296.1353, found: 296.1356.

IR: $\tilde{\nu}$ (cm⁻¹) = 3393 *m*, 3272 *m*, 2928 *m*, 2780 *m*, 2449 *w*, 1596 *s*, 1534 *m*, 1480 *m*, 1428 *m*, 1404 *m*, 1348 *m*, 1306 *m*, 1272 *m*, 1204 *m*, 1181 *m*, 1125 *m*, 1114 *m*, 1083 *s*, 1033 *s*, 985 *m*, 960 *w*, 894 *m*, 861 *s*, 791 *m*, 755 *m*, 695 *s*, 656 *s*, 628 *s*.

d₃-N⁶,N⁶-Dimethyladenosine (d₃-m⁶₂A)

Compound **7** (100 mg, 0.24 mmol) was dissolved in 6 mL methanol and treated with d₃-dimethylamine (170 mg, 3.53 mmol). After addition of NEt₃ (700 μL) the reaction mixture was stirred for 18 h at 60 °C. Then the solvent was removed *in vacuo* and the product purified *via* RP-HPLC (eluent A: H₂O, eluent B: MeCN, gradient: 100% A, 0% B → 40% A, 100% B in 45 min, retention time = 38.0 min). Isotope-labeled nucleoside **d₃-m⁶₂A** (57.0 mg, 0.19 mmol, 80%) was dried *in vacuo* and was obtained as a white solid.

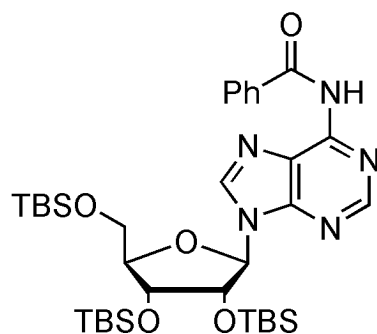
¹H NMR (D₂O, 400 MHz) δ (ppm) = 8.14 (s, 1H, C2H), 7.95 (s, 1H, C8H), 5.96 (d, ³J=5.9 Hz, 1H, C₁H), 4.71 (t, ³J=5.5 Hz, 1H, C₂H), 4.42 (dd, ³J=2.6 Hz, ³J=6.0 Hz, 1H, C₃H), 4.30 (d, ³J=2.6 Hz, 1H, C₄H), 3.96 (dd, ³J=2.3 Hz, ²J=12.7 Hz, 1H, C₅H_a), 3.86 (dd, ³J=3.3 Hz, ²J=12.9 Hz, 1H, C₅H_b), 3.22 (s, br, 3H, NCH₃).

¹³C NMR (D₂O, 101 MHz) δ (ppm) = 153.7, 151.4, 148.2, 138.2, 119.0, 88.1, 85.5, 73.6, 70.5, 61.4, 38.6.

HRMS (ESI⁺): calcd. for C₁₂H₁₄D₃N₅O₄ [M+H]⁺: 299.1539, found: 299.1547.

10.6.5 Synthesis of m⁶t⁶A

2',3',5'-Tri-*O*-(*tert*-butyldimethylsilyl)-*N*⁶-benzoyladenosine (**16**)^[142]



Compound **1** (0.10 g, 0.16 mmol) was dissolved in pyridine (2.0 mL) and treated with benzoylchloride (28.5 μ L, 0.25 mmol) at $-5\text{ }^{\circ}\text{C}$. The reaction mixture was stirred for 5 min at $-5\text{ }^{\circ}\text{C}$, slowly warmed to rt and stirred for another 2 h. Afterwards the reaction mixture was stopped with H_2O , diluted with CH_2Cl_2 (20 mL) and washed with H_2O ($3 \times 10\text{ mL}$). All aqueous layers were again extracted with CH_2Cl_2 (20 mL). The combined CH_2Cl_2 -layers were dried over MgSO_4 , filtrated and the solvent was removed *in vacuo*. Pure product **16** (78.0 mg, 0.11 mmol, 67%) was obtained after column chromatographic separation (EtOAc/cyclohexane = 20:80) as a colorless foam.

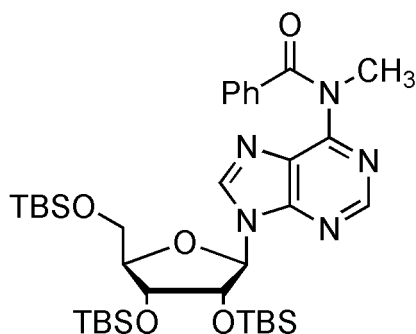
$R_f = 0.79$ (cyclohexane/EtOAc 1:1).

$^1\text{H NMR}$ (CDCl_3 , 599 MHz) δ (ppm) = 9.10 (s, br, 1H, NH), 8.80 (s, 1H, C8H), 8.35 (s, 1H, C2H), 8.01 (d, $^3J = 7.1\text{ Hz}$, 2H, H_{Ph}), 7.57 (d, $^3J = 7.5\text{ Hz}$, 1H, H_{Ph}), 7.50 (t, $^3J = 7.7\text{ Hz}$, 2H, H_{Ph}), 6.10 (d, $^3J = 5.2\text{ Hz}$, 1H, C_1H), 4.66 (t, $^3J = 4.7\text{ Hz}$, 1H, C_2H), 4.30 (t, $^3J = 3.9\text{ Hz}$, 1H, C_3H), 4.14 (d, $^3J = 3.0\text{ Hz}$, 1H, C_4H), 4.06 – 3.75 (m, 2H, C_5H_2), 0.94 – 0.78 (3s, 27H, $\text{Si}(\text{CH}_3)_3$), 0.16 – (-0.32) (m, 18H, $\text{Si}(\text{CH}_3)_2$).

$^{13}\text{C NMR}$ (CDCl_3 , 151 MHz) δ (ppm) = 164.6, 152.7, 151.6, 149.4, 141.9, 133.8, 132.7, 128.8, 127.8, 123.1, 88.4, 85.7, 75.9, 71.9, 62.5, 26.1, 25.8, 25.6, 18.5, 18.1, 17.8, -4.4, -4.7, -4.7, -5.0, -5.4, -5.4.

HRMS (ESI⁺): calcd. for $\text{C}_{35}\text{H}_{59}\text{N}_5\text{O}_5\text{Si}_3$ $[\text{M}+\text{H}]^+$: 714.3897, found: 714.3907.

IR: $\tilde{\nu}$ (cm^{-1}) = 2952 s, 2929 s, 2896 m, 2857 s, 1704 m, 1610 s, 1581 s, 1513 w, 1453 s, 1390 w, 1328 w, 1251 s, 1155 m, 1071 s, 999 m, 969 m, 939 m, 843 s, 775 s, 705 m, 671 m.

2',3',5'-Tri-*O*-(*tert*-butyldimethylsilyl)-*N*⁶-benzoyl-*N*⁶-methyl-adenosine (29)^[142]

Compound **16** (0.50 g, 0.70 mmol) was dissolved in CH₂Cl₂ (16.5 mL), treated with methyl iodide (0.17 mL, 2.80 mmol) and afterwards cooled to -5 °C. After addition of tetrabutylammoniumbromide (0.23 g, 0.70 mmol) and a NaOH solution (1M, 7.0 mL), the reaction mixture was stirred for 2 h at -5 °C, followed by 1 h at rt. The reaction was stopped with H₂O, then the crude mixture was diluted with CH₂Cl₂ (30 mL) and washed with H₂O (3 × 50 mL). All aqueous layers were extracted again with CH₂Cl₂ (50 mL), the combined organic layers were dried over MgSO₄ and filtrated. After removing the solvent *in vacuo*, the crude material was purified *via* column chromatography (EtOAc/cyclohexane = 30:70). Product **29** (0.33 g, 0.46 mmol, 65%) was obtained as a colorless foam.

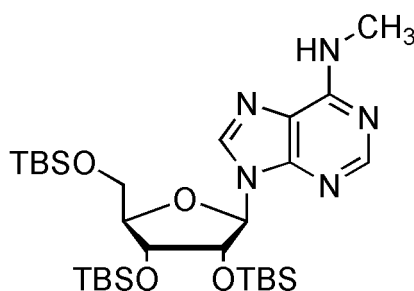
R_f = 0.87 (cyclohexane/EtOAc 1:1).

¹H NMR (CDCl₃, 599 MHz) δ (ppm) = 8.53 (s, 1H, C8H), 8.24 (s, 1H, C2H), 7.41 (dd, ³J = 1.2 Hz, ³J = 8.3 Hz, 2H, H_{Ph}), 7.23 – 7.21 (m, 1H, H_{Ph}), 7.12 (t, ³J = 7.8 Hz, 2H, H_{Ph}), 6.01 (d, ³J = 5.6 Hz, 1H, C₁'H), 4.58 (dd, ³J = 4.4 Hz, ³J = 5.5 Hz, 1H, C₂'H), 4.23 (dd, ³J = 3.2 Hz, 4.2 Hz, 1H, C₃'H), 4.10 (dd, ³J = 2.8 Hz, ³J = 7.0 Hz, 1H, C₄'H), 3.96 (dd, ³J = 4.2 Hz, ²J = 11.4 Hz, 1H, C₅'H_a), 3.77 (s, 3H, CH₃), 3.75 (dd, ³J = 2.8 Hz, ²J = 11.4 Hz, 1H, C₅'H_b), 0.95 - 0.71 (3s, 27H, SiC(CH₃)₃), 0.15 – -0.42 (6s, 18H, Si(CH₃)₂).

¹³C NMR (CDCl₃, 151 MHz) δ (ppm) = 172.3, 155.0, 152.8, 151.9, 142.8, 136.4, 130.8, 128.9, 128.0, 126.8, 88.4, 86.2, 76.0, 72.3, 62.8, 36.1, 26.3, 26.0, 25.8, 18.7, 18.3, 18.0, -4.2, -4.4, -4.5, -4.9, -5.2, -5.2.

HRMS (ESI⁺): calcd. for C₃₆H₆₁N₅O₅Si₃ [M+H]⁺: 728.4053, found: 728.4062.

IR: $\tilde{\nu}$ (cm⁻¹) = 2953 s, 2929 s, 2896 m, 2857 s, 1642 s, 1580 m, 1544 m, 1462 m, 1377 w, 1309 w, 1251 s, 1160 m, 1071 s, 1004 m, 968 w, 939 w, 847 s, 774 s, 722 m, 660 m.

2',3',5'-Tri-*O*-(*tert*-butyldimethylsilyl)-*N*⁶-methyladenosine (8)

Method A: *N*⁶-Methyladenosine (**m⁶A**, 7.41 g, 26.3 mmol) and imidazole (16.2 g, 0.24 mol) were dissolved in dry DMF (36 mL), then TBSCl (16.0 g, 0.11 mol) was added to the yellow solution and stirred for 18 h at rt. Afterwards CH₂Cl₂ (250 mL) was added to the reaction mixture and then washed with H₂O (3 × 200 mL). The combined organic layers were dried over MgSO₄, evaporated *in vacuo* and the crude material was purified *via* column chromatography (EtOAc/cyclohexane = 40:60). Product **8** (15.8 g, 25.4 mmol, 96%) was obtained as a colorless oil.

Method B: Compound **29** (0.05 g, 68.7 μmol) was treated with an ethanolic methylamin solution (33%, 1.5 mL) and stirred for 30 min. Afterwards the solvent was removed *in vacuo* and the crude material was purified by column chromatography (EtOAc/cyclohexane = 50:50). Compound **8** (0.04 g, 65.7 μmol, 96%) was obtained as a foam.

R_f(EtOAc/cyclohexane = 1:1) = 0.74.

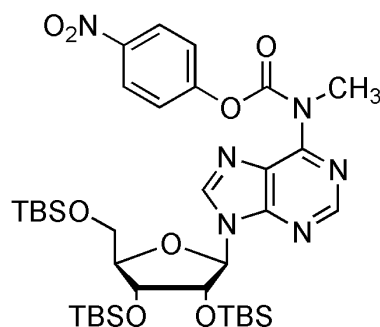
¹H NMR (d₆-DMSO, 400 MHz) δ (ppm) = 8.32 (s, 1H, C2H), 8.22 (s, 1H, C8H), 7.76 (s, br, 1H, NH), 5.93 (d, ³J=6.4 Hz, 1H, C1'H), 4.91 (dd, ³J=4.4 Hz, ³J=6.3 Hz, 1H, C2'H), 4.32 (dd, ³J=1.8 Hz, ³J=4.4 Hz, 1H, C3'H), 4.08 – 3.93 (m, 2H, C4'H, C5'H_b), 3.74 (dd, ³J=6.6 Hz, ²J=13.5 Hz, 1H, C5'H_b), 2.95 (s, br, 3H, CH₃), 0.91 – 0.71 (3s, 27H, SiC(CH₃)₃), 0.10 – (-0.36) (6s, 18H, Si(CH₃)₂).

¹³C NMR (d₆-DMSO, 101 MHz) δ (ppm) = 155.4, 153.0, 148.8, 139.6, 120.1, 87.3, 85.7, 74.7, 72.8, 62.9, 26.2, 26.1, 25.9, 18.4, 18.2, 17.9, -2.8, -4.2, -4.4, -4.5, -5.0, -5.1.

HRMS (ESI⁺): calcd. for C₂₉H₅₇N₅O₄Si₃ [M+H]⁺: 624.3791, found: 624.3796.

IR: $\tilde{\nu}$ (cm⁻¹) = 3344 w, 2952 m, 2929 m, 2896 m, 2857 m, 1622 m, 1582 m, 1472 w, 1362 w, 1253 m, 1158 m, 1070 m, 1043 w, 1000 w, 968 m, 938 m, 831 s, 773 s, 671 m, 651 m.

2',3',5'-Tri-*O*-(*tert*-butyldimethylsilyl)-*N*⁶-methyl-*N*⁶-(4-nitrophenoxy)carbonyl adenosine (12)



The reagent (4-Nitrophenoxy)chloroformate (12.6 g, 62.5 mmol) was added to a solution of 2',3',5'-Tri-*O*-(*tert*-butyldimethylsilyl)-*N*⁶-methyladenosine (**8**, 15.6 g, 25.0 mmol) in dry pyridine (130 mL). The resulting suspension was stirred at 50 °C for 3 h and subsequently diluted with CH₂Cl₂ (250 mL). After washing with H₂O (3 × 200 mL) the combined organic layers were dried over MgSO₄, filtrated and the solvent removed *in vacuo*. The crude product was purified *via* column chromatography (EtOAc/cyclohexane = 10:90) and the solvent was removed *in vacuo* to yield compound **12** as a colorless solid in 80% (15.8 g, 20.1 mmol).

R_f(EtOAc/cyclohexane = 1:1) = 0.83. M.p.: 137 °C.

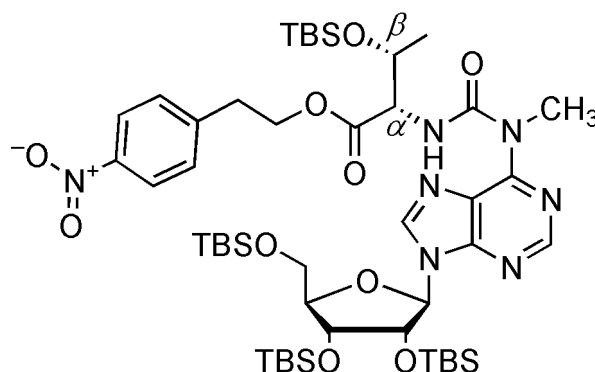
¹H NMR (CDCl₃, 600 MHz) δ (ppm) = 8.81 (s, 1H, C2H), 8.48 (s, 1H, C8H), 8.23 – 8.17 [d, ³J=9.2 Hz, 2H, H_{Npe}(o-NO₂)], 7.41 [d, ³J=9.3 Hz, 2H, H_{Npe}(m-NO₂)], 6.11 (d, ³J=4.9 Hz, 1H, C₁H), 4.53 (t, ³J=4.6 Hz, 1H, C₂H), 4.28 (t, ³J=4.1 Hz, 1H, C₃H), 4.13 (dd, ³J=3.6 Hz, ³J=6.2 Hz, 1H, C₄H), 4.00 (dd, ³J=3.6 Hz, ²J=11.5 Hz, 1H, C₅H_a), 3.78 (dd, ³J=2.4 Hz, ²J=11.5 Hz, 1H, C₅H_b), 3.66 (s, 3H, CH₃), 0.91 – 0.75 (3s, 27H, SiC(CH₃)₃), 0.08 – (-0.29) (6s, 18H, Si (CH₃)₂).

¹³C NMR (CDCl₃, 151 MHz) δ (ppm) = 156.1, 152.8, 152.6, 152.5, 152.2, 145.3, 143.0, 127.7, 125.1, 122.7, 88.6, 85.8, 76.7, 71.9, 62.6, 35.9, 26.3, 26.0, 25.8, 18.7, 18.3, 18.0, -4.2, -4.5, -4.5, -4.9, -5.1, -5.2.

HRMS (ESI⁺): calcd. for C₃₆H₆₀N₆O₈Si₃ [M+H]⁺: 789.3853, found: 789.3892.

IR: $\tilde{\nu}$ (cm⁻¹) = 2952 *m*, 2929 *m*, 2858 *m*, 1743 *s*, 1592 *m*, 1574 *s*, 1525 *s*, 1461 *m*, 1345 *s*, 1309 *s*, 1253 *m*, 1217 *s*, 1155 *s*, 1108 *s*, 968 *w*, 864 *m*, 835 *s*, 776 *s*, 691 *m*, 648 *w*.

***N*⁶-Methyl-2',3',5'-Tri-*O*-(*Tert*-butyldimethylsilyl)-*N*⁶-{{{(1*S*,2*R*)-2-[[*tert*-butyl)-dimethyl]silyloxy}-1-[[2-(4-nitrophenyl)ethoxy]carbonyl]propyl}amino}carbonyl}adenosine (**13**)**



Compound **12** (1.10 g, 1.39 mmol) and *O*-(*tert*-butyldimethylsilyl)-L-threonine-[2-(4-nitrophenyl)ethyl]ester (**11**, 0.80 g, 2.09 mmol) were dissolved in dry pyridine (20 mL) and stirred for 18 h at rt. The solvent was removed *in vacuo*, then CH₂Cl₂ (80 mL) were added and washed with water (3 × 120 mL). The crude product was dried over MgSO₄, filtrated and purified *via* column chromatography (EtOAc/cyclohexane = 20:80). Compound **13** (1.21 g, 1.17 mmol, 84%) was obtained as a colorless foam.

R_f(EtOAc/cyclohexane = 1:1) = 0.79.

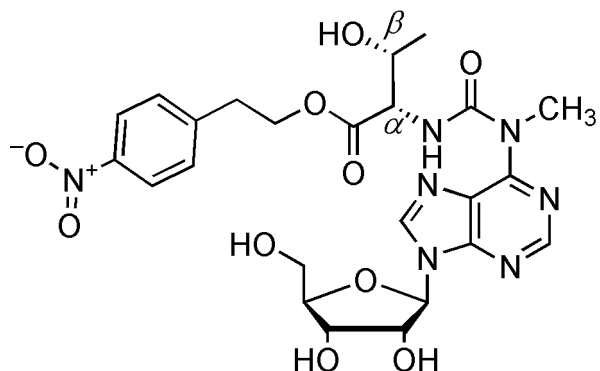
¹H NMR (CDCl₃, 300 MHz) δ (ppm) = 11.00 (d, ³J=8.7 Hz, 1H, C_αNH), 8.46 (s, 1H, C2H), 8.26 (s, 1H, C8H), 8.03 [d, ³J=8.5 Hz, 2H, H_{Npe}(o-NO₂)], 7.31 [d, ³J=8.5 Hz, 2H, H_{Npe}(m-NO₂)], 6.10 (d, ³J=5.3 Hz, 1H, C1'H), 4.71 – 4.64 (t, ³J=4.6 Hz, 1H, C2'H), 4.57 (dd, ³J=1.6 Hz, ³J=8.6 Hz, 1H, C_αH), 4.51 – 4.22 (m, 4H, C_βH, C₃H, OCH₂CH₂), 4.13 (dd, ³J=3.4 Hz, ³J=6.5 Hz, 1H, C4'H), 4.06 – 3.94 (m, 4H, C₅H_a, NCH₃), 3.78 (dd, ³J=2.9 Hz, ²J=11.4 Hz, 1H, C₅H_b), 3.01 (t, ³J=6.6 Hz, 2H, OCH₂CH₂), 1.22 (d, ³J=6.3 Hz, 3H, β-CH₃), 0.87 (4s, 36H, SiC(CH₃)₃), 0.22 – (-0.32) (8s, 24H, Si(CH₃)₂).

¹³C NMR (CDCl₃, 75 MHz) δ (ppm) = 171.5, 156.6, 153.4, 152.6, 150.1, 147.1, 145.7, 140.4, 130.0, 123.9, 122.8, 99.6, 88.4, 85.9, 76.1, 72.3, 69.0, 64.8, 62.8, 60.7, 35.1, 26.3, 26.1, 25.9, 25.8, 21.4, 18.8, 18.3, 18.1, 18.0, -4.1, -4.2, -4.4, -4.5, -4.8, -5.1, -5.2, -5.2.

HRMS (ESI⁺): calcd. for C₄₈H₈₅N₇O₁₀Si₄ [M+H]⁺: 1032.5508, found: 1032.5551.

IR: $\tilde{\nu}$ (cm⁻¹) = 2941 *m*, 2930 *m*, 2857 *m*, 2361 *w*, 1734 *m*, 1685 *m*, 1570 *m*, 1520 *s*, 1464 *m*, 1346 *s*, 1251 *s*, 1215 *w*, 1165 *m*, 1138 *m*, 1087 *m*, 1023 *m*, 834 *s*, 775 *s*, 748 *m*, 669 *m*.

***N*⁶-Methyl-*N*⁶-{[(1*S*,2*R*)-2-hydroxy-1-[[2-(4-nitrophenyl)ethoxy]carbonyl]propyl]-amino}carbonyl}adenosine (**22**)**



Compound **13** (3.00 g, 2.95 mmol) was dissolved in dry CH₂Cl₂ (2.5 mL), then treated with triethylamine-*tris*(hydrofluoride) (3.89 mL, 24.1 mmol) and stirred at rt for 24 h. After evaporation of the solvent *in vacuo*, the reaction mixture was left for 48 h at 25 °C. Afterwards CH₂Cl₂ (2 mL) was added and the reaction stopped with trimethylmethoxysilane (1 mL). After subsequent removal of the solvent *in vacuo* the crude mixture was purified *via* column chromatography (CH₂Cl₂/MeOH = 10:1) and obtained **22** (1.62 g, 2.89 mmol, 98%) as a colorless foam.

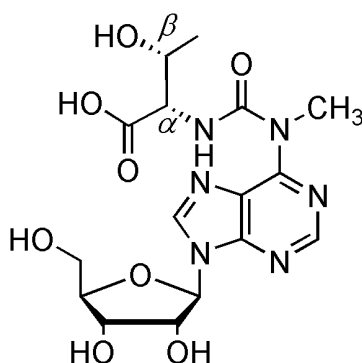
R_f (CH₂Cl₂/MeOH 10:1) = 0.34.

¹H NMR (d₆-DMSO, 400 MHz) δ (ppm) = 10.69 (d, ³J=7.8 Hz, 1H, C_αNH), 8.74 (s, 1H, C2H), 8.54 (s, 1H, C8H), 8.07 [d, ³J=8.9 Hz, 2H, H_{Npe}(o-NO₂)], 7.52 (d, ³J=8.9 Hz, 2H, H_{Npe}(m-NO₂)], 6.05 (d, ³J=5.3 Hz, 1H, C₁H), 5.53 (d, ³J=5.9 Hz, 1H, C₂H), 5.21 (dd, ³J=4.9 Hz, ³J=7.8 Hz, 2H, C₂OH, C₃OH), 5.12 (t, ³J=5.5 Hz, 1H, C₅OH), 4.56 (dd, ³J=5.3 Hz, ³J=10.8 Hz, 1H, C₂H), 4.41 – 4.29 (m, 2H, OCH₂CH₂), 4.27 (dd, ³J=2.9 Hz, ³J=7.8 Hz, 1H, C_αH), 4.21 – 4.11 (m, 2H, C₃H, C_βH), 3.99 (q, ³J=3.9 Hz, 1H, C₄H), 3.82 (s, 3H, NCH₃), 3.70 (dd, ³J=5.4 Hz, ²J=10.5 Hz, 1H, C₅H_a), 3.60 (dd, ³J=6.0 Hz, ²J=11.8 Hz, 1H, C₅H_b), 3.05 (t, ³J=6.3 Hz, 2H, OCH₂CH₂), 1.10 (d, ³J=6.3 Hz, 3H, β-CH₃).

¹³C NMR (d₆-DMSO, 101 MHz) δ (ppm) = 170.8, 155.3, 152.3, 152.1, 149.8, 146.6, 146.1, 141.5, 130.1, 123.2, 121.8, 87.6, 85.5, 73.9, 70.1, 66.2, 64.2, 61.1, 59.9, 34.3, 34.0, 20.6.

HRMS (ESI⁺): calcd. for C₂₄H₂₉N₇O₁₀ [M+H]⁺: 576.2049, found: 576.2054.

IR: $\tilde{\nu}$ (cm⁻¹) = 3342 *m*, 2930 *m*, 2361 *w*, 1734 *m*, 1670 *m*, 1570 *s*, 1516 *s*, 1464 *s*, 1343 *s*, 1269 *m*, 1180 *m*, 1107 *s*, 1079 *s*, 1022 *s*, 854 *m*, 746 *m*, 697 *m*, 644 *m*.

***N*⁶-Methyl-*N*⁶-threonylcarbamoyladenine (m⁶t⁶A)**

Compound **22** (50.0 mg, 86.9 μmol) were dissolved in 900 μL THF and treated with 1,8-Diazabicyclo[5.4.0]undec-7-en (100 μL , 0.66 mmol). The reaction mixture was shaken for 3 h at 40 $^{\circ}\text{C}$ at 700 rpm. Afterwards the solvent was removed *in vacuo* and the crude product purified *via* RP-HPLC (eluent A: 0.1 M NEt_3/HOAc in H_2O , pH = 7.0, eluent B: 0.1 M NEt_3/HOAc in MeCN, pH = 7.0, gradient: 100% A, 0% B \rightarrow 40% A, 100% B in 45 min, retention time = 18.7 min) to yield nucleoside **m⁶t⁶A** (33.0 mg, 69.2 μmol , 80%) as a colorless hygroscopic salt with NEt_3 (ratio of 2:1).

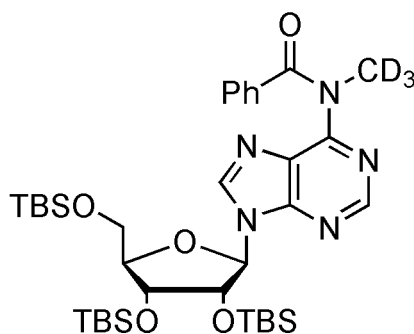
^1H NMR (CD_3OD , 400 MHz) δ (ppm) = 8.61 (s, 1H, C8H), 8.54 (s, 1H, C2H), 6.10 (d, $^3J=5.8$ Hz, 1H, C1'H), 4.75 – 4.70 (m, 1H, C2'H), 4.41 – 4.30 (m, 3H, C3'H, C $_{\alpha}$ H, C $_{\beta}$ H), 4.17 (s, 1H, C4'H), 3.92 (s, 3H, NCH₃), 3.90 (dd, $^3J=2.8$ Hz, $^2J=12.4$ Hz, 1H, C5'H_a), 3.77 (dd, $^3J=3.1$ Hz, $^2J=12.4$ Hz, 1H, C5'H_b), 3.20 (q, $^3J=7.3$ Hz, 3H, N(CH₂CH₃)₃), 1.30 (t, $^3J=7.3$ Hz, 6H, N(CH₂CH₃)₃), 1.25 (d, $^3J=6.4$ Hz, 3H, β -CH₃).

^{13}C NMR (CD_3OD , 101 MHz) δ (ppm) = 174.9, 156.3, 153.1, 151.8, 149.8, 141.5, 122.6, 89.4, 86.2, 74.2, 70.8, 67.5, 61.7, 60.7, 46.3 (NEt_3), 34.0, 19.1, 7.7 (NEt_3).

HRMS (ESI): calcd. for $\text{C}_{16}\text{H}_{22}\text{N}_6\text{O}_8$ [M-H]⁻: 425.1426, found: 425.1417.

10.6.6 Synthesis of d₃-m⁶t⁶A

d₃-2',3',5'-Tri-*O*-(*tert*-butyldimethylsilyl)-*N*⁶-benzoyl-*N*⁶-methyladenosine (17)

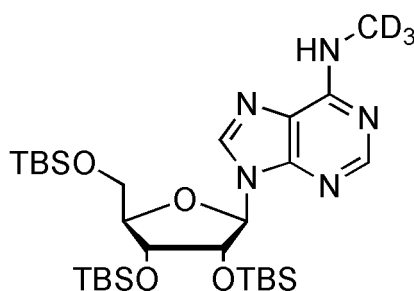


Compound **16** (732 mg, 1.03 mmol) was dissolved in CH₂Cl₂ (24 mL) and treated with methyl iodide (255 μ L, 4.10 mmol). After addition of tetrabutylammoniumbromide (0.23 g, 0.70 mmol) and a NaOH solution (1M, 7.0 mL) the solution was stirred for 3 h at rt. The reaction was stopped with H₂O, then the crude mixture was diluted with CH₂Cl₂ (30 mL) and washed with H₂O (3 \times 20 mL). All aqueous layers were extracted again with CH₂Cl₂ (20 mL), the combined organic layers were dried over MgSO₄ and filtrated. After removing the solvent *in vacuo*, the crude material was purified *via* column chromatography (EtOAc/ cyclohexane = 30:70 \rightarrow 50:50). The crude reaction mixture was added to the column using pure CH₂Cl₂ due to solubility reasons. Product **17** (508 mg, 0.69 mmol, 68%) was obtained as a colorless foam.

¹H NMR (CDCl₃, 599 MHz) δ (ppm) = 8.57 (s, 1H, C8H), 8.29 (s, 1H, C2H), 7.43 (d, ³J=7.6 Hz, 2H, H_{Ph}), 7.26 (d, ³J=7.4 Hz, 1H, H_{Ph}), 7.14 (t, ³J=7.6 Hz, 2H, H_{Ph}), 6.02 (d, ³J=5.5 Hz, 1H, C₁'H), 4.56 (t, ³J=4.8 Hz, 1H, C₂'H), 4.26 – 4.21 (m, 1H, C₃'H), 4.10 (dd, ³J=2.9 Hz, ³J=6.4 Hz, 1H, C₄'H), 3.96 (dd, ³J=4.1 Hz, ²J=11.4 Hz, 1H, C₅'H_a), 3.76 (dd, ³J=2.7 Hz, ²J=11.4 Hz, 1H, C₅'H_b), 0.95 – 0.69 (3s, 27H, SiC(CH₃)₃), 0.12 – -0.43 (6s, 18H, Si(CH₃)₂).

¹³C NMR (CDCl₃, 151 MHz) δ (ppm) = 172.3, 154.9, 152.8, 151.6, 142.9, 136.2, 130.9, 128.9, 128.1, 126.4, 88.5, 86.2, 76.1, 72.3, 62.8, 26.3, 26.0, 25.8, 18.7, 18.3, 18.0, -4.2, -4.4, -4.5, -4.9, -5.1.

HRMS (ESI⁺): calcd. for C₃₆H₅₈D₃N₅O₅Si₃ [M+H]⁺: 731.4239, found: 731.4231.

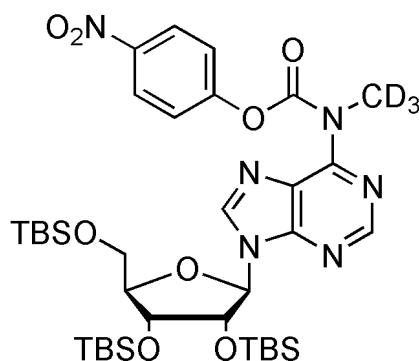
d₃-2',3',5'-Tri-*O*-(*tert*-butyldimethylsilyl)-*N*⁶-methyladenosine (18)

Compound **17** (2.98 g, 4.08 mmol) was treated with an ethanolic methylamin solution (33%, 80 mL) and stirred for 2 h. Afterwards the solvent was removed *in vacuo* and the crude material was purified by column chromatography (EtOAc/cyclohexane = 50:50). The crude mixture was dissolved in CH₂Cl₂ before it was load to the column. Compound **18** (2.39 g, 3.82 mmol, 94%) was obtained as a pure colorless foam.

¹H NMR (CDCl₃, 599 MHz) δ (ppm) = 8.36 (s, 1H, C2H), 8.05 (s, 1H, C8H), 5.99 (d, ³J=5.4 Hz, 1H, C₁H), 5.67 (s, br, 1H, NH), 4.69 (t, ³J=4.8 Hz, 1H, C₂H), 4.29 (t, ³J=3.8 Hz, 1H, C₃H), 4.10 (dd, ³J=3.4 Hz, ³J=7.0 Hz, 1H, C₄H), 4.01 (dd, ³J=4.4 Hz, ²J=11.3 Hz, 1H, C₅H_a), 3.76 (dd, ³J=2.9 Hz, ²J=11.3 Hz, 1H, C₅H_b), 0.97 – 0.73 (3s, 27H, SiC(CH₃)₃), 0.14 – (-0.31) (6s, 18H, Si(CH₃)₂).

¹³C NMR (CDCl₃, 151 MHz) δ (ppm) = 155.6, 153.2, 149.1, 139.1, 120.6, 88.4, 85.8, 75.9, 72.4, 62.9, 26.3, 26.1, 25.9, 18.7, 18.3, 18.1, -4.2, -4.5, -4.5, -4.9, -5.2.

HRMS (ESI⁺): calc. for C₂₉H₅₄D₃N₅O₄Si₃ [M+H]⁺: 627.3976, found: 627.3967.

d₃-2',3',5'-O-Tris(*tert*-butyldimethylsilyl)-N⁶-methyl-N⁶-(4-nitrophenoxy)carbonyl adenosine (19)

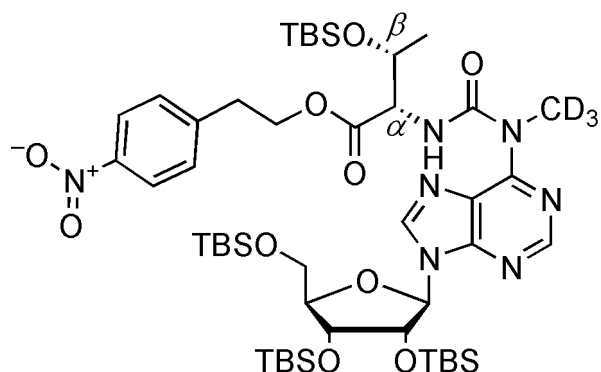
(4-Nitrophenoxy)chloroformate (0.30 g, 1.69 mmol) was added to a solution of d₃-2',3',5'-Tri-*O*-(*tert*-butyldimethylsilyl)-N⁶-methyladenosine (**18**, 353 mg, 563 μmol) in dry pyridine (4 mL). The resulting suspension was stirred at 50 °C for 5.5 h and subsequently diluted in CH₂Cl₂ (20 mL). After washing with H₂O (3 × 40 mL) the combined organic layers were dried over MgSO₄, filtrated and the solvent removed *in vacuo*. The crude product was purified *via* column chromatography (EtOAc/cyclohexane = 10:90) and compound **19** (411 mg, 0.52 mmol, 92%) was obtained as a colorless foam.

¹H NMR (CDCl₃, 599 MHz) δ (ppm) = 8.80 (s, 1H, C2H), 8.46 (s, 1H, C8H), 8.21 [d, ³J=9.2 Hz, 2H, H_{Npe}(o-NO₂)], 7.40 [d, ³J=9.2 Hz, 2H, H_{Npe}(m-NO₂)], 6.11 (d, ³J=4.9 Hz, 1H, C₁H), 4.53 (t, ³J=4.6 Hz, 1H, C₂H), 4.28 (t, ³J=4.1 Hz, 1H, C₃H), 4.13 (d, ³J=2.6 Hz, 1H, C₄H), 4.00 (dd, ³J=3.6 Hz, ²J=11.5 Hz, 1H, C₅H_a), 3.78 (dd, ³J=2.4 Hz, ²J=11.5 Hz, 1H, C₅H_b), 0.91 – 0.73 (3s, 27H, SiC(CH₃)₃), 0.17 – (-0.31) (6s, 18H, Si(CH₃)₂).

¹³C NMR (CDCl₃, 151 MHz) δ (ppm) = 156.1, 152.9, 152.6, 152.5, 152.2, 145.3, 143.1, 127.9, 125.1, 122.7, 88.6, 85.8, 76.6, 72.0, 62.6, 26.3, 26.0, 25.8, 18.7, 18.3, 18.1, -4.2, -4.4, -4.5, -4.9, -5.1, -5.2.

HRMS (ESI⁺): calcd. for C₃₆H₅₇D₃N₆O₈Si₃ [M+H]⁺: 792.4038, found: 789.4031.

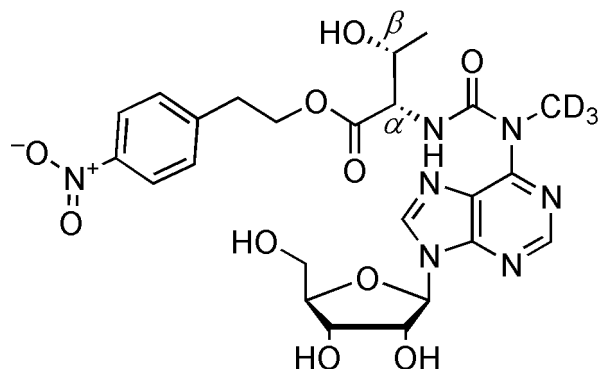
d₃-N⁶-Methyl-2',3',5'-Tri-*O*-(*Tert*-butyldimethylsilyl)-N⁶-{{{(1*S*,2*R*)-2-[[(*tert*-butyl)-dimethyl]silyloxy}-1-[2-(4-nitrophenyl)ethoxy]carbonyl]propyl}amino}carbonyl} adenosine (20**)**



Compound **19** (2.40 g, 3.03 mmol) and *O*-(*tert*-Butyldimethylsilyl)-L-threonine-[2-(4-nitrophenyl)ethyl]ester (**11**, 1.74 g, 4.54 mmol) were dissolved in dry pyridine (26 mL) and stirred for 15 h at rt. Extra addition of compound **11** (0.30 g, 0.78 mmol) completed the reaction by stirring at rt for another 7 h. CH₂Cl₂ (100 mL) was added after removal of the solvent *in vacuo* and washed with water (3 × 150 mL). The crude product was dried over MgSO₄, filtrated and purified *via* column chromatography (EtOAc/cyclohexane = 30:70). Compound **20** (2.62 g, 2.53 mmol, 84%) was obtained as colorless foam.

¹H NMR (CDCl₃, 200 MHz) δ (ppm) = 11.01 (d, ³*J*=8.8 Hz, 1H, C_αNH), 8.46 (s, 1H, C2H), 8.27 (s, 1H, C8H), 8.03 [d, ³*J*=8.8 Hz, 2H, H_{Npe(o-NO₂)}], 7.31 [d, ³*J*=8.6 Hz, 2H, H_{Npe(o-NO₂)}], 6.10 (d, ³*J*=5.2 Hz, 1H, C₁H), 4.66 (t, ³*J*=4.7 Hz, 1H, C₂H), 4.61 – 4.24 (m, 5H, C_βH, C₄H, C₃H, OCH₂CH₂), 4.13 (dd, ³*J*=3.5 Hz, ³*J*=6.3 Hz, 1H, C_αH), 4.01 (dd, ³*J*=3.9 Hz, ²*J*=11.4 Hz, 1H, C₅H_a), 3.77 (dd, ³*J*=2.9 Hz, ²*J*=11.4 Hz, 1H, C₅H_b), 3.01 (t, ³*J*=6.1 Hz, 2H, OCH₂CH₂), 1.21 (d, ³*J*=6.3 Hz, 3H, β-CH₃), 0.95 – 0.75 (4s, 36H, SiC(CH₃)₃), 0.22 – (-0.35) (8s, 24H, Si(CH₃)₂).

HRMS (ESI⁺): calcd. for C₄₈H₈₂D₃N₇O₁₀Si₄ [M+H]⁺: 1035.5693, found: 1035.5665.

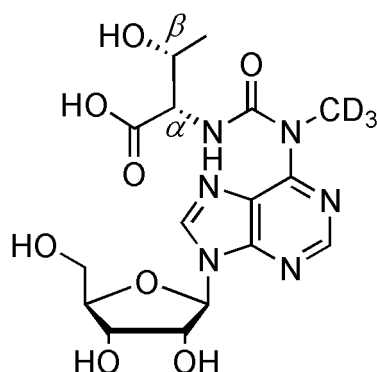
d₃-N⁶-Methyl-N⁶-{[(1*S*,2*R*)-2-hydroxy-1-[[2-(4-nitrophenyl)ethoxy]carbonyl]propyl]-amino}carbonyl}adenosine (30)

Compound **20** (1.50 g, 1.45 mmol) was dissolved in dry CH₂Cl₂ (2 mL), then treated with triethylamine-*tris*(hydrofluoride) (3.89 mL, 24.1 mmol) and stirred at 25 °C for 24 h. After evaporation of the solvent *in vacuo*, the reaction mixture was left for 48 h at 25 °C. Afterwards CH₂Cl₂ (2 mL) was added and the reaction stopped with trimethylmethoxysilane (1 mL). After subsequent removal of the solvent *in vacuo* the crude mixture was purified *via* column chromatography (CH₂Cl₂/MeOH = 10:1) to obtain compound **30** (372 mg, 643 μg, 44%).

¹H NMR (CD₃OD, 400 MHz) δ (ppm) = 8.53 (s, 1H, C8H), 8.50 (s, 1H, C2H), 7.99 [d, ³J=8.8 Hz, 2H, H_{Npe(o-NO₂)}], 7.42 [d, ³J=8.8 Hz, 2H, H_{Npe(o-NO₂)}], 6.10 (d, ³J=5.5 Hz, 1H, C₁H), 4.70 (t, ³J=5.3 Hz, 1H, C₂H), 4.46 – 4.38 (m, 3H, OCH₂CH₂, C_βH), 4.35 (dd, ³J=3.8 Hz, ³J=5.1 Hz, 1H, C₃H), 4.31 (qd, ³J=2.9 Hz, ³J=6.4 Hz, 1H, C_αH), 4.15 (dd, ³J=3.1 Hz, 6.6 Hz, 1H, C₄H), 3.89 (dd, ³J=2.8 Hz, ²J=12.3 Hz, 1H, C₅H_a), 3.76 (dd, ³J=3.2, ²J=12.4 Hz, 1H, C₅H_b), 3.06 (t, ³J=6.3 Hz, 2H, OCH₂CH₂), 1.21 (d, ³J=6.4, 3H, β-CH₃).

¹³C NMR (CD₃OD, 101 MHz) δ (ppm) = 171.1, 156.6, 152.8, 151.9, 149.5, 146.6, 146.2, 141.6, 129.6, 122.9, 122.5, 89.4, 86.1, 74.3, 70.7, 66.9, 64.4, 61.6, 60.1, 34.1, 19.2.

HRMS (ESI⁺): calcd. for C₂₄H₂₆D₃N₇O₁₀ [M+H]⁺: 579.2234, found: 579.2238.

d₃-N⁶-Methyl-N⁶-threonylcarbamoyladenine (d₃-m⁶t⁶A)

Compound **30** (50.0 mg, 86.4 μmol) were dissolved in 900 μL THF and treated with 1,8-Diaza-bicyclo[5.4.0]undec-7-en (100 μL , 0.66 mmol). The reaction mixture was shaken for 3 h at 40 $^{\circ}\text{C}$. Afterwards the solvent was removed *in vacuo* and purified *via* RP-HPLC (eluent A: H_2O , eluent B: MeCN, gradient: 100% A, 0% B \rightarrow 40% A, 100% B in 45 min, retention time = 23.0 min) to yield nucleoside **d₃-m⁶t⁶A** (28.5 mg, 48.9 μmol , 57%) as a colorless hygroscopic salt with DBU as counterion (ratio of 1:1).

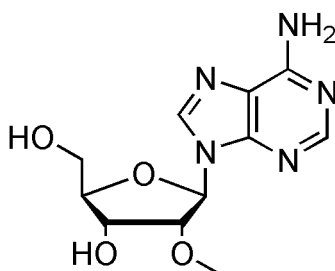
^1H NMR (D_2O , 400 MHz) δ (ppm) = 8.70 (s, 1H, C8H), 8.57 (s, 1H, C2H), 6.19 (d, $^3J=5.7$ Hz, 1H, C1H), 4.85 (t, $^3J=5.5$ Hz, 1H, C2'H), 4.48 (t, $^3J=4.6$ Hz, 1H, C3'H), 4.32 (m, 2H, C $_{\alpha}$ H, C $_{\beta}$ H), 4.26 (d, $^3J=3.9$ Hz, 1H, C4'H), 3.92 (m, 2H, C5'H₂), 3.61 – 3.49 (m, 4H, DBU), 3.34 (t, $^3J=5.8$ Hz, 2H, DBU), 2.67 – 2.61 (m, 2H, DBU), 2.08 – 1.98 (m, 2H, DBU), 1.71 (m, 6H, DBU), 1.28 (d, $^3J=6.4$ Hz, 3H, C $_{\beta}$ CH₃).

^{13}C NMR (D_2O , 101 MHz) δ (ppm) = 177.4, 165.8 (DBU), 157.1, 153.2, 151.4, 150.6, 142.0, 122.8, 88.3, 85.5, 73.6, 70.3, 68.2, 62.1, 61.2, 54.0 (DBU), 48.1 (DBU), 37.9 (DBU), 32.7 (DBU), 28.3 (DBU), 25.8 (DBU), 23.2 (DBU), 19.3, 18.8 (DBU).

HRMS (ESI⁻): calcd. for $\text{C}_{16}\text{H}_{19}\text{D}_3\text{N}_6\text{O}_8$ [M-H]⁻: 428.1612, found: 428.1607.

10.6.7 Synthesis of Am, d₃-Am, and d₃-m¹A

2'-*O*-Methyladenosine (Am)^[143]



Adenosine (1.36 g, 5.09 mmol) was dissolved in dry DMF (20 mL) at 80 °C and cooled to 0 °C. Then sodiumhydride (60% in mineral oil, 0.22 g, 9.17 mmol) was added. Afterwards methyl iodide (0.24 mL, 3.82 mmol) was dissolved in DMF (2.5 mL) and added under vigorously shaking. After stirring for 4 h at 0 °C, the suspension was filtrated. The solvent of the filtrate removed *in vacuo*. The residue was dissolved in methanol (25 mL) and adsorbed on silica (3 g). The raw material was purified *via* column chromatography (CH₂Cl₂/MeOH = 50:1 → 20:1). For further purification of the monomethylated adenosine fractions were recrystallized twice in ethanol to yield nucleoside **Am** (0.17 g, 0.60 mmol, 16%) as a colorless solid.

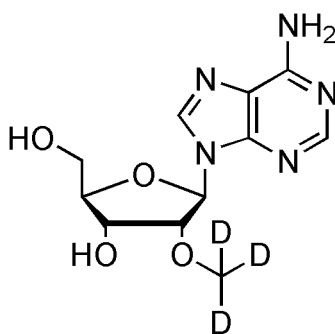
M.p.: 205 °C.

¹H NMR (d₆-DMSO, 400 MHz) δ (ppm) = 8.38 (s, 1H, C8H), 8.14 (s, 1H, C2H), 7.34 (s, 2H, NH₂), 6.00 (d, ³J=6.0 Hz, 1H, C1'H), 5.40 (dd, ³J=4.7 Hz, ³J=6.9 Hz, 1H, C5'OH), 5.25 (d, ³J=4.9 Hz, 1H, C3'OH), 4.39 – 4.32 (m, 2H, C2'H, C3'H), 3.98 (q, ³J=3.5 Hz, 1H, C4'H), 3.72 – 3.62 (m, 1H, C5'H_a), 3.53 – 3.60 (m, 1H, C5'H_b), 3.30 (s, 3H, CH₃).

¹³C NMR (d₆-DMSO, 101 MHz) δ (ppm) = 156.1, 152.5, 149.0, 139.7, 119.2, 86.4, 85.8, 82.4, 68.8, 61.5, 57.4.

HRMS (ESI⁺): calcd. for C₁₁H₁₅N₅O₄ [M+H]⁺: 282.1197, found: 282.1198.

IR: $\tilde{\nu}$ (cm⁻¹) = 3264 s, 3236 s, 3104 s, 2915 m, 2830 m, 1693 s, 1613 s, 1568 m, 1475 m, 1422 m, 1382 m, 1344 m, 1292 s, 1194 m, 1121 s, 1075 s, 1021 m, 980 m, 874 w, 809 w, 778 w, 727 m, 700 m, 638 m.

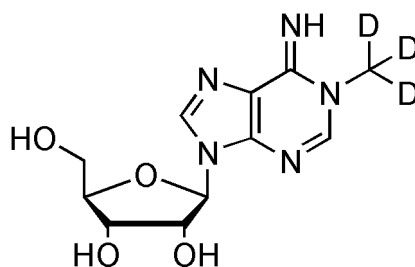
d₃-2'-O-Methyladenosine (d₃-Am)

Adenosine (2.00 g, 7.48 mmol) was dissolved in dry DMF (25 mL) at 80 °C and cooled to 0 °C. Then sodiumhydride (60% in mineral oil, 0.32 g, 13.5 mmol) was added, stirred for 20 min. Methyl iodide (0.81 mL, 5.61 mmol), dissolved in DMF (3.7 mL) was added under vigorous shaking after completed H₂-formation. After stirring for 3.75 h at 0 °C, MeOH (4 mL) was added to stop the reaction. Then the suspension was filtrated and the solvent of the filtrate was removed *in vacuo*. The residue was dissolved in methanol (30 mL) and adsorbed on silica (3 g). The raw material was purified by column chromatography (CH₂Cl₂/MeOH = 50:1 → 20:1). For further purification the monomethylated adenosine fractions were recrystallized twice in ethanol to yield isotope-labeled compound **d₃-Am** (0.34 g, 1.20 mmol, 21%) as a colorless solid.

¹H NMR (d₆-DMSO, 400 MHz) δ (ppm) = 8.38 (s, 1H, C8H), 8.14 (s, 1H, C2H), 7.34 (s, 2H, NH₂), 6.00 (d, ³J=5.9 Hz, 1H, C1'H), 5.41 (dd, ³J=4.8 Hz, ³J=6.6 Hz, 1H, C5'OH), 5.25 (d, ³J=3.4 Hz, 1H, C3'OH), 4.40 – 4.29 (m, 2H, C2'H, C3'H), 3.98 (q, ³J=3.5 Hz, 1H, C4'H), 3.67 (dt, ³J=4.1 Hz, ²J=12.0 Hz, 1H, C5'H_a), 3.60 – 3.51 (m, 1H, C5'H_b).

¹³C NMR (d₆-DMSO, 101 MHz) δ (ppm) = 156.1, 152.5, 149.0, 139.7, 119.2, 86.4, 85.8, 82.3, 68.8, 61.5 (sept, ¹J=21 Hz) CD₃.

HRMS (ESI⁺): calcd. for C₁₁H₁₂D₃N₅O₄ [M+H]⁺: 285.1382, found: 285.1388.

d₃-1-Methyladenosine (d₃-m¹A)^[145]

Adenosine (5.00 g, 18.7 mmol) and d₃-methyl iodide were dissolved in dry DMA (60 mL) and stirred for 16 h at rt. Then 0.5 g celite was added, stirred for 20 min and afterwards filtrated. After addition of acetone (250 mL) the solution was left standing for 24 h at 4 °C. The resulting precipitate was filtrated, washed with cold acetone, diethylether and dried *in vacuo* afterwards. The slightly yellow product was detected as pure **d₃-m¹A** hydroiodide (5.31 g, 12.9 mmol, 69%). Afterwards 2.00 g of the hydroiodide was adjusted to pH 8 with conc. NH₃ and acetone (40 mL) was added. Then the solution was left at 4 °C for 16 h and the formed crystals were filtered off and purified *via* RP-HPLC (eluent A: H₂O (2 mM NH₄HCOO, pH = 5.5), eluent B: H₂O/MeCN = 80:20 (2 mM NH₄HCOO, pH = 5.5), gradient: 100% A, 0% B → 40% A, 100% B in 45 min, retention time = 41.5 min).

M.p.: 211 °C.

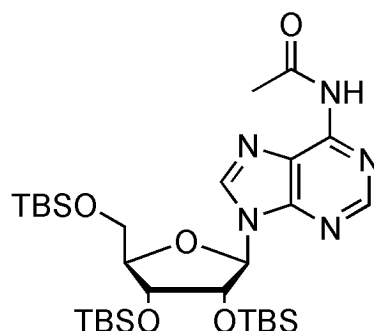
¹H NMR (d₆-DMSO, 200 MHz) δ (ppm) = 8.15 (s, 1H, C2H), 8.08 (s, 1H, C8H), 7.01 (s, 1H, HCOOH), 5.75 (d, ³J=5.9 Hz, 1H, C₁H), 5.48 (s, 1H, C₂OH), 5.27 – 5.05 (m, 2H, C₅OH, C₃OH), 4.47 (dd, ³J=5.1 Hz, ³J=10.3 Hz, 1H, C₂H), 4.11 (dd, ³J=4.1 Hz, ³J=7.9 Hz, 1H, C₃H), 3.92 (q, ³J=3.7 Hz, 1H, C₄H), 3.73 – 3.45 (m, 2H, C₅H₂).

HRMS (ESI⁺): calcd. for C₁₁H₁₂D₃N₅O₄ [M+H]⁺: 285.1382, found: 285.1386.

IR: $\tilde{\nu}$ (cm⁻¹) = 3102 m, 2928 m, 1687 m, 1644 m, 1570 s, 1505 s, 1425 m, 1378 m, 1327 m, 1217 m, 1171 m, 1081 s, 1052 s, 982 w, 866 w, 775 w, 699 w, 676 w, 638 m.

10.6.8 Synthesis of ac⁶A

2',3',5'-Tri-*O*-(*tert*-butyldimethylsilyl)-*N*⁶-acetyladenosine (**21**)



Compound **1** (200 mg, 0.33 mmol) was dissolved in dry pyridine (4 mL), slowly treated with acetylchloride (0.79 mL, 11.2 mmol) at -5 °C and stirred for 5 min. Then the reaction mixture was warmed to rt and stirred for another 1 h. The reaction was stopped with water (2 mL), extracted with CH₂Cl₂ (20 mL) and washed three times with H₂O (3 × 25 mL). The combined organic layers were dried over MgSO₄, filtrated and the solvent was removed *in vacuo*. The crude product was purified by column chromatography (EtOAc/cyclohexane = 30:70) to obtain compound **21** (140 mg, 0.21 mmol, 66%) as colorless foam.

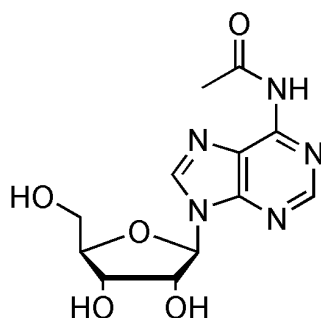
R_f (EtOAc/cyclohexane 1:1) = 0.60. M.p.: 64 °C.

¹H NMR (CDCl₃, 400 MHz) δ (ppm) = 8.66 (s, 1H, C8H), 8.61 (s, br, 1H, NH), 8.33 (s, 1H, C2H), 6.06 (d, ³J=5.2 Hz, 1H, C1H), 4.62 (t, ³J=4.7 Hz, 1H, C₂H), 4.29 (t, ³J=4.0 Hz, 1H, C₃H), 4.13 (dd, ³J=3.6 Hz, ³J=6.4 Hz, 1H, C₄H), 4.00 (dd, ³J=3.9 Hz, ²J=11.4 Hz, 1H, C₅H_a), 3.77 (dd, ³J = 2.6 Hz, ²J=11.4 Hz, 1H, C₅H_b), 2.59 (s, 3H, CH₃), 0.97 – 0.69 [3s, 27H, SiC(CH₃)₃], 0.17 – (-0.41) (6s, 18H, Si(CH₃)₂).

¹³C NMR (CDCl₃, 101 MHz) δ (ppm) = 152.5, 151.3, 149.2, 142.0, 122.2, 88.6, 85.8, 76.3, 72.1, 62.7, 27.1, 26.3, 26.0, 25.9, 25.9, 18.7, 18.3, 18.1, -4.2, -4.5, -4.5, -4.9, -5.2, -5.2.

HRMS (ESI): ber. für C₃₀H₅₇N₅O₅Si₃ [M+H]⁺: 652.3740, found: 652.3756.

IR: $\tilde{\nu}$ (cm⁻¹) = 2953 w, 2929 m, 2897 w, 2857 m, 2341 w, 1703 m, 1608 m, 1584 m, 1463 m, 1372 m, 1294 m, 1281 m, 1251 m, 1153 m, 1123 m, 1071 m, 1031 m, 1000 m, 969 m, 939 m, 835 s, 775 s, 668 m, 644 m, 572 m.

***N*⁶-Acetyladenosine (ac⁶A)**

Compound **21** (0.20 g, 0.31 mmol) and triethylamin-trihydrofluoride (0.16 mL, 0.98 mmol) were dissolved in CH₂Cl₂ (2.0 mL) and stirred at rt for 15 h. Then more triethylamin-trihydrofluoride (0.16 mL, 0.98 mmol) was added and the reaction mixture was stirred for another 30 h. After the reaction mixture was diluted with CH₂Cl₂, trimethylmethoxysilane (3.2 mL) was added to stop the reaction and the solution was stirred for 30 min at rt. The solvent was removed *in vacuo*, followed by dissolving the residue in hot EtOH and subsequent filtration. After the solvent was removed *in vacuo*, the crude product was purified *via* RP-HPLC (eluent A: H₂O, eluent B: MeCN, gradient: 100% A, 0% B → 0% A, 100% B in 45 min, retention time = 18.2 min) to obtain nucleoside **ac⁶A** (77.0 mg, 0.25 mmol, 80%) as a pure solid.

R_f (CH₂Cl₂/MeOH 10:1) = 0.08. M.p.: 176 °C

¹H NMR (CD₃OD, 200 MHz) δ (ppm) = 8.59 (s, 1H, C8H), 8.58 (s, 1H, C2H), 6.09 (d, ³J=5.8 Hz, 1H, C1'H), 4.74 (t, ³J= 5.5 Hz 1H, C2'H), 4.36 (dd, ³J=3.4 Hz, 5.1 Hz, 1H, C3'H), 4.17 (dd, ³J=3.1 Hz, ³J=6.2 Hz, 1H, C4'H), 3.83 (qd, ³J=3.0 Hz, ²J=12.4 Hz, 2H, C5'H₂), 2.37 (s, 3H, COCH₃).

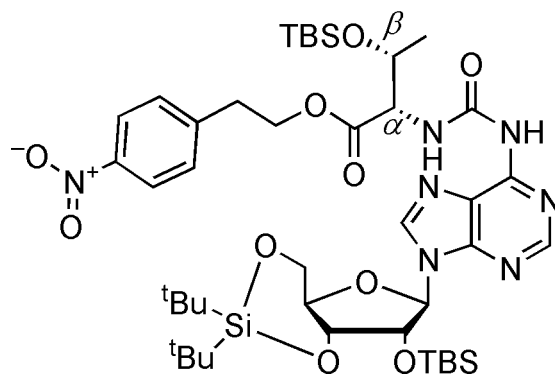
¹³C NMR (CD₃OD, 101 MHz) δ (ppm) = 170.5, 152.0, 151.5, 151.3, 143.1, 123.2, 89.4, 86.3, 74.3, 70.8, 61.7, 23.2.

HRMS (ESI⁺): calcd. for C₁₂H₁₅N₅O₅ [M+H]⁺: 310.1146, found: 310.1148.

IR: $\tilde{\nu}$ (cm⁻¹) = 3261 *s*, 3133 *s*, 2923 *s*, 2855 *m*, 1682 *s*, 1623 *s*, 1584 *s*, 1536 *w*, 1462 *s*, 1414 *m*, 1372 *m*, 1307 *s*, 1251 *m*, 1190 *m*, 1103 *s*, 1077 *s*, 1038 *m*, 896 *w*, 870 *w*, 795 *w*, 680 *w*, 643 *m*.

10.6.9 Synthesis towards incorporation of t⁶A into RNA

2'-O-(Tert-butyl dimethylsilyl)-[3',5'-O-bis(tert-butyl)silylen]-N⁶-{[(1S,2R)-2-[(tert-butyl)dimethylsilyloxy]-1-[2-(4-nitrophenyl)ethoxy]carbonyl]propyl}amino}carbonyl adenosine (23**)**^[147-148]



Compound **15** (400 mg, 712 μmol) was dissolved in dry DMF (8 mL). Then di-*tert*-butylsilylbis(trifluoromethanesulfonate) (97%, 346 μL , 1.07 mmol) was added dropwise at $-5\text{ }^{\circ}\text{C}$ for 15 min and the reaction mixture stirred for 2 h. Afterwards imidazole was added (242 mg, 3.56 mmol) and stirred for 5 min at $-5\text{ }^{\circ}\text{C}$. The reaction was warmed to rt, then TBSCl (429 mg, 2.85 mmol) was added and the reaction mixture stirred for 15 h. Afterwards the reaction mixture was extracted with CH_2Cl_2 (60 mL), followed by washing with water ($3 \times 80\text{ mL}$) and extraction of the aqueous layers with additional CH_2Cl_2 (60 mL). The combined organic layers were dried over MgSO_4 , filtrated and the solvent evaporated *in vacuo*. The crude product was purified *via* column chromatography (EtOAc/cyclohexane = 20:80) to obtain **23** (468 mg, 503 μmol , 71%) as colorless foam.

$R_f(\text{CHCl}_3/\text{MeOH } 10:1) = 0.73$.

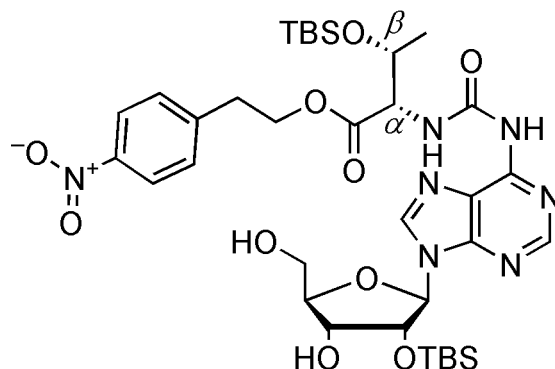
$^1\text{H NMR}$ (CDCl_3 , 600 MHz) δ (ppm) = 9.97 (d, $^3J=8.9\text{ Hz}$, 1H, C_αNH), 8.46 (s, 1H, C_8H), 8.40 (s, 1H, C_2H), 8.15 (s, 1H, C_6NH), 7.92 [d, $^3J=8.7\text{ Hz}$, 2H, $H_{\text{Npe}}(\text{o-NO}_2)$], 7.30 [d, $^3J=8.4\text{ Hz}$, 2H, $H_{\text{Npe}}(\text{m-NO}_2)$], 5.98 (s, 1H, C_1H), 4.63 (d, $^3J=4.6\text{ Hz}$, 1H, C_2H), 4.55 (dd, $^3J=1.5\text{ Hz}$, $^3J=9.1\text{ Hz}$, 1H, C_3H), 4.53 – 4.44 (m, 3H, C_4H , C_αH , C_βH), 4.41 – 4.30 (m, 2H, $\text{CH}_2\text{CH}_2\text{O}$), 4.23 (td, $^3J=5.1\text{ Hz}$, $^2J=10.1\text{ Hz}$, 1H, C_5H_a), 4.07 – 4.01 (m, 1H, C_5H_b), 3.01 (t, $^3J=6.5\text{ Hz}$, 2H, $\text{CH}_2\text{CH}_2\text{O}$), 1.23 (d, $^3J=6.3\text{ Hz}$, 3H, $\text{C}_\beta\text{CH}_3$), 1.07 – 1.03 (2s, 18H, $\text{Si}[\text{C}(\text{CH}_3)_3]_2$), 0.94 – 0.87 (2s, 18H, $\text{SiC}(\text{CH}_3)_3$), 0.08 (4s, 12H, $\text{Si}(\text{CH}_3)_2$).

^{13}C NMR (CDCl_3 , 151 MHz) δ = 171.0, 154.5, 151.3, 150.3, 149.8, 146.9, 145.7, 141.5, 129.9, 123.7, 121.1, 92.7, 76.0, 75.8, 75.0, 68.8, 68.0, 64.7, 59.8, 35.0, 27.7, 27.2, 26.1, 25.7, 22.9, 21.3, 20.6, 18.5, 18.0, -4.1, -4.8, -5.2.

HRMS (ESI⁺): calcd. for $\text{C}_{43}\text{H}_{71}\text{N}_7\text{O}_{10}\text{Si}_3$ $[\text{M}+\text{H}]^+$: 930.4643, found: 930.4675.

IR: $\tilde{\nu}$ (cm^{-1}) = 3245 *w*, 2932 *m*, 2895 *w*, 2858 *m*, 1737 *w*, 1702 *m*, 1611 *m*, 1588 *m*, 1521 *s*, 1466 *m*, 1345 *m*, 1251 *s*, 1165 *m*, 1133 *m*, 1097 *m*, 999 *m*, 940 *w*, 895 *w*, 828 *s*, 778 *s*, 751 *m*, 695 *w*, 652 *m*.

2'-O-(Tert-butyl dimethylsilyl)-N⁶-{[(1S,2R)-2-[(tert-butyl)dimethylsilyloxy]-1-[2-(4-nitrophenyl)ethoxy]carbonyl]propyl}amino}carbonyl}adenosine (25**)^[147-148]**



Compound **23** (447 mg, 480 μmol) was dissolved in a polypropylene tube in dry CH_2Cl_2 (5 mL) and dry pyridine (50 μL). The solution was cooled to 0 $^\circ\text{C}$ and subsequently treated with pyridine \cdot HF (70%, 65.0 μL , 504 μmol). The reaction was stopped after 3 h using methoxytrimethylsilane (600 μL) and stirred for another 30 min at rt. Then the solvent was removed *in vacuo* and the crude product purified *via* column chromatography ($\text{CH}_2\text{Cl}_2/\text{MeOH}$ = 50:1). Compound **25** (327 mg, 414 μmol , 86%) was obtained as a colorless foam.

R_f ($\text{CH}_2\text{Cl}_2/\text{MeOH}$ 10:1) = 0.48.

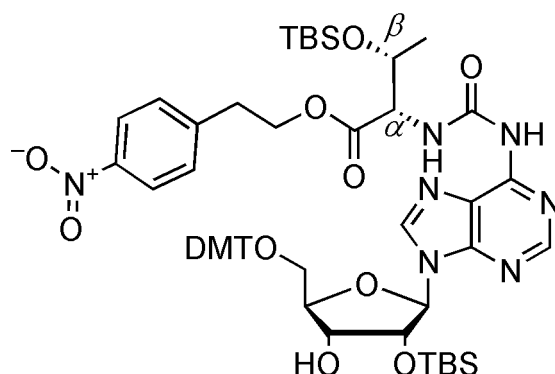
^1H NMR (CDCl_3 , 600 MHz) δ (ppm) = 9.99 (d, $^3J=8.6$ Hz, 1H, C_αNH), 8.90 (s, 1H, C_8H), 8.46 (s, 1H, C_2H), 8.22 (s, 1H, C_6NH), 8.05 [d, $^3J=7.9$ Hz, 2H, $H_{\text{Npe}}(\text{o-NO}_2)$], 7.33 [d, $^3J=7.9$ Hz, 2H, $H_{\text{Npe}}(\text{m-NO}_2)$], 5.85 (m, 1H, C_1H), 5.15 – 5.00 (m, 1H, C_2H), 4.56 (d, $^3J=8.7$ Hz, 1H, C_αH), 4.51 – 4.16 (m, 5H, C_4H , C_3H , C_βH , $\text{CH}_2\text{CH}_2\text{O}$), 3.94 (d, $^2J=12.6$ Hz, 1H, C_5H_a), 3.74 (d, $^2J=11.9$ Hz, 1H, C_5H_b), 3.08 – 2.95 (m, 2H, $\text{CH}_2\text{CH}_2\text{O}$), 1.21 (d, $^3J=5.9$ Hz, 3H, $\text{C}_\beta\text{CH}_3$), 0.81 (2s, 18H, $\text{Si}(\text{CH}_3)_3$), -0.16 (4s, 12H, $\text{Si}(\text{CH}_3)_2$).

^{13}C NMR (CDCl_3 , 151 MHz) δ (ppm) = 170.9, 154.3, 151.1, 151.0, 149.5, 147.0, 145.6, 143.6, 130.0, 123.9, 122.2, 91.3, 87.6, 74.8, 72.9, 68.8, 65.1, 63.4, 59.7, 35.0, 25.7, 21.3, 18.0, 18.0, -4.1, -5.2, -5.3.

HRMS (ESI⁺): calcd. for $\text{C}_{35}\text{H}_{55}\text{N}_7\text{O}_{10}\text{Si}_2$ $[\text{M}+\text{H}]^+$: 790.3622, found: 790.3649.

IR: $\tilde{\nu}$ (cm^{-1}) = 3244 w, 2953 m, 2930 m, 2857 m, 1736 w, 1697 s, 1611 m, 1588 m, 1520 s, 1470 m, 1345 m, 1312 m, 1250 s, 1214 m, 1129 m, 1093 s, 1035 m, 996 w, 840 w, 856 m, 835 s, 777 s, 747 m, 696 w, 671 w, 645 w, 564 w.

2'-O-(Tert-butyl dimethylsilyl)-5'-O-(4,4'-dimethoxytrityl)-N⁶-{[(1S,2R)-2-[(tert-butyl)dimethylsilyloxy]-1-[2-(4-nitrophenyl)ethoxy]carbonyl}propyl]amino}carbonyl}adenosine (27**)^[147-148]**



Compound **25** (145 mg, 184 μmol) was dissolved in dry pyridine (8 mL) and treated with DMTC1 (78.0 mg, 0.23 mmol). The reaction mixture was stirred for 16 h at rt, then another portion of DMTC1 was added (20.0 mg, 59.0 μmol) and the reaction mixture stirred for another 2.5 h. The reaction was stopped afterwards with MeOH (1.8 mL), extracted with CH_2Cl_2 (30 mL), washed with conc. NaHCO_3 (2×40 mL) and conc. NaCl (2×40 mL). All aqueous layers were extracted again with extra CH_2Cl_2 (30 mL). The combined organic layers were dried over MgSO_4 , filtrated and the solvent evaporated *in vacuo*. The crude product was purified *via* column chromatography ($\text{CH}_2\text{Cl}_2/\text{MeOH}/\text{NEt}_3 = 98:0:2 \rightarrow 96:2:2$), followed by a second purification *via* NP-HPLC (eluent A: heptane, eluent B: EtOAc, gradient: 100% A, 0% B \rightarrow 70% A, 30% B in 45 min, retention time = 43.1 min) to obtain **27** (138 mg, 126 μmol , 69%) as colorless foam.

R_f ($\text{CH}_2\text{Cl}_2/\text{MeOH}/\text{NEt}_3$ 20:1:0.2) = 0.76.

^1H NMR (acetone, 400 MHz) δ (ppm) = 9.95 (d, $^3J=9.2$ Hz, 1H, C_αNH), 8.64 (s, 1H, C_6NH), 8.50 (s, 1H C_8H), 8.40 (s, 1H, C_2H), 8.02 [d, $^3J=8.7$ Hz, 2H, $H_{\text{Npe(o-NO}_2)}$], 7.55 – 7.48 [m, 4H, $H_{\text{Npe(m-NO}_2)}$, H_{DMT}], 7.37 (dd, $^3J=2.4$ Hz, $^3J=8.9$ Hz, 4H, H_{DMT}), 7.31 – 7.15 (m, 3H, H_{DMT}), 6.84 (dd, $^3J=2.7$ Hz, $^3J=9.0$ Hz, 4H, H_{DMT}), 6.16 (d, $^3J=4.5$ Hz, 1H, C_1H), 5.16 (t, $^3J=4.7$ Hz, 1H, C_2H), 4.60 – 4.49 (m, 3H, C_3H , C_αH , C_βH), 4.47 – 4.34 (m, 2H, $\text{CH}_2\text{CH}_2\text{O}$), 4.29 (dd, $^3J=4.6$ Hz, $^3J=8.1$ Hz, 1H, C_4H), 3.92 (d, $^3J=5.8$ Hz, 1H, C_3OH), 3.77 (s, 6H, OCH_3), 3.53 – 3.42 (m, 2H, C_5H_2), 3.13 (t, $^3J=6.2$ Hz, 2H, $\text{CH}_2\text{CH}_2\text{O}$), 1.28 (d, $^3J=6.2$ Hz, 3H, $\text{C}_\beta\text{CH}_3$), 0.92 – 0.86 (2s, 18H, $\text{Si}(\text{CH}_3)_3$), 0.10 – (-0.04) (4s, 12H, $\text{Si}(\text{CH}_3)_2$).

^{13}C NMR (d_6 -acetone, 101 MHz) δ (ppm) = 171.6, 159.7, 159.7, 154.7, 151.6, 151.5, 151.4, 147.7, 147.5, 146.2, 143.6, 136.8, 136.8, 131.2, 131.1, 131.1, 129.1, 128.6, 127.6, 124.2,

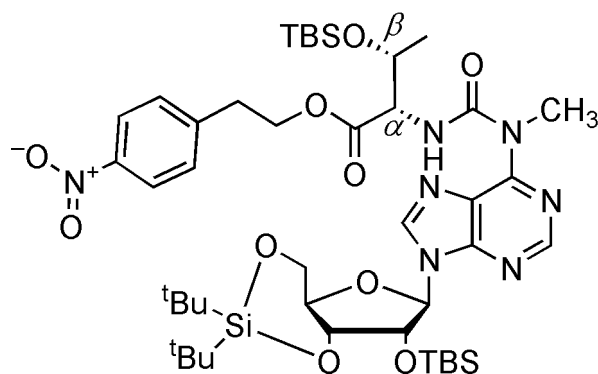
122.0, 114.0, 90.3, 87.2, 85.0, 76.5, 72.1, 69.7, 65.7, 64.5, 60.4, 55.6, 35.4, 30.7, 27.6, 26.2, 26.1, 21.6, 18.8, 18.5, -4.0, -4.5, -4.7, -5.1.

HRMS (ESI⁺): calcd. for C₅₆H₇₃N₇O₁₂Si₂ [M+H]⁺: 1092.4929, found: 1092.4967.

IR: $\tilde{\nu}$ (cm⁻¹) = 2929 *w*, 2855 *w*, 1734 *w*, 1700 *m*, 1608 *m*, 1588 *m*, 1520 *s*, 1509 *s*, 1465 *m*, 1345 *m*, 1248 *s*, 1175 *m*, 1129 *w*, 1095 *m*, 1033 *s*, 994 *m*, 939 *w*, 908 *m*, 828 *s*, 778 *s*, 750 *w*, 698 *w*, 673 *w*, 644 *w*.

10.6.10 Synthesis towards incorporation of m⁶t⁶A into RNA

*N*⁶-Methyl-2'-*O*-(*tert*-butyldimethylsilyl)-[3',5'-*O*-bis(*tert*-butyl)silylen]-*N*⁶-{[(1*S*,2*R*)-2-[[(*tert*-butyl)dimethylsilyloxy]-1-[2-(4-nitrophenyl)ethoxy]carbonyl}propyl]amino}carbonyl} adenosine (**24**)^[147-148]



Compound **22** (286 mg, 497 μ mol) was dissolved in dry DMF (7 mL), then di-*tert*-butylsilylbis(trifluoromethanesulfonate) (97%, 300 μ L, 928 μ mol) was added dropwise at -5 °C for 15 min and the reaction mixture was stirred for 1.5 h. An additional portion of di-*tert*-butylsilylbis(trifluoromethanesulfonate) (97%, 50.0 μ L, 155 μ mol) was added and the reaction mixture stirred for another 2.5 h. Afterwards imidazole (169 mg, 2.48 mmol) was added and stirred for 5 min at -5 °C. The reaction was warmed to rt, TBSCl (375 mg, 2.48 mmol) was added afterwards, the reaction mixture stirred for 16 h and subsequently extracted with CH₂Cl₂ (60 mL). The organic layer was washed with water (3 \times 80 mL) and the aqueous layers again extracted with CH₂Cl₂ (60 mL). The combined organic layers were dried over MgSO₄, filtrated and the solvent evaporated *in vacuo*. The crude product was dissolved in CH₂Cl₂ and purified *via* column chromatography (EtOAc/cyclohexane = 20:80) to obtain **24** (389 mg, 412 μ mol, 83%) as colorless foam.

R_f (CH₂Cl₂/MeOH 10:1) = 0.89.

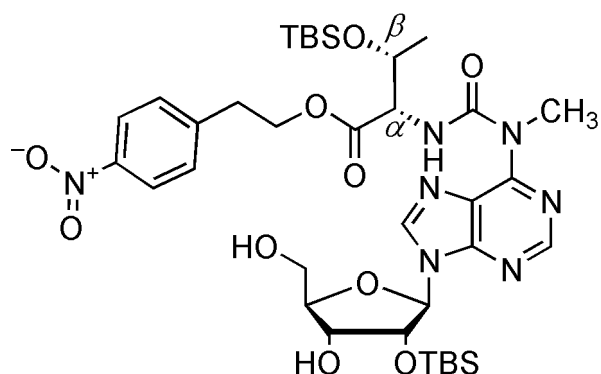
¹H NMR (CDCl₃, 600 MHz) δ (ppm) = 10.96 (d, ³J=8.6 Hz, 1H, C _{α} NH), 8.41 (s, 1H, C8H), 7.99 – 7.96 [m, 3H, C2H, H_{Npe}(o-NO₂)], 7.30 [d, ³J=8.7 Hz, 2H, H_{Npe}(m-NO₂)], 6.00 (s, 1H, C₁H), 4.58 (d, ³J=4.6 Hz, 1H, C₂H), 4.56 (dd, ³J=1.2 Hz, ³J=8.2 Hz, 1H, C _{α} H), 4.51 – 4.44 (m, 3H, C₃H, C₄H, C _{β} H), 4.38 (dt, ³J=6.5 Hz, ²J=11.1 Hz, 1H, CH₂CH_aO), 4.31 (dt, ³J=6.6 Hz, ²J=11.1 Hz, 1H, CH₂CH_bO), 4.24 (td, ³J=5.2 Hz, ²J=10.1 Hz, 1H, C₅H_a), 4.02 (dd, ³J=9.4 Hz, ²J=10.4 Hz, 1H, C₅H_b), 3.96 (s, 3H, N₆CH₃), 3.01 (t, ³J=6.5 Hz, 2H, CH₂CH₂O), 1.21 (d, ³J=6.3 Hz, 3H, C _{β} CH₃), 1.10 – 0.84 (4s, 36H, Si[C(CH₃)₃]₂, SiC(CH₃)₃), 0.17 – (-0.08) (m, 12H, Si(CH₃)₂).

^{13}C NMR (CDCl_3 , 151 MHz) δ (ppm) = 171.4, 156.5, 153.5, 151.7, 150.2, 146.9, 145.7, 139.4, 129.9, 123.7, 122.8, 92.6, 76.1, 75.7, 74.9, 69.0, 68.0, 64.7, 60.7, 35.0, 35.0, 27.7, 27.5, 27.2, 26.1, 25.8, 23.0, 21.4, 20.6, 20.0, 18.5, 18.0, -4.1, -4.1, -4.8, -5.2.

HRMS (ESI⁺): calcd. for $\text{C}_{44}\text{H}_{73}\text{N}_7\text{O}_{10}\text{Si}_3$ $[\text{M}+\text{H}]^+$: 944.4800, found: 944.4822.

IR: $\tilde{\nu}$ (cm^{-1}) = 3290 *w*, 2934 *m*, 2892 *w*, 2859 *m*, 1738 *w*, 1681 *m*, 1585 *w*, 1569 *w*, 1520 *m*, 1466 *m*, 1389 *w*, 1362 *m*, 1343 *m*, 1251 *m*, 1171 *w*, 1138 *m*, 1078 *m*, 1061 *m*, 1012 *m*, 1000 *m*, 938 *m*, 896 *w*, 825 *s*, 798 *s*, 654 *s*.

***N*⁶-Methyl-2'-*O*-(*tert*-butyldimethylsilyl)-*N*⁶-{[(1*S*,2*R*)-2-[(*tert*-butyl)dimethyl]silyloxy]-1-[[2-(4-nitrophenyl)ethoxy]carbonyl]propyl]amino}carbonyl}adenosine (**26**)^[147-148]**



Compound **24** (185 mg, 196 μmol) was dissolved in a polypropylene tube in dry CH_2Cl_2 (3.5 mL) and dry pyridine (40 μL). The solution was cooled to $-5\text{ }^\circ\text{C}$ and subsequently treated with pyridine \cdot HF (70%, 26.0 μL , 206 μmol). After 5 h the reaction was stopped using methoxytrimethylsilane (200 μL) and stirred for 30 min at rt. Then the solvent was removed *in vacuo* and the crude product purified *via* column chromatography ($\text{CH}_2\text{Cl}_2/\text{MeOH} = 50:1$). Compound **26** (122 mg, 152 μmol , 77%) was obtained as colorless foam.

R_f ($\text{CH}_2\text{Cl}_2/\text{MeOH} 10:1$) = 0.53.

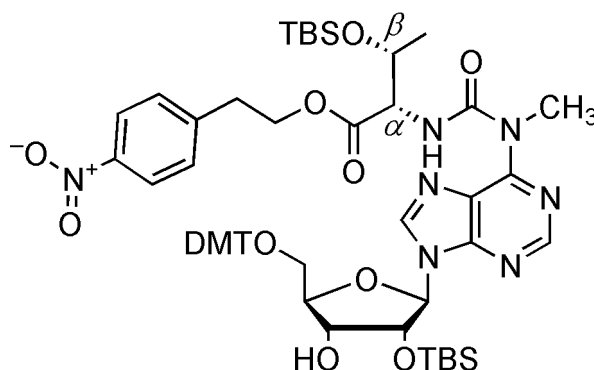
^1H NMR (CDCl_3 , 600 MHz) δ (ppm) = 10.87 (d, $^3J=8.6$ Hz, 1H, C_αNH), 8.46 (s, 1H, $\text{C}8\text{H}$), 8.08 [d, $^3J=8.5$ Hz, 2H, $H_{\text{Npe(o-NO}_2)}$], 7.95 (s, 1H, $\text{C}2\text{H}$), 7.35 [d, $^3J=8.6$ Hz, 2H, $H_{\text{Npe(m-NO}_2)}$], 5.80 (d, $^3J=7.3$ Hz, 1H, C_1H), 5.12 (dd, $^3J=4.8$ Hz, $^3J=7.2$ Hz, 1H, C_2H), 4.54 (dd, $^3J=1.7$ Hz, $^3J=8.6$ Hz, 1H, C_αH), 4.47 – 4.41 (m, 2H, C_4H , C_βH), 4.37 – 4.33 (m, 2H, $\text{CH}_2\text{CH}_a\text{O}$), 4.24 (dt, $^3J=6.9$ Hz, 11.0 Hz, 1H, $\text{CH}_2\text{CH}_b\text{O}$), 3.97 (s, 3H, N_6CH_3), 3.94 (dd, $^3J=1.5$ Hz, $^2J=12.9$ Hz, 1H, C_5H_a), 3.74 (dd, $^3J=1.3$ Hz, $^2J=12.9$ Hz, 1H, C_5H_b), 3.04 (t, $^3J=6.7$ Hz, 2H, $\text{CH}_2\text{CH}_2\text{O}$), 1.20 (d, $^3J=6.3$ Hz, 3H, $\text{C}_\beta\text{CH}_3$), 0.91 – 0.87 (2s, 18H, $\text{SiC}(\text{CH}_3)_3$), 0.03 – (-0.16) (4s, 12H, $\text{Si}(\text{CH}_3)_2$).

^{13}C NMR (CDCl_3 , 151 MHz) δ (ppm) = 171.2, 156.2, 154.2, 151.3, 149.8, 147.1, 145.7, 141.5, 130.0, 123.9, 91.5, 87.7, 74.3, 72.9, 68.9, 65.0, 63.5, 60.7, 35.2, 35.1, 25.8, 25.7, 21.4, 18.0, 18.0, -4.0, -5.1, -5.2, -5.2.

HRMS (ESI⁺): calcd. for $\text{C}_{36}\text{H}_{57}\text{N}_7\text{O}_{10}\text{Si}_2$ [$\text{M}+\text{H}$]⁺: 804.3778, found: 804.3799.

IR: $\tilde{\nu}$ (cm^{-1}) = 3206 w, 2953 m, 2930 m, 2856 m, 1734 m, 1683 m, 1570 m, 1519 s, 1463 m, 1423 w, 1346 s, 1253 s, 1215 w, 1177 w, 1129 m, 1088 s, 1024 m, 976 w, 857 m, 836 s, 811 w, 778 s, 748 m, 696 m, 672 w, 646 w, 526 w.

***N*⁶-Methyl-2'-*O*-(*tert*-butyldimethylsilyl)-5'-*O*-(4,4'-dimethoxytrityl)-*N*⁶-{[(1*S*,2*R*)-2-[(*tert*-butyl)dimethyl]silyloxy]-1-[2-(4-nitrophenyl)ethoxy]carbonyl}propyl}amino}carbonyl}adenosine (**28**)^[147-148]**



Compound **26** (239 mg, 297 μmol) was dissolved in dry pyridine (10 mL) and treated with DMTC1 (131 mg, 386 μmol). The reaction mixture was stirred for 16 h at rt. The reaction was stopped afterwards with MeOH (1.8 mL), extracted with CH_2Cl_2 (30 mL), washed with conc. NaHCO_3 (2×40 mL) and conc. NaCl (2×40 mL). All aqueous layers were extracted again with another CH_2Cl_2 (30 mL). The combined organic layers were dried over MgSO_4 , filtrated and the solvent evaporated *in vacuo*. The crude product was purified *via* column chromatography ($\text{CH}_2\text{Cl}_2/\text{MeOH}/\text{pyridine} = 98:0:2 \rightarrow 97:1:2$), followed by a second purification *via* NP-HPLC (eluent A: heptane, eluent B: EtOAc, gradient: 100% A, 0% B \rightarrow 70% A, 30% B in 45 min, retention time = 43.1 min) to obtain compound **28** (232 mg, 210 μmol , 71%) as colorless foam.

$R_f(\text{CH}_2\text{Cl}_2/\text{MeOH}/\text{pyridine } 20:1:0.2) = 0.63$.

^1H NMR (d_6 -acetone, 400 MHz) δ (ppm) = 10.90 (d, $^3J=8.7$ Hz, 1H, C_αNH), 8.49 (s, 1H, C8H), 8.44 (s, 1H, C2H), 8.01 [d, $^3J=8.7$ Hz, 2H, $H_{\text{Npe}(o-\text{NO}_2)}$], 7.50 [d, $^3J=8.7$ Hz, 2H, $H_{\text{Npe}(m-\text{NO}_2)}$], 7.48 – 7.42 (m, 2H, H_{DMT}), 7.37 – 7.31 (m, 4H, H_{DMT}), 7.29 – 7.17 (m, 3H, H_{DMT}), 6.83 (dd, $^3J=1.9$ Hz, $^3J=8.9$ Hz, 4H, H_{DMT}), 6.19 (d, $^3J=4.4$ Hz, 1H, C_1H), 5.01 (dd, $^3J=4.9$ Hz, $^3J=10.0$ Hz, 1H, C_2H), 4.79 (t, $^3J=5.0$ Hz, 1H, C_3H), 4.52 (dd, $^3J=1.8$ Hz, 7.5 Hz, 2H, C_αH), 4.47 – 4.33 (m, 2H, $\text{CH}_2\text{CH}_2\text{O}$), 4.28 (d, $^3J=5.7$ Hz, 1H, C_3OH), 4.24 (dd, $^3J=4.7$ Hz, $^3J=8.5$ Hz, 1H, C_4H), 3.94 (s, 3H, NCH_3), 3.76 (s, 6H, OCH_3), 3.54 (dd, $^3J=3.6$ Hz, $^2J=10.6$ Hz, 1H, C_5H_a), 3.35 (dd, $^3J=4.7$ Hz, $^2J=10.6$ Hz, 1H, C_5H_b), 3.12 (t, $^3J=6.2$ Hz, 2H, $\text{CH}_2\text{CH}_2\text{O}$), 1.26 (d, $^3J=6.2$ Hz, 3H, $\text{C}_\beta\text{CH}_3$), 0.94 – 0.79 (2s, 18H, $\text{SiC}(\text{CH}_3)_3$), 0.15 – (-0.02) (4s, 12H, $\text{Si}(\text{CH}_3)_2$).

^{13}C NMR (d_6 -acetone, 101 MHz) δ (ppm) = 171.8, 159.7, 156.8, 154.0, 153.2, 150.4, 147.7, 147.5, 146.1, 142.5, 136.8, 136.7, 131.1, 131.1, 131.0, 129.1, 128.6, 127.6, 124.1, 123.5, 114.0, 113.9, 90.3, 87.2, 85.0, 74.7, 73.3, 69.8, 65.5, 64.2, 61.4, 55.6, 35.3, 35.1, 32.7, 26.4, 26.1, 23.4, 21.7, 18.9, 18.5, 14.4, -4.1, -4.2, -4.5, -5.1.

HRMS (ESI⁺): calcd. for $\text{C}_{57}\text{H}_{75}\text{N}_7\text{O}_{12}\text{Si}_2$ $[\text{M}+\text{H}]^+$: 1106.5085, found: 1106.5123.

IR: $\tilde{\nu}$ (cm^{-1}) = 2952 *w*, 2929 *w*, 2856 *w*, 1734 *w*, 1685 *m*, 1607 *w*, 1569 *m*, 1510 *s*, 1464 *m*, 1346 *s*, 1301 *m*, 1250 *s*, 1176 *m*, 1131 *m*, 1088 *m*, 1026 *s*, 975 *m*, 938 *w*, 912 *w*, 835 *s*, 778 *s*, 751 *m*, 699 *m*, 673 *w*, 646 *w*, 616 *w*.

11. Abbreviations

A	Adenosine
A site	Aminoacyl tRNA binding site
ac ⁶ A	N ⁶ -Acetyladenosine
ac ⁴ C	N ⁴ -Acetylcytidine
ac ⁴ Cm	N ⁴ -Acetyl-2'-O-methylcytidine
AID	Activation-induced deaminase
AIDS	Acquired immune deficiency syndrome
Am	2'-O-Methyladenosine
ASL	Anticodon stem and loop
ATT	6-Aza-2-thiothymine
BER	Base excision repair
C	Cytidine
calcd.	Calculated
caC	5-Carboxylcytosine
CNS	Central nervous system
conc.	Concentrated
D	Dihydrouridine
dA	Deoxyadenosine
DBU	1,8-Diazabicyclo[5.4.0]undec-7-en
dC	Deoxycytidine
dG	Deoxyguanosine
DG	Dentate gyrus
DMA	N,N-Dimethylacetamide
DMEM	Dulbecco's Modified Eagle's Medium
DMF	N,N-Dimethylformamide
DMT	Dimethoxytrityl
DNA	Deoxyribonucleic acid
DSL	Dihydrouridine stem and loop
dT	Deoxythymidine
<i>E. coli</i>	Escherichia coli
EDTA	Ethylendiamine tetraacetate
EI	Electron ionization
ES cells	Embryonic stem cells
ESI	Electrospray ionization
fC	5-Formylcytosine
g ⁶ A	N ⁶ -Glycinylicarbamoyladenine
G	Guanosine
Gm	2'-O-Methylguanosine
HGT	Horizontal gene transfer
HIV-1	Human immunodeficiency virus type 1

hmC	5-Hydroxymethylcytosine
hmU	5-Hydroxymethyluracil
hn ⁶ A	N ⁶ -Hydroxynorvalylcarbamoyladenosine
HPLC	High performance liquid chromatography
HRMS	High resolution mass spectrometry
Hz	Hertz
I	Inosine
i ⁶ A	N ⁶ -Isopentenyladenosine
io ⁶ A	N ⁶ -(<i>cis</i> -Hydroxyisopentenyl)adenosine
ICAT	Isotope-coded affinity tagging
IR	Infra red
k ² C	Lysidine
LB	Lysogeny broth
LC	Liquid chromatography
LUCA	Last universal common ancestor
m ¹ A	1-Methyladenosine
m ¹ I	1-Methylinosine
m ¹ G	1-Methylguanosine
m ² A	2-Methyladenosine
m ² G	N ² -Methylguanosine
m ² ₂ G	N ² ,N ² -Dimethylguanosine
m ⁶ A	N ⁶ -Methyladenosine
m ⁶ ₂ A	N ⁶ ,N ⁶ -Dimethyladenosine
m ⁶ t ⁶ A	N ⁶ -Methyl-N ⁶ -threonylcarbamoyladenosine
m ⁷ G	7-Methylguanosine
m ⁸ A	8-Methyladenosine
M.p.	Melting point
mC	5-Methylcytosine
mcm ⁵ s ² U	5-Methoxycarbonylmethyl-2-thiouridine
MeCN	Acetonitrile
MeCP2	Methyl-CpG binding protein 2
MELAS	Myopathy, encephalopathy, lactic acidosis, and stroke-like episodes
MeOTMS	Methoxytrimethylsilane
MERRF	Myoclonus epilepsy associated with ragged red fibers
mnm ⁵ s ² U	5-Methylaminomethyl-2-thiouridine
MOPS	3-(<i>N</i> -morpholino)propanesulfonic acid
mRNA	Messenger ribonucleic acid
MS	Mass spectrometry
ms ² i ⁶ A	2-Methylthio-N ⁶ -isopentenyladenosine
ms ² io ⁶ A	2-Methylthio-N ⁶ -(<i>cis</i> -hydroxyisopentenyl)adenosine
ms ² t ⁶ A	2-Methylthio-N ⁶ -threonylcarbamoyladenosine
ms ² hn ⁶ A	2-Methylthio-N ⁶ -hydroxynorvalylcarbamoyladenosine
n	Amount of substance
nano-LC-MS/MS	nano-liquid chromatography-tandem MS

NMR	Nuclear magnetic resonance
NPE	4-Nitrophenylethyl
OD	Optical density
OHyW	Hydroxywybutosine
oQ	Epoxyqueuosine
P site	Peptidyl tRNA binding site
pH	Pondus hydrogenii
Ph.D.	Doctor of philosophy
ppm	Parts per million
Q	Queuosine
R _f	Rate of flow
RNA	Ribonucleic acid
rpm	Rotation per minute
rRNA	Ribosomal ribonucleic acid
RS	tRNA synthase
RSD	Relative standard deviation
rt	Room temperature
s ² C	2-Thiocytidine
SAM	S-Adenosylmethionine
SILAC	Stable isotope labeling with amino acids in cell culture
snoRNP	Small nucleolar ribonucleoprotein
snRNA	Small nuclear ribonucleic acid
t ⁶ A	N ⁶ -Threonylcarbamoyladenosine
TBS	<i>tert</i> -Butyldimethylsilyl
THF	Tetrahydrofuran
TLC	Thin layer chromatography
τm ⁵ U	5-Taurinomethyluridine
τm ⁵ s ² U	5-Taurinomethyl-2-thiouridine
TMS	Trimethylsilyl
TSL	Thymidine stem and loop
tRNA	Transfer ribonucleic acid
U	Uridine
UV	Ultraviolet
vol.	Volume
Ψ	Pseudouridine
yW	Wybutosine
ZNS	Zentralnervensystem

12. References

- [1] J. M. Berg, J. L. Tymoczko, L. Stryer, *Biochemistry, 5th Edition*, W. H. Freeman and Co., **2002**.
- [2] D. Kuch, Ph.D. thesis, Ludwig-Maximilians-University (Munich) **2008**. *Synthese und Charakterisierung neuartiger Inhibitoren für die humane DNA Methyltransferase DNMT1*.
- [3] S. Dunin-Horkawicz, A. Czerwoniec, M. J. Gajda, M. Feder, H. Grosjean, J. M. Bujnicki, *Nucleic Acids Res.* **2006**, *34*, D145-D149. *MODOMICS: a database of RNA modification pathways*.
- [4] P. A. Limbach, P. F. Crain, J. A. McCloskey, *Nucleic Acids Res.* **1994**, *22*, 2183-2196. *Summary: the modified nucleosides of RNA*.
- [5] H. Grosjean, M. Sprinzl, S. Steinberg, *Biochimie* **1995**, *77*, 139-141. *Posttranscriptionally modified nucleosides in transfer RNA: their locations and frequencies*.
- [6] C. Horn, M. Sprinzl, M. Brown, A. Ioudovitch, S. Steinberg, *Nucleic Acids Res.* **1998**, *26*, 148-153. *Compilation of tRNA sequences and sequences of tRNA genes*.
- [7] G. R. Björk, C. E. Gustafsson, J. U. Ericson, T. G. Hagervall, Y. H. Jönsson, P. M. Wikström, *Annu. Rev. Biochem.* **1987**, *56*, 263-287. *Transfer RNA modification*.
- [8] M. Helm, *Nucleic Acids Res.* **2006**, *34*, 721-733. *Post-transcriptional nucleotide modification and alternative folding of RNA*.
- [9] P. F. Agris, *EMBO Rep.* **2008**, *9*, 629-635. *Bringing order to translation: the contributions of transfer RNA anticodon-domain modifications*.
- [10] P. F. Agris, F. A. P. Vendeix, W. D. Graham, *J. Mol. Biol.* **2007**, *366*, 1-13. *tRNA's wobble decoding of the genome: 40 years of modification*.
- [11] P. F. Agris, *Nucleic Acids Res.* **2004**, *32*, 223-238. *Decoding the genome: a modified view*.
- [12] H. Grosjean, V. de Crécy-Lagard, C. Marck, *FEBS Lett.* **2010**, *584*, 252-264. *Deciphering synonymous codons in the three domains of life: co-evolution with specific tRNA modification enzymes*.
- [13] A. Bird, *Nature* **2007**, *447*, 396-398. *Perceptions of epigenetics*.
- [14] P. A. Jones, D. Takai, *Science* **2001**, *293*, 1068-1070. *The role of DNA methylation in mammalian epigenetics*.
- [15] A. P. Feinberg, *Nature* **2007**, *447*, 433-440. *Phenotypic plasticity and the epigenetics of human disease*.
- [16] W. Reik, W. Dean, J. Walter, *Science* **2001**, *293*, 1089-1093. *Epigenetic reprogramming in mammalian development*.
- [17] W. Reik, *Nature* **2007**, *447*, 425-432. *Stability and flexibility of epigenetic gene regulation in mammalian development*.
- [18] C. Popp, W. Dean, S. Feng, S. J. Cokus, S. Andrews, M. Pellegrini, S. E. Jacobsen, W. Reik, *Nature* **2010**, *463*, 1101-1105. *Genome-wide erasure of DNA methylation in mouse primordial germ cells is affected by AID deficiency*.
- [19] J. J. Day, J. D. Sweatt, *Nat. Neurosci.* **2010**, *13*, 1319-1323. *DNA methylation and memory formation*.
- [20] S. Kriaucionis, N. Heintz, *Science* **2009**, *324*, 929-930. *The nuclear DNA base 5-hydroxymethylcytosine is present in Purkinje neurons and the brain*.
- [21] M. Tahiliani, et al., *Science* **2009**, *324*, 930-935. *Conversion of 5-methylcytosine to 5-hydroxymethylcytosine in mammalian DNA by MLL partner TET1*.

- [22] P. F. Crain, J. A. McCloskey, *Nucleic Acids Res.* **1996**, *24*, 98-99. *The RNA modification database.*
- [23] Y. Ikeuchi, S. Kimura, T. Numata, D. Nakamura, T. Yokogawa, T. Ogata, T. Wada, T. Suzuki, T. Suzuki, *Nat. Chem. Biol.* **2010**, *6*, 277-282. *Agmatine-conjugated cytidine in a tRNA anticodon is essential for AUA decoding in archaea.*
- [24] D. Mandal, et al., *Proc. Natl. Acad. Sci. U. S. A.* **2010**, *107*, 2872-2877. *Agmatidine, a modified cytidine in the anticodon of archaeal tRNA(Ile), base pairs with adenosine but not with guanosine.*
- [25] Y. Motorin, M. Helm, *Biochemistry* **2010**, 4934-4944. *tRNA stabilization by modified nucleotides.*
- [26] A. L. Konevega, N. G. Soboleva, V. I. Makhno, A. V. Peshekhonov, V. I. Katunin, *Mol. Biol.* **2006**, *40*, 597-610. *Effect of modification of tRNA nucleotide 37 on the tRNA interaction with the A and P sites of the Escherichia coli 70S ribosome.*
- [27] A. L. Konevega, N. G. Soboleva, V. I. Makhno, Y. P. Semenov, W. Wintermeyer, M. V. Rodnina, V. I. Katunin, *RNA* **2004**, *10*, 90-101. *Purine bases at position 37 of tRNA stabilize codon-anticodon interaction in the ribosomal A site by stacking and Mg²⁺-dependent interactions.*
- [28] L. B. Jenner, N. Demeshkina, G. Yusupova, M. Yusupov, *Nat. Struct. Mol. Biol.* **2010**, *17*, 555-560. *Structural aspects of messenger RNA reading frame maintenance by the ribosome.*
- [29] M. Yarus, *Science* **1982**, *218*, 646-652. *Translational efficiency of transfer RNA's: uses of an extended anticodon.*
- [30] M. Sprinzl, N. Dank, S. Nock, A. Schön, *Nucleic Acids Res.* **1991**, *19 Suppl*, 2127-2171. *Compilation of tRNA sequences and sequences of tRNA genes.*
- [31] S. H. Kim, F. L. Suddath, G. J. Quigley, A. McPherson, J. L. Sussman, A. H. J. Wang, N. C. Seeman, A. Rich, *Science* **1974**, *185*, 435-440. *Three-dimensional tertiary structure of yeast phenylalanine transfer RNA.*
- [32] J. D. Robertus, J. E. Ladner, J. T. Finch, D. Rhodes, R. S. Brown, B. F. C. Clark, A. Klug, *Nature* **1974**, *250*, 546-551. *Structure of yeast phenylalanine tRNA at 3 Å resolution.*
- [33] J. Cabello-Villegas, M. E. Winkler, E. P. Nikonowicz, *J. Mol. Biol.* **2002**, *319*, 1015-1034. *Solution Conformations of Unmodified and A37N6-dimethylallyl Modified Anticodon Stem-loops of Escherichia coli tRNAPhe.*
- [34] H. Grosjean, M. Sprinzl, S. Steinberg, *Biochimie* **1995**, *77*, 139-141. *Posttranscriptionally modified nucleosides in transfer RNA: their locations and frequencies.*
- [35] M. Sprinzl, K. S. Vassilenko, *Nucleic Acids Res.* **2005**, *33*, D139-D140. *Compilation of tRNA sequences and sequences of tRNA genes.*
- [36] S. S. Ashraf, R. H. Guenther, G. Ansari, A. Malkiewicz, E. Sochacka, P. F. Agris, *Cell Biochem. Biophys.* **2000**, *33*, 241-252. *Role of modified nucleosides of yeast tRNA(Phe) in ribosomal binding.*
- [37] C. Yarian, M. Marszalek, E. Sochacka, A. Malkiewicz, R. Guenther, A. Miskiewicz, P. F. Agris, *Biochemistry* **2000**, *39*, 13390-13395. *Modified Nucleoside Dependent Watson-Crick and Wobble Codon Binding by tRNA Lys UUU Species.*
- [38] J. W. Stuart, Z. Gdaniec, R. Guenther, M. Marszalek, E. Sochacka, A. Malkiewicz, P. F. Agris, *Biochemistry* **2000**, *39*, 13396-13404. *Functional Anticodon Architecture of Human tRNA Lys3 Includes Disruption of Intraloop Hydrogen Bonding by the Naturally Occurring Amino Acid Modification, t6A.*
- [39] J. Cabello-Villegas, I. Tworowska, E. P. Nikonowicz, *Biochemistry* **2004**, *43*, 55-66. *Metal ion stabilization of the U-turn of the A37 N6-dimethylallyl-modified anticodon stem-loop of Escherichia coli tRNAPhe.*

- [40] J. Weissenbach, H. Grosjean, *Eur. J. Biochem.* **1981**, *116*, 207-213. *Effect of Threonylcarbamoyl Modification (t6A) in Yeast tRNA^{ArgIII} on Codon-Anticodon and Anticodon-Anticodon Interactions.*
- [41] M. Sundaram, P. C. Durant, D. R. Davis, *Biochemistry* **2000**, *39*, 12575-12584. *Hypermethylated Nucleosides in the Anticodon of tRNA^{Lys} Stabilize a Canonical U-Turn Structure.*
- [42] P. C. Durant, A. C. Bajji, M. Sundaram, R. K. Kumar, D. R. Davis, *Biochemistry* **2005**, *44*, 8078-8089. *Structural effects of hypermodified nucleosides in the Escherichia coli and human tRNA^{Lys} anticodon loop: the effect of nucleosides s2U, mcm5U, mcm5s2U, mnm5s2U, t6A, and ms2t6A.*
- [43] J. W. Stuart, K. M. Koshlap, R. Guenther, P. F. Agris, *J. Mol. Biol.* **2003**, *334*, 901-918. *Naturally-occurring Modification Restricts the Anticodon Domain Conformational Space of tRNA^{Phe}.*
- [44] E. Lescrinier, K. Nauwelaerts, K. Zanier, K. Poesen, M. Sattler, P. Herdewijn, *Nucleic Acids Res.* **2006**, *34*, 2878-2886. *The naturally occurring N6-threonyl adenine in anticodon loop of Schizosaccharomyces pombe tRNAⁱ causes formation of a unique U-turn motif.*
- [45] F. V. Murphy, V. Ramakrishnan, A. Malkiewicz, P. F. Agris, *Nat. Struct. Mol. Biol.* **2004**, *11*, 1186-1191. *The role of modifications in codon discrimination by tRNA^{(Lys)UUU}.*
- [46] N. E. McCrate, M. E. Varner, K. I. Kim, M. C. Nagan, *Nucleic Acids Res.* **2006**, *34*, 5361-5368. *Molecular dynamics simulations of human tRNA^{Lys,3 UUU}: the role of modified bases in mRNA recognition.*
- [47] U. von Ahsen, R. Green, R. Schroeder, H. F. Noller, *RNA* **1997**, *3*, 49-56. *Identification of 2'-hydroxyl groups required for interaction of a tRNA anticodon stem-loop region with the ribosome.*
- [48] V. Boudou, J. Langridge, A. Van Aerschot, C. Hendrix, A. Millar, P. Weiss, P. Herdewijn, *Helv. Chim. Acta* **2000**, *83*, 152-161. *Synthesis of the Anticodon Hairpin tRNA^{fMet} containing t6A.*
- [49] A. Morin, S. Auxilien, B. Senger, R. Tewari, H. Grosjean, *RNA* **1998**, *4*, 24-37. *Structural requirements for enzymatic formation of threonylcarbamoyladenine (t6A) in tRNA: an in vivo study with Xenopus laevis oocytes.*
- [50] M. Sundaram, P. F. Crain, D. R. Davis, *J. Org. Chem.* **2000**, *65*, 5609-5614. *Synthesis and characterization of the native anticodon domain of E. coli tRNA^{Lys}: simultaneous incorporation of modified nucleosides mnm5s2U, t6A, and pseudouridine using phosphoramidite chemistry.*
- [51] C. Yarian, H. Townsend, W. Czystkowski, E. Sochacka, A. J. Malkiewicz, R. Guenther, A. Miskiewicz, P. F. Agris, *J. Biol. Chem.* **2002**, *277*, 16391-16395. *Accurate translation of the genetic code depends on tRNA modified nucleosides.*
- [52] R. P. Fahlman, T. Dale, O. C. Uhlenbeck, *Mol. Cell* **2004**, *16*, 799-805. *Uniform binding of aminoacylated transfer RNAs to the ribosomal A and P sites.*
- [53] S. S. Ashraf, E. Sochacka, R. Cain, R. Guenther, A. Malkiewicz, P. F. Agris, *RNA* **1999**, *5*, 188-194. *Single atom modification (O->S) of tRNA confers ribosome binding.*
- [54] D. Brégeon, V. Colot, M. Radman, F. Taddei, *Genes Dev.* **2001**, *15*, 2295-2306. *Translational misreading: a tRNA modification counteracts a +2 ribosomal frameshift.*
- [55] P. J. Farabaugh, G. R. Björk, *EMBO J.* **1999**, *18*, 1427-1434. *How translational accuracy influences reading frame maintenance.*
- [56] J. F. Atkins, G. R. Björk, *Microbiol. Mol. Biol. Rev.* **2009**, *73*, 178-210. Figure reproduced with permission from American Society for Microbiology. *A gripping tale*

- of ribosomal frameshifting: extragenic suppressors of frameshift mutations spotlight P-site realignment.*
- [57] J. Urbonavicius, Q. Qian, J. M. B. Durand, T. G. Hagervall, G. R. Björk, *EMBO J.* **2001**, *20*, 4863-4873. *Improvement of reading frame maintenance is a common function for several tRNA modifications.*
- [58] G. R. Björk, P. M. Wikström, A. S. Byström, *Science* **1989**, *244*, 986-989. *Prevention of translational frameshifting by the modified nucleoside 1-methylguanosine.*
- [59] G. R. Björk, J. M. Durand, T. G. Hagervall, R. Leipuviene, H. K. Lundgren, K. Nilsson, P. Chen, Q. Qian, J. Urbonavicius, *FEBS Lett.* **1999**, *452*, 47-51. *Transfer RNA modification: influence on translational frameshifting and metabolism.*
- [60] J. Urbonavicius, G. Stahl, J. M. Durand, S. N. B. Salem, Q. Qian, P. J. Farabaugh, G. R. Björk, *RNA* **2003**, *9*, 760-768. *Transfer RNA modifications that alter +1 frameshifting in general fail to affect -1 frameshifting.*
- [61] G. R. Björk, K. Jacobsson, K. Nilsson, M. J. O. Johansson, A. S. Byström, O. P. Persson, *EMBO J.* **2001**, *20*, 231-239. *A primordial tRNA modification required for the evolution of life?*
- [62] B. A. Carlson, J. F. Mushinski, D. W. Henderson, S. Y. Kwon, P. F. Crain, B. J. Lee, D. L. Hatfield, *Virology* **2001**, *279*, 130-135. *1-Methylguanosine in place of Y base at position 37 in phenylalanine tRNA is responsible for its shiftiness in retroviral ribosomal frameshifting.*
- [63] S. S. Phelps, A. Malkiewicz, P. F. Agris, S. Joseph, *J. Mol. Biol.* **2004**, *338*, 439-444. *Modified nucleotides in tRNA(Lys) and tRNA(Val) are important for translocation.*
- [64] J. Pütz, C. Florentz, F. Benseler, R. Giegé, *Nat. Struct. Biol.* **1994**, *1*, 580-582. *A single methyl group prevents the mischarging of a tRNA.*
- [65] V. Perret, A. Garcia, H. Grosjean, J. P. Ebel, C. Florentz, R. Giegé, *Nature* **1990**, *344*, 787-789. *Relaxation of a transfer RNA specificity by removal of modified nucleotides.*
- [66] K. Nakanishi, L. Bonnefond, S. Kimura, T. Suzuki, R. Ishitani, O. Nureki, *Nature* **2009**, *461*, 1144-1148. *Structural basis for translational fidelity ensured by transfer RNA lysidine synthetase.*
- [67] T. Muramatsu, K. Nishikawa, F. Nemoto, Y. Kuchino, S. Nishimura, T. Miyazawa, S. Yokoyama, *Nature* **1988**, *336*, 179-181. *Codon and amino-acid specificities of a transfer RNA are both converted by a single post-transcriptional modification.*
- [68] M. K. Krüger, M. A. Sørensen, *J. Mol. Biol.* **1998**, *284*, 609-620. *Aminoacylation of hypomodified tRNA^{Glu} in vivo.*
- [69] A. Soma, R. Kumagai, K. Nishikawa, H. Himeno, *J. Mol. Biol.* **1996**, *263*, 707-714. *The anticodon loop is a major identity determinant of Saccharomyces cerevisiae tRNA(Leu).*
- [70] J. Li, B. Esberg, J. F. Curran, G. R. Björk, *J. Mol. Biol.* **1997**, *271*, 209-221. *Three modified nucleosides present in the anticodon stem and loop influence the in vivo aa-tRNA selection in a tRNA-dependent manner.*
- [71] L. A. Sylvers, K. C. Rogers, M. Shimizu, E. Ohtsuka, D. Söll, *Biochemistry* **1993**, *32*, 3836-3841. *A 2-thiouridine derivative in tRNA^{Glu} is a positive determinant for aminoacylation by Escherichia coli glutamyl-tRNA synthetase.*
- [72] K. Nakanishi, Y. Ogiso, T. Nakama, S. Fukai, O. Nureki, *Nat. Struct. Mol. Biol.* **2005**, *12*, 931-932. *Structural basis for anticodon recognition by methionyl-tRNA synthetase.*
- [73] M. A. Rould, J. J. Perona, T. A. Steitz, *Nature* **1991**, *352*, 213-218. *Structural basis of anticodon loop recognition by glutaminyl-tRNA synthetase.*
- [74] S. Fukai, O. Nureki, S. I. Sekine, A. Shimada, D. G. Vassylyev, S. Yokoyama, *RNA* **2003**, *9*, 100-111. *Mechanism of molecular interactions for tRNA^{Val} recognition by valyl-tRNA synthetase.*

- [75] L. F. Silvián, J. Wang, T. A. Steitz, *Science* **1999**, 285, 1074-1077. *Insights into Editing from an Ile-tRNA Synthetase Structure with tRNA^{Ile} and Mupirocin.*
- [76] J. M. B. Durand, G. R. Björk, A. Kuwae, M. Yoshikawa, C. Sasakawa, *J. Bacteriol.* **1997**, 179, 5777-5782. *The modified nucleoside 2-methylthio-N⁶-isopentenyladenosine in tRNA of Shigella flexneri is required for expression of virulence gene.*
- [77] J. M. Durand, B. Dagberg, B. E. Uhlin, G. R. Björk, *Mol. Microbiol.* **2000**, 35, 924-935. *Transfer RNA modification, temperature and DNA superhelicity have a common target in the regulatory network of the virulence of Shigella flexneri: the expression of the virF gene.*
- [78] A. C. Bajji, M. Sundaram, D. G. Myszka, D. R. Davis, *J. Am. Chem. Soc.* **2002**, 124, 14302-14303. *An RNA Complex of the HIV-1 A-Loop and tRNA^{Lys,3} Is Stabilized by Nucleoside Modifications.*
- [79] P. Bénas, G. Bec, G. Keith, R. Marquet, C. Ehresmann, B. Ehresmann, P. Dumas, *RNA* **2000**, 6, 1347-1355. *The crystal structure of HIV reverse-transcription primer tRNA(Lys,3) shows a canonical anticodon loop.*
- [80] S. Kurata, et al., *J. Biol. Chem.* **2008**, 283, 18801-18811. *Modified uridines with C5-methylene substituents at the first position of the tRNA anticodon stabilize U.G wobble pairing during decoding.*
- [81] Y. Kirino, T. Yasukawa, S. Ohta, S. Akira, K. Ishihara, K. Watanabe, T. Suzuki, *Proc. Natl. Acad. Sci. U. S. A.* **2004**, 101, 15070-15075. *Codon-specific translational defect caused by a wobble modification deficiency in mutant tRNA from a human mitochondrial disease.*
- [82] T. Suzuki, T. Suzuki, T. Wada, K. Saigo, K. Watanabe, *EMBO J.* **2002**, 21, 6581-6589. *Taurine as a constituent of mitochondrial tRNAs: new insights into the functions of taurine and human mitochondrial diseases.*
- [83] T. Yasukawa, T. Suzuki, N. Ishii, S. Ohta, K. Watanabe, *EMBO J.* **2001**, 20, 4794-4802. *Wobble modification defect in tRNA disturbs codon-anticodon interaction in a mitochondrial disease.*
- [84] K. M. Harrington, I. A. Nazarenko, D. B. Dix, R. C. Thompson, O. C. Uhlenbeck, *Biochemistry* **1993**, 32, 7617-7622. *In vitro analysis of translational rate and accuracy with an unmodified tRNA.*
- [85] B. S. Vold, *Nucleic Acids Res.* **1979**, 7, 193-204. *Radioimmunoassays for the modified nucleosides N-[9-(β-D-ribofuranosyl)purin-6-ylcarbonyl]-L-threonine and 2-methylthioadenosine.*
- [86] B. S. Vold, J. M. Lazar, A. M. Gray, *J. Biol. Chem.* **1979**, 254, 7362-7367. *Characterization of a deficiency of N⁶-(delta 2-isopentenyl)-2-methylthioadenosine in the Escherichia coli mutant trpX by use of antibodies to N⁶-(delta 2-isopentenyl)adenosine.*
- [87] P. F. Agris, J. G. Tompson, C. W. Gehrke, K. C. Kuo, R. H. Rice, *J. Chromatogr. A* **1980**, 194, 205-212. *High-performance liquid chromatography and mass spectrometry of transfer RNA bases for isotopic abundance.*
- [88] C. W. Gehrke, R. W. Zumwalt, R. A. McCune, K. C. Kuo, *J. Cancer Res. Clin. Oncol.* **1982**, 103, 323-324. *Quantitative high-performance liquid chromatography analysis of modified nucleosides in physiological fluids, tRNA, and DNA.*
- [89] K. R. Noon, R. Guymon, P. F. Crain, J. A. McCloskey, M. Thomm, J. Lim, R. Cavicchioli, *J. Bacteriol.* **2003**, 185, 5483-5490. *Influence of Temperature on tRNA Modification in Archaea: Methanococcus burtonii (Optimum Growth Temperature [Topt], 23 C) and Stetteria hydrogenophila (Topt, 95 C).*
- [90] J. A. McCloskey, D. E. Graham, S. Zhou, P. F. Crain, M. Ibba, J. Konisky, D. Söll, G. J. Olsen, *Nucleic Acids Res.* **2001**, 29, 4699-4706. *Post-transcriptional modification in*

- archaeal tRNAs: identities and phylogenetic relations of nucleotides from mesophilic and hyperthermophilic Methanococcales.*
- [91] J. A. Kowalak, J. J. Dalluge, J. A. McCloskey, K. O. Stetter, *Biochemistry* **1994**, *33*, 7869-7876. *The role of posttranscriptional modification in stabilization of transfer RNA from hyperthermophiles.*
- [92] C. G. Edmonds, P. F. Crain, R. Gupta, T. Hashizume, C. H. Hocart, J. A. Kowalak, S. C. Pomerantz, K. O. Stetter, J. A. McCloskey, *J. Bacteriol.* **1991**, *173*, 3138-3148. *Posttranscriptional modification of tRNA in thermophilic archaea (Archaeobacteria).*
- [93] C. W. Gehrke, K. C. Kuo, *J. Chromatogr.* **1989**, *471*, 3-36. *Ribonucleoside analysis by reversed-phase high-performance liquid chromatography.*
- [94] M. Buck, M. Connick, B. N. Ames, *Anal. Biochem.* **1983**, *129*, 1-13. *Complete analysis of tRNA-modified nucleosides by high-performance liquid chromatography: the 29 modified nucleosides of Salmonella typhimurium and Escherichia coli tRNA.*
- [95] A. Costa, J.-P. Pais de Barros, G. Keith, W. Baranowskic, J. Desgrès, *J. Chromatogr. B* **2004**, *801*, 237-247. *Determination of queuosine derivatives by reverse-phase liquid chromatography for the hypomodification study of Q-bearing tRNAs from various mammal liver cells.*
- [96] B. F. Cravatt, J. R. Yates, G. M. Simon, *Nature* **2007**, *450*, 991-1000. *The biological impact of mass-spectrometry-based proteomics.*
- [97] S.-E. Ong, M. Mann, *Nat. Chem. Biol.* **2005**, *1*, 252-262. *Mass spectrometry-based proteomics turns quantitative.*
- [98] S. D. Patterson, R. H. Aebersold, *Nat. Genet.* **2003**, *33 Suppl*, 311-323. *Proteomics: the first decade and beyond.*
- [99] T. Böttcher, M. Pitscheider, S. A. Sieber, *Angew. Chem., Int. Ed.* **2010**, *49*, 2680-2698. *Natural products and their biological targets: proteomic and metabolomic labeling strategies.*
- [100] J. C. Venter, S. Levy, T. Stockwell, K. Remington, A. Halpern, *Nat. Genet.* **2003**, *33 Suppl*, 219-227. *Massive parallelism, randomness and genomic advances.*
- [101] D. J. Lockhart, E. A. Winzeler, *Nature* **2000**, *405*, 827-836. *Genomics, gene expression and DNA arrays.*
- [102] B. D. Bennett, E. H. Kimball, M. Gao, R. Osterhout, S. J. Van Dien, J. D. Rabinowitz, *Nat. Chem. Biol.* **2009**, *5*, 593-599. *Absolute metabolite concentrations and implied enzyme active site occupancy in Escherichia coli.*
- [103] N. Gehlenborg, et al., *Nat. Meth.* **2010**, *7*, S56-S68. *Visualization of omics data for systems biology.*
- [104] M. Mann, *Nat. Rev. Mol. Cell Biol.* **2006**, *7*, 952-958. *Functional and quantitative proteomics using SILAC.*
- [105] S. P. Gygi, B. Rist, S. A. Gerber, F. Turecek, M. H. Gelb, R. Aebersold, *Nat. Biotechnol.* **1999**, *17*, 994-999. *Quantitative analysis of complex protein mixtures using isotope-coded affinity tags.*
- [106] F. Turecek, *J. Mass Spectrom.* **2002**, *37*, 1-14. *Mass spectrometry in coupling with affinity capture-release and isotope-coded affinity tags for quantitative protein analysis.*
- [107] Y. Yang, D. Nikolic, S. M. Swanson, R. B. van Breemen, *Anal. Chem.* **2002**, *74*, 5376-5382. *Quantitative determination of N7-methyldeoxyguanosine and O6-methyldeoxyguanosine in DNA by LC-UV-MS-MS.*
- [108] E. P. Quinlivan, J. F. Gregory, *Nucleic Acids Res.* **2008**, *36*, e119. *DNA methylation determination by liquid chromatography-tandem mass spectrometry using novel biosynthetic [U-15N]deoxycytidine and [U-15N]methyldeoxycytidine internal standards.*

- [109] K. Taghizadeh, J. L. McFaline, B. Pang, M. Sullivan, M. Dong, E. Plummer, P. C. Dedon, *Nat. Protoc.* **2008**, *3*, 1287-1298. *Quantification of DNA damage products resulting from deamination, oxidation and reaction with products of lipid peroxidation by liquid chromatography isotope dilution tandem mass spectrometry.*
- [110] J. J. Dalluge, J. A. McCloskey, T. Hashizume, *Nucleic Acids Res.* **1996**, *24*, 3242-3245. *Quantitative measurement of dihydrouridine in RNA using isotope dilution liquid chromatography-mass spectrometry (LC/MS).*
- [111] G. B. Chheda, R. H. Hall, D. I. Magrath, J. Mozejko, M. P. Schweizer, L. Stasiuk, P. R. Taylor, *Biochemistry* **1969**, *8*, 3278-3282. *Aminoacyl nucleosides. VI. Isolation and preliminary characterization of threonyladenine derivatives from transfer ribonucleic acid.*
- [112] M. P. Schweizer, G. B. Chheda, L. Baczynskyj, R. H. Hall, *Biochemistry* **1969**, *8*, 3283-3289. *Aminoacyl nucleosides. VII. N-(purin-6-ylcarbamoyl)threonine. A new component of transfer ribonucleic acid.*
- [113] B. El Yacoubi, et al., *Nucleic Acids Res.* **2009**, *37*, 2894-2909. *The universal YrdC/Sua5 family is required for the formation of threonylcarbamoyladenine in tRNA.*
- [114] B. N. Elkins, E. B. Keller, *Biochemistry* **1974**, *13*, 4622-4628. *Enzymic synthesis of N-(purin-6-ylcarbamoyl)threonine, an anticodon-adjacent base in transfer ribonucleic acid.*
- [115] A. Körner, D. Söll, *FEBS Lett.* **1974**, *39*, 301-306. *N-(purin-6-ylcarbamoyl)threonine: biosynthesis in vitro in transfer RNA by an enzyme purified from Escherichia coli.*
- [116] M. P. Schweizer, K. McGrath, L. Baczynskyj, *Biochem. Biophys. Res. Commun.* **1970**, *40*, 1046-1052. *The isolation and characterization of N-[9-(β -D-ribofuranosyl-purin-6-ylcarbamoyl)]glycine from yeast transfer RNA.*
- [117] F. Kimura-Harada, D. L. von Minden, J. A. McCloskey, S. Nishimura, *Biochemistry* **1972**, *11*, 3910-3915. *N-[(9-D-Ribofuranosylpurin-6-yl)-N-methylcarbamoyl]threonine, a modified nucleoside isolated from Escherichia coli threonine transfer ribonucleic acid.*
- [118] Q. Qian, J. F. Curran, G. R. Bjork, *J. Bacteriol.* **1998**, *180*, 1808-1813. *The methyl group of the N6-methyl-N6-threonylcarbamoyladenine in tRNA of Escherichia coli modestly improves the efficiency of the tRNA.*
- [119] T. H. Tsang, B. N. Ames, M. Buck, *Biochim. Biophys. Acta* **1983**, *741*, 180-196. *Sequence specificity of tRNA-modifying enzymes. An analysis of 258 tRNA sequences.*
- [120] M. Raba, K. Limburg, M. Burghagen, J. R. Katze, M. Simsek, J. E. Heckman, U. L. Rajbhandary, H. J. Gross, *Eur. J. Biochem.* **1979**, *97*, 305-318. *Nucleotide sequence of three isoaccepting lysine tRNAs from rabbit liver and SV40-transformed mouse fibroblasts.*
- [121] Z. Yamaizumi, S. Nishimura, K. Limburg, M. Raba, H. J. Gross, P. F. Crain, J. A. McCloskey, *J. Am. Chem. Soc.* **1979**, *101*, 2224-2225. *Structure elucidation by high resolution mass spectrometry of a highly modified nucleoside from mammalian transfer RNA. N-[(9-beta-D-Ribofuranosyl-2-methylthiopurin-6-yl)carbamoyl]threonine.*
- [122] S. Arragain, et al., *J. Biol. Chem.* **2010**, *285*, 28425-28433. *Identification of Eukaryotic and Prokaryotic Methylthiotransferase for Biosynthesis of 2-Methylthio-N6-threonylcarbamoyladenine in tRNA.*
- [123] J. W. Littlefield, D. B. Dunn, *Biochem. J.* **1958**, *70*, 642-651. *The occurrence and distribution of thymine and three methylated-adenine bases in ribonucleic acids from several sources.*
- [124] J. W. Littlefield, D. B. Dunn, *Nature* **1958**, *181*, 254-255. *Natural occurrence of thymine and three methylated adenine bases in several ribonucleic acids.*

- [125] M. Kempenaers, M. Roovers, Y. Oudjama, K. L. Tkaczuk, J. M. Bujnicki, L. Droogmans, *Nucleic Acids Res.* **2010**, 1-11. *New archaeal methyltransferases forming 1-methyladenosine or 1-methyladenosine and 1-methylguanosine at position 9 of tRNA.*
- [126] R. Raettig, H. Kersten, J. Weissenbach, G. Dirheimer, *Nucleic Acids Res.* **1977**, 4, 1769-1782. *Methylation of an adenosine in the D-loop of specific transfer RNAs from yeast by a procaryotic tRNA (adenine-1) methyltransferase.*
- [127] M. Klagsbrun, *J. Biol. Chem.* **1973**, 248, 2612-2620. *An evolutionary study of the methylation of transfer and ribosomal ribonucleic acid in prokaryote and eukaryote organisms.*
- [128] S. Ozanick, A. Krecic, J. Andersland, J. T. Anderson, *RNA* **2005**, 11, 1281-1290. *The bipartite structure of the tRNA m1A58 methyltransferase from *S. cerevisiae* is conserved in humans.*
- [129] Z. Bodi, J. D. Button, D. Grierson, R. G. Fray, *Nucleic Acids Res.* **2010**, 1-9. *Yeast targets for mRNA methylation.*
- [130] M. L. Wilkinson, S. M. Crary, E. J. Grayhack, J. E. Jackman, E. M. Phizicky, *RNA* **2007**, 13, 404-413. *The 2'-O-methyltransferase responsible for modification of yeast tRNA at position 4.*
- [131] L. Droogmans, H. Grosjean, *Biochimie* **1991**, 73, 1021-1025. *2-O-methylation and inosine formation in the wobble position of anticodon-substituted tRNA-Phe in a homologous yeast in vitro system.*
- [132] A. M. B. Giessing, S. S. Jensen, A. Rasmussen, L. H. Hansen, A. Gondela, K. Long, B. Vester, F. Kirpekar, *RNA* **2009**, 15, 327-336. *Identification of 8-methyladenosine as the modification catalyzed by the radical SAM methyltransferase Cfr that confers antibiotic resistance in bacteria.*
- [133] K. H. Kaminska, E. Purta, L. H. Hansen, J. M. Bujnicki, B. Vester, K. S. Long, *Nucleic Acids Res.* **2010**, 38, 1652-1663. *Insights into the structure, function and evolution of the radical-SAM 23S rRNA methyltransferase Cfr that confers antibiotic resistance in bacteria.*
- [134] B. Poldermans, H. Bakker, P. H., *Nucleic Acids Res.* **1980**, 8, 143-151. *Studies on the function of two adjacent N6,N6-dimethyladenosines near the 3' end of 16S ribosomal RNA of *Escherichia coli*. IV. The effect of the methylgroups on ribosomal subunit interaction.*
- [135] M. D. Metodiev, N. Lesko, C. B. Park, Y. Cámara, Y. Shi, R. Wibom, K. Hultenby, C. M. Gustafsson, N.-G. Larsson, *Cell Metab.* **2009**, 9, 386-397. *Methylation of 12S rRNA is necessary for in vivo stability of the small subunit of the mammalian mitochondrial ribosome.*
- [136] A. Sauerwald, D. Sitaramaiah, J. A. McCloskey, D. Söll, P. F. Crain, *FEBS Lett.* **2005**, 579, 2807-2810. *N6-Acetyladenosine: a new modified nucleoside from *Methanopyrus kandleri* tRNA.*
- [137] G. B. Chheda, C. I. Hong, *J. Med. Chem.* **1971**, 14, 748-753. *Synthesis of naturally occurring 6-ureidopurines and their nucleosides.*
- [138] V. Nair, S. D. Chamberlain, *J. Org. Chem.* **1985**, 50, 5069-5075. *Novel photoinduced functionalized C-alkylations in purine systems.*
- [139] C. Höbartner, C. Kreutz, E. Flecker, E. Ottenschläger, W. Pils, K. Grubmayr, R. Micura, *Monatsh. Chem.* **2003**, 134, 851-873. *The Synthesis of 2'-O-[(Triisopropylsilyl)oxy]methyl (TOM) Phosphoramidites of Methylated Ribonucleosides (m1G, m2G, m22G, m1I, m3U, m4C, m6A, m62A) for Use in Automated RNA Solid-Phase Synthesis.*

- [140] T. Brückl, Ph.D. thesis, Ludwig-Maximilians-University (Munich), **2010**. *Synthesis of natural and isotope-labeled tRNA nucleosides and their mass spectrometric quantification*.
- [141] S. P. Dutta, C. I. Hong, G. P. Murphy, A. Mittelman, G. B. Chheda, *Biochemistry* **1975**, *14*, 3144-3151. *Synthesis and properties of the naturally occurring N-[(9-D-ribofuranosylpurin-6-yl)-N-methylcarbamoyl]-L-threonine (mt6A) and other related synthetic analogs*.
- [142] K. Aritomo, T. Wada, M. Sekine, *J. Chem. Soc., Perkin Trans. I* **1995**, 1837-1844. *Alkylation of 6-N-acylated adenosine derivatives by the use of phase transfer catalysis*.
- [143] J. Yano, L. S. Kan, P. O. Ts'o, *Biochim. Biophys. Acta* **1980**, *629*, 178-183. *A simple method of the preparation of 2'-O-methyladenosine. Methylation of adenosine with methyl iodide in anhydrous alkaline medium*.
- [144] P. J. L. M. Quaedflieg, A. P. van der Heiden, L. H. Koole, A. J. J. M. Coenen, S. van der Wal, E. M. Meijer, *J. Org. Chem.* **1991**, *56*, 5846-5859. *Synthesis and conformational analysis of phosphate-methylated RNA dinucleotides*.
- [145] J. W. Jones, R. K. Robins, *J. Am. Chem. Soc.* **1963**, *85*, 193-201. *Purine Nucleosides. III. Methylation studies of certain naturally occurring purine nucleosides*.
- [146] S. L. Beaucage, R. P. Iyer, *Tetrahedron* **1992**, *39*, 2095-2135. *Advances in the synthesis of oligonucleotides by the phosphoramidite approach*.
- [147] V. Serebryany, L. Beigelman, *Tetrahedron Lett.* **2002**, *43*, 1983-1985. *An efficient preparation of protected ribonucleosides for phosphoramidite RNA synthesis*.
- [148] V. Serebryany, L. Beigelman, *Nucleosides, Nucleotides Nucleic Acids* **2003**, *22*, 1007-1009. *Synthesis of 2'-O-Substituted Ribonucleosides*.
- [149] M. Szymański, M. Z. Barciszewska, V. A. Erdmann, J. Barciszewski, *Biochem. J.* **2003**, *371*, 641-651. *5 S rRNA: structure and interactions*.
- [150] E. Bruenger, J. A. Kowalak, Y. Kuchino, J. A. McCloskey, H. Mizushima, K. O. Stetter, P. F. Crain, *FASEB J.* **1993**, *7*, 196-200. *5S rRNA modification in the hyperthermophilic archaea *Sulfolobus solfataricus* and *Pyrodictium occultum**.
- [151] P. F. Crain, *Methods Enzymol.* **1990**, *193*, 782-790. *Preparation and enzymatic hydrolysis of DNA and RNA for mass spectrometry*.
- [152] C. W. Gehrke, K. C. Kuo, R. A. McCune, K. O. Gerhardt, P. F. Agris, *J. Chromatogr.* **1982**, *230*, 297-308. *Quantitative enzymatic hydrolysis of tRNAs: reversed-phase high-performance liquid chromatography of tRNA nucleosides*.
- [153] P. M. E. Gramlich, C. T. Wirges, J. Gierlich, T. Carell, *Org. Lett.* **2008**, *10*, 249-251. *Synthesis of modified DNA by PCR with alkyne-bearing purines followed by a click reaction*.
- [154] J. F. Gregory, E. P. Quinlivan, *Nucleic Acids Res.* **2008**, *36*, e119. *DNA methylation determination by liquid chromatography-tandem mass spectrometry using novel biosynthetic [U-15N]deoxycytidine and [U-15N]methyldeoxycytidine internal standards*.
- [155] O. Dimroth, *Justus Liebigs Ann. Chem.* **1910**, *373*, 336-370. *Über intramolekulare Umlagerungen*.
- [156] J. D. Engel, *Biochem. Biophys. Res. Commun.* **1975**, *64*, 581-586. *Mechanism of the dimroth rearrangement in adenosine*.
- [157] S. N. Mikhailov, J. Rozenski, E. V. Efimtseva, R. Busson, A. Van Aerschot, P. Herdewijn, *Nucleic Acids Res.* **2002**, *30*, 1124-1131. *Chemical incorporation of 1-methyladenosine into oligonucleotides*.
- [158] C. Frezza, E. Gottlieb, *Semin. Cancer Biol.* **2009**, *19*, 4-11. *Mitochondria in cancer: Not just innocent bystanders*.

- [159] R. A. Gatenby, R. J. Gillies, *Nat. Rev. Cancer* **2004**, 4, 891-899. *Why do cancers have high aerobic glycolysis?*
- [160] V. Gogvadze, S. Orrenius, B. Zhivotovsky, *Trends Cell Biol.* **2008**, 18, 165-173. *Mitochondria in cancer cells: what is so special about them?*
- [161] I. Samudio, M. Fiegl, M. Andreeff, *Cancer Res.* **2009**, 69, 2163-2166. *Mitochondrial Uncoupling and the Warburg effect: Molecular basis for the reprogramming of cancer cell metabolism.*
- [162] M. A. Kiebish, X. Han, H. Cheng, J. H. Chuang, T. N. Seyfried, *J. Lipid Res.* **2008**, 49, 2545-2556. *Cardiolipin and electron transport chain abnormalities in mouse brain tumor mitochondria: lipidomic evidence supporting the Warburg theory of cancer.*
- [163] T. Brückl, D. Globisch, M. Wagner, M. Müller, T. Carell, *Angew. Chem. Int. Ed.* **2009**, 48, 7932-7934. *Parallel isotope-based quantification of modified tRNA nucleosides.*
- [164] T. Brückl, F. Klepper, K. Gutsmedl, T. Carell, *Org. Biomol. Chem.* **2007**, 5, 3821-3825. *A short and efficient synthesis of the tRNA nucleosides PreQ0 and archaeosine.*
- [165] F. Klepper, E.-M. Jahn, V. Hickmann, T. Carell, *Angew. Chem. Int. Ed.* **2007**, 46, 2325-2327. *Synthesis of the transfer-RNA nucleoside queuosine by using a chiral allyl azide intermediate.*
- [166] F. Klepper, K. Polborn, T. Carell, *Helv. Chim. Acta* **2005**, 88, 2610-2616. *Robust Synthesis and Crystal-Structure Analysis of 7-Cyano-7-deazaguanine (PreQ0 Base) and 7-(Aminomethyl)-7-deazaguanine (PreQ1 Base).*
- [167] T. Brückl, I. Thoma, A. J. Wagner, P. Knochel, T. Carell, *Eur. J. Org. Chem.* **2010**, 2010, 6517-6519. *Efficient Synthesis of Deazaguanosine-Derived tRNA Nucleosides PreQ0, PreQ1, and Archaeosine Using the Turbo-Grignard Method.*
- [168] F. Jühling, M. Mörl, K. Hartmann Roland, M. Sprinzl, F. Stadler Peter, J. Pütz, *Nucleic Acids Res.* **2009**, 37, D159-162. *tRNADB 2009: compilation of tRNA sequences and tRNA genes.*
- [169] A. C. Kneuttinger, Master thesis, Ludwig-Maximilians-University (Munich) **2010**. *Isolation and characterisation of Spore Photoproduct Lyase from Geobacillus stearothermophilus.*
- [170] C. Frezza, S. Cipolat, L. Scorrano, *Nature Protoc.* **2007**, 2, 287-295. *Organelle isolation: functional mitochondria from mouse liver, muscle and cultured fibroblasts.*
- [171] B.-H. Ahn, H.-S. Kim, S. Song, I. H. Lee, J. Liu, A. Vassilopoulos, C.-X. Deng, T. Finkel, *Proc. Natl. Acad. Sci. USA* **2008**, 105, 14447-14452. *A role for the mitochondrial deacetylase Sirt3 in regulating energy homeostasis.*
- [172] D. P. Kelly, J. I. Gordon, R. Alpers, A. W. Strauss, *J. Biol. Chem.* **1989**, 264, 18921-18925. *The Tissue-specific Expression and Developmental Regulation of Two Nuclear Genes Encoding Rat Mitochondrial Proteins.*
- [173] G. Benard, et al., *Am. J. Physiol., Cell Physiol.* **2006**, 291, C1172-C1182. *Physiological diversity of mitochondrial oxidative phosphorylation.*
- [174] <http://library.med.utah.edu/masspec/mongo.htm>
- [175] C. M. Castleberry, P. A. Limbach, *Nucleic Acids Res.* **2010**, 38, e162. *Relative quantitation of transfer RNAs using liquid chromatography mass spectrometry and signature digestion products.*
- [176] R. J. Jackson, S. Naphine, I. Brierley, *RNA* **2001**, 7, 765-773. *Development of a tRNA-dependent in vitro translation system.*
- [177] H. A. Johnson, R. L. Baldwin, J. France, C. C. Calvert, *J. Nutr.* **1999**, 129, 728-739. *A model of whole-body protein turnover based on leucine kinetics in rodents.*
- [178] A. Suryawan, P. M. J. O'Connor, J. A. Bush, H. V. Nguyen, T. A. Davis, *Amino Acids* **2009**, 37, 97-104. *Differential regulation of protein synthesis by amino acids and insulin in peripheral and visceral tissues of neonatal pigs.*

- [179] J. B. Plotkin, H. Robins, A. J. Levine, *Proc. Natl. Acad. Sci. USA* **2004**, *101*, 12588-12591. *Tissue-specific codon usage and the expression of human genes.*
- [180] K. A. Dittmar, J. M. Goodenbour, T. Pan, *PLoS Genet.* **2006**, *2*, 2107-2115. *Tissue-specific differences in human transfer RNA expression.*
- [181] J. Ling, N. Reynolds, M. Ibba, *Annu. Rev. Microbiol.* **2009**, *63*, 61-78. *Aminoacyl-tRNA synthesis and translational quality control.*
- [182] J. W. Gray, C. Collins, *Carcinogenesis* **2000**, *21*, 443-452. *Genome changes and gene expression in human solid tumors.*
- [183] G. L. Nicolson, *Biochim. Biophys. Acta* **1982**, *695*, 113-176. *Cancer metastasis - Organ colonization and the cell-surface properties of malignant cells.*
- [184] T. Reya, S. J. Morrison, M. F. Clarke, I. L. Weissman, *Nature* **2001**, *414*, 105-111. *Stem cells, cancer, and cancer stem cells.*
- [185] M. Wu, J. A. Eisen, *Genome Biol.* **2008**, *9*, R151. *A simple, fast, and accurate method of phylogenomic inference.*
- [186] H. Hori, *J. Mol. Evol.* **1975**, *7*, 75-86. *Evolution of 5sRNA.*
- [187] C. R. Woese, *Microbiol. Mol. Biol. Rev.* **1987**, *51*, 221-271. *Bacterial evolution.*
- [188] P. Yarza, M. Richter, J. Peplies, J. Euzéby, R. Amann, K.-H. Schleifer, W. Ludwig, F. O. Glöckner, R. Rosselló-Móra, *Syst. Appl. Microbiol.* **2008**, *31*, 241-250. *The All-Species Living Tree project: a 16S rRNA-based phylogenetic tree of all sequenced type strains.*
- [189] J. O. McInerney, J. A. Cotton, D. Pisani, *Trends Ecol. Evol.* **2008**, *23*, 276-281. *The prokaryotic tree of life: past, present... and future?*
- [190] J. O. McInerney, D. Pisani, *Science* **2007**, *318*, 1390-1391. *Genetics - Paradigm for life.*
- [191] F. D. Ciccarelli, T. Doerks, C. von Mering, C. J. Creevey, B. Snel, P. Bork, *Science* **2006**, *311*, 1283-1287. *Toward automatic reconstruction of a highly resolved tree of life.*
- [192] K. Shiba, H. Motegi, P. Schimmel, *Trends Biochem. Sci.* **1997**, *12*, 453-457. *Maintaining genetic code through adaptations of tRNA synthetases to taxonomic domains.*
- [193] K. Sheppard, D. Söll, *J. Mol. Biol.* **2008**, *377*, 831-844. *On the Evolution of the tRNA-Dependent Amidotransferases, GatCAB and GatDE.*
- [194] T. Okayasu, K. Sorimachi, *Amino Acids* **2009**, *36*, 261-271. *Organisms can essentially be classified according to two codon patterns.*
- [195] A. K. Hopper, E. M. Phizicky, *Genes Dev.* **2003**, *17*, 162-180. *tRNA transfers to the limelight.*
- [196] R. S. Gupta, *Microbiol. Mol. Biol. Rev.* **1998**, *62*, 1435-1491. *Protein phylogenies and signature sequences: A reappraisal of evolutionary relationships among archaeobacteria, eubacteria, and eukaryotes.*
- [197] J. R. Battista, *Annu. Rev. Microbiol.* **1997**, *51*, 203-224. *Against all odds: the survival strategies of *Deinococcus radiodurans*.*
- [198] Y. Nitzan, H. Ashkenazi, *Photochem. Photobiol.* **2008**, *69*, 505-510. *Photoinactivation of *Deinococcus radiodurans*: an unusual gram-positive microorganism.*
- [199] L. Olendzenski, L. Liu, O. Zhaxybayeva, R. Murphey, D. G. Shin, J. P. Gogarten, *J. Mol. Evol.* **2000**, *51*, 587-599. *Horizontal transfer of archaeal genes into the deinococcaceae: detection by molecular and computer-based approaches.*
- [200] S. Chimnaronk, F. Forouhar, J. Sakai, M. Yao, C. M. Tron, M. Atta, M. Fontecave, J. F. Hunt, I. Tanaka, *Biochemistry* **2009**, *48*, 5057-5065. *Snapshots of dynamics in synthesizing *N*(6)-isopentenyladenosine at the tRNA anticodon.*
- [201] K. H. Kaminska, U. Baraniak, M. Boniecki, K. Nowaczyk, A. Czerwoniec, J. M. Bujnicki, *Proteins* **2008**, *70*, 1-18. *Structural bioinformatics analysis of enzymes*

- involved in the biosynthesis pathway of the hypermodified nucleoside ms(2)io(6)A37 in tRNA.*
- [202] J. J. Janzer, J. P. Raney, B. D. McLennan, *Nucleic Acids Res.* **1982**, *10*, 5663-5672. *The transfer RNA of certain Enterobacteriaceae contain 2-methylthiozeatin riboside (ms2io6A) an isopentenyl adenosine derivative.*
- [203] B. Thimmappaya, J. D. Cherayil, *Biochem. Biophys. Res. Commun.* **1974**, *60*, 665-672. *Unique presence of 2-methylthio-ribosylzeatin in the transfer ribonucleic acid of the bacterium.*
- [204] M. B. Eisen, P. T. Spellman, P. O. Brown, D. Botstein, *Proc. Natl. Acad. Sci. U.S.A.* **1998**, *95*, 14863-14868. *Cluster analysis and display of genome-wide expression patterns.*
- [205] N. Jessani, Y. Liu, M. Humphrey, B. F. Cravatt, *Proc. Natl. Acad. Sci. U.S.A.* **2002**, *99*, 10335-10340. *Enzyme activity profiles of the secreted and membrane proteome that depict cancer cell invasiveness.*
- [206] E. Griffiths, R. S. Gupta, *J. Bacteriol.* **2004**, *186*, 3097-3107. *Distinctive Protein Signatures Provide Molecular Markers and Evidence for the Monophyletic Nature of the Deinococcus-Thermus Phylum.*
- [207] A. J. Spiers, A. Buckling, P. B. Rainey, *Microbiology* **2000**, *146*, 2345-2350. *The causes of Pseudomonas diversity.*
- [208] M. Mulet, J. Lalucat, E. García-Valdés, *Environ. Microbiol.* **2010**, *12*, 1513-1530. *DNA sequence-based analysis of the Pseudomonas species.*
- [209] E. Lerat, V. Daubin, N. A. Moran, *PLoS Biol.* **2003**, *1*, e19. *From gene trees to organismal phylogeny in prokaryotes: the case of the gamma-Proteobacteria.*
- [210] E. V. Koonin, K. S. Makarova, L. Aravind, *Annu. Rev. Microbiol.* **2001**, *55*, 709-742. *Horizontal gene transfer in prokaryotes: quantification and classification.*
- [211] J. C. Dohm, M. Vingron, E. Staub, *J. Mol. Evol.* **2006**, *63*, 437-447. *Horizontal gene transfer in aminoacyl-tRNA synthetases including leucine-specific subtypes.*
- [212] J. R. Brown, D. Gentry, J. A. Becker, K. Ingraham, D. J. Holmes, M. J. Stanhope, *EMBO Rep.* **2003**, *4*, 692-698. *Horizontal transfer of drug-resistant aminoacyl-transfer-RNA synthetases of anthrax and Gram-positive pathogens.*
- [213] S. S. Phelps, C. Gaudin, S. Yoshizawa, C. Benitez, D. Fourmy, S. Joseph, *J. Mol. Biol.* **2006**, *360*, 610-622. *Translocation of a tRNA with an extended anticodon through the ribosome.*
- [214] L. Cegelski, G. R. Marshall, G. R. Eldridge, S. J. Hultgren, *Nat. Rev. Microbiol.* **2008**, *6*, 17-27. *The biology and future prospects of antivirulence therapies.*
- [215] P. S. Stewart, J. W. Costerton, *Lancet* **2001**, *358*, 135-138. *Antibiotic resistance of bacteria in biofilms.*
- [216] R. M. Klevens, et al., *JAMA* **2007**, *298*, 1763-1771. *Invasive methicillin-resistant Staphylococcus aureus infections in the United States.*
- [217] T. Böttcher, S. A. Sieber, *ChemBioChem* **2009**, *10*, 663-666. *Structurally refined beta-lactones as potent inhibitors of devastating bacterial virulence factors.*
- [218] C. A. Lowery, T. Abe, J. Park, L. M. Eubanks, D. Sawada, G. F. Kaufmann, K. D. Janda, *J. Am. Chem. Soc.* **2009**, *131*, 15584-15585. *Revisiting AI-2 quorum sensing inhibitors: direct comparison of alkyl-DPD analogues and a natural product fimbrolide.*
- [219] C. A. Lowery, et al., *J. Am. Chem. Soc.* **2009**, *131*, 14473-14479. *Defining the mode of action of tetramic acid antibacterials derived from Pseudomonas aeruginosa quorum sensing signals.*
- [220] H. Suga, K. M. Smith, *Curr. Opin. Chem. Biol.* **2003**, *7*, 586-591. *Molecular mechanisms of bacterial quorum sensing as a new drug target.*

- [221] C. Burtscher, S. Wuertz, *Appl. Environ. Microbiol.* **2003**, *69*, 4618-4627. *Evaluation of the Use of PCR and Reverse Transcriptase PCR for Detection of Pathogenic Bacteria in Biosolids from Anaerobic Digestors and Aerobic Composters.*
- [222] N. M. Carroll, E. E. Jaeger, S. Choudhury, A. A. Dunlop, M. M. Matheson, P. Adamson, N. Okhravi, S. Lightman, *J. Clin. Microbiol.* **2000**, *38*, 1753-1757. *Detection of and discrimination between gram-positive and gram-negative bacteria in intraocular samples by using nested PCR.*
- [223] S. D. Tyler, C. A. Strathdee, K. R. Rozee, W. M. Johnson, *Clin. Diagn. Lab. Immunol.* **1995**, *2*, 448-453. *Oligonucleotide primers designed to differentiate pathogenic pseudomonads on the basis of the sequencing of genes coding for 16S-23S rRNA internal transcribed spacers.*
- [224] K. Shigemura, T. Shirakawa, H. Okada, K. Tanaka, S. Kamidono, S. Arakawa, A. Gotoh, *Clin. Exp. Med.* **2005**, *4*, 196-201. *Rapid detection and differentiation of Gram-negative and Gram-positive pathogenic bacteria in urine using TaqMan probe.*
- [225] P. Kiratisin, P. Santanirand, N. Chantratita, S. Kaewdaeng, *Diagn. Microbiol. Infect. Dis.* **2007**, *59*, 277-281. *Accuracy of commercial systems for identification of Burkholderia pseudomallei versus Burkholderia cepacia.*
- [226] J. E. Gee, C. T. Sacchi, M. B. Glass, B. K. De, R. S. Weyant, P. N. Levett, A. M. Whitney, A. R. Hoffmaster, T. Popovic, *J. Clin. Microbiol.* **2003**, *41*, 4647-4654. *Use of 16S rRNA Gene Sequencing for Rapid Identification and Differentiation of Burkholderia pseudomallei and B. mallei.*
- [227] B. Soufi, C. D. Kelstrup, G. Stoehr, F. Fröhlich, T. C. Walther, J. V. Olsen, *Mol. BioSyst.* **2009**, *5*, 1337-1346. *Global analysis of the yeast osmotic stress response by quantitative proteomics.*
- [228] A. Y. Golovina, P. V. Sergiev, A. V. Golovin, M. V. Serebryakova, I. Demina, V. M. Govorun, O. A. Dontsova, *RNA* **2009**, *15*, 1134-1141. *The yfiC gene of E. coli encodes an adenine-N6 methyltransferase that specifically modifies A37 of tRNA^IVal(cmo5UAC).*
- [229] S. M. Kinghorn, C. P. O'Byrne, I. R. Booth, I. Stansfield, *Microbiology* **2002**, *148*, 3511-3520. *Physiological analysis of the role of truB in Escherichia coli: a role for tRNA modification in extreme temperature resistance.*
- [230] M. P. Deutscher, *J. Biol. Chem.* **2003**, *278*, 45041-45044. *Degradation of stable RNA in bacteria.*
- [231] E. Turlin, O. Sismeiro, J. Pierre, V. Labas, A. Danchin, F. Biville, *Res. Microbiol.* **2005**, *156*, 312-321. *3-Phenylpropionate catabolism and the Escherichia coli oxidative stress response.*
- [232] D. M. Thompson, C. Lu, P. J. Green, R. Parker, *RNA* **2008**, *14*, 2095-2103. *tRNA cleavage is a conserved response to oxidative stress in eukaryotes.*
- [233] F. Walter, J. Pu, R. Giege, E. Westhof, *EMBO J.* **2002**, *21*, 760-768. *Binding of tobramycin leads to conformational changes in yeast tRNA and its inhibition of aminoacylation.*
- [234] S. R. Kirk, Y. Tor, *Bioorg. Med. Chem.* **1999**, *7*, 1979-1991. *tRNA^{Phe} binds aminoglycoside antibiotics.*
- [235] S. Corvaisier, V. Bordeau, B. Felden, *J. Biol. Chem.* **2003**, *278*, 14788-14797. *Inhibition of transfer messenger RNA aminoacylation and trans-translation by aminoglycoside antibiotics.*
- [236] N. E. Mikkelsen, K. Johansson, L. A. Kirsebom, A. Virtanen, *Nat. Struct. Biol.* **2001**, *8*, 510-514. *Aminoglycoside binding displaces a divalent metal ion in a tRNA-neomycin B complex.*
- [237] F. C. Neidhardt, P. L. Bloch, D. F. Smith, *J. Bacteriol.* **1974**, *119*, 736-747. *Culture Medium for Enterobacteria.*

- [238] B. Frey, J. McCloskey, W. Kersten, H. Kersten, *J. Bacteriol.* **1988**, *170*, 2078-2082. *New function of vitamin B12: cobamide-dependent reduction of epoxyqueuosine to queuosine in tRNAs of Escherichia coli and Salmonella typhimurium.*
- [239] D. W. Phillipson, C. G. Edmonds, P. F. Crain, D. L. Smith, D. R. Davis, J. A. McCloskey, *J. Biol. Chem.* **1987**, *262*, 3462-3471. *Isolation and structure elucidation of an epoxide derivative of the hypermodified nucleoside queuosine from Escherichia coli transfer RNA.*
- [240] S. G. Van Lanen, S. D. Kinzie, S. Matthieu, T. Link, J. Culp, D. Iwata-Reuyl, *J. Biol. Chem.* **2003**, *278*, 10491-10499. *tRNA modification by S-adenosylmethionine:tRNA ribosyltransferase-isomerase. Assay development and characterization of the recombinant enzyme.*
- [241] J. D. Watson, F. H. C. Crick, *Nature* **1953**, *171*, 737-738. *Molecular structure of nucleic acids.*
- [242] G. R. Wyatt, *Nature* **1950**, *166*, 237-238. *Occurrence of 5-methylcytosine in nucleic acids.*
- [243] M. Esteller, *N. Engl. J. Med.* **2008**, *358*, 1148-1159. *Epigenetics in cancer.*
- [244] M. G. Goll, T. H. Bestor, *Annu. Rev. Biochem.* **2005**, *74*, 481-514. *Eukaryotic cytosine methyltransferases.*
- [245] S. Ito, A. C. D'Alessio, O. V. Taranova, K. Hong, L. C. Sowers, Y. Zhang, *Nature* **2010**. *Role of Tet proteins in 5mC to 5hmC conversion, ES-cell self-renewal and inner cell mass specification.*
- [246] N. W. Penn, R. Suwalski, C. O'Riley, K. Bojanowski, R. Yura, *Biochem. J.* **1972**, *126*, 781-790. *The presence of 5-hydroxymethylcytosine in animal deoxyribonucleic acid.*
- [247] R. M. Kothari, V. Shankar, *J. Mol. Evol.* **1976**, *7*, 325-329. *5-Methylcytosine content in the vertebrate deoxyribonucleic acids: species specificity.*
- [248] P. Borst, R. Sabatini, *Annu. Rev. Microbiol.* **2008**, *62*, 235-251. *Base J: discovery, biosynthesis, and possible functions.*
- [249] U. M. Ünlügil, J. M. Rini, *Curr. Opin. Struct. Biol.* **2000**, *10*, 510-517. *Glycosyltransferase structure and mechanism.*
- [250] M. A. Gama-Sosa, R. M. Midgett, V. A. Slagel, S. Githens, K. C. Kuo, C. W. Gehrke, M. Ehrlich, *Biochim. Biophys. Acta* **1983**, *740*, 212-219. *Tissue-specific differences in DNA methylation in various mammals.*
- [251] M. A. Gama-Sosa, V. A. Slagel, R. W. Trewyn, R. Oxenhandler, K. C. Kuo, C. W. Gehrke, M. Ehrlich, *Nucleic Acids Res.* **1983**, *11*, 6883-6894. *The 5-methylcytosine content of DNA from human tumors.*
- [252] L. Song, S. R. James, L. Kazim, A. R. Karpf, *Anal. Chem.* **2005**, *77*, 504-510. *Specific method for the determination of genomic DNA methylation by liquid chromatography-electrospray ionization tandem mass spectrometry.*
- [253] B. F. Vanyushin, S. G. Tkacheva, A. N. Belozersky, *Nature* **1970**, *225*, 948-949. *Rare bases in animal DNA.*
- [254] D. Globisch, M. Münzel, M. Müller, S. Michalakis, M. Wagner, S. Koch, T. Brückl, M. Biel, T. Carell, *PLoS ONE* **2010**, *5*, e15367. *Tissue Distribution of 5-Hydroxymethylcytosine and Search for Active Demethylation Intermediates.*
- [255] M. Münzel, D. Globisch, T. Brückl, M. Wagner, V. Welzmler, S. Michalakis, M. Müller, M. Biel, T. Carell, *Angew. Chem. Int. Ed.* **2010**, 5375-5377. *Quantification of the Sixth DNA Base Hydroxymethylcytosine in the Brain.*
- [256] G. L. Ming, H. J. Song, *Annu. Rev. Neurosci.* **2005**, *28*, 223-250. *Adult neurogenesis in the mammalian central nervous system.*
- [257] F. H. Gage, *Science* **2000**, *287*, 1433-1438. *Mammalian neural stem cells.*
- [258] C.-X. Song, et al., *Nat. Biotechnol.* **2011**, *29*, 68-72. *Selective chemical labeling reveals the genome-wide distribution of 5-hydroxymethylcytosine.*

- [259] V. Valinluck, H. H. Tsai, D. K. Rogstad, A. Burdzy, A. Bird, L. C. Sowers, *Nucleic Acids Res.* **2004**, *32*, 4100-4108. *Oxidative damage to methyl-CpG sequences inhibits the binding of the methyl-CpG binding domain (MBD) of methyl-CpG binding protein 2 (MeCP2).*
- [260] Z. Liutkeviciute, G. Lukinavicius, V. Masevicius, D. Daujotyte, S. Klimasauskas, *Nat. Chem. Biol.* **2009**, *5*, 400-402. *Cytosine-5-methyltransferases add aldehydes to DNA.*
- [261] S. C. Wu, Y. Zhang, *Nat. Rev. Mol. Cell Biol.* **2010**, *11*, 607-620. *Active DNA demethylation: many roads lead to Rome.*
- [262] K. N. Houk, J. K. Lee, D. J. Tantillo, S. Bahmanyar, B. N. Hietbrink, *ChemBioChem* **2001**, *2*, 113-118. *Crystal structures of orotidine monophosphate decarboxylase: Does the structure reveal the mechanism of nature's most proficient enzyme?*
- [263] R. D. Palmatier, R. P. McCroskey, M. T. Abbott, *J. Biol. Chem.* **1970**, *245*, 6706-6710. *Enzymatic conversion of uracil 5-carboxylic acid to uracil and carbon dioxide.*
- [264] P. M. Shaffer, C. A. Hsu, M. T. Abbott, *J. Bacteriol.* **1975**, *121*, 648-655. *Metabolism of pyrimidine deoxyribonucleosides in neurospora-crassa.*
- [265] J. M. Simmons, T. A. Muller, R. P. Hausinger, *Dalton Trans.* **2008**, 5132-5142. *Fe-II/alpha-ketoglutarate hydroxylases involved in nucleobase, nucleoside, nucleotide, and chromatin metabolism.*
- [266] J.-K. Zhu, *Annu. Rev. Genet.* **2009**, *43*, 143-166. *Active DNA demethylation mediated by DNA glycosylases.*
- [267] R. J. Boorstein, L. N. Chiu, G. W. Teebor, *Nucleic Acids Res.* **1989**, *17*, 7653-7661. *Phylogenetic Evidence of a Role for 5-Hydroxymethyluracil-DNA Glycosylase in the Maintenance of 5-Methylcytosine in DNA.*
- [268] V. Rusmintratip, L. C. Sowers, *Proc. Natl. Acad. Sci. U. S. A.* **2000**, *97*, 14183-14187. *An unexpectedly high excision capacity for mispaired 5-hydroxymethyluracil in human cell extracts.*
- [269] S. V. Cannon, A. Cummings, G. W. Teebor, *Biochem. Biophys. Res. Commun.* **1988**, *151*, 1173-1179. *5-Hydroxymethylcytosine DNA glycosylase activity in mammalian tissue.*

PERSONAL DATA

Date of birth 13th of October 1981
Place of birth Kaiserslautern
Nationality German

RESEARCH EXPERIENCE

03/2007 – 03/2011 **Research for Ph.D.**
Faculty of Chemistry and Pharmacy
Ludwig-Maximilians-University (LMU) in Munich, Germany
Group of Prof. Dr. Thomas Carell
“Synthesis of natural modified nucleosides and their mass spectrometric quantification in cells and tissue”

04/2006 – 02/2007 **Research for Diploma thesis**
Nucleic Acid Center (NAC), University of Southern Denmark (SDU) in Odense, Denmark, Group of Prof. Dr. Erik B. Pedersen
“Novel Triplex Forming Oligonucleotides Trapping the Phosphate Backbone of the Duplex”

04/2005 – 07/2005 **Research internship**
SDU in Odense, Denmark Group of Prof. Dr. Erik B. Pedersen
“Synthesis of MC-1220 and TMC-125 Analogues and their Pro-Drugs as Novel Non-Nucleoside Reverse Transcriptase Inhibitors (NNRTIs)”

UNIVERSITY EDUCATION

10/2001 – 03/2006 Undergraduate studies, graduate studies and Diploma exams
Faculty of Chemistry
Technical University Kaiserslautern, Germany

SCHOOL EDUCATION

08/1992 – 06/2001 **High school “Abitur”**
“Gymnasium an der Burgstraße”
Kaiserslautern, Germany

